

UC San Diego

UC San Diego Electronic Theses and Dissertations

Title

Vanadium-dependent bromoperoxidase in a marine *Synechococcus* /

Permalink

<https://escholarship.org/uc/item/34x4t8rp>

Author

Johnson, Todd Laurel

Publication Date

2013

Peer reviewed|Thesis/dissertation

UNIVERSITY OF CALIFORNIA, SAN DIEGO

Vanadium-dependent bromoperoxidase in a marine *Synechococcus*

A dissertation submitted in partial satisfaction of the requirements for the degree of
Doctor of Philosophy

in

Marine Biology

by

Todd L. Johnson

Committee in charge:

Brian Palenik, Chair
Bianca Brahamsha, Co-Chair
Lihini Aluwihare
James Golden
Jens Mühle
Bradley Moore

2013

Copyright

Todd L. Johnson, 2013

All rights reserved.

The dissertation of Todd L. Johnson is approved, and it is acceptable in quality and form for publication on microfilm and electronically:

Co-Chair

Chair

University of California, San Diego

2013

DEDICATION

To Janet, Tim, and Andrew Johnson, for unconditional love and support.

TABLE OF CONTENTS

Signature Page.....	iii
Dedication	iv
Table of Contents.....	v
List of Abbreviations.....	vi
List of Figures.....	viii
List of Tables.....	xi
Acknowledgements.....	xiii
Vita.....	xiv
Abstract.....	xv
Chapter 1: Introduction.....	1
Chapter 2: Characterization of a functional vanadium-dependent bromoperoxidase in the marine cyanobacterium <i>Synechococcus</i> sp. CC9311	10
Chapter 3: Expression patterns of vanadium-dependent bromoperoxidase in <i>Synechococcus</i> sp. CC9311 as a response to physical agitation and a bacterial assemblage	27
Chapter 4: Halomethane production by vanadium-dependent bromoperoxidase in marine <i>Synechococcus</i>	107
Chapter 5: Conclusions.....	149
Appendix 1.....	154

LIST OF ABBREVIATIONS

VBPO – vanadium-dependent bromoperoxidase

bp – base pair

kDa – kilodalton

°C – degrees Celsius

DNA – deoxyribonucleic acid

PCR – polymerase chain reaction

MES - 2-(*N*-morpholino)ethanesulfonic acid

Na₃VO₄ – sodium orthovanadate

H₂O₂ – hydrogen peroxide

hr - hour

min – minute

μmol - micromole

μM - micromolar

nM – nanomolar

ppt – parts per trillion

SDS-PAGE – sodium dodecyl sulfate - polyacrylamide gel electrophoresis

Br⁻ – bromide

I⁻ - iodide

Cl⁻ - chloride

ppt – parts per trillion

mTorr – millitorr

VHOC – volatile halogenated organic compounds

CH_3Br – methyl bromide

CH_3I – methyl iodide

CH_3Cl – methyl chloride

CH_2Br_2 - dibromomethane

CH_2Cl_2 - dichloromethane

CHBr_3 - bromoform

CHCl_3 - chloroform

LIST OF FIGURES

- Figure 1: SDS-PAGE gels of total proteins from *Synechococcus* strains WH8102, CC9311, and VBPO from *Corallina officinalis* (Co VBPO, Sigma) stained with Sypro Ruby (left) and with phenol red (right) for bromoperoxidase activity. The migrations of molecular mass standards are indicated on the left in kDa.....13
- Figure 2: Amino acid alignment of VBPO from *Synechococcus sp.* strain CC9311 and strain WH8020. Active site is shown by the solid bar while vanadium-coordinating residues are shown in bold, as determined by homology to *Ascophyllum nodosum*. Arrows indicate residues used for the design of environmental probes14
- Figure 3: Neighbor-joining tree of known bromoperoxidase sequences and related genes. Amino acid sequences obtained from NCBI using *Synechococcus sp.* strain CC9311 (YP_731869.1) in a BLASTp. Asterisk (*) indicates only node with less than 50% bootstrap support. Accession numbers are shown in *Supplementary Table 1*.....14
- Figure 4: Neighbor-Joining tree of environmental VBPO sequences. Nucleotide sequences were trimmed to a conserved region of approximately 180-bp (alignment shown in *Supplementary Figure 2*). “Pier#” samples were obtained from a degenerate primer (PierF and PierR) clone library from the Scripps Pier in La Jolla, CA.....15
- Fig. S1: Alignment of the well-conserved region between cyanobacterial and eukaryotic algal vanadium-dependent bromoperoxidases (VBPOs) used to construct the phylogenetic tree shown in Figure 3. Sequences were obtained from the National Center for Biotechnology Information’s nr protein database.....20
- Fig. S2: Nucleotide alignment of the Scripps Pier clone library to metagenomic sequences (see “Materials and Methods”). This alignment was used for the neighbor-joining analysis and phylogenetic tree construction shown in Figure 4.....23
- Figure 3.1: A diagram of the insertional gene inactivation of VBPO (sync_2681) in *Synechococcus* CC9311 (shown in A) to form the VMUT genotype (shown in B). Steps: 1. PCR amplification of gene fragment, 2. Clone into TOPO vector to form pTOP2681, 3. Excise new fragment with *EcoRI* and cloned into pMUT100 form pVBR1, 4.....84
- Figure 3.2: Mutant genotyping, a 1% agarose gel showing PCR products from boiling DNA extraction of stock cultures using A) RPOC1 primers (303 bp) and B) verifications primers (750 bp). Lanes left to right: 1 Kb Plus Ladder (bp); CC9311; VMUT; VMUT2; no DNA control.....85
- Figure 3.3: Mutant growth curves showing the cell counts (lines) comparing the growth of CC9311 and the original mutant, VMUT, under stirred and still conditions over the first three growth curves (A-C) as well as CC9311 and VMUT2 (D-F). VBPO specific activities (bars) are also shown comparing CC9311 to VMUT2 (D-F) over three.....86

Figure 3.4: VBPO specific activity of proteins harvested from cultures of A) CC9311 and B) VMUT2 at different phases of growth. VBPO activities of biological triplicates are shown from cultures grown under still conditions (white bars), cultures grown under still conditions and subjected to a short term (4 hr) period of stirring (grey bars), and87

Figure 3.5: Genotype of VMUT after disappearance of stir-sensitive phenotype. PCR products from boiling DNA extraction shown on 1% agarose gels. Panel A: verifications primers (750 bp) lanes left to right: 1) 1 Kb Plus Ladder (bp); 2) CC9311; 3) VMUT stir; 4) VMUT still; 5) no DNA control. Panel B: RPOC1 primers (303 bp)88

Figure 3.6: Duplicate SDS-PAGE of proteins extracted from CC9311 and VMUT2 in stationary phase; grown still, still with only four hours of stirring, or constant stirring. Each lane was loaded with 55 μg protein and stained with A) sypro ruby or B) phenol-red in the presence of Na_3VO_4 , KBr , and H_2O_2 for VBPO activity. Lanes left to right.....89

Figure 3.7: Induction and persistence of VBPO with stirring. A) Cell counts from cultures of CC9311 used to test the induction of VBPO with stirring over time. Vertical solid line shows when stirring was either initiated or halted in cultures. Growth rates of the cultures after the vertical line are 0.56 d^{-1} for the culture that was stirred from inoculation.....90

Figure 3.8: VBPO and cell resistance to hydrogen peroxide. Phycoerythrin autofluorescence of CC9311 and VMUT cultures after the addition of hydrogen peroxide. Solid lines represent cultures that have been preconditioned with stirring while dotted lines represent cultures that have been grown still from inoculation. Top left: Trial 1....91

Figure 3.9: VBPO specific activities of CC9311 cultures exposed to A) 25 μM hydrogen peroxide and b) 0.1 μM methyl viologen (MV).....92

Figure 3.10: Cell counts of *Acaryochloris marina* cultures tested for VBPO activity (trial 2).93

Figure 3.11: Native PAGE Gel of *Synechococcus* sp. CC9311 and *Acaryochloris marina* proteins, 21 μg protein per lane, from still and stirred cultures. Gel in panel A was stained with Sypro Ruby for total proteins, Gel in panel B was stained with phenol red for VBPO activity. Lanes left to right A) 1. Benchmark Protein ladder; 2. CC9311, still.....94

Figure 3.12: SDS-PAGE of *Synechococcus* CC9311 and *Acaryochloris marina* proteins, 26.5 μg protein per lane. Gel in panel A was stained with Sypro Ruby for total proteins, Gel in panel B was stained with phenol red for VBPO activity. Lanes left to right A) 1. Benchmark Protein ladder; 2. CC9311, still; 3. CC9311, stirred; 4. *A. marina*.95

Figure 3.13: Neighbor-joining tree showing the 16S gene library constructed of the bacterial assemblage that induces VBPO in *Synechococcus* CC9311, the 19 isolates, as well known sequences. TJ# refers to a clone from the 16S rRNA gene library and PTB# refers to a strain isolated from the *Pteridomonas* enrichment.96

Figure 3.14: Alignment of the 421 bp fragment of the 16s rRNA genes from the PTB enrichment clone library (TJ#), 19 isolated strains (PTB#) and known sequences.....97

Figure 4.1: Experimental design used to measure halomethane production in *Synechococcus* cultures..... 140

Figure 4.2: Cell concentrations of cultures (1.5 L) used in the purge-and-trap experiment (solid lines days 2-7). Vertical solid line at day seven indicates when CC9311 (Black) and VMUT2 (light grey) cultures were split and sealed in a serum bottle for 24 hrs with (dotted) and without (dotted) stirring. Vertical dotted line at day 8 indicates when.....141

Figure 4.3: Reaction mechanism for the biosynthesis of polyhalomethanes mediated by bromoperoxidase activity as proposed by Beissner *et al.* (1981).....142

Figure 4.4: Reaction scheme for vanadium-dependent bromoperoxidase determined for VBPO in the red algae, *Corallina officinalis*. This figure is adapted from Carter *et al.* (2002).....143

LIST OF TABLES

Table 1: Primer sequences used in this study. Degenerate primer code is as follows: S, G or C; R, A or G; Y, C or T; N, any base.....	12
Table 2: Vanadium-dependent bromoperoxidase specific activity found in <i>Synechococcus</i>	13
Table S1. Gene codes and accession numbers of the sequences used in the neighbor-joining tree of vanadium-dependent bromoperoxidase (VBPO) genes shown in Figure 3	25
Table 3.1: List of primers used in the construction and verification of the insertional gene inactivation for VMUT and VMUT2, as well as the universal primers used with the PTB enrichment.....	70
Table 3.2: Growth rate constants (k , day ⁻¹) comparing the growth of CC9311 and VMUT (shaded) and CC9311 and VMUT2 (not shaded) under still and stirred conditions.....	71
Table 3.3: VBPO activities measured in protein extracts of <i>Synechococcus</i> sp. CC9311 after exposure to different conditions and stresses.....	72
Table 3.4: VBPO specific activity in CC9311 proteins after 24 hour exposure to different grazer cultures.....	74
Table 3.5: Specific VBPO activities of <i>Acaryochloris marina</i> cultures.....	75
Table 3.6: Summary of peptide spectra and significant protein numbers from the two iTRAQ experiments.	76
Table 3.7: Table of colonies isolated from the PTB enrichment culture, including VBPO activity of CC9311 after 24 hr co-culturing experiment.....	77
Table 3.8: Isobaric iTRAQ mass tags used and VBPO specific activities of each treatment iTRAQ proteomic experiments	79
Table 3.9: Proteins identified with a significant iTRAQ ratio ($p \leq 0.05$) in at least two treatments. Sorted by descending order of iTRAQ ratio (stir divided still) from WT after 24 hrs.....	80
Table 3.10: List of functional gene categories enriched in iTRAQ experiments determined by DAVID (<i>see methods</i>).	84

Table 4.1: Dimensionless Henry's constants (K_H) used in calculations for the headspace experiment as well as purge efficiency calculations for the purge-and-trap experiment.	131
Table 4.2: Cell concentrations (cells ml^{-1}), VBPO activity ($\mu\text{mol dibromothymolblue min}^{-1} \text{mg}^{-1}$), and halomethane concentrations (pmol L^{-1}) measured in the headspace of <i>Synechococcus</i> cultures..	132
Table 4.3: Halomethane concentrations ($\text{pmol L}^{-1} \text{cell}^{-1}$) measured in the headspace above cultures of <i>Synechococcus</i> , blank (SN medium) subtracted and normalized to cell concentration.....	133
Table 4.4: Cell concentrations and VBPO activities measured in cultures used in the purge-and-trap experiment.....	134
Table 4.5: Purge efficiencies (percent recovered) by compound from the purge-and-trap experiment.....	135
Table 4.6: Halomethane concentrations (pmol L^{-1}) of each bottle measured in the purge-and-trap experiment.	136
Table 4.7: Cell-normalized halomethane concentrations ($\text{pmol L}^{-1} \text{cell}^{-1} \times 10^9$) measured in <i>Synechococcus</i> cultures in the purge-and-trap experiment.....	137
Table 4.8: Production rates ($\text{molecules cell}^{-1} \text{day}^{-1}$) of halomethanes in two strains of <i>Synechococcus</i> and a VBPO-gene inactivated mutant from the purge-and-trap experiment, normalized to the initial cell concentrations.....	138
Table 4.9: Production rates ($\text{molecules cell}^{-1} \text{day}^{-1}$) of halomethanes in two strains of <i>Synechococcus</i> and a VBPO-gene inactivated mutant from the purge-and-trap experiment, normalized by the averaged cell concentrations between time 0 and 24 hours.....	139

ACKNOWLEDGMENTS

First and foremost, I would like to thank my advisors, Dr. Brian Palenik and Dr. Bianca Brahamsha for providing tremendous support and guidance as well as for having patience with me as a developing scientist. I also extend tremendous gratitude to all of the members on my committee who have provided advice, corrections, frank discussions, and lab space to help me achieve my goals.

I would like to give a special thanks to Dr. Jens Mühle for help in understanding and designing experiments for the measurement of trace gases. Your discussions and help in the lab were invaluable for accomplishing my research. Thank you also to the entire laboratory of Ray Weiss, who allowed me to use their instruments and supplies, as well as helped me to make precise measurements of trace gases from my cultures.

Thank you Dr. Lihini Aluwihare for providing both advice and lab space to develop my skills in chemical extractions. I would also like to thank Dr. Brad Moore for discussions about vanadium dependent bromoperoxidase. Thank you Dr. James Golden for taking time to serve on my committee and guide my research.

Thank you to all of the past and present lab members of the Palenik and Brahamsha labs for creating a great work environment. I would like to thank Rhona Stuart, Javier Paz-Yepes, and Emy Daniels for helpful discussions relating to both science and life, both in and out of the lab. In addition, thank you Nellie Shaul, who also provided discussions on numerous aspects of halogenating enzymes.

Finally, I have endless gratitude to my friends and family who have helped me develop tremendously as a person over the past several years. My family has always been available to lend a listening ear and provide perspective. And to all of my friends at SIO,

who continuously inspire me to develop as a scientist and a human being through discussions, distractions, traveling, cooking, exercise, and music, thank you.

Chapter 2, in full, is a reprint of the material as it appears in *Journal of Psychology* 2011, 47:792-801. Johnson, Todd; Palenik, Brian; and Brahamsha, Bianca. The dissertation author was the primary investigator and author of this paper.

Chapter 3, in part, is currently being prepared for submission for publication of the material by Johnson, Todd; Paz-Yepes, Javier; Palenik, Brian; and Brahamsha, Bianca. The dissertation author was the primary investigator and will be first author of this paper.

Chapter 4, in part, is currently being prepared for submission for publication of the material by Johnson, Todd; Mühle, Jens; Palenik, Brian; and Brahamsha, Bianca. The dissertation author was the primary investigator and will be first author of this paper.

VITA

- 2007 Bachelor of Science in Ecology and Evolutionary Biology, California
State University, Fresno
- 2013 Doctor of Philosophy in Marine Biology, University of California, San
Diego

PUBLICATIONS

- Johnson, T. L., Palenik, B., and Brahamsha, B. 2011. Characterization of a functional vanadium-dependent bromoperoxidase in the marine cyanobacterium *Synechococcus* sp. *CC9311*. *Journal of Phycology*. 47:792-801.
- Johnson, T., G. L. Newton, R. C. Fahey, and M. Rawat. 2009. Unusual production of glutathione in *Actinobacteria*. *Archives of Microbiology* 191:89-93.
- Miller, C.C., Rawat, M., Johnson, T., Av-Gay, Y. 2007. Innate protection of *Mycobacteria* against the antimicrobial activity of nitric oxide is provided by mycothiol. *Antimicrobial Agents and Chemotherapy*. 51:9. 3364-3366

PRESENTATIONS

- Johnson, T.L., Palenik, B., Brahamsha, B. 2010. American Society for Microbiology.
- Johnson, T.L., Palenik, B., Brahamsha, B. 2013. Association for the Sciences of Limnology and Oceanography. Poster Presentation.

FIELDS OF STUDY

Major Field: Marine Biology, Microbiology

Studies in Marine Biology and Microbiology
Dr. Brian Palenik, Dr. Bianca Brahamsha

ABSTRACT OF THE DISSERTATION

Vanadium-dependent bromoperoxidase in a marine *Synechococcus*

by

Todd L. Johnson

Doctor of Philosophy in Marine Biology

University of California, San Diego, 2013

Professor Brian Palenik, Chair
Professor Bianca Brahamsha, Co-Chair

Vanadium-dependent bromoperoxidase (VBPO) carries out the two-electron oxidation of halides using hydrogen peroxide to create a hypohalous acid-like intermediate, which then halogenates electron-rich organic molecules. While this enzyme is well-characterized in marine eukaryotic macroalgae, the activity and function of VBPO in prokaryotes remains vastly unexplored. A gene (*sync_2681*) encoding a putative VBPO was recently annotated in the genome of *Synechococcus* sp. CC9311, however the activity, function, and consequences of the expression of VBPO in cyanobacteria remained unknown. The first goal of this dissertation was to better characterize the activity of VBPO in CC9311, finding that the observed activity resulted from the single, expected gene product. One highly neglected aspect of studies of VBPO is the use of

genetic manipulation to test natural physiological and ecological functions of this enzyme. Thus the second goal of this dissertation was to explore the function of VBPO in CC9311 through the creation of a mutant lacking a functional VBPO, then tracking activity under diverse conditions in coordination with global quantitative proteomics. The final goal of this dissertation was to explore the chemical consequences of the expression of VBPO in cyanobacteria, specifically measuring the production of halomethanes. VBPO has long been implicated in the production of polyhalogenated methanes, such as bromoform and dibromomethane through the use of eukaryotic algal protein extracts, however, this dissertation offers the first evidence that the VBPO in a marine cyanobacterium is responsible for the production of halogenated methanes in a laboratory setting.

Chapter 1: Introduction

Technological advancements, particularly in DNA sequencing, have facilitated an abundance of genomic-based studies for marine microbial populations, revealing novel organisms, genes, and potential gene functions (Rusch *et al.*, 2007, Scanlan *et al.*, 2009). While this has provided tremendous insights in determining the ingredients of the oceanic biological “soup,” it has opened the door to many questions. When the genome of *Synechococcus sp.* CC9311 was sequenced (Palenik *et al.*, 2006), a hypothetical gene (sync_2681) was annotated as a vanadium-dependent bromoperoxidase (VBPO) and was located in a region of horizontally transferred genes. VBPOs are primarily associated with marine eukaryotic macroalgae and have long been of interest for the production of halogenated organic molecules through the oxidation of halides and consumption of H₂O₂ (Moore & Okuda, 1996, Carter-Franklin & Butler, 2004). Though such sequence similarity-based annotations are useful, they do not guarantee the expression or function of a gene in another organism. It is still important to experimentally define these genetic elements in order to accurately relate them to the physiological and ecological context of an organism’s natural history.

The presence of VBPO suggests a potentially novel protein function in *Synechococcus* as this enzyme has never been characterized in a cyanobacterium and the ecological function of VBPO in prokaryotes remains uninvestigated. This dissertation takes the opportunity to expand upon a genetic observation and provide insight on how *Synechococcus* responds to its physical and biological environment as well as on the function of VBPO in marine cyanobacteria.

Synechococcus is a genus of marine chroococcoid cyanobacteria that is widely distributed throughout the world's oceans and plays a significant role in global biogeochemical cycles, responsible for up to 30% of photosynthetically-fixed carbon production in some areas (Li, 1994, Jardillier *et al.*, 2010). The genomic age has shown us the staggering degree of genetic diversity among microbial populations, for example in comparing the genomes of isolates in the genus *Synechococcus* (Scanlan *et al.*, 2009). Genomes of marine *Synechococcus* range in size from 2.235 to 3.043 Mbp (Hess, 2011), however, only an estimated 1,572 genes are common among the 14 genomes from 11 clades tested and are considered to be "core" genes. The remaining genes belong to the "flexible" genome (Dufresne *et al.*, 2008). These genes are either unique to a particular strain or only a few strains of *Synechococcus*. Many genes in this "flexible genome" are often considered to be horizontally transferred and are sometimes concentrated in specific locations in the genome, areas that are referred to as genomic islands (Dufresne *et al.*, 2008). While the utility of these genetic islands has been postulated to result in adaptation to specific environments, only a few recent studies have demonstrated specific functions for these concentrated segments of horizontally transferred genes (Coleman *et al.*, 2006, Avrani *et al.*, 2011, Stuart *et al.*, 2009, Stuart *et al.*, 2013). The gene encoding VBPO is located in a genomic island of putatively horizontally transferred genes in the genome of CC9311 as indicated by Dufresne *et al.* (2008).

VBPOs are generally associated with the marine environment as opposed to other halogenating enzymes. One reason for this may be that the primary substrates for the enzymatic reaction are readily available. In sea water, chloride is one of the most abundant ions (590 mM), while bromide (0.9 mM) and iodide (0.5 μ M) are successively

less common ions (Channer *et al.*, 1997). The transition metal co-factor, vanadium, is also present in seawater. While it is considered a trace element, dissolved vanadium has a conservative distribution in the open ocean with concentrations around 34-45 nM (Wang and Wihelmy, 2009) with a depletion of dissolved vanadium in coastal and estuarine waters (Shiller and Mao, 1999). Vanadium exists in several oxidation states in seawater, for which the biological accessibility is thought to vary. In seawater, vanadium primarily exists as vanadium(V) and vanadium(IV), with relative concentrations proportional to redox conditions. Vanadium(V) is more abundant in oxygenated water (Wang and Wihelmy, 2009) and is also used by VBPO, binding with trigonal bipyrimidal coordination (Carter *et al.*, 2002). Vanadium(IV) is more common in low oxygen seawater and is thought to be more freely diffusible through biological membranes (Wang and Wihelmy, 2009). Vanadium(IV) is also used by several vanadium utilizing enzymes, such as the nitrogenases in some diazotrophic cyanobacteria. A third oxidation state, vanadium(III), is found in Ascidians, which are also known for taking up vanadium(IV) and storing vanadium(III) in vanadocytes (Michibata *et al.*, 2002).

While the function in *Synechococcus* is unknown, haloperoxidases in eukaryotic macroalgae are regulated in response to a variety of environmental stresses. In the Rhodophyte *Gracilaria changii*, micro-array studies revealed that a vanadium dependent chloroperoxidase is up-regulated during light deprivation (Ho *et al.*, 2009). In the same species, a vanadium dependent bromoperoxidase is up-regulated during both hypo- and hyperosmotic stress (Teo *et al.*, 2009). VBPO activity has also been correlated to changes in temperature in Rhodophytes (Latham, 2008) and copper shock in the phaeophyte *Ectocarpus* (Ritter *et al.*, 2010). These findings support the role of VBPO in maintaining

physiological homeostasis, particularly in regards to oxidative stress. Weinberger *et al.* (2007), found that two species of *Gracilaria* have greater bromoperoxidase activity and release of halomethanes after cell-wall damage, supporting the role of this enzyme as part of an allelopathic defense strategy. These results agree with a study correlating the release of bromoform to the prevention of epiphytic diatoms on red algae (Ohsawa *et al.*, 2001). On the other hand, VBPO in *Corallina pilulifera* is expressed constitutively, though detectable activity was found to be seasonally regulated by the availability of vanadate (Itoh *et al.*, 1996).

The presence of VBPO in a prokaryote such as *Synechococcus* CC9311 provides a chance to use genetic manipulations not available in other organisms in order to directly identify consequences of the presence or absence of VBPO (Paul & Pohnert, 2011). The overarching goal of this dissertation is to explore the activity of VBPO in *Synechococcus* sp. CC9311 in the context of establishing a physiological and/or ecological role for this enzyme in this marine, photosynthetic prokaryote.

The first objective of this dissertation was to characterize the activity of VBPO in *Synechococcus* CC9311. The inception of this project was based on the presence of the predicted VBPO gene in the CC9311 genome and the ability of protein extracts from CC9311 to brominate monochlorodimedone in the presence of hydrogen peroxide, a common method used to detect VBPO activity. However, it was still vital to determine which protein(s) were responsible for this observed activity. For this, I used multiple assays on protein extracts of CC9311 aimed at determining halide specificity by adapting techniques for detecting VBPO activity in both spectrophotometric and polyacrylamide gel (PAGE) based assays. This allowed me to determine the halide specificity and

compare the specific activity of VBPO in CC9311 to those found in eukaryotic macroalgae. I further showed that the observed VBPO activity is the result of a single gene product in CC9311. The distribution of predicted VBPO genes in other cyanobacteria was explored by searching reference databases using the VBPO gene sequence in CC9311 (sync_2681). The presence of cyanobacterial-like VBPO genes in the environment was explored by using degenerate primer PCR probes on DNA extracted from marine water samples.

The second major goal of this dissertation was to put the activity of VBPO into a physiological and ecological context for *Synechococcus*, primarily through characterizing the regulation of VBPO activity in cultures of CC9311. The two main hypotheses for the function of VBPO in eukaryotic macroalgae are its role as an antioxidant through the use of hydrogen peroxide as a substrate versus its role as a defensive enzyme through the production of halogenated organic molecules. Both of these roles may help elucidate the functionality of VBPO in the cyanobacteria, though this has never been investigated.

To address the role of VBPO in *Synechococcus* CC9311, I used a previously established genetic manipulation system to inactivate the gene (sync_2681) encoding VBPO in *Synechococcus*. After identifying the expression patterns of VBPO in CC9311, a quantitative proteomic approach was used to determine major differences in protein expression patterns between cultures of CC9311 with and without VBPO. The mutant was also used in combination with quantitative proteomics to identify proteins or physiological systems that are affected by the presence or, rather absence, of VBPO.

The third major goal for this dissertation was to identify and quantify the production of halogenated metabolites in *Synechococcus* resulting from VBPO with a

specific focus on the production of halomethanes. A wide variety of brominated metabolites have been isolated from the marine environment, having broad implications for ecological interactions (Gribble, 2003; Paul and Pohnert, 2011). While VBPO has been both suggested and shown to be involved in the production of a wide range of brominated organic molecules (Flodin & Whitfield, 1999, Ohsawa et al., 2001, Arnoldsson *et al.*, 2012), this chapter focuses on the production of halogenated methanes, as VBPO is implicated in the production of the polyhalomethanes bromoform and dibromomethane (Biessner, 1981). Halomethane production in *Synechococcus* was determined by measuring a suite of halogenated methanes in the air above cultures (headspace) as well as well in air passed through cultures to “purge” dissolved portions of these volatile gases.

References

- Arnoldsson, K., Andersson, P. L. & Haglund, P. 2012. Formation of environmentally relevant brominated dioxins from 2,4,6,-tribromophenol via bromoperoxidase-catalyzed dimerization. *Environmental Science & Technology* **46**:7239-44.
- Avrani, S., Wurtzel, O., Sharon, I., Sorek, R. & Lindell, D. 2011. Genomic island variability facilitates *Prochlorococcus*-virus coexistence. *Nature* **474**:604-08.
- Beissner, R. S., Guilford, W. J., Coates, R. M. & Hager, L. P. 1981. Synthesis of brominated heptanones and bromoform by bromoperoxidase of marine origin. *Biochemistry* **20**:3724-31.
- Carter, J. N., Beatty, K. E., Simpson, M. T. & Butler, A. 2002. Reactivity of recombinant and mutant vanadium bromoperoxidase from the red alga *Corallina officinalis*. *Journal of Inorganic Biochemistry* **91**:59-69.
- Carter-Franklin, J. N. & Butler, A. 2004. Vanadium bromoperoxidase-catalyzed biosynthesis of halogenated marine natural products. *Journal of the American Chemical Society* **126**:15060-66.
- Channer, D. M. D., deRonde, C. E. J. & Spooner, E. T. C. 1997. The Cl--Br--I-composition of similar to 3.23 Ga modified seawater: implications for the geological evolution of ocean halide chemistry. *Earth and Planetary Science Letters* **150**:325-35.
- Coleman, M. L., Sullivan, M. B., Martiny, A. C., Steglich, C., Barry, K., DeLong, E. F. & Chisholm, S. W. 2006. Genomic islands and the ecology and evolution of *Prochlorococcus*. *Science* **311**:1768-70.
- Dufresne, A., Ostrowski, M., Scanlan, D., Garczarek, L., Mazard, S., Palenik, B., Paulsen, I., de Marsac, N., Wincker, P., Dossat, C., Ferriera, S., Johnson, J., Post, A., Hess, W. & Partensky, F. 2008a. Unraveling the genomic mosaic of a ubiquitous genus of marine cyanobacteria. *Genome Biology*. **9**(5):R90. DOI 10.1186/gb-2008-9-5-r90.
- Flodin, C. & Whitfield, F. B. 1999. 4-hydroxybenzoic acid: a likely precursor of 2,4,6-tribromophenol in *Ulva lactuca*. *Phytochemistry* **51**:249-55.
- Hess, W. R. 2011. Cyanobacterial genomics for ecology and biotechnology. *Current Opinion in Microbiology* **14**:608-14.
- Ho, C. L., Teoh, S., Teo, S. S., Rahim, R. A. & Phang, S. M. 2009. Profiling the transcriptome of *Gracilaria changii* (Rhodophyta) in response to light deprivation. *Marine Biotechnology* **11**:513-19.

- Itoh, N., Sasaki, H., Ohsawa, N., Shibata, M. S. & Miura, J. 1996. Bromoperoxidase in *Corallina pilulifera* is regulated by its vanadate content. *Phytochemistry* **42**:277-81.
- Jardillier, L., Zubkov, M. V., Pearman, J. & Scanlan, D. J. 2010. Significant CO₂ fixation by small prymnesiophytes in the subtropical and tropical northeast Atlantic Ocean. *Isme Journal* **4**:1180-92.
- Latham, H. 2008. Temperature stress-induced bleaching of the coralline alga *Corallina officinalis*: a role for the enzyme bromoperoxidase. *BioscienceHorizons*, pp. 104-13.
- Li, W. K. W. 1994. Primary production of Prochlorophytes, cyanobacteria, and eukaryotic ultraphytoplankton - measurements from flow cytometric sorting. *Limnology and Oceanography* **39**:169-75.
- Michibata, H., Uyama, T., Ueki, T. & Kanamori, K. 2002. Vanadocytes, cells hold the key to resolving the highly selective accumulation and reduction of vanadium in ascidians. *Microscopy Research and Technique* **56**:421-34.
- Moore, C. A. & Okuda, R. K. 1996. Bromoperoxidase activity in 94 species of marine algae. *Journal of Natural Toxins* **5**:295-305.
- Ohsawa, N., Ogata, Y., Okada, N. & Itoh, N. 2001. Physiological function of bromoperoxidase in the red marine alga, *Corallina pilulifera*: production of bromoform as an allelochemical and the simultaneous elimination of hydrogen peroxide. *Phytochemistry* **58**:683-92.
- Palenik, B., Ren, Q., Dupont, C., Myers, G., Heidelberg, J., Badger, J., Madupu, R., Nelson, W., Brinkac, L., Dodson, R., Durkin, A., Daugherty, S., Sullivan, S., Khouri, H., Mohamoud, Y., Halpin, R. & Paulsen, I. 2006. Genome sequence of *Synechococcus* CC9311: Insights into adaptation to a coastal environment. *Proceedings of the National Academy of Sciences of the United States of America* **103**:13555-59.
- Paul, C. & Pohnert, G. 2011. Production and role of volatile halogenated compounds from marine algae. *Natural Product Reports* **28**:186-95.
- Ritter, A., Ubertini, M., Romac, S., Gaillard, F., Delage, L., Mann, A., Cock, J. M., Tonon, T., Correa, J. A. & Potin, P. 2010. Copper stress proteomics highlights local adaptation of two strains of the model brown alga *Ectocarpus siliculosus*. *Proteomics* **10**:2074-88.

- Rusch, D. B., Halpern, A. L., Sutton, G., Heidelberg, K. B., Williamson, S., Yooseph, S., Wu, D. Y., Eisen, J. A., Hoffman, J. M., Remington, K., Beeson, K., Tran, B., Smith, H., Baden-Tillson, H., Stewart, C., Thorpe, J., Freeman, J., Andrews-Pfannkoch, C., Venter, J. E., Li, K., Kravitz, S., Heidelberg, J. F., Utterback, T., Rogers, Y. H., Falcon, L. I., Souza, V., Bonilla-Rosso, G., Eguiarte, L. E., Karl, D. M., Sathyendranath, S., Platt, T., Bermingham, E., Gallardo, V., Tamayo-Castillo, G., Ferrari, M. R., Strausberg, R. L., Nealson, K., Friedman, R., Frazier, M. & Venter, J. C. 2007. The Sorcerer II Global Ocean Sampling expedition: Northwest Atlantic through Eastern Tropical Pacific. *Plos Biology* **5**:398-431.
- Scanlan, D. J., Ostrowski, M., Mazard, S., Dufresne, A., Garczarek, L., Hess, W. R., Post, A. F., Hagemann, M., Paulsen, I. & Partensky, F. 2009. Ecological Genomics of Marine Picocyanobacteria. *Microbiology and Molecular Biology Reviews* **73**(2):249-99.
- Stuart, R. K., Dupont, C. L., Johnson, D. A., Paulsen, I. T. & Palenik, B. 2009. Coastal strains of marine *Synechococcus* species exhibit increased tolerance to copper shock and a distinctive transcriptional response relative to those of open-ocean strains. *Applied and Environmental Microbiology* **75**:5047-57.
- Stuart, R. K., Brahamsha, B., Busby, K., Palenik, B. 2013. Genomic island genes in a coastal marine *Synechococcus* strain confer enhanced tolerance to copper and oxidative stress. *The ISME Journal*. 1-11. DOI 10.1038/ismej.2012.175.
- Teo, S. S., Ho, C. L., Teoh, S., Rahim, R. A. & Phang, S. M. 2009. Transcriptomic analysis of *Gracilaria changii* (*Rhodophyta*) in response to hyper- and hypoosmotic stresses. *Journal of Phycology* **45**:1093-99.
- Wang, D. & Wilhelmly, S. A. S. 2009. Vanadium speciation and cycling in coastal waters. *Marine Chemistry* **117**:52-58.
- Weinberger, F., Coquempot, B., Forner, S., Morin, P., Kloareg, B. & Potin, P. 2007. Different regulation of haloperoxidation during agar oligosaccharide-activated defence mechanisms in two related red algae, *Gracilaria* sp and *Gracilaria chilensis*. *Journal of Experimental Botany* **58**:4365-72.

CHAPTER 2

J. Phycol. 47, 792–801 (2011)
© 2011 Phycological Society of America
DOI: 10.1111/j.1529-8817.2011.01007.x

CHARACTERIZATION OF A FUNCTIONAL VANADIUM-DEPENDENT BROMOPEROXIDASE IN THE MARINE CYANOBACTERIUM *SYNECHOCOCCUS* SP. CC9311¹

Todd L. Johnson, Brian Palenik, and Bianca Brahamsha²

Scripps Institution of Oceanography, University of California San Diego, 8750 Biological Grade, La Jolla, California 92093-0202, USA.

Vanadium-dependent bromoperoxidases (VBPOs) are characterized by the ability to oxidize halides using hydrogen peroxide. These enzymes are well-studied in eukaryotic macroalgae and are known to produce a variety of brominated secondary metabolites. Though genes have been annotated as VBPO in multiple prokaryotic genomes, they remain uncharacterized. The genome of the coastal marine cyanobacterium *Synechococcus* sp. CC9311 encodes a predicted VBPO (YP_731869.1, sync_2681), and in this study, we show that protein extracts from axenic cultures of *Synechococcus* possess bromoperoxidase activity, oxidizing bromide and iodide, but not chloride. In-gel activity assays of *Synechococcus* proteins separated using PAGE reveal a single band having VBPO activity. When sequenced via liquid chromatography/mass spectrometry/mass spectrometry (LC/MS/MS), peptides from the band aligned to the VBPO sequence predicted by the open reading frame (ORF) sync_2681. We show that a VBPO gene is present in a closely related strain, *Synechococcus* sp. WH8020, but not other clade I *Synechococcus* strains, consistent with recent horizontal transfer of the gene into *Synechococcus*. Diverse cyanobacterial-like VBPO genes were detected in a pelagic environment off the California coast using PCR. Investigation of functional VBPOs in unicellular cyanobacteria may lead to discovery of novel halogenated molecules and a better understanding of these organisms' chemical ecology and physiology.

Key index words: cyanobacteria; horizontal gene transfer; specific activity; *Synechococcus*; vanadium-dependent bromoperoxidase

Abbreviations: GOS database, Global Ocean Sampling database; HGT, horizontal gene transfer; MCD, monochlorodimedone; PhR, phenol red; ThB, thymol blue; VBPO, vanadium-dependent bromoperoxidase

Vanadium-dependent haloperoxidases are found in a wide range of organisms and are well-studied for their ability to oxidize halides (Winter and

Moore 2009). A subset of these halogenating enzymes, VBPOs, has been predominantly identified and characterized in eukaryotic macroalgae (Ohsawa et al. 2001, Carter et al. 2002, Kamenarska et al. 2007), though they have been suggested to be present in prokaryotes. The reaction mechanism of VBPO from the rhodophyte *Corallina officinalis* has been described by Carter et al. (2002). The enzyme first binds to a molecule of hydrogen peroxide. The peroxy-bound form of the enzyme carries out the two-electron oxidation of bromide, forming hypobromous acid. This reactive intermediate attaches bromine to organic molecules through an electrophilic reaction. The hypobromous acid intermediate is generally thought to be freely dispersing. However, strong evidence supports specificity toward a final organic substrate (Butler and Carter-Franklin 2004, Kamenarska et al. 2007, Hartung et al. 2009).

VBPOs have two proposed functions in vivo. Primarily, the enzyme is associated with the ability to synthesize a variety of brominated organic compounds, thought to serve as an allelopathic defense. In eukaryotic macroalgae, bromoform production prevents growth of epiphytic diatoms (Ohsawa et al. 2001), whereas brominated compounds in rhodophytes have antimicrobial and other bioactive properties (Butler and Carter-Franklin 2004). Though an active bromoperoxidase has not been characterized in a cyanobacterium, brominated compounds are produced by some groups. The first demonstration of halogenated molecules in cyanobacteria was the finding of brominated phenols in *Calothrix brevissima* (Pedersén and DaSilva 1973). Other studies have also shown that polybrominated diphenyl ethers are produced by *Oscillatoria*, a sponge endosymbiont (Unson et al. 1994, Agrawal and Bowden 2005). Monohalomethane and polyhalomethane production has been associated with the cyanobacterial fraction of a bloom in the Baltic Sea, in which *Pseudoanabaena* sp. was the dominant species along with other filamentous cyanobacteria (Karlsson et al. 2008). Halogenated compounds could serve as an allelopathic defense for marine *Synechococcus*, which is subject to high grazing pressure from eukaryotes and competition from heterotrophic bacteria (Caron et al. 1991, Strom 2002).

¹Received 1 September 2010. Accepted 14 January 2011.

²Author for correspondence: e-mail brahamsha@ucsd.edu.

CYANOBACTERIAL BROMOPEROXIDASE

VBPO also has a possible physiological role as an antioxidant. Hydrogen peroxide, a metabolic by-product of photosynthesis, is a damaging reactive oxygen species that is present in seawater up to nanomolar concentrations (Drabkova et al. 2007). VBPO reduces hydrogen peroxide to water with the oxidation of bromide. Manley and Barbero (2001) explored the role of VBPO in the remediation of photosynthetically produced H_2O_2 , finding a correlation between bromoperoxidase activity in the chlorophyte *Ulva lactuca* and light and dark cycles. Another study found that vanadium chloroperoxidase was down-regulated under light deprivation in the transcriptome of *Gracilaria algae* (Ho et al. 2009). VBPO could act as an antioxidant system for marine cyanobacteria, decreasing internally produced H_2O_2 ; however, VBPOs have been primarily found and studied in eukaryotic macroalgae.

Synechococcus is a genus of unicellular chroococoid cyanobacteria that contributes up to 20%–30% of photosynthetically fixed marine primary production (Li 1994, Jardillier et al. 2010). Due to the abundance and global distribution of *Synechococcus*, it is important to understand the ecology and physiology of these photoautotrophs. As a primary producer, *Synechococcus* is subject to high predation rates by heterotrophic plankton (Christaki et al. 2002, Chan et al. 2009). An increasing number of isolated *Synechococcus* strains from different clades (species) with available whole genome sequences provide an opportunity to investigate physiological differences at the clade and strain levels, as well as address questions such as the role of horizontally transferred genes. At least 10 distinct clades of *Synechococcus* have been observed (Dufresne et al. 2008), based on both internal transcribed spacer (ITS) and 16S rRNA sequences, demonstrative of the fine-scale diversity within this genus.

To date, the presence of VBPO in prokaryotic photoautotrophs has only been inferred from genome sequencing. A VBPO was recently annotated in the genome of *Synechococcus* sp. CC9311 (Palenik et al. 2006) and could have been acquired by horizontal gene transfer (HGT), supported by the fact that it is found in an island of genes unique to *Synechococcus* sp. CC9311 among sequenced *Synechococcus* genomes (Dufresne et al. 2008), with many of the island's genes showing atypical trinucleotide composition (Palenik et al. 2006). Putative bromoperoxidases are present in several other sequenced cyanobacterial genomes (Swingley et al. 2008; *Crocospaera watsonii* WH8501, GenBank AADV00000000.2, *Synechococcus* sp. PCC 7335, GenBank ABRV00000000). However, the distribution, activity, and function of this enzyme among cyanobacteria have remained undefined.

We report here on the first characterization of a functional bromoperoxidase in a cyanobacterium and investigate the distribution of bromoperoxidase

genes in strains of marine *Synechococcus* and in the pelagic marine environment.

MATERIALS AND METHODS

Strains and culture conditions. *Synechococcus* sp. used in this study include strains CC9311 (Palenik et al. 2006, CCMP2515), WH8102 (Waterbury et al. 1986, CCMP2370), WH8020 (Waterbury et al. 1986), CC9617 (Toledo et al. 1999), and WH8016 (Waterbury et al. 1986). All stock cultures were maintained in SN medium (Waterbury and Willey 1988) prepared using seawater from the Scripps Pier (La Jolla, CA; 32°52' N, 117°15.4' W). For assays, cultures were grown at constant light ($\sim 20 \mu E \cdot m^{-2} \cdot s^{-1}$) at 18°C with stirring. Cultures of *Synechococcus* sp. CC9311 and WH8102 were axenic, whereas *Synechococcus* sp. WH8020, CC9617, and WH8016 were not axenic.

Protein extractions. Proteins were collected from *Synechococcus* cultures in late exponential growth. Cell pellets from 1 L cultures were suspended in 3 mL 100 mM 2(N-morpholino) ethanesulfonic acid (MES) buffer, pH 7.0, and broken using a French pressure cell with three passes at 20,000 psi. Unbroken cells were removed by centrifugation (Sorvall RC28S, Thermo Fisher Scientific, Waltham, MA, USA) at 6,278g for 10 min at room temperature. The supernatant, consisting of soluble and membrane-bound fractions, was taken as crude protein extract. Subsequent centrifugation at 100,446g for 90 min (4°C) was performed to separate membrane from soluble proteins (Brahamsa 1996). The membrane fraction pellet was washed with 3 mL of 100 mM MES buffer, pH 7.0, and collected by centrifugation for 90 min at 100,446g. All proteins were handled on ice and stored at $-80^\circ C$ until use. Protein concentrations were determined using the Pierce BCA Protein Assay (Thermo Fisher Scientific, Rockford, IL, USA) with BSA standards.

Enzyme activity. Protein extracts from *Synechococcus* cultures were tested for bromoperoxidase activity using monochlorodimedone (MCD; Sigma Inc., St. Louis, MO, USA) and thymol blue (ThB; ACROS, Geel, Belgium), as described in Carter et al. (2002), Kamenarska et al. (2007), and Verhaeghe et al. (2008) with the following modifications. Crude protein extracts were incubated with sodium orthovanadate at a final concentration of 1.98 mM at room temperature for 20 min prior to the assay. For the MCD assay, crude, soluble, and membrane-bound protein extracts (0.05–0.1 mg $\cdot mL^{-1}$ final conc.) were added to 100 mM KBr in 100 mM MES buffer (pH 7.0) and 60 μM MCD. The reaction was started with the addition of hydrogen peroxide to a final concentration of 2 mM and monitored spectrophotometrically at 290 nm (MCD, $\epsilon = 19.9 \text{ mM}^{-1} \cdot \text{cm}^{-1}$). In the second bromoperoxidase assay, 10 μM ThB (final concentration) replaced MCD. The absorbance of the dihalogenated product was monitored at 620 nm (ThB1₂, $\epsilon = 40.3 \text{ mM}^{-1} \cdot \text{cm}^{-1}$; ThBBr₂, $\epsilon = 37.2 \text{ mM}^{-1} \cdot \text{cm}^{-1}$). Specific activities are reported as $\mu\text{mol substrate brominated} \cdot \text{min}^{-1} \cdot \text{mg protein}^{-1}$.

Halide specificity, kinetics. We tested halide specificity by substituting potassium bromide (1–100 mM) with either potassium iodide (0.5–50 mM) or potassium chloride (100 mM) in the reaction. We used MCD assays to compare bromide oxidation with chloride oxidation in crude extracts. We used ThB, however, to compare VBPO oxidation of bromide and iodide. We also measured the ability of VBPO in crude extracts to oxidize iodide by measuring the accumulation of triiodide at 350 nm in the presence of hydrogen peroxide and iodide as described by Kamenarska et al. (2007).

The reaction velocities for the enzyme were determined over the first minute at each concentration, then fitted to a Michaelis–Menten, nonlinear regression using GraphPad Prism software version 5.0b (GraphPad Software, San Diego, CA, USA).

TODD L. JOHNSON ET AL.

SDS-PAGE. To identify the proteins responsible for the observed activity, polyacrylamide gels were run under native and denaturing conditions, and then stained for bromoperoxidase activity. For native conditions, *Synechococcus* protein extracts were loaded on Novex Nupage 7% Tris-Acetate gels (Invitrogen, Carlsbad, CA, USA) and run with Tris-Glycine Native Running buffer consisting of 25 mM Tris-base and 192 mM glycine, pH 8.3 (Invitrogen) at 150 V for 2 h. For denaturing conditions, protein extracts were incubated at 70°C for 10 min in the presence of Novex Reducing Agent (Invitrogen) following the manufacturer's recommendations and run with Tris-Acetate SDS Running Buffer (Invitrogen) at 150 V for 1 h.

Duplicate gels were run simultaneously and stained for total protein using Sypro Ruby (Invitrogen) according to the manufacturer's directions. A stain for bromoperoxidase activity was used as described in Suthiphongchai et al. (2008) with the following modifications. Gels run under denaturing conditions were soaked in the Tris-glycine buffer lacking SDS for 1 h, then placed in a PhR stain containing 100 mM MES (pH 7.0), 40 mM H₂O₂, 200 μM Na₂VO₄, 100 mM potassium bromide, and 2 mM PhR.

For protein sequencing, the gel was stained with Coomassie Brilliant Blue as recommended by the NuPAGE Technical Guide (Invitrogen), and the protein band corresponding to the active band observed with PhR on a duplicate gel was excised in 1 mm × 1 mm cubes, placed in MilliQ (Milli-Q Plus Ultrapur Water Purification System, Millipore, Billerica, MA, USA) water, and kept at 4°C until sequencing. Peptide sequencing was performed using LC/MS/MS as described in (McCormack et al. 1997) at the University of California San Diego (UCSD) Biomolecular/Proteomics Mass Spectrometry Facility.

Phylogeny. *Synechococcus* sp. CC9311 VBPO (YP_731869.1) was compared with the National Center for Biotechnology Information's (NCBI; Bethesda, MD, USA) nr protein database using blastp (Altschul et al. 1997). Amino acid sequences from the results with highest similarity were aligned in ClustalX (Chenna et al. 2003) and trimmed in SE-AL v.2.0 (Rambaut 1996) to a 183-amino-acid region (see Fig. S1 in the supplementary material) that includes active site residues known to be conserved between VBPO sequences (Winter and Moore 2009). A neighbor-joining analysis was performed (Fig. 3) from 100 bootstrap replicates using PHYLIP (Felsenstein 1989), and the resulting tree was viewed in Figtree (Rambaut 2008).

VBPO in *Synechococcus*. We tested closely related (clade I) strains of *Synechococcus* (sp. CC9617, WH8020, WH8016) for the presence of a bromoperoxidase gene. Degenerate PCR primers (Table 1; VDEGF, VDEGR) were designed based on residues conserved between cyanobacteria and rhodophyte VBPOs (see Fig. S1), to yield a 262 bp product for sync_2681 (CC9311 VBPO). Amplified products were cloned into the pcr4-TOPO vector (Invitrogen) as recommended by the manufacturer. Plasmids were isolated using a plasmid mini prep kit (Qiagen, Valencia, CA, USA) and sequenced using the T7 universal primer. For *Synechococcus* sp. WH8020, new primers (Table 1; VWholeF, VWholeR) were designed based on the 5' and 3' ends of sync_2681 in CC9311 to amplify the whole gene (1.8 kb), and the PCR product was sequenced. The active site and vanadium-coordinating residues, conserved between vanadium bromo-peroxidases and chloro-peroxidases, are annotated based on homology to those described in *Curvularia inaequalis* (Raugei and Carloni 2006) and *Ascophyllum nodosum* (Weyand et al. 1999).

Cyanobacterial VBPO in the environment. To test whether cyanobacterial-like VBPO genes were present in the coastal pelagic environment, samples were taken from the pier at Scripps Institution of Oceanography (La Jolla, CA, USA) on seven dates through 2006 (February, April, May, August,

TABLE 1. Primer sequences used in this study. Degenerate primer code is as follows: S, G or C; R, A or G; Y, C or T; N, any base.

Primer name	Sequence
VDEGF	5'-GCR TGN CCN GCN CCR TAN GMN GG -3'
VDEGR	5'-AAR GCN GTN CGN TAY CAR AAR TT -3'
VWholeF	5'-ATG ACA GAT CAA CGC AAA CTC AC-3'
VWholeR	5'-CTA TCG GTG ACC GAT GCG ACG-3'
PierF	5'-AAG GCS GTG CGY TAY CAR AAG TTC AA-3'
PierR	5'-GCN AGY TTR TTN AGY TGN CCY TC-3'

October) and 2007 (April, May). Half-liter water samples were filtered on a 0.2 μm Supor filter disk (Pall Life Sciences, Ann Arbor, MI, USA), and the DNA was extracted (Palenik et al. 2009, Tai 2009). Degenerate PCR primers were designed for a conserved region of cyanobacterial VBPO (Table 1; PierF, PierR). Touch-down PCR was the most successful method of amplification. Starting at 63°C, the annealing temperature was decreased by 1°C every cycle for 13 cycles, and then kept at 54°C for 27 cycles. A clone library was constructed from PCR products using pcr-4 Topo vector (Invitrogen). Multiple clones were sequenced from successful PCR amplifications.

Two environmental metagenomic databases were also accessed for this study. Sequences were retrieved using blastp with VBPO from *Synechococcus* sp. CC9311 against the GOS database (Seshadri et al. 2007). *Synechococcus* VBPO from CC9311 was also used to look for sequences in *Synechococcus* metagenomes from water taken at the Scripps Pier in La Jolla, California (B. Palenik and I. T. Paulsen, unpublished). Nucleotide sequences from pier samples were aligned in ClustalX and trimmed to an overlapping region (see Fig. S2 in the supplementary material). A neighbor-joining analysis was used to construct a phylogenetic tree in PHYLIP with 100 bootstrap replicates. *Acaryochloris marina* VBPO (YP_001515553) was used as an outgroup.

RESULTS

Activity assays. Haloperoxidase activity was detected in *Synechococcus* sp. CC9311 crude, soluble, and membrane protein extracts using multiple assays. Specific haloperoxidase activities of *Synechococcus* proteins used with the MCD, ThB, and triiodide assays are shown in Table 2. When *Synechococcus* sp. CC9311 crude extracts were used with MCD, the V_{max} for bromide oxidation was $0.400 \pm 0.046 \mu\text{mol} \cdot \text{min}^{-1} \cdot \text{mg}^{-1}$. No detectable activity was observed in crude protein extracts using chloride as the halide for the MCD assay. Crude protein extracts from *Synechococcus* sp. WH8020, a strain closely related to *Synechococcus* sp. CC9311, had lower activity levels than those of *Synechococcus* sp. CC9311. No detectable activity was seen in crude, soluble, or membrane protein extracts from *Synechococcus* sp. WH8102 using bromide as the halide in the MCD or ThB assay. Furthermore, when the MCD assay is used with crude protein from *Synechococcus* sp. CC9311, <0.01% VBPO specific activity is observed when no vanadium incubation step is included (Table 2).

We used the ThB assay to compare Br⁻ and I⁻ as VBPO substrates in crude protein extracts. When a

CYANOBACTERIAL BROMOPEROXIDASE

TABLE 2. Vanadium-dependent bromoperoxidase specific activity found in *Synechococcus*.

Organism	Halide*	Specific activity ($\mu\text{mol} \cdot \text{min}^{-1} \cdot \text{mg}^{-1}$)	Assay
<i>Synechococcus</i> sp. CC9311	I [0.1 mM]	0.910 ± 0.110^a	I_3^-
	Br	0.019 ± 0.001^a	ThB
	Br	0.400 ± 0.046^a	MCD
	Br	0.165 ± 0.003^a	ThB
	Br	0.560 ± 0.085^b	MCD
	Br	1.01^c	MCD
	Br	0.002 ± 0.0003^d	MCD
<i>Synechococcus</i> sp. WH8020	Cl	ND ^a	MCD
	Cl	ND ^a	ThB
<i>Synechococcus</i> sp. WH8102	Br	0.074 ± 0.013^a	MCD
	Br	ND ^a	MCD

^aCrude protein extracts used in assay.

^bSoluble protein fraction from *Synechococcus* sp. CC9311.

^cMembrane-protein fraction from *Synechococcus* sp. CC9311, $n = 1$.

^dCrude protein extracts not preincubated with sodium orthovanadate.

^e100 mM halide used unless otherwise indicated.

ND, not detected; MCD, monochlorodimedone; ThB, thymol blue.

Michaelis–Menten nonlinear regression was fit to the ThB assay results, VBPO in *Synechococcus* sp. CC9311 has a greater V_{max} with bromide ($0.165 \pm 0.005 \mu\text{mol} \cdot \text{min}^{-1} \cdot \text{mg}^{-1}$) than with iodide ($0.019 \pm 0.001 \mu\text{mol} \cdot \text{min}^{-1} \cdot \text{mg}^{-1}$). The half-saturation constant, K_m , was also larger for bromide ($1.525 \pm 0.184 \text{ mM}$) than iodide ($0.0237 \pm 0.003 \text{ mM}$). No activity was detected when chloride was used as the halide in the ThB assay.

The membrane protein fraction had 1.8 times greater specific activity than the soluble protein fraction ($0.56 \pm 0.085 \mu\text{mol} \cdot \text{min}^{-1} \cdot \text{mg}^{-1}$ and $1.01 \mu\text{mol} \cdot \text{min}^{-1} \cdot \text{mg}^{-1}$, respectively) using the MCD assay.

SDS-PAGE and in-gel staining. In-gel staining for bromoperoxidase activity using PhR showed a single band of 220,000 Da in crude protein extracts (Fig. 1) as well as in soluble and membrane proteins extracted from *Synechococcus* sp. CC9311. The development of the band was dependent on the presence of both bromide and hydrogen peroxide (data not shown). Active bands appeared more slowly in the absence of vanadium, usually developing over 10 min without vanadium, while developing sooner when vanadium is present. No bands developed in lanes containing proteins from *Synechococcus* sp. WH8102.

The active band from the membrane fraction (see Materials and Methods) of *Synechococcus* sp. CC9311 was excised and sequenced using LC/MS/MS. A single protein was shown to be dominant, having 80% amino acid coverage from 51 peptides of the annotated VBPO (sync_2681). Though no other proteins were present in significant quantity or coverage, a ferritin (sync_1539) was present with three peptides providing 26% coverage of the gene.

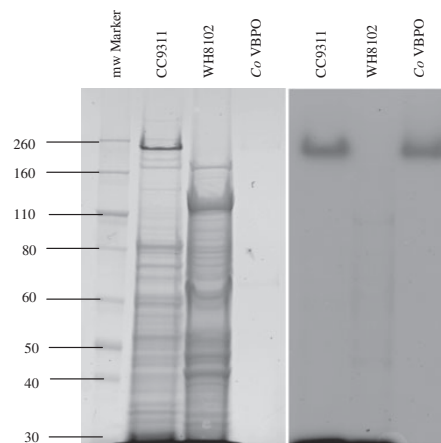


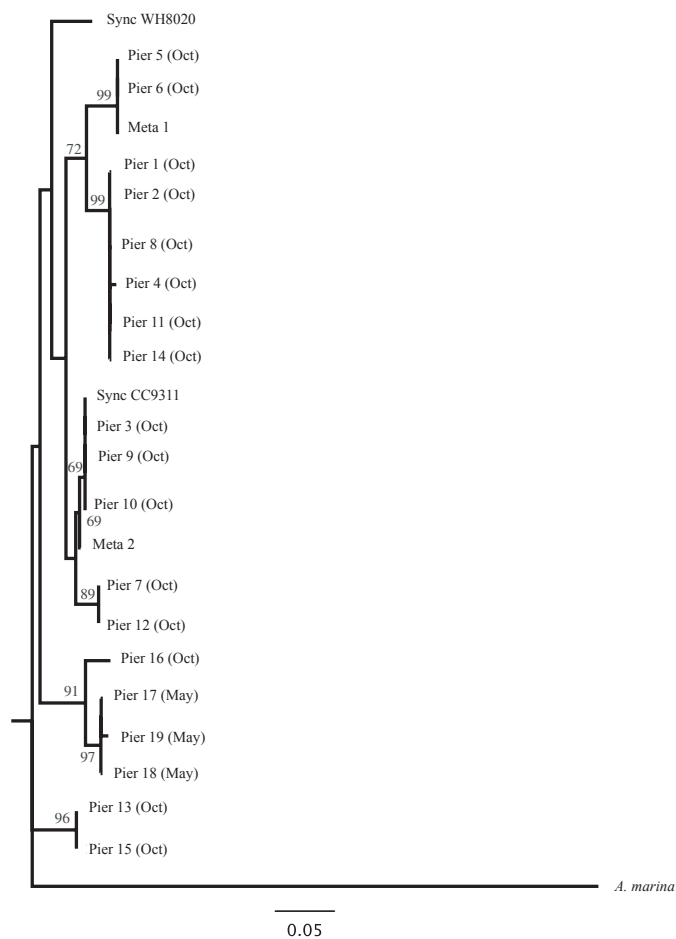
FIG. 1. SDS-PAGE gels of crude protein extracts from *Synechococcus* strains WH8102, CC9311, and vanadium-dependent bromoperoxidase (VBPO) from *Corallina officinalis* (Co VBPO, Sigma) stained with Sypro Ruby (left) and with phenol red (right) for bromoperoxidase activity. The migrations of molecular mass standards are indicated on the left in kDa.

VBPO in *Synechococcus*. Clade I *Synechococcus* strains for which genome data are not available (WH8020, CC9617, WH8016) were screened for VBPO genes using degenerate primers designed to amplify a short region of the bromoperoxidase gene. PCR amplification was only seen in CC9311 and WH8020. Subsequent sequencing of the entire VBPO gene found in *Synechococcus* sp. WH8020 revealed 92.88% nucleotide identity and 95% amino acid identity with *Synechococcus* sp. CC9311, with no gaps (Fig. 2). These results correlate with *Synechococcus* sp. CC9311 whole-genome microarray studies using DNA–DNA hybridizations with these clade I strains, which showed a lack of VBPO gene hybridization in CC9617 and WH8016 (B. Palenik and I. T. Paulsen, unpublished).

Phylogeny. A phylogenetic analysis of vanadium bromoperoxidases and related haloperoxidases is shown in Figure 3. *Synechococcus* sp. CC9311 VBPO has the greatest amino acid identity to the two VBPO genes found in *Acaryochloris marina* MC11017 (53%, 35%), as well as the VBPO gene found in *Synechococcus* PCC7335 (46%). With respect to eukaryotic macroalgae, VBPO in *Synechococcus* sp. CC9311 has a greater similarity to rhodophyte bromoperoxidase (34% amino acid identity to *C. officinalis* 1 and 2) than to phaeophyte bromo- and iodo-peroxidases (18% identity to *L. digitata* B1 and B2; *L. digitata* I1 and I3). There are several cyanobacterial sequences annotated as type 2 phosphatidic acid phosphatases (PAP2)/haloperoxidases for which no enzyme

CYANOBACTERIAL BROMOPEROXIDASE

FIG. 4. Neighbor-joining tree of environmental vanadium-dependent bromoperoxidase sequences. Nucleotide sequences were trimmed to a conserved region of ~180 bp (alignment shown in Figure S2 (see the supplementary material). "Pier #" samples were obtained from a degenerate primer (PierF and PierR) clone library from the Scripps Pier in La Jolla, California. Samples labeled "Meta" were obtained from *Synechococcus*-specific metagenomes. Bootstrap values >50 shown as significant, from 100 replicates.



degenerate PCR primers were applied to environmental DNA samples from surface samples taken off the Scripps Pier (La Jolla, CA, USA), designed to amplify a conserved region of the VBPO gene, including the active site. Amplification was successful for the February, May, and October 2006 samples. Clones were obtained and sequenced from May (three total) and October of 2006 (16 total) and are shown in our analysis. When compared with known VBPO sequences, the clone sequences are closely related to *Synechococcus* sp. CC9311 VBPO (Fig. 4), with >87% nucleotide identified among all clones. Multiple clusters of sequences were observed from our clone library and local metagenomic data, with one cluster of sequences very closely related to

VBPO from *Synechococcus* sp. CC9311 (98%–99.8% nucleotide identities to *Synechococcus* sp. CC9311 for Pier 3, 9, and 10 clones).

When a blastp search of the VBPO amino acid sequence from *Synechococcus* sp. CC9311 was performed against the GOS All Metagenomic ORFs (P) database (<http://camera.calit2.net/>) with a cutoff of E-06, 24 peptides were obtained representing 10 scaffolds. The scaffold sequences are from coastal, hypersaline lagoon, and mangrove sites. The top hit, JCVI_PEP_1105086041153 from GS033-Punta Cormorant, Floreana Island (Hypersaline Lagoon), Ecuador, is 55% identical to *Synechococcus* sp. CC9311 VBPO over a 300-amino-acid region. As this sequence and few of the scaffolds overlapped the

VBPO region obtained from PCR from the Scripps Pier, we did not include them in Figure 4. However, nine scaffolds appear to be from cyanobacteria, although none are demonstrably from clade I *Synechococcus*.

DISCUSSION

This is the first study to establish the presence of a functional VBPO in *Synechococcus*. Presence of this gene is not a genus-wide characteristic, as it is only found in some strains of clade I *Synechococcus* sp. (CC9311 and WH8020), but not found in other clade I strains tested (CC9617, WH8016), nor in representatives of other marine *Synechococcus* clades for which genome sequences are available, such as WH8102 (clade III), CC9902 (clade IV), or CC9605 (clade II). Homologous sequences are present in the genomes of *Acaryochloris marina*, *Synechococcus* sp. PCC7335, and *Crocospaera watsonii*, suggesting the presence of functional bromoperoxidases in other marine or estuarine cyanobacteria.

Determining the distribution of VBPO among related organisms is important in exploring the link between red algal and cyanobacterial bromoperoxidases. In doing so, an important consideration is that VBPO (sync_2681) in *Synechococcus* sp. CC9311 appears to be in a cluster of horizontally transferred genes, encompassing a region of ~ 29 kbp. These 32 genes, including a putative mechanosensitive ion channel (sync_2685), amidotransferase (sync_2679), diguanylate cyclase (sync_2671), as well as hypothetical proteins, all lack homologues in 11 other marine *Synechococcus* with whole genomes sequenced (Dufresne et al. 2008). Furthermore, along with neighboring genes, VBPO is not represented in a coastal *Synechococcus* environmental metagenome, suggestive of a gene recently acquired by *Synechococcus* sp. CC9311 and closely related strains (Palenik et al. 2009). *A. marina* has one of the largest prokaryotic genomes, which includes two bromoperoxidase sequences that are the most similar known amino acid sequences to VBPO in *Synechococcus* sp. CC9311 (Swingley et al. 2008). *A. marina* is also a common epiphyte of red algae (Murakami et al. 2004) that have bromo-peroxidases and chloroperoxidases and produce a variety of halogenated metabolites. One possibility is that the bromoperoxidase gene was transferred from a red alga to an epiphytic cyanobacterium and subsequently spread to other photoautotrophic prokaryotes. This concept may be supported by the lack of ubiquity of the gene among *Synechococcus* strains. Alternately, the gene could have been acquired by a eukaryotic alga from an epiphytic prokaryote. However, more genomes and homologous gene sequences are necessary to support either lineage.

One example of a gene of eukaryotic origin acquired by cyanobacteria is the class I algal fructose biphosphate aldolase (FBA) gene. This eukaryotic

version of the FBA gene was recently found in several *Synechococcus* strains, including *Synechococcus* sp. CC9311 and CC9902 as well as multiple *Prochlorococcus* strains (Rogers et al. 2007). Cyanobacterial class I FBA genes cluster with the rhodophyte homologues of this plastid-targeted, metabolically important enzyme. Though the origin of VBPO in *Synechococcus* is not clear at this time, a similar evolutionary relationship may exist to rhodophyte VBPO homologues.

Enzyme activity. VBPO in *Synechococcus* sp. CC9311 is capable of oxidizing bromide and iodide but is not able to measurably oxidize chloride. Specific VBPO activities measured in this study are similar to previously reported VBPO activities ($U = \mu\text{mol MCD brominated} \cdot \text{min}^{-1}$) measured in crude protein extracts from eukaryotic macroalgae, which include $3.2 U \cdot \text{mg}^{-1}$ (Krenn et al. 1989) in *A. nodosum*, $0.14 U \cdot \text{mg}^{-1}$ in the rhodophyte *Kappaphycus alvarezii* (Kamenarska et al. 2007), and $1.6 U \cdot \text{mg}^{-1}$ in crude extracts from *Gracilaria* sp. (Suthiphongchai et al. 2008). VBPO from *Synechococcus* sp. CC9311 had a stronger affinity (lower K_m) toward iodide than bromide, though on the same order of magnitude as results found in *K. alvarezii* (Kamenarska et al. 2007). Also, a greater specific activity was observed when triiodide accumulation was used to measure VBPO activity compared with using the thymol assay, which is a more direct comparison to the ability of VBPO to oxidize bromide.

Protein extracts from *Synechococcus* sp. WH8020 have similar specific activity toward bromide as *Synechococcus* sp. CC9311. However, *Synechococcus* sp. WH8102, which lacks a predicted bromoperoxidase gene in its genome, has no detectable bromoperoxidase activity when using MCD, ThB, or PhR as the organic substrate.

VBPO is active in both soluble and membrane-protein fractions in *Synechococcus* sp. CC9311. The soluble fraction maintains about half the specific activity of the membrane fraction, suggesting that this may primarily be a membrane-associated protein. Alternately, if the active enzyme is multimeric, this increase in mass may cause the protein to partially pellet during the ultracentrifugation, membrane protein isolation step used in this study. Bromoperoxidases have been shown to be outer-membrane bound as well as plastid-targeted enzymes in eukaryotic algae (Manley 2002).

SDS-PAGE analysis. The protein band that displayed VBPO activity ran at 220 kDa under both native and denaturing conditions, despite a predicted mass of 68 kDa for the product of sync_2681. The active band ran at the same mass as the bromoperoxidase from *C. officinalis*, which has a predicted MW of 64 kDa and is a homododecamer in situ (Coupe et al. 2007). VBPO is also known to form homodimers in brown algae (Weyand et al. 1999). An inactive band appeared ~ 64 kDa under denaturing conditions in the *C. officinalis* VBPO

CYANOBACTERIAL BROMOPEROXIDASE

control. Bromoperoxidases are known to have high thermostability, only showing a gradual loss in activity at 80°C in *A. nodosum* (Krenn et al. 1989) and thus may not have been denatured after heating at 70°C for 10 min.

By sequencing the active band from SDS-PAGE gels stained with PhR, we have demonstrated that the only protein responsible is the single gene product of the annotated bromoperoxidase.

It will be important to determine if an organic molecule(s) is being halogenated in vivo before inferring a physiological function for VBPO in *Synechococcus* sp. CC9311. VBPO does not appear to be in a putative biosynthetic operon in *Synechococcus* sp. CC9311, as is the case for the vanadium-dependent haloperoxidase gene in two strains of *Streptomyces* (Winter et al. 2007), in which a vanadium chloroperoxidase is active as part of the biosynthetic pathway for napyridiomycin. This possibility does not preclude the interaction of VBPO with other gene products of *Synechococcus* sp. CC9311 but does not suggest an obvious organic substrate that is being brominated by the enzyme. Alternatively, the molecule may not originate from *Synechococcus* itself. For example, in pelagic ecosystems, dissolved organic carbon (DOC) has been implicated in providing the organic material that is brominated and found in diatoms (Hill and Manley 2006). An extracellular source, such as DOC, may be the substrate for pelagic *Synechococcus* VBPO.

The production of brominated organic compounds has been demonstrated in numerous microalgae including cyanobacteria. Symbiotic *Oscillatoria* sp. produce polybrominated diphenyl ethers (Unson et al. 1994, Agrawal and Bowden 2005). Other filamentous cyanobacteria, such as *Lynbya*, are renowned for the production of halogenated natural products (Nogle and Gerwick 2003, Edwards et al. 2004). Interestingly, volatile halogenated organic compounds (VHOCs) have been associated with a mixed-cyanobacterial bloom in the Baltic sea (Karlsson et al. 2008), but no enzyme was tested as the source. VHOCs, particularly methyl halides, have also been suggested as by-products of the bromoperoxidase reaction in eukaryotic algae. Moore et al. (1996) demonstrated that multiple diatom cultures produce bromo- and iodo-methane while simultaneously finding haloperoxidase activity in these cultures. Brownell et al. (2010) reported that despite finding methyl halide production in cultures of both *Synechococcus* and *Prochlorococcus*, extrapolated production rates did not appear to contribute significantly to oceanic production rates of these molecules and conflicted with previously reported values. As the presence of VBPO in *Synechococcus* is strain specific, more work is needed to correlate methyl halide production to VBPO activity in cyanobacteria, particularly *Synechococcus*. Halomethane production has also been observed in several macroalgae. Further work should focus on deter-

mining the brominated organic products of VBPO in *Synechococcus*. Such information could lead to novel compounds or insights into substrate specificity.

Alternatively, the *Synechococcus* VBPO could contribute to the detoxification of photosynthetically produced hydrogen peroxide in vivo, as evidence has previously supported this role in eukaryotic macroalgae (Manley and Barbero 2001, and Ho et al. 2009). Future physiological studies will address this possibility as well. A better understanding of the function of VBPO may provide insights into ecological adaptations of *Synechococcus* as well as the roles of this enzyme in other organisms.

Bromoperoxidase in the environment. We found that *Synechococcus*-like bromoperoxidase genes are present and diverse in the coastal environment. After combining sequences from our clone library with those obtained from coastal *Synechococcus* metagenomes (Palenik et al. 2009, B. Palenik and I. Paulsen, unpublished), several clusters of sequences become apparent. However, all sequences were >87% identical. Metagenome sequences with 80% or higher sequence identity tile reliably to reference genomes (Tai 2009), suggesting that VBPO sequences with >87% identity are from clade I *Synechococcus* strains. However, we cannot rule out the possibility of recent HGT to other microbes. There was no correlation between the sampling date and the clustering of a sequence, suggesting that the VBPO genes detected in this study are in organisms that are found in May and October. Interestingly, VBPO was not detected on other sampling dates (April, August). All but one sequence from our library had conserved active site residues as predicted in previous literature (Carter et al. 2002), suggesting that these cyanobacterial-like VBPOs are functional in the pelagic environment.

Concluding remarks. This study brings light to the diversity of bromoperoxidase genes in free-living, unicellular cyanobacteria. We have demonstrated that *Synechococcus* sp. CC9311 encodes an active bromoperoxidase, the product of sync_2681. We have further observed an active bromoperoxidase gene in another clade I strain of *Synechococcus* as well as genetically related bromoperoxidase genes in coastal ocean samples.

We thank Mike Smanski for initial experiments demonstrating VBPO activity in *Synechococcus* sp. CC9311. We also thank Vera Tai for providing environmental DNA samples. Protein sequencing was done by the Biomolecular Proteomics Mass Spectrometry Facility at UCSD. This work was funded by NSF grant OCE-0648175 to B. P. and B. B.

Agrawal, M. S. & Bowden, B. F. 2005. Marine sponge *Dysidea herbacea* revisited: another brominated diphenyl ether. *Mar. Drugs* 3:9–14.

Altschul, S. F., Madden, T. L., Schaffer, A. A., Zhang, J., Zhang, Z., Miller, W. & Lipman, D. J. 1997. Gapped BLAST and PSI-BLAST: a new generation of protein database search programs. *Nucleic Acids Res.* 25:3389–402.

- Brahmsha, B. 1996. An abundant cell-surface polypeptide is required for swimming by the nonflagellated marine cyanobacterium *Synechococcus*. *Proc. Natl. Acad. Sci. U. S. A.* 93:6504–9.
- Brownell, D. K., Moore, R. M. & Cullen, J. J. 2010. Production of methyl halides by *Prochlorococcus* and *Synechococcus*. *Glob. Biogeochem. Cycles* 24:GB2002.
- Butler, A. & Carter-Franklin, J. N. 2004. The role of vanadium bromoperoxidase in the biosynthesis of halogenated marine natural products. *Nat. Prod. Rep.* 21:180–8.
- Caron, D. A., Lim, E. L., Miceli, G., Waterbury, J. B. & Valois, F. W. 1991. Grazing and utilization of chroococcoid cyanobacteria and heterotrophic bacteria by protozoa in laboratory cultures and a coastal plankton community. *Mar. Ecol. Prog. Ser.* 76: 205–17.
- Carter, J. N., Beatty, K. E., Simpson, M. T. & Butler, A. 2002. Reactivity of recombinant and mutant vanadium bromoperoxidase from the red alga *Corallina officinalis*. *J. Inorg. Biochem.* 91:59–69.
- Chan, Y. F., Tsai, A. Y., Chiang, K. P. & Hsieh, C. H. 2009. Pigmented nanoflagellates grazing on *Synechococcus*: seasonal variations and effect of flagellate size in the coastal ecosystem of subtropical Western Pacific. *Microb. Ecol.* 58:548–57.
- Chenna, R., Sugawara, H., Koike, T., Lopez, R., Gibson, T. J., Higgins, D. G. & Thompson, J. D. 2003. Multiple sequence alignment with the Clustal series of programs. *Nucleic Acids Res.* 31:3497–500.
- Christaki, U., Courties, C., Karayanni, H., Giannakourou, A., Maravelias, C., Komas, K. A. & Lebaron, P. 2002. Dynamic characteristics of *Prochlorococcus* and *Synechococcus* consumption by bacterivorous nanoflagellates. *Microb. Ecol.* 43:341–52.
- Coupe, E. E., Smyth, M. G., Fosberry, A., Hall, R. M. & Littlechild, J. A. 2007. The dodecameric vanadium-dependent haloperoxidase from the marine alga *Corallina officinalis*: cloning, expression, and refolding of the recombinant enzyme. *Protein Expr. Purif.* 52:265–72.
- Drabkova, M., Matthijs, H. C. P., Admiraal, W. & Marsalek, B. 2007. Selective effects of H₂O₂ on cyanobacterial photosynthesis. *Photosynthetica* 45:363–9.
- Dufresne, A., Ostrowski, M., Scanlan, D., Garczarek, L., Mazard, S., Palenik, B., Paulsen, I., et al. 2008. Unraveling the genomic mosaic of a ubiquitous genus of marine cyanobacteria. *Genome Biol.* 9:R90.
- Edwards, D. J., Marquez, B. L., Nogle, L. M., McPhail, K., Goeger, D. E., Roberts, M. A. & Gerwick, W. H. 2004. Structure and biosynthesis of the jamaicamides, new mixed polyketide-peptide neurotoxins from the marine cyanobacterium *Lynghya majuscula*. *Chem. Biol.* 11:817–33.
- Felsenstein, J. 1989. PHYLIP – Phylogeny Inference Package (Version 3.2). *Cladistics* 5:164–6.
- Hartung, J., Dumont, Y., Greb, M., Hach, D., Kohler, F., Schulz, H., Casny, M., Rehder, D. & Vilter, H. 2009. On the reactivity of bromoperoxidase I (*Ascophyllum nodosum*) in buffered organic media: formation of carbon bromine bonds. *Pure Appl. Chem.* 81:251–64.
- Hill, V. L. & Manley, S. L. 2006. Does an extracellular bromoperoxidase of marine diatoms halogenate doc? *J. Phycol.* 42(Suppl.):46.
- Ho, C. L., Teoh, S., Teo, S. S., Rahim, R. A. & Phang, S. M. 2009. Profiling the transcriptome of *Gracilaria changii* (Rhodophyta) in response to light deprivation. *Mar. Biotechnol.* 11:513–9.
- Jardillier, L., Zubkov, M. V., Pearman, J. & Scanlan, D. J. 2010. Significant CO₂ fixation by small prymnesiophytes in the subtropical and tropical northeast Atlantic Ocean. *ISME J.* 4:1180–92.
- Kamenarska, Z., Taniguchi, T., Ohsawa, N., Hiraoka, M. & Itoh, N. 2007. A vanadium-dependent bromoperoxidase in the marine red alga *Kappaphycus alvarezii* (Doty) Doty displays clear substrate specificity. *Phytochemistry* 68:1358–66.
- Karlsson, A., Auer, N., Schulz-Bull, D. & Abrahamsson, K. 2008. Cyanobacterial blooms in the Baltic – a source of halocarbons. *Mar. Chem.* 110:129–39.
- Krenn, B., Izumi, Y., Yamada, H. & Wever, R. 1989. A comparison of different (vanadium) bromoperoxidases – the bromoperoxidase from *Corallina pilulifera* is also a vanadium enzyme. *Biochim. Biophys. Acta* 998:63–8.
- Li, W. K. W. 1994. Primary production of prochlorophytes, cyanobacteria, and eukaryotic ultraphytoplankton – measurements from flow cytometric sorting. *Limnol. Oceanogr.* 39:169–75.
- Manley, S. L. 2002. Phylogenesis of halomethanes: a product of selection or a metabolic accident? *Biogeochemistry* 60:163–80.
- Manley, S. L. & Barbero, P. E. 2001. Physiological constraints on bromoform (CHBr₃) production by *Ulva lactuca* (Chlorophyta). *Limnol. Oceanogr.* 46:1392–9.
- McCormack, A. L., Schieltz, D. M., Goode, B., Yang, S., Barnes, G., Drubin, D. & Yates, J. R. 1997. Direct analysis and identification of proteins in mixtures by LC/MS/MS and database searching at the low-femtomole level. *Anal. Chem.* 69:767–76.
- Moore, R. M., Webb, M., Tokarczyk, R. & Wever, R. 1996. Bromoperoxidase and iodoperoxidase enzymes and production of halogenated methanes in marine diatom cultures. *J. Geophys. Res.* 101:899–908.
- Murakami, A., Miyashita, H., Iseki, M., Adachi, K. & Mimuro, M. 2004. Chlorophyll d in an epiphytic cyanobacterium of red algae. *Science* 303:1633.
- Nogle, L. M. & Gerwick, W. H. 2003. Diverse secondary metabolites from a Puerto Rican collection of *Lynghya majuscula*. *J. Nat. Prod.* 66:217–20.
- Ohsawa, N., Ogata, Y., Okada, N. & Itoh, N. 2001. Physiological function of bromoperoxidase in the red marine alga, *Corallina pilulifera*: production of bromoform as an allelochemical and the simultaneous elimination of hydrogen peroxide. *Phytochemistry* 58:683–92.
- Palenik, B., Ren, Q., Dupont, C., Myers, G., Heidelberg, J., Badger, J., Madupu, R., et al. 2006. Genome sequence of *Synechococcus* CC9311: insights into adaptation to a coastal environment. *Proc. Natl. Acad. Sci. U. S. A.* 103:13555–9.
- Palenik, B., Ren, Q., Tai, V. & Paulsen, I. T. 2009. Coastal *Synechococcus* metagenome reveals major roles for horizontal gene transfer and plasmids in population diversity. *Environ. Microbiol.* 11:349–59.
- Pedersen, M. & DaSilva, E. J. 1973. Simple brominated phenols in the blue-green alga *Catolrix brevissima* West. *Planta* 115:83–6.
- Rambaut, A. 1996. *Se-Al: Sequence Alignment Editor*. Available at: <http://tree.bio.ed.ac.uk/software/seal/> (last accessed 28 January 2009).
- Rambaut, A. 2008. *FigTree. 1.2 ed.* Available at: <http://tree.bio.ed.ac.uk/software/figtree/> (last accessed 13 May 2009).
- Raugei, S. & Carloni, P. 2006. Structure and function of vanadium haloperoxidases. *J. Phys. Chem. B* 110:3747–58.
- Rogers, M. B., Patron, N. J. & Keeling, P. J. 2007. Horizontal transfer of a eukaryotic plastid-targeted protein gene to cyanobacteria. *BMC Biol.* 5:R26.
- Seshadri, R., Kravitz, S. A., Smarr, L., Gilna, P. & Frazier, M. 2007. CAMERA: a community resource for metagenomics. *PLoS Biol.* 3:394–7.
- Strom, S. 2002. Novel interactions between phytoplankton and microzooplankton: their influence on the coupling between growth and grazing rates in the sea. *Hydrobiologia* 480: 41–54.
- Suthiphongchai, T., Boonsiri, P. & Panijpan, B. 2008. Vanadium-dependent bromoperoxidases from *Gracilaria* algae. *J. Appl. Phycol.* 20:271–8.
- Swingle, W. D., Chen, M., Cheung, P. C., Conrad, A. L., Dejesa, L. C., Hao, J., Honchak, B. M., et al. 2008. Niche adaptation and genome expansion in the chlorophyll d-producing cyanobacterium *Acaryochloris marina*. *Proc. Natl. Acad. Sci. U. S. A.* 105:2005–10.
- Tai, V. 2009. Diversity and dynamics of *Synechococcus* populations in the Southern California Bight. PhD dissertation, University of California, San Diego, 255 pp.
- Toledo, G., Palenik, B. & Brahmsha, B. 1999. Swimming marine *Synechococcus* strains with widely different photosynthetic pigment ratios form a monophyletic group. *Appl. Environ. Microbiol.* 65:5247–51.
- Unson, M. D., Holland, N. D. & Faulkner, D. J. 1994. A brominated secondary metabolite synthesized by the cyanobacterium

CYANOBACTERIAL BROMOPEROXIDASE

- symbiont of a marine sponge and accumulation of the crystalline metabolite in the sponge tissue. *Mar. Biol.* 119:1–11.
- Verhaeghe, E., Buisson, D., Zekri, E., Leblanc, C., Potin, P. & Ambroise, Y. 2008. A colorimetric assay for steady-state analyses of iodo- and bromoperoxidase activities. *Anal. Biochem.* 379:60–5.
- Waterbury, J. B., Watson, S. W., Valois, F. W. & Franks, D. G. 1986. Biological and ecological characterization of the marine unicellular cyanobacterium *Synechococcus*. *Can. J. Fish. Aquat. Sci.* 214:71–120.
- Waterbury, J. B. & Willey, J. M. 1988. Isolation and growth of marine planktonic cyanobacteria. *Methods Enzymol.* 167:100–5.
- Weyand, M., Hecht, H. J., Kiess, M., Liaud, M. F., Vilter, H. & Schomburg, D. 1999. X-ray structure determination of a vanadium-dependent haloperoxidase from *Azophyllum nodosum* at 2.0 angstrom resolution. *J. Mol. Biol.* 293:595–611.
- Winter, J. M., Moffitt, M. C., Zazopoulos, E., McAlpine, J. B., Dorrestein, P. C. & Moore, B. S. 2007. Molecular basis for chloronium-mediated meroterpene cyclization – cloning, sequencing, and heterologous expression of the napyradiomycin biosynthetic gene cluster. *J. Biol. Chem.* 282:16362–8.
- Winter, J. M. & Moore, B. S. 2009. Exploring the chemistry and biology of vanadium-dependent haloperoxidases. *J. Biol. Chem.* 284:18577–81.

Supplementary Material

The following supplementary material is available for this article:

Figure S1. Alignment of the well-conserved region between cyanobacterial and eukaryotic algal vanadium-dependent bromoperoxidases (VBPOs) used to construct the phylogenetic tree shown in Figure 3. Sequences were obtained from the National Center for Biotechnology Information's nr protein database, and accession numbers can be found in Table S1 (see supplementary material). Arrows indicate regions used to design the primers VDEGF and VDEGR.

Figure S2. Nucleotide alignment of the Scripps Pier clone library to metagenomic sequences (see Materials and Methods). This alignment was used for the neighbor-joining analysis and phylogenetic tree construction shown in Figure 4.

Table S1. Gene codes and accession numbers of the sequences used in the neighbor-joining tree of vanadium-dependent bromoperoxidase (VBPO) genes shown in Figure 3.

This material is available as part of the online article.

Please note: Wiley-Blackwell are not responsible for the content or functionality of any supporting materials supplied by the authors. Any queries (other than missing material) should be directed to the corresponding author for the article.

		→
<i>Synechococcus</i> sp. CC9311	(373)	KAVRYQKFNNHLRLRPEALAARIEKAQEIESR----FPTICGCFSEMASD----LQQVVD
<i>Synechococcus</i> sp. WH8020	(373)	KAVRYQKFNNHLRLRPEALAARIEKAQEIESR----FPEICGCFSEMASD----LQQTVD
<i>Synechococcus</i> sp. PCC7335 a	(384)	KAVRYQKFNIHRRRLRPEA IAGRIHQWRNTQPT----NLAPVAELSTQINQ---TLQAVKA
<i>A. marina</i> 1	(399)	KAVRFQKFNNH IRLRPEALAARIELVNSFDGL----SQADKDTVPEVLKK---YIGLFSN
<i>A. marina</i> 2	(422)	KAVRFQKFNVHRRRLRPEALGGLVDRYKHGKGA-GD-ELKPVAALVEALENV-GLLSKVVA
<i>C. watsonii</i>	a (255)	KAMRYQKFNVHSRLRPEGEGGLIDRYLTIPNL-QDGELKPIAPLVEALRNE-RLLDREV--
<i>Verrucomicrobiae</i> sp.	a (426)	KAVRFQKFNLHRRRLRPEALAGRIHAQMTGK-----IDLPEIDALIGKQQT-DILDRVKA
<i>N. spumigena</i>	a (336)	KAVWFQKWYVHRRIRPEAFGGLLHNLHTG-----KAKYPIDQEIFGS--SALEKVYS
<i>M. chthonoplastes</i>	a (340)	KAVWYQKWFVHRRRLRPEAFGGLIHNLMTG-----RAEYPIHPEILNS--QALKAMFD
<i>S. tropica</i>	a (317)	RAVWYQKWFVHRRMRPEVFGARVHQRLTGG-----RAYEFDREVLES--DAVDRVFS
<i>S. usitatus</i>	a (307)	KAVWYQKWFVHRRRLRPEAYGGLVQNTVSS-----GQKYPLHSDVLNS--EALSRIHS
<i>C. officinalis</i> 1	(394)	KAVRYQKFNIHRRRLRPEATGGLISVNKNAFLK-SESVFPEVDV LVEELSS---ILDDSAS
<i>C. officinalis</i> 2	(392)	KAVRYQKFNIHRRRLRPEATGGLISVNKIAAEK-GESVFP EVDLAVEELED---ILEKAEI
<i>C. pilulifera</i> 1	(394)	KAVRYQKFNIHRRRLRPEATGGLISVNKKSFLAGSDIIFPEVSELVEELSS---ILDDVAE
<i>C. pilulifera</i> 2	(392)	KAVRYQKFNIHRRRLRPEATGGLISVNKIAAQK-GESIFPEVDLAVEELGD---ILEKAEI
<i>L. digitata</i> B1	(371)	RHAWYAKWQVHRMLRPEAYGALVHNTLMR-----DVI TPLPDSILRN-TELLNRVEV
<i>L. digitata</i> B2	(407)	RHAWYAKWQVHRMLRPEAYGALVHNTLMR-----DVI TPLPDSILRN-TELLNRVEV
<i>L. digitata</i> B3	(373)	RHAWYTKWQVHRVLRPQAYGGLLHNTLMK-----DVI TPLPQSILGN-TDLLSRVAA
<i>L. digitata</i> B4	(370)	RHAWYTKWQVHRVLRPEAYGGLLHNTLME-----DVI TPLPQSILGN-TDLLSRVAA
<i>L. digitata</i> B5	(358)	RHAWYTKWQVHRVLRPEAYGGLLHNTLMK-----DVI TPLPQSILGN-TDLLSRVAA
<i>L. digitata</i> B6	(339)	RHAWYTKWQVHRVLRPEAYGGLLHNTLMN-----DVI TPLPQSILGN-TDLLSRVAA
<i>L. digitata</i> 11	(397)	KSAWYQKWNVHMFVRPEAFGGSIHNVLLG-----KLDVEIAPSLK N-TDLLDRVAA
<i>L. digitata</i> 13	(390)	KSAWYQKWNVHMFVRPEAFGGTIHNVLLG-----KLNVDINPSLLKN-TELLERVAE
<i>F. distichus</i>	(458)	RASCYQKWQVHRFARPEALGGTLHNTIAG-----DL DADFDISLLEN-DELLKRVAE
<i>A. nodosum</i>	(339)	RSSWYQKWQVHRFARPEALGGTLHNTIKG-----ELNADFDLSLLEN-AELLKRVAA
		: : * : * ** : . . : . :
		←

Figure S1: Alignment of the well-conserved region between cyanobacterial and eukaryotic algal vanadium-dependent bromoperoxidases (VBPOs) used to construct the phylogenetic tree shown in Figure 3. Sequences were obtained from the National Center for Biotechnology Information's nr protein database, and accession numbers can be found in Table S1 (see supplementary material). Arrows indicate regions used to design the primers VDEGF and VDEGR.

<i>Synechococcus</i> sp. CC9311	--LIRNHN--QSLAG-----EATALLPMAFAEGSPMHPAYGAGHATVAGACVTILKAFFN
<i>Synechococcus</i> sp. WH8020	--LIRNHN--QSLAG-----DATALLPMAFAEGSPMHPAYGAGHATVAGACVTILKAFFN
<i>Synechococcus</i> sp. PCC7335	HNKAQNDQYKSSIGGEEFDRDEVYLLPMAFAEGSPMHPAYGAGHAAVAGACVTILKAFFD
<i>A. marina</i> 1	--ALKPTL--NALGG-----N--YLLPMAFPEGSPMHPAYGAGHATVAGACVTILKAFFD
<i>A. marina</i> 2	HNQLQNQN--LDRSGDPSSAGDNYFLPMAFPEGSPMHPAYGAGHATVAGACVTILKAFFD
<i>C. watsonii</i>	-NQFNN-----GQSYLLPMAFPEGSPMHPAYGAGHATVAGACVTILKAFFD
<i>Verrucomicrobiae</i> sp.	HNAARNPV--GPHKGDASAGSNLYLLPMAFPEGSPMHPAYGAGHATVAGACVTILKAFFD
<i>N. spumigena</i>	-----LCGTYLLPMAFPEGSPMHPAYGAGHATVAGACVTILKAFFD
<i>M. chthonoplastes</i>	-----KNGNYLLPQVFPPEGSPMHPAYGAGHATVAGACVTILKAFFD
<i>S. tropica</i>	-----KWGSYLLPQAFPEGSPMHPAYGAGHATVAGACVTILKAFFD
<i>S. usitatus</i>	-----RYGSYLLPMAYPEGSPMHPAYGAGHATVAGASITILKSLFD
<i>C. officinalis</i> 1	SNEKQN-----IADGDVSPGKSFLLPMAFAEGSPMHPAYGAGHATVAGACVTILKAFFD
<i>C. officinalis</i> 2	SNRKQN-----IADGDVSPGKSFLLPMAFAEGSPMHPAYGAGHATVAGACVTILKAFFD
<i>C. pilulifera</i> 1	SNEKQN-----RADGIVSPDKSFLLPMAFAEGSPMHPAYGAGHATVAGACVTILKAFFD
<i>C. pilulifera</i> 2	SNRKQN-----IADGDVSPDKSFLLPMAFAEGSPMHPAYGAGHATVAGACVTILKAFFD
<i>L. digitata</i> B1	HNQRMN-----PDG-----EKTFLPMAAAQGSPTHAYPSGHAINNGAYITALKAFGLG
<i>L. digitata</i> B2	HNQRMN-----PDG-----EKTFLPMAAAQGSPTHAYPSGHAINNGAYITALKAFGLG
<i>L. digitata</i> B3	NNIRMN-----PDG-----EKTFLPMAAAQGSPTHAYPSGHAINNGAYITALKAFGLG
<i>L. digitata</i> B4	NNIRMN-----PDG-----EKTFLPMAAAQGSPTHAYPSGHAINNGAYITALKAFGLG
<i>L. digitata</i> B5	NNIRMN-----PDG-----EKTFLPMAAAQGSPTHAYPSGHAINNGAYITALKAFGLG
<i>L. digitata</i> B6	NNIRMN-----PDG-----EKTFLPMAAAQGSPTHAYPSGHAINNGAYITALKAFGLG
<i>L. digitata</i> I1	RNGEIN---GRPGV---LDRTYLLSQALPEGSPMHPAYGAGHATVAGACVTILKALVGLG
<i>L. digitata</i> I3	RNGVIN---GRPGV---LDRTYLLSQAVIEGSPMHPAYGAGHATVAGACVTILKALVGLG
<i>F. distichus</i>	INAAQN-----PNN-----EVTYLLPQAIQVGSPTHAYPSGHAINNGAYITALKALIG
<i>A. nodosum</i>	INAAQN-----PNN-----EVTYLLPQAIQVGSPTHAYPSGHAINNGAYITALKALIG
	:* . . * . * ** : * : ** . . * ** : . .
<i>Synechococcus</i> sp. CC9311	TS---ALFVKINDVAGFHSHKQHI LARLKC GDSVEAGAYQETDCGKRLEFERCGSFHLLIEG
<i>Synechococcus</i> sp. WH8020	TS---ALFVKINDLAGFYSKQHI LDRLKC GDSVEAGAYQVTDCCGKRLEFERCGSFHLLIEG
<i>Synechococcus</i> sp. PCC7335	HS---YVLP-----GPVVTPTSTNGQ-----
<i>A. marina</i> 1	TS---AVLAKSQSQSIAFK-----RLENGD--KPIAFRAPDLPGSGPGE-----
<i>A. marina</i> 2	HG---WQLNLG--MANGK-----YISYEPNQDGSS-----
<i>C. watsonii</i>	HG---WQLPLGKDETTGR-----YIAYEPNADGSG-----
<i>Verrucomicrobiae</i> sp.	HG---QELG---TK-----SYEANANGSK-----
<i>N. spumigena</i>	ES---WKIPH-----PVVFNDDGTE-----
<i>M. chthonoplastes</i>	ES---YQIPK-----PMVFNDDGTE-----
<i>S. tropica</i>	ET---AVLDN-----PIQANEDGTA-----
<i>S. usitatus</i>	EN---FVIPN-----PVVASPDGLS-----
<i>C. officinalis</i> 1	AN---FQIDQV-----FEVDTDEDK-----
<i>C. officinalis</i> 2	SN---FQIDQV-----FEVDKDEDK-----
<i>C. pilulifera</i> 1	AN---FQIDKV-----FEVDTDEDK-----
<i>C. pilulifera</i> 2	SG---IEIDQV-----FEVDKDEDK-----
<i>L. digitata</i> B1	YEAGQKCFPN-----PVVSNDEGTK-----
<i>L. digitata</i> B2	YEAGQKCFPN-----PVVSNDEGTK-----
<i>L. digitata</i> B3	FEAGQKCFPN-----LVESDDGGLA-----
<i>L. digitata</i> B4	FEAGQKCFPN-----LVESDDGGLA-----
<i>L. digitata</i> B5	FEAGQKCFPN-----LVESDDGGLA-----
<i>L. digitata</i> B6	FEAGQKCFPN-----LVESDDGGLA-----
<i>L. digitata</i> I1	LERGSVCFND-----PVFPDDEGLT-----
<i>L. digitata</i> I3	LERGSDCFRD-----PKVPDDEGLT-----
<i>F. distichus</i>	LDRGGECFPN-----PVFPDDEGLE-----
<i>A. nodosum</i>	LDRGGDCYPD-----PVYPPDDGLK-----

Figure S1: continued

<i>Synechococcus</i> sp. CC9311	KYATFKPDGKTNQ-----SCCPLTLEGELNKLA-
<i>Synechococcus</i> sp. WH8020	KDATFKPDGT TNK-----SCCPLTLEGELNKLA-
<i>Synechococcus</i> sp. PCC7335	-----KLQ RVPSE-----ELS-LTIEGELNKLA-
<i>A. marina</i> 1	--GVPKDDLKPFK-----PNHFLTLEGELNKLA-
<i>A. marina</i> 2	-----LQQVL-----LDCPLTVEGELNKIA-
<i>C. watsonii</i>	-----LVEVL-----LEQPLTVEGELNKVA-
<i>Verrucomicrobiae</i> sp.	-----LTAVN-----LKAPLTVEGELNKLA-
<i>N. spumigena</i>	-----LIAYT-----GADAEKLT VGGELNKVA-
<i>M. chthonoplastes</i>	-----LVS YIPYS-----GPGTEVLT VGGELNKLA-
<i>S. tropica</i>	-----LVPYE-----GQDAGRLT VGGELNKLA-
<i>S. usitatus</i>	-----LIPYQ-----GPDANQLT VGGELNKLA-
<i>C. officinalis</i> 1	-----LVKSS-----FPGPLTVAGELNKLA-
<i>C. officinalis</i> 2	-----LVKSS-----FKGTLTVAGELNKLA-
<i>C. pilulifera</i> 1	-----LVKSS-----FKGTLTVAGELNKLA-
<i>C. pilulifera</i> 2	-----LVKSS-----FKGTLTVAGELNKLA-
<i>L. digitata</i> B1	-----RIKYKPSGREIVGECVNEKGKLV EGLTYEGELNKISA
<i>L. digitata</i> B2	-----RIKYKPSGREIVGECVNEKGKLV EGLTYEGELNKISA
<i>L. digitata</i> B3	-----RVPYVPTGTEFLEDCV DKG NKT TGLTIEGELNKVA-
<i>L. digitata</i> B4	-----RVPYVPTGTEFLEDCV DKG NKT TGLTIEGELNKVA-
<i>L. digitata</i> B5	-----RVPYVPTGTEFLEDCV DKG NKT TGLTIEGELNKVA-
<i>L. digitata</i> B6	-----RVPYVPTGTEFLEDCV DKG NKT TGLTIEGELNKVA-
<i>L. digitata</i> I1	-----LLPYTGDDG-----NNCLTFEGEINKLA-
<i>L. digitata</i> I3	-----LLDFTGD-----CLTFEGEINKLA-
<i>F. distichus</i>	-----LINFEGA-----CLTYEGEINKLA-
<i>A. nodosum</i>	-----LIDFRGS-----CLTFEGEINKLA-

** **:*:*:.

a. Not annotated as putative VBPO

Figure S1: continued


```

SyncCC9311 CTTGCGGGGGGAAGCCACGGCTCTGCTGCCGATGGCTTTCGCGGAAGGTTGCGCCGATGCAC
SyncWH8020 CTCGCTGGGGACGCCACGGCTCTGCTGCCGATGGCTTTCGCGGAAGGTTGCGCCGATGCAC
Pier1      CTTACTGGTGACGCCACAGCTCTGCTGCCGATGGCTTTCGCGGAAGGTTGCGCCGATGCAC
Pier2      CTTACTGGTGACGCCACAGCTCTGCTGCCGATGGCTTTCGCGGAAGGTTGCGCCGATGCAC
Pier3      CTTGCGGGGGGAAGCCACGGCTCTGCTGCCGATGGCTTTCGCGGAAGGTTGCGCCGATGCAC
Pier4      CTTACTGGTGACGCCACAGCTCTGCTGCCGATGGCTTTCGCGGAAGGTTGCGCCGATGCAC
Pier5      CTCGCTGGGGACGCCACTGCCCTCCTACCGATGGCATTTCGCGGAAGGTTGCGCCGATGCAC
Pier6      CTCGCTGGGGACGCCACTGCCCTCCTACCGATGGCATTTCGCGGAAGGTTGCGCCGATGCAC
Pier7      CTTGCGGGGGGAAGCCACGGCTCTGCTGCCGATGGCTTTCGCGGAAGGTTGCGCCGATGCAC
Pier8      CTTACTGGTGACGCCACAGCTCTGCTGCCGATGGCTTTCGCGGAAGGTTGCGCCGATGCAC
Pier9      CTTGCGGGGGGAAGCCACGGCTCTGCTGCCGATGGCTTTCGCGGAAGGTTGCGCCGATGCAC
Pier10     CTTGCGGGGGGAAGCCACGGCTCTGCTGCCGATGGCTTTCGCGGAAGGTTGCGCCGATGCAC
Pier11     CTTACTGGTGACGCCACAGCTCTGCTGCCGATGGCTTTCGCGGAAGGTTGCGCCGATGCAC
Pier12     CTTGCGGGGGGAAGCCACGGCTCTGCTGCCGATGGCTTTCGCGGAAGGTTGCGCCGATGCAC
Pier13     CTCGCTGGGGGAAGCCACTGCCCTCCTGCCGATGGCTTTCGCGGAAGGTTGCGCCGATGCAC
Pier14     CTTACTGGTGACGCCACAGCTCTGCTGCCGATGGCTTTCGCGGAAGGTTGCGCCGATGCAC
Pier15     CTCGCTGGGGGAAGCCACTGCCCTCCTGCCGATGGCTTTCGCGGAAGGTTGCGCCGATGCAC
Pier16     CTCGCTGGGGACGCCACGGCCCTGTTGCCGATGGCTTTCGCGGAAGGTTCTCCGATGCAC
Pier17     CTCGCTGGGGACGCCACGGCCCTGTTGCCGATGGCTTTCGCGGAAGGTTGCGCCGATGCAC
Pier18     CTCGCTGGGGACGCCACGGCCCTGTTGCCGATGGCTTTCGCGGAAGGTTGCGCCGATGCAC
Pier19     CTCGCTGGGGACGCCACGGCCCTGTTGCCGATGGCTTTCGCGGAAGGTTGCGCCGATGCAC
Meta1      CTCGCTGGGGACGCCACTGCCCTCCTACCGATGGCATTTCGCGGAAGGTTGCGCCGATGCAC
Meta2      CTTGCGGGGGGAAGCCACGGCTCTGCTGCCGATGGCTTTCGCGGAAGGTTGCGCCGATGCAC
A. marina TTAGGGGGG-----AATTATTTACTACCAATGGCTTTCCTGAAGGCTCGCCAATGCAT
          *      **          *      *  *  *  *  *  *  *  *  *  *  *  *  *  *  *

```

Figure S2: Nucleotide alignment of the Scripps Pier clone library to metagenomic sequences (see “Materials and Methods”). This alignment was used for the neighbor-joining analysis and phylogenetic tree construction shown in Figure 4.

Table S1: Gene codes and accession numbers of the sequences used in the neighbor-joining tree of vanadium-dependent bromoperoxidase (VBPO) genes shown in Figure 3.

Tree label	Organism	Gene accession no.
Sync CC9311	<i>Synechococcus</i> sp. CC9311	YP_731869
Sync WH8020	<i>Synechococcus</i> sp. WH8020	HQ154623.1 (This Study)
<i>A. marina</i> 1	<i>Acaryochloris marina</i>	YP_001515553
<i>A. marina</i> 2	<i>Acaryochloris marina</i>	YP_001519261
Sync PCC7335	<i>Synechococcus</i> sp. PCC7335	ZP_05035964.1
<i>S. tropica</i>	<i>Salinispora tropica</i>	YP_001157472
<i>S. usitatus</i>	<i>Solibacter usitatus</i>	YP_828805
<i>C. officinalis</i> 1	<i>Corallina officinalis</i>	AAM46061
<i>C. officinalis</i> 2	<i>Corallina officinalis</i>	1UP8.A
<i>C. pilulifera</i> 1	<i>Corallina pilulifera</i>	BAA31261
<i>C. pilulifera</i> 2	<i>Corallina pilulifera</i>	BAA31262
<i>M. chthonoplastes</i>	<i>Microcoleus chthonoplastes</i> PCC7420	ZP_05023600.1
<i>C. watsonii</i>	<i>Crocospaera watsonii</i> WH8501	ZP_00515257
<i>N. spumigena</i>	<i>Nodularia spumigena</i> CCY9414	ZP_01629010
<i>Verrucomicrobiae</i> sp.	<i>Verrucomicrobiae</i> bacterium DG1235	ZP_05058612.1
<i>L. digitata</i> B1	<i>Laminaria digitata</i>	CAD37191.1
<i>L. digitata</i> B2	<i>Laminaria digitata</i>	CAD37192.1
<i>L. digitata</i> B3	<i>Laminaria digitata</i>	CAQ51441.4
<i>L. digitata</i> B4	<i>Laminaria digitata</i>	CAQ51442.1
<i>L. digitata</i> B5	<i>Laminaria digitata</i>	CAQ51443.1
<i>L. digitata</i> B6	<i>Laminaria digitata</i>	CAQ51444.1
<i>L. digitata</i> I1	<i>Laminaria digitata</i> I	CAI04025.1
<i>L. digitata</i> I3	<i>Laminaria digitata</i> I	CAQ51446.1
<i>A. nodosum</i>	<i>Ascophyllum nodosum</i>	P81701
<i>F. distichus</i>	<i>Fucus distichus</i>	AAC35279

Chapter 2, in full, is a reprint of the material as it appears in Johnson, T. L., Palenik, B., and Brahamsha, B. 2011. Characterization of a functional vanadium-dependent bromoperoxidase in the marine cyanobacterium *Synechococcus* sp. CC9311. *Journal of Phycology*. 47:792-801. The dissertation author was the primary investigator and the first author of this paper.

Chapter 3

Expression patterns of vanadium-dependent bromoperoxidase in *Synechococcus* sp.

CC9311 as a response to physical agitation and a bacterial assemblage.

Abstract

Vanadium-dependent bromoperoxidase (VBPO, sync_2681) activity was recently characterized in *Synechococcus* sp. CC9311. While this enzyme has several reported functions in eukaryotic macroalgae, its physiological function in cyanobacteria is unknown. To address this question, this study used enzyme activity, a VBPO-inactive mutant, and quantitative iTRAQ proteomics to determine induction patterns as well as identify specific proteins that may be involved in the same processes as VBPO. VBPO activity is highly upregulated when *Synechococcus* sp. CC9311 is exposed to physical agitation or to a specific bacterial assemblage, but not by oxidative stress. The use of quantitative iTRAQ proteomics indicated that VBPO was the protein most upregulated by stirring after 4 and 24 hrs. Additionally, the mutant showed an enrichment of cell wall related proteins upregulated by stirring, indicating a biochemical response to physical stress. This study further reports VBPO activity in *Acaryochloris marina* and suggests a similar regulation pattern of VBPO activity by physical agitation.

Introduction

Vanadium-dependent bromoperoxidases (VBPO) are halogenating enzymes that are widely distributed and have been well characterized in eukaryotic macroalgae

(Kamenarska *et al.*, 2007, Krenn *et al.*, 1989, Moore & Okuda, 1996, Ohsawa *et al.*, 2001). However, there are only two recent examples of functional vanadium-dependent haloperoxidases in prokaryotes (Bernhardt *et al.*, 2011, Johnson *et al.*, 2011, Winter, 2009). VBPOs coordinate the two-electron oxidation of halides using hydrogen peroxide, forming a hypohalous acid intermediate, and are named for the most electronegative halide oxidized, which is bromide in the case of VBPO. The highly reactive intermediate, in the form of hypohalous acid, halogenates electron-rich organic molecules (Carter *et al.*, 2002, Kamenarska *et al.*, 2007). The long hypothesized and experimentally examined functions of VBPO in eukaryotes are the detoxification of hydrogen peroxide or a defensive strategy through the production of halogenated organic molecules (Ohsawa *et al.*, 2001, Butler & Carter-Franklin, 2004, Manley, 2002). However, the physiological and ecological role of this enzyme in bacteria is unknown.

Marine chroococcoid cyanobacteria are widely distributed primary producers in the global oceans, contributing as much as 30% of marine photosynthetic carbon fixation in some locations (Li, 1994, Jardillier *et al.*, 2010). Marine *Synechococcus* exhibit niche adaptation and have been divided into at least 20 distinct clades, with more still being resolved (Penno *et al.*, 2006, Huang *et al.*, 2012). Genomes have been sequenced from at least 10 distinct clades of marine *Synechococcus* (Dufresne *et al.*, 2008), which has provided many insights into their niche adaptations and their staggering genetic diversity. One aspect of this diversity is reflected by the amount of horizontal gene transfer found in the genomes. Horizontally transferred genes are often grouped into genetic islands (Dufresne *et al.*, 2008), and it has recently been shown that some of these genes have

specific physiological or ecological functions. Recent examples include resistance to cyanophage (Avrani *et al.*, 2011) and copper stress (Stuart *et al.*, 2013).

Upon the sequencing of the genome of *Synechococcus* sp. CC9311 (referred to as CC9311, Palenik *et al.*, 2006) a putative gene (sync_2681) annotated as a vanadium-dependent bromoperoxidase was found in a genomic island of horizontally transferred genes. This VBPO (sync_2681) was recently characterized in CC9311 (Johnson *et al.*, 2011) with the gene product being the only protein displaying VBPO activity when separated by SDS-PAGE. The study also found VBPO activity in a closely related clade I strain, *Synechococcus* sp. WH8020. Furthermore, VBPO gene sequences are found in other cyanobacterial genomes as well as environmental samples. The physiological function of VBPO in cyanobacteria, however, is still unknown.

Acaryochloris is a genus of marine cyanobacteria with the unique production of chlorophyll d (Ohkubo *et al.*, 2006), which was once attributed to red algae. Swingley *et al.* (2008), recently sequenced the genome of *Acaryochloris marina* MBIC11017 revealing a large genome of over 8 Mbp, with seven plasmids as well as numerous gene duplications and horizontal gene transfer. *A. marina* MBIC11017 also contains two genes annotated as vanadium-dependent bromoperoxidases with high similarity to VBPO in *Synechococcus* sp. CC9311 (YP_001515553.1, 53.7% amino acid identities; YP_00151926.1, 40% amino acid identities). One of these sequences shares the greatest known sequence similarity (53.7% amino acid identities) to VBPO in *Synechococcus* sp. CC9311 (Johnson *et al.*, 2011). Testing VBPO activity in *A. marina* presents an opportunity to verify that VBPO is produced and active in another genus of

cyanobacteria, as well as a chance to investigate the role of this enzyme in another cyanobacterium based on expression patterns of VBPO activity.

Expression studies are valuable tools for determining cellular responses to specific conditions. Quantitative proteomics is a method of using isobaric mass tags to label digested proteins, which are separated through high pH reverse phase chromatography as well as HPLC, and sequenced via tandem mass spectrometry (Ross *et al.*, 2004). This process allows for efficient and quantitative comparisons of expressed proteins to be made between multiple treatments of the same organism. This technology is complemented in this study by the creation of a mutant, in which the gene for VBPO was disrupted. Comparing the wild-type to the mutant allows for a direct method for determining the consequences of VBPO expression.

This study offers the first application of direct genetic manipulation to demonstrate the physiological and ecological implications of VBPO activity in a cyanobacterium. In this study, we have created a VBPO-inactive mutant, explored the regulation of VBPO using induction cues, and investigated the physiological implications of VBPO through the use of quantitative proteomics.

Materials and Methods

Chemicals

A vanadium-dependent bromoperoxidase standard was purchased (Sigma) as a recombinant enzyme from *Corallina officinalis*. Chemicals used to detect VBPO specific activity were sodium orthovanadate (Na_3VO_4 , Alexis Biochemicals), 2-(*N*-

morpholino)ethanesulfonic acid (MES >99%, Acros Organics) buffer, potassium bromide (KBr, Fisher), and hydrogen peroxide (H₂O₂) 30% stock (Fisher).

Strains and Growth conditions

Synechococcus sp. CC9311 (Palenik *et al.*, 2006) and mutant strains were grown in liquid SN medium (Waterbury & Willey, 1988) supplemented with 250 nM sodium orthovanadate (Na₃VO₄) at 23°C in constant light (20 μmol photons m⁻² s⁻¹). A *Pteridomonas* clone, isolated from the Scripps Pier (B. Palenik), was grown in F/4 medium (Guillard & Ryther, 1962) amended with 2 barley grains per 50 ml in constant light. Heterotrophic bacteria tested included marine bacterium strain TW6 (Bidle & Azam, 2001), *Alteromonas* strain TW-7 (Bidle & Azam, 2001), *Silicibacter* strain TrichCH4B (Roe *et al.*, 2012). *Silicibacter* was grown at 30°C with slow shaking in Marine Broth 2216 medium (Difco). *Alteromonas* TW7 and marine bacterium TW6 (gamma-proteobacteria) bacterial strains were grown in Marine Broth 2216 medium at room temperature without shaking. *Acaryochloris marina* MCIC11017 (Swingley *et al.*, 2008) was grown and maintained in SN medium with constant light of 20 μmol photons m⁻² s⁻¹ at 23°C.

Insertional Gene Inactivation

VBPO (sync_2681) in *Synechococcus* sp. CC9311 was inactivated using methods from Brahamsha (1996) as summarized in Figure 3.1. Genomic DNA was extracted from *Synechococcus* sp. CC9311 as described in Brahamsha (1996). Polymerase chain reaction (PCR) was used on CC9311 genomic DNA to amplify a 482 bp fragment (primers VBF,

VBR; Table 1) of the gene for VBPO (sync_2681), cloned into the pCR4-Topo vector (Invitrogen) and transformed into Topo OneShot competent cells (Invitrogen). The TOPO construct, pTOP2681, was isolated using a plasmid prep kit (Qiagen), digested with *EcoRI* (New England Biolabs) and the gene fragment (sync_2681 amplified with VBF/VBR, now flanked by the TOPO vector to the *EcoRI* sites on either end) was gel purified and excised. The excised fragment was then cloned into the *EcoRI* site of pMUT100 (Brahamsha, 1996), resulting in the plasmid pVBR1, which was transformed into *Escherichia coli* strain MC1061 containing the conjugal plasmids pRK24 and pRL528, and grown in LB with 50 $\mu\text{g/ml}$ kanamycin, 100 $\mu\text{g/ml}$ ampicillin, and 10 $\mu\text{g/ml}$ chloramphenicol. The plasmid construct, pVBR1, was introduced into *Synechococcus* sp. CC9311 via conjugation with *Escherichia coli* strain MC1061 (pVBR1, pRK24, pRL528) as described in (Brahamsha, 1996) with the exception that 0.4% Sea Plaque agarose (Lonza) was used for pour-plating. Colonies appeared in 3 weeks and were picked and maintained in SN liquid medium with 20 $\mu\text{g/ml}$ kanamycin.

Mutant verification

The genotype of the mutant was verified using PCR. Primers were designed (VBPO Verif long F / VBPO Verif long R, Table 3.1) to amplify a 700 bp fragment including approximately 100 bp outside the original PCR fragment in the wild-type. This fragment should not amplify in the mutant under the conditions used due to the 4,000 bp vector insert. Primers specific to the CC9311 *rpoC* gene were used as a positive control for the PCR reaction and DNA quality, as seen in Figure 3.2. PCR reactions were also carried out to further verify the correct insert was present as well as the orientation of the

vector insert. Primers were designed based on the pMUT100 vector (pBR322 forward a, pBR322 reverse a, Table 1) and used individually in PCR reactions with VBPO verif 2F (Table 1) on boiling DNA extractions of VMUT cultures. VBPO Verif 2F is located towards the N-terminus end of sync_2681, outside of the original 482 bp fragment, so that PCR amplification is only possible if paired with only one of the pBR322 primers. VBPO Verif 2F and pBR322 reverse a amplified the expected 609 bp region while no product was observed when pBR322 forward a and VBPO Verif 2F were used. A 750 bp fragment was successfully amplified in CC9311 but not in VMUT indicating that the mutant was segregated. Primers successfully amplified a 303 bp fragment from *rpoC* (Figure 3.2) in both CC9311 as well as VMUT. The original mutant, VMUT, was constructed in April 2010. A second mutant, referred to as VMUT2, was recreated using the same technique in September 2011 to verify the possible phenotype reversion.

Growth Measurements

Cultures (1.5 L in a 2.8L flask) of CC9311 and VMUT were inoculated to a cell concentration of 1.0×10^5 cells ml^{-1} in SN media supplemented with 250 nM Na_3VO_4 and kanamycin (mutant only, final concentration of 20 $\mu\text{g}/\text{ml}$). Each culture was grown with or without stirring at 200 rpm with a magnetic stir bar (6.0 cm length). *Synechococcus* cell concentrations were determined via flow cytometer (FACSort, Becton Dickinson) or by hemacytometer at 400X magnification. Phycoerythrin autofluorescence of 5 ml aliquots of cultures was measured using phycoerythrin specific cutoff filters (excitation = 544 nm, emission = 577 nm) on a Turner 10AU fluorometer (Turner Designs). Proteins were extracted from 500 ml cultures harvested at different phases of growth and VBPO

activity was determined using the thymol blue- based spectrophotometric assay. Some protein samples were also separated on SDS-PAGE and stained for total proteins and VBPO activity. Growth rates were determined by fitting cell ml^{-1} counts to the exponential growth equation in Prism v 5.0 software (GraphPad Software Inc.).

In growth experiments involving CC9311 and VMUT2, short term VBPO inducibility was also tested. Proteins were extracted from the stirred cultures at different stages of growth and tested for VBPO activity. Additionally, 200 ml aliquots from the still culture were transferred to a 500 ml flask and a) subjected to stirring for 4 hrs or b) remained still for 4 hrs. Proteins were then harvested and tested for VBPO activity.

VBPO Accumulation

For more detailed measurements of VBPO activity as a response to stirring over time in cultures of CC9311, four flasks (2.8 L) of SN medium (2.0 L) containing 250 nM Na_3VO_4 were inoculated with CC9311. After inoculation, two cultures were grown still while two cultures were subjected to stirring. When the cultures entered mid-log phase, stirring was applied to one of the still cultures. Stirring was also halted in one of the stirred cultures. Samples (200 ml) from each culture were harvested via centrifugation after 2, 4, 8, 12, 24, 32, 48, and 72 hrs of the treatment. Proteins were extracted and tested for VBPO activity. Samples (1 ml) were taken from each culture, fixed with 0.25% glutaraldehyde and frozen at -80°C until cell concentrations were measured.

Protein extraction

Cells were harvested via centrifugation at 13,175 xg for 10 min at 18°C. The medium was discarded and cell pellets were resuspended in 100 mM MES buffer, pH 7.0. Cells were broken using a French Pressure cell (SLM Instruments) with 3 passes at 20,000 psi. Protein concentrations were determined using the BCA Protein kit (Pierce, Thermo) microplate assay carried out according to the manufacturer's directions. The working reagent (200 µL) was added to each protein sample (25 µL), incubated at 37°C for 30 min, then the absorbance was measured at 562 nm. BSA provided by the kit as a 2,000 µg/ml stock was diluted in 100 mM MES buffer, pH 7.0 and used as a standard curve of 25-2,000 µg/mL to determine protein concentrations.

Sensitivity to hydrogen peroxide

Resistance to hydrogen peroxide was tested in *Synechococcus* CC9311 and VMUT or VMUT2 cultures preconditioned with and without stirring to induce VBPO. In trial one, 1.5 L cultures of *Synechococcus* CC9311 and VMUT were grown still or stirred at 200 rpm to log phase (experiments were started when cell concentrations were 1.0 – 3.0 x 10⁷ cells ml⁻¹ for each experiment). The cultures were then divided, adding 20 ml culture per 50 ml flat-bottom glass culture tube. No cultures were stirred after being divided into the smaller tubes, making the stirring a preconditioned treatment. Hydrogen peroxide was diluted from a 30% stock in sterile MilliQ water and added to tubes in triplicate at the following final concentrations: 0 µM, 10 µM, 25 µM, 50 µM. VMUT preconditioned with stirring was not tested at that time due to the sensitivity of VMUT to stirring. The second trial used VMUT2 and included cultures that were preconditioned

with stirring. Hydrogen peroxide concentrations were adjusted in the second trial to include 0 μM , 10 μM , 20 μM , 30 μM , 50 μM , and 100 μM . For each experiment, phycoerythrin autofluorescence was recorded after 0, 2, 4, 6, 12, 24, 48, and 72 hours after the addition of H_2O_2 for each replicate. Additionally, a 1 ml sample from one replicate at each H_2O_2 concentration was taken, glutaraldehyde was added to a final concentration of 0.25%, and the sample was frozen at -80°C for cell counts by flow cytometry. Protein was extracted from 400 ml of the source cultures before being divided and VBPO activity was tested.

SDS-PAGE Analysis

Protein extracts were mixed with SDS loading buffer (Invitrogen) and denaturing reagent (Invitrogen), and heated at 70°C for 10 min, then loaded onto duplicate Novex NuPAGE 3-8% tris-acetate gels (Invitrogen) and used with tris-acetate SDS running buffer (Invitrogen). Gels were run at 150 V for 1 hr with constant voltage. Total proteins were visualized by overnight staining with Sypro Ruby (Invitrogen) and imaged with UV light using a Typhoon Scanner. VBPO activity was tested in a duplicate gel by immersing the gel in a phenol red solution (Johnson, *et al.*, 2011). Purified bromoperoxidase (0.5 U) from *Corallina officinalis* (Sigma) was used as a positive control for VBPO activity.

VBPO Assay

A spectrophotometric assay for vanadium-dependent bromoperoxidase activity was used as in Johnson *et al.* (2011). Protein extracts (100 μl , 0.02-0.08 mg ml^{-1} , final concentration in the reaction) were incubated with 2.2 μl of 90 mM Na_3VO_4 at room

temperature for 20 min. The protein was then added to 10 μl of 1 mM thymol blue and 840 μl of 100 mM MES buffer with 100 mM KBr, pH 8.0, in a 1 ml cuvette and blanked at 620 nm. To start the reaction, 50 μl of 40 mM H_2O_2 were added and the absorbance was monitored at 620 nm. Hydrogen peroxide stocks were prepared fresh before each experiment in autoclaved MilliQ water.

VBPO Induction Experiments

To investigate the nature of VBPO induction, still cultures of *Synechococcus* sp. CC9311 in exponential growth were exposed to a variety of conditions and stresses. Cultures were grown in large (1.5 L cultures in 2.8 L flasks) batches to mid-log phase ($1.0 - 6.0 \times 10^7$ cells ml^{-1}) then distributed (200 ml) into 500 ml flasks. Each treatment was applied for 4, 6, or 24 hrs. For each experiment, a still culture served as a negative control for VBPO activity while a culture stirred with a 5.0 cm magnetic stir bar at 200 rpm served as a positive control for VBPO induction. After each experiment, protein was extracted from the 200 ml culture as described above and tested for VBPO activity using the spectrophotometric assay with thymol blue. VBPO activity was considered to be significant if the assay slope ($A_{620} \text{ min}^{-1}$) was greater than three standard deviations above a no protein control, otherwise the activity was considered below the limits of detection. Furthermore, VBPO activity was considered induced if the treatment was significantly greater than the still control as determined by a t-test ($p < 0.05$) performed in Prism Graphpad. All experiments were done on *Synechococcus* cultures grown in SN medium supplemented with 250 nM Na_4VO_3 and incubated in constant light at 20-25 μM photons $\text{m}^{-2} \text{ s}^{-1}$ at 23°C, unless otherwise indicated. Experimental setups are described below in

the following categories of 1) Physical stress, 2) Gas exchange 3) Light, 4) Cell wall stress, 5) Oxidative stress, and 6) Addition of bacteria

1) *Physical stress*

Shaking: Cultures (200 ml) were poured into a 500 ml flask and then placed on a shaking plate, moving at 120 revolutions per minute. Flask size and rotation were based on low-shear (0.028 s^{-1}) control measured in Sahoo *et al.* (2003).

Shear Stress: Laminar shear stress was applied to cultures of *Synechococcus* using Couette chambers; clear plastic, hollow cylinders that remain stationary while an inner cylinder rotates. Friction forces the liquid in the gap between the cylinders to move at varied speeds within the gap causing laminar shear. Greater rotation speeds of the cylinders cause greater shear stress. Shear rates from $10\text{-}50 \text{ s}^{-1}$ were applied using an upright Couette chamber with a 5.0 mm gap as described in Juhl *et al.*, (2000). Shear rates from 100 s^{-1} to 1000 s^{-1} were applied for 6 hours using a slanted Couette chamber with a 2.5 mm gap as described in Latz *et al.*, (1994). For each treatment, the still, negative control for VBPO induction was a culture that was sealed in a still Couette chamber and incubated next to the actively rotating chamber.

2) *Gas Exchange*

Stirring with no headspace: A 500 ml flask was filled to the top with culture and sealed with a layer of parafilm as well as tin foil to prevent gas exchange. The culture was then stirred for 4 hours with a 5.0 cm magnetic stir bar at 200 rpm. The positive control was 250 ml culture in a 500 ml flask, with a foam stopper and tin foil.

Bubbling: Gas exchange was increased by introducing a slow stream of non-sterile lab air to the culture through a 5.0 ml glass (Fisher) pipette secured by a foam stopper.

3) *Light*

The effect of light on VBPO induction was tested with stirring and shaking conditions described above with and without light. Dark conditions were set up identically to light conditions, with the exception that the treatment flask was covered in foil at the beginning of the induction.

4) *Cell Wall Stress*

Osmotic shock: Cultures were grown still with constant light in SN medium (75% seawater). To apply osmotic shock, cultures were divided then centrifuged in 200 ml batches at 13,175 $\times g$, 10 min, 18°C. Cell pellets were resuspended in SN medium adjusted with MilliQ water to 50% salinity of seawater, non-adjusted SN medium, or SN medium adjusted to 125% seawater with sterile 5 M NaCl. The full salinity of seawater was assumed to be 0.5 M. Each osmotic condition was tested under still and stirred conditions. After 24 hours, proteins were extracted from 200 ml of each treatment and VBPO activity was tested.

Broken *Synechococcus*: A portion (100 ml) of a still culture of CC9311 was centrifuged for 10 min at 18° C at 8,200 $\times g$ and resuspended in 3 ml sterile SN medium. The cells were broken using a French Pressure cell at 20,000 psi with three passes. The broken cells (2.5 ml) were added back to the original still culture (250 ml) of CC9311 in a 500 ml flask.

Antibiotics: Ampicillin, a lactam-based antibiotic that interrupts peptidoglycan synthesis, was added to a still culture of CC9311 at a final concentration of $10 \mu\text{g ml}^{-1}$ for 24 hrs. Protein was harvested from 200 ml culture and tested for VBPO activity.

5) *Oxidative stress*

Hydrogen peroxide: To test whether the addition of oxidative stress induced VBPO activity, hydrogen peroxide (H_2O_2 , 30% stock) was added to both a still and a stirred culture of CC9311 at a final concentration of $25 \mu\text{M}$, a concentration pre-determined not to be toxic (See *Sensitivity to Hydrogen Peroxide*). After a 24 hr incubation in constant light, proteins were extracted and tested for VBPO activity.

Methyl viologen: Another form of oxidative stress was also tested using methyl viologen to increase intracellular superoxide (O_2^-). Methyl viologen was added to still cultures of CC9311 at a final concentration of $0.10 \mu\text{M}$, a concentration determined to shock, but not to be toxic to CC9311 (*R. Stuart*, personal communication). Proteins were harvested after 4 hours and tested for VBPO activity.

6) *Addition of heterotrophic bacteria*

Three known heterotrophic bacterial isolates were co-cultured with CC9311 for 24 hrs to determine if they provided an induction cue for VBPO activity. Cultures of marine bacterium TW6, *Alteromonas* TW7, and *Silicibacter* TrichCH4B were grown overnight in marine broth 2216 medium and cell abundance determined by hemacytometer. A volume of heterotrophic bacterial culture (0.5-1.0 ml depending on cell counts) was transferred to a 1.5 ml microfuge tube, centrifuged at $6,275 \times g$ for 10 min at room temperature, the used medium was discarded, and the cell pellet was resuspended in 1 ml fresh, sterile SN medium. The washed bacterial cells were then

added to a culture of CC9311 that had been grown still to log phase ($1.0\text{-}5.0 \times 10^7$ cells ml^{-1}). Heterotrophic bacteria were diluted to a final cell concentration of 1.0×10^6 cells ml^{-1} in the co-culture. The co-cultures were harvested after 24 hours via centrifugation as described above. The proteins were extracted and then analyzed for VBPO activity.

VBPO in Acarychloris marina

Acaryochloris marina strain MBIC11017 was grown in 500 ml cultures of SN medium supplemented with 250 nM sodium orthovanadate (Na_3VO_4) in 1 L flasks. Cultures were grown either still or stirred at 200 rpm with a magnetic stir bar (5.0 cm in length) from inoculation to late log phase as monitored by cell concentration, with the final cell densities at $1.0\text{-}2.0 \times 10^7$ cells ml^{-1} . Cell concentrations were monitored by flow cytometry (FACsort). Cultures (400 ml) were harvested via centrifugation as described above under *Protein Extraction* and resuspended in 1 ml 100 mM MES buffer, pH 7.0. VBPO activity was tested in protein extracts using 1) Thymol blue spectrophotometric assay, 2) native-PAGE, and SDS-PAGE as described above.

Induction of VBPO with grazers and associated bacteria

VBPO activity in CC9311 was also measured after exposure to several organisms known to consume *Synechococcus*. Grazers tested include *Oxyrrhis marina* (“Oxy”, S. Strom), a *Pteridomonas* clone (“Pt”, B. Palenik), a Choanoflagellate clone (“10tr”, B. Palenik), a Cercozoan (“Cerc”, B. Palenik), and *Goniomonas* sp. (“Go” S. Strom). Grazers were maintained in constant light at 23°C on F/2 medium supplemented with barley grains. Grazer cell counts were accomplished by staining 1 ml of culture with

DAPI (adding 30 μl of 10 $\mu\text{g ml}^{-1}$ DAPI stock and 20 μl of 25% glutaraldehyde to a final concentration of 0.5%, incubated overnight at 4°C) and counted via hemacytometer.

Grazers were diluted in 16 ml SN medium and added to a still culture of CC9311 (1.0×10^7 cells ml^{-1}) so that the final grazer cell concentration was about 5.0×10^3 cells ml^{-1} except for *Oxyrrhis marina*, for which live cells were counted via drop counts (in 4×10 μl drops) and diluted to 100 cells ml^{-1} . Grazers were counted again right after mixing as well as after 24 hours and are as follows for 0 and 24 hours respectively: the Choanoflagellate (14.8 to 7.4×10^3 cells ml^{-1}), *Cercozoan* (5.5 to 6.9×10^3 cells ml^{-1}), *Goniomonas* (3.70 to 4.6×10^3 cells ml^{-1}), *Paraphysomonas* (8.33 to 12.9×10^3 cells ml^{-1}), and *Pteridomonas* (4.6 to 6.4×10^3 cells ml^{-1}). *O. marina* cells could not be counted after the dilution by hemacytometer. After the addition of grazers, cultures were incubated for 24 hrs, then 200 ml of each co-culture were harvested and the extracted proteins were tested for VBPO activity. The filtrates (2.0 μm TTTP, Millipore) of *Pteridimonas* sp. and *Goniomonas* sp. were also added to CC9311 cultures to test induction by the bacterial fractions of the grazer cultures.

VBPO Inductions using PTB enrichment

A separate bacterial enrichment culture was started from the 1.2 μm filtrate of *Pteridomonas* in F/4 media amended with 2 barley grains, hereby after referred to as the Pt-bacterial (PTB) enrichment culture. A culture of the PTB bacterial enrichment was grown for 7 days, then mixed with CC9311 (grown to 3.7×10^7 cells ml^{-1}) and tested for VBPO activity. Cell counts of the PTB enrichment were not taken. The experiment was set up to determine whether it is the presence of heterotrophic bacteria inducing VBPO as

well as to demonstrate that the VBPO activity is coming from CC9311 and not the additional organism(s). To accomplish this, several treatments were set up. First, dilutions (1:5, 1:20, 1:100) of the PTB bacterial enrichment were added to CC9311. The 0.2 μm , “bacteria free” filtrate of the PTB enrichment was also added to CC9311. To determine if any potential signals (such as a peptide) were being removed by the filter, the PTB bacterial culture (40 ml) was centrifuged at 8,200 $\times g$ for 10 min at 18°C. Half (20 ml) of the supernatant was added directly to CC9311, the remaining half was passed through a 0.2 μm filter (Cellulose acetate, Thermo Scientific) and then added to a culture of CC9311. A 16s rRNA gene clone library was constructed from the cell pellet at this step and is discussed in the next sections.

To verify the source of VBPO activity, the PTB enrichment was added to SN medium as a control as well as to VMUT2 (grown to 5.2×10^7 cells ml^{-1}) that been washed in fresh SN to remove the kanamycin.

As an additional control, VBPO inductions were done using whole cultures of *Pteridomonas sp.*, the 2.0 μm (Millipore, TTTP) filtrate, representing the bacterial fraction, and the 0.2 μm (Cellulose acetate, Thermo Scientific) filtrate, representing the “bacteria-free” fraction. For these experiments, the treatment was added in a volume of 20 ml (diluted in F/4 when necessary) to 200 ml CC9311 in a 500 ml flask. After a 24 hour incubation, the cells were harvested and then the proteins were extracted and tested for VBPO activity.

Identification of bacteria in PTB enrichment

A 16S ribosomal RNA gene library was constructed to identify the diversity of the PTB culture. Cells from 40 ml of the PTB bacterial enrichment were centrifuged (8,200 xg, 10 min, 18°C) and the pellet was frozen at -20°C. The bacterial pellet was thawed on ice, resuspended in 400 ml TE buffer with 5 mM Na₂EDTA, and the genomic DNA was extracted as described in Brahamsha (1996). The 16S rRNA gene was then amplified using the universal bacterial primers 27F and 1492R (Table 1). PCR products were cloned directly into the PCR2.1 vector (Invitrogen) according to the manufacturer's directions, transformed into OneShot Top 10F competent cells, and plated on LB agar with 50 µg ml⁻¹ kanamycin. Plasmid DNA was isolated from 20 clones and the insert was sequenced using M13F-20 as well as the M13R primers.

Isolation of bacteria from Pt-Bacterial enrichment

To examine whether an individual strain was inducing VBPO activity in CC9311, bacterial colonies were isolated from the Pt-bacterial enrichment using several media types and plating methods. Serial dilutions of the PTB culture were made in autoclaved, 0.2 µm filtered seawater and spread on to 2216 (Difco) 1.5% agar (premixed), 2216/2 (half strength 2216) agar amended with SeaPlaque agarose to a final agar/agarose concentration of 1.5%, SWC (Ruby & Nealson, 1978) with 1.5% agarose, SWC/10 with 1.5% agarose, SN with 0.2% glucose, 0.05% tryptone (Brahamsha, 1996), and 1.5% agarose. Dilutions were also pour-plated in SN agar with 0.2% glucose and 0.05% tryptone. SeaPlaque agarose was used with all media types at 1.5% except with 2216 agar, which came pre-mixed at 1.5%. SN pour plates used 0.6% SeaPlaque agarose.

Colony PCR was used on the PTB isolates to amplify the 16S rRNA gene using the universal primers 27F and 1492R. PCR products were purified using the Qiaquick PCR Cleanup kit before direct sequencing using the universal 27F primer. Homologous sequences to the 16S rRNA gene of the isolates as well as the 16S rRNA library were identified using a blastn megablast search against the nucleotide collection (nr/nt) at <http://www.ncbi.nlm.nih.gov/> (Altschul *et al.*, 1997).

A neighbor-joining analysis was performed to compare the 16S rRNA genes from the 16S rRNA clone library of the PTB enrichment used for VBPO induction and the 19 strains isolated from the PTB enrichment. 16S rRNA genes from 20 clones, 19 strain isolates, and the top BLAST hits from representative groups were aligned in CLUSTALX v. 2.0 (Chenna *et al.*, 2003, Rambaut, 1996) and trimmed in SE-AL (Rambaut, 1996) to a 421 bp section downstream of the 27F primer region. A neighbor-joining analysis was performed in CLUSTALX and the tree was viewed in FigTree v. 1.3.1 (Rambaut, 2008).

VBPO inductions using PTB isolates

To determine if any individual bacterial isolates were responsible for VBPO induction in CC9311, each of the 19 PTB isolates were individually co-cultured with CC9311 for 24 hours as well as 7 days. For 24 hour experiments, PTB isolates were grown overnight in 50 ml cultures of 2216/2 liquid medium, at 23°C, with constant light. Cell counts were done by staining 1:100 dilutions of cultures in 1X SYBRgreen (Molecular Probes) and counting via hemacytometer. A portion of each culture (6-20 ml) was centrifuged (8,200 xg, 10 min, 18°C), the spent 2216/2 discarded, and each cell pellet was resuspended in 20 ml F/4 medium. The full 20 ml of each culture was then

added to 200 ml of CC9311 (3.0×10^7 cells ml^{-1}) so that the PTB isolates would be diluted to 1.0×10^7 cells ml^{-1} . After the 24-hour incubation, proteins were harvested from 200 ml cells and tested for VBPO activity. For 7 day co-culturing, PTB isolate cultures were grown for 2 days in 2216/2, then 0.2-1.2 ml of each culture was added directly to 100 ml CC9311. At the T=0, PTB isolates were diluted to 1.0×10^5 cells ml^{-1} and CC9311 cell concentration was 1.9×10^7 cells ml^{-1} in a 250 ml flask. After seven days, Optical density (750 nm) measurements were taken and proteins were harvested and then tested for VBPO activity.

iTRAQ Proteomics

A quantitative proteomics approach was used to determine the expression patterns of proteins in *Synechococcus* in response to stirring. Two separate experiments were performed using 1) *Synechococcus* CC9311 and VMUT and 2) CC9311 and VMUT2. Strains were grown in 2.0 L cultures of SN to exponential growth phase, and then divided into two 1.0 L cultures in 2.0 L flasks. One culture was subjected to stirring with a magnetic stir bar (5.0 cm) at 200 rpm for 4 hrs (trial 1) or 24 hrs (trial 2) while the other half remained still over the same period. At the end of the treatment, cultures were centrifuged at 13,175 xg for 10 min at 18°C, resuspended in 3 ml 100 mM MES buffer pH 7.0, and broken using the French Pressure cell. The extracts were subjected to centrifugation at 6,275 xg, 4°C for 10 min. The supernatant served as the protein extract used for iTRAQ quantification and for measuring VBPO specific activity.

Trypsin digested proteins for each treatment were individually labeled with unique iTRAQ isobaric mass tags (ABSciex) as described by Ross et al. (2004) and then

combined. Proteins quantification was carried out by the Biomolecular/Proteomics Mass Spectrometry facility at the University of California, San Diego.

Protein Pilot v. 4.0 software (AB-Sciex) was used to search sequenced peptides against the *Synechococcus* sp. CC9311 genome (GenBank accession number CP000435, including the amino acid sequence of the kanamycin cassette from pUC4K). Proteins with isobaric mass tag ratios greater than 1.2 or less than 0.8 with a corresponding *p*-value of less than 0.05 in any ratio were treated as significantly regulated. All proteins identified with at least one peptide (95% confidence) were considered for functional group analysis.

Results

VMUT Phenotype and VBPO expression patterns

To characterize the growth of VMUT compared to wild-type, cell counts, phycoerythrin autofluorescence, and VBPO activity were measured daily in cultures grown with and without stirring (Figure 3.3). Growth rate constants (k , d^{-1} ; Table 3.2) were similar when CC9311 and VMUT cultures were grown without agitation. However, the application of stirring prevented or severely inhibited the growth of VMUT, but not CC9311 in the first three trials. After several months of being maintained in constant light and no agitation, a fourth growth experiment was performed and VMUT grew at the same rate as WT with stirring. The VBPO⁻ genotype had not reverted as indicated by PCR (VBPO_{verif} F, VBPO_{verif} R, Table 3.1, Figure 3.5), suggesting that a secondary mutation occurred or the strain had become acclimated to the absence of VBPO by compensating with other proteins. This prompted the creation and use of a second

mutant, VMUT2. The first trial showed inhibited growth of VMUT2 with stirring compared to WT as well as final cell density two orders of magnitude less than other cultures (Figure 3.3 D, E). However, growth rates were comparable to CC9311 in the last two trials of VMUT2, started approximately one month apart (Table 3.2). All cultures were maintained in constant light without stirring between experiments.

VBPO activity was only detected in cultures of CC9311 (Figure 3.4, Figure 3.6). VBPO activity was greatest in cultures of CC9311 grown with continuous stirring, increasing from $0.035 \pm 0.034 \mu\text{mol min}^{-1} \text{mg}^{-1}$ in early log-phase to $0.176 \pm 0.080 \mu\text{mol min}^{-1} \text{mg}^{-1}$ in stationary phase (Figure 3.4). Inducibility of VBPO activity by short-term stirring (4 hrs) was greatest during exponential growth ($0.085 \pm 0.029 \mu\text{mol min}^{-1} \text{mg}^{-1}$). VBPO activity in the control culture (CC9311 that was grown still, transferred to a new flask, and then remained still for four hours) was detectable, having a maximum value of $0.016 \pm 0.011 \mu\text{mol min}^{-1} \text{mg}^{-1}$ in early stationary phase. No VBPO activity was detected in cultures of VMUT2 (Figure 3.4, Figure 3.6).

Protein extracts from growth experiments were separated by SDS-PAGE and stained for total proteins and VBPO activity (Figure 3.6). Banding patterns were similar between all treatments with the exception of a strong band at $\sim 140 \text{ kDa}$ in CC9311 that had been stirred from inoculation to stationary phase. This single band had strong VBPO activity indicated by staining with phenol red and was consistent in MW with previous work (Johnson *et al.*, 2011). A faint VBPO-active band was present when the culture was stirred for four hours while no comparable bands were visible in CC9311 grown without stirring. VMUT cultures grown still, with short-term stirring, or with long-term stirring lacked bands with VBPO activity.

VBPO activity was measured in protein extracts at time intervals over 72 hours after stirring was either applied or halted in log-phase cultures of CC9311 (Figure 3.7). When stirring is applied to a log-phase, still-grown culture, VBPO activity was detected after two hours and increased exponentially over the 48 hrs, with an r^2 of 0.98 when fit to the exponential growth equation compared to an r^2 of 0.91 when fit to a linear regression in GraphPad (Prism), and then continued to accumulate. No activity was detected in the culture that was grown and remained still (Figure 3.6A). When stirring was halted in a log-phase culture that had been stirred from inoculation, VBPO specific activity (normalized to mg protein) remained stable for 12 hr and then gradually decreased, but VBPO activity normalized to the culture volume remained nearly constant. VBPO specific activity continued to increase in the control culture that was stirred constantly from inoculation (Figure 3.7B).

VBPO induction cues

A variety of conditions and stresses were applied to cultures of *Synechococcus* CC9311 to determine the nature of VBPO induction as detailed above. Conditions and VBPO activities are provided in Table 3.3.

1) *Physical agitation*

Physical agitation in the form of stirring was the strongest inducer of VBPO activity, which ranged from about 0.003 - 0.0319 $\mu\text{mol min}^{-1} \text{mg}^{-1}$ after four hours of stirring.

Cultures subjected to shaking induced VBPO activity, but only to 25% of the stirred control. The application of laminar shear stress from a Couette chamber (see

methods) at a shear stress of 10 s^{-1} caused a slight induction ($0.00174 \pm 0.0002 \mu\text{mol min}^{-1} \text{ mg}^{-1}$) over the still control based on a t-test. Shear stress failed to induce VBPO from shear rates of 50 s^{-1} , 100 s^{-1} , and 1000 s^{-1} .

2) *Gas Exchange*

Stirring in the absence of a headspace induced VBPO activity by the same amount when compared to the positive, stirred control. There was no induction of VBPO activity when a culture remained still with no headspace. When cultures were gently bubbled with air, VBPO activity was the same within error as the still control. However, when the culture was bubbled, there was noticeable clumping of the *Synechococcus* culture near the air outlet (Table 3.3).

3) *Light*

Cultures were exposed to physical agitation (both stirring and shaking) in the presence and absence of light. When light became a factor with physical agitation, 3.8 times more VBPO activity was detected after four hours of stirring in the light ($0.0319 \pm 0.0021 \mu\text{mol min}^{-1} \text{ mg}^{-1}$) compared to four hours of stirring in the dark ($0.0083 \pm 0.0005 \mu\text{mol min}^{-1} \text{ mg}^{-1}$). Similarly, 2.7 times higher induction was observed after four hours of shaking in the light compared to shaking in the dark. Still cultures exposed to dark conditions had no induction of VBPO activity.

4) *Cell wall stress*

Osmotic shock, by adjusting the culture medium to 50% or 125% seawater salinity, did not induce VBPO in still cultures. Stirring under hyperosmotic (125% seawater salinity) conditions induced VBPO activity similarly to stirring in normal SN medium (75% Seawater). Stirring under hypoosmotic conditions did induce VBPO

activity ($0.0009 \pm 0.0005 \mu\text{mol min}^{-1} \text{mg}^{-1}$), though 16 times less than the positive, stirred control. Cell viability under hypoosmotic conditions was not tested after the induction period. Neither exposure to $10 \mu\text{g/ml}$ ampicillin nor the addition of broken *Synechococcus* cells induced VBPO activity in CC9311 after 24 hours.

5) *Oxidative stress*

VBPO activity was not present after cultures were exposed to oxidative stress from $25 \mu\text{M}$ hydrogen peroxide or $0.1 \mu\text{M}$ methyl viologen (Table 3.3, Figure 3.9).

6) *Addition of heterotrophic bacteria*

No VBPO activity was observed when *Alteromonas* TW7 was co-cultured with CC9311 for 24 hours. Activity was detected when Marine Bacterium TW6 was co-cultured with CC9311 for 24 hours ($0.0014 \mu\text{mol min}^{-1} \text{mg}^{-1}$), but the activity was less than the still control so induction was not observed. Similarly, no upregulation of VBPO activity was observed in *Silicibacter* TrichCH4B co-cultures.

VBPO and resistance to hydrogen peroxide

Cultures of CC9311 and VMUT or VMUT2 preconditioned with and without stirring to induce VBPO were tested for resistance to hydrogen peroxide (Figure 3.7) by monitoring phycoerythrin autofluorescence and cell counts after exposure of log-phase cultures to varied concentrations of hydrogen peroxide. In the first trial, CC9311 grown with stirring from inoculation was able to recover, as judged by an increase in phycoerythrin autofluorescence, after the addition of hydrogen peroxide at $50 \mu\text{M}$ while cultures of CC9311 and VMUT grown still lost PE fluorescence. In the second trial, cultures of VMUT2 and CC9311 were grown with and without stirring from inoculation.

Both CC9311 and VMUT2 were resistant to H₂O₂ at 100 μM while cultures grown without agitation were sensitive at 100 μM. Trial 1 was performed when VMUT was sensitive to stirring, about 2 months after verification, while Trial 2 was performed after the period in which VMUT2 was sensitive to stirring, about 6 months after verification.

VBPO in Acaryochloris marina

Acaryochloris marina cultures grew to late exponential phase in SN media, at similar growth rates for both the stirred (0.53 day⁻¹) and still (0.61 day⁻¹) cultures. Growth curves are shown in Figure 3.10. Cells grew visibly clumpy in the still culture relative to the stirred cultures in both trials. Proteins were extracted from both stirred and still cultures and specific VBPO activity was determined using the thymol blue assay (Table 3.5). In the first trial, VBPO activity was only detected in the stirred culture (0.063 ± 0.006 μmol min⁻¹ mg⁻¹), while no activity was found in the still culture. In the second trial, four times more VBPO activity was found in the stirred culture compared to the still culture.

When proteins from trial 2 were separated using native-PAGE gel electrophoresis and stained for VBPO activity, a single band that migrated the same distance as CC9311 VBPO had VBPO activity and was present in both the still and stirred cultures (Figure 3.11), with a more intense band in the stirred culture, agreeing with the specific activities. *A. marina* proteins separated via SDS-PAGE and stained with phenol red did not show any bands with VBPO activity in contrast to CC9311 and the *C. officinalis* controls. However, there was a protein band at the same MW as the denatured *C. officinalis* VBPO (Figure 3.12)

VBPO activity in response to grazers

Pteridomonas sp. and the 2.0 μm filtrate from *Pteridomonas* sp. were the strongest inducers of VBPO activity (0.011 ± 0.005 , $0.022 \pm 0.0002 \mu\text{mol min}^{-1} \text{mg}^{-1}$, respectively; Table 3.4), showing up to 15% VBPO activity of the stirred control. *Goniomonas* sp. as well as the 2.0 μm filtrate of the *Goniomonas* sp. culture also induced VBPO activity (0.006 ± 0.0003 , $0.005 \pm 0.0002 \mu\text{mol min}^{-1} \text{mg}^{-1}$, respectively; Table 3.4), but less than *Pteridomonas* sp. *Oxyrrhis marina* also induced VBPO activity ($0.002 \pm 0.00008 \mu\text{mol min}^{-1} \text{mg}^{-1}$), but less than the other induced treatments. No VBPO activity was detected when the cercozoan or the choanoflagellate were mixed with CC9311.

VBPO induction in response to a bacterial assemblage

VBPO was strongly induced in CC9311 when the culture was mixed with a non-axenic culture of *Pteridomonas* as well as the PTB bacterial enrichment (PT-bacteria) derived from the 1.2 μm filtrate of the same *Pteridomonas* culture, but maintained separately (Table 3.3). The 2.0 μm filtrate from both of the *Pteridomonas* and PTB cultures also induced VBPO activity in CC9311. Similarly, VBPO activity was induced less as greater dilutions of the PTB enrichment were added to CC9311. VBPO activity was not induced when CC9311 was mixed with the 0.2 μm filtrate of the *Pteridomonas* culture. When the PTB enrichment culture was centrifuged and the supernatant was added to CC9311, VBPO activity was induced. However, if the supernatant from the PTB enrichment was filtered through a 0.2 μm filter, it no longer induced VBPO in CC9311.

Furthermore, no VBPO activity was detected when the PTB enrichment was added to cultures of VMUT (stirred or still) or to SN medium.

Sequencing of a 16S rRNA gene library (20 clones) from a culture used for VBPO induction revealed two dominant groups of bacteria, *Alteromonas* sp. (gamma-proteobacteria) and a group of alpha-proteobacteria (neighbor-joining tree in Figure 3.13; Alignment in Figure 3.14).

Nineteen bacterial strains were isolated from the PTB enrichment (Table 3.7) on a variety of media. When 16S rRNA genes were sequenced, all isolates matched closely to either alphaproteobacteria (PTB isolates 3, 7, 10, 11, 12, 13, 14, 15, 16, 17, 18, and 19) or gammaproteobacteria (PTB isolates 1, 2, 4, 5, 6, 8, and 9). A neighbor-joining analysis was performed on a 480 bp region of the 16S rRNA gene, including the sequences from the 16S rDNA gene library, the bacterial isolates, and the closest BLAST hits of each group (Figure 3.13). Three groups of alpha-proteobacteria were abundant in the cultured isolates but not detected in the 16S rDNA clone library from the assemblage, suggesting a lower abundance. The alpha-proteobacteria also grew more slowly in F/4 media (Table 3.7).

Isolates from the PTB enrichment did not induce VBPO activity when individually co-cultured with CC9311 in both short term (24 hr) and long-term (7 day) exposures. VBPO activities from the 24 hour exposures are shown in Table 3.7.

iTRAQ proteomics

A quantitative proteomics approach was applied to evaluate the response of *Synechococcus* to stirring. Proteins were extracted from CC9311 and VMUT after 4 hr

(trial 1) and CC9311 and VMUT2 after 24 hr (trial 2), and quantified using iTRAQ proteomics. A total of 102,888 and 55,234 spectra were analyzed from each experiment, respectively, with 17,408 and 35,444 aligning to peptides with at least 95% confidence. In the first experiment, 1,293 proteins were identified with at least one peptide and 1,108 proteins were significantly identified with 2 or more peptide hits, of which 30 proteins had iTRAQ ratios with a p-value less than or equal to 0.05. In the second trial, 1,173 proteins were identified with at least one peptide, 989 proteins were significantly identified with 2 or more peptides, of which 73 proteins had an iTRAQ ratio with a p-value of less than or equal to 0.05. Results are summarized in Table 3.6. A full list of proteins identified with iTRAQ mass tag ratios for each treatment is available in Appendix 1.

Proteins with an iTRAQ mass tag ratio with a p-value of ≤ 0.05 were considered significant by convention. To determine regulation patterns, proteins with a ratio of greater than 1.2 or less than 0.8 were considered significantly upregulated or down regulated, respectively, by using the 5th and 95th percentiles. Proteins with a significant p-value within at least one ratio are listed in Table 3.9. VBPO activity was seen only in CC9311 stirred cultures and no VBPO activity was found in VMUT cultures (Table 3.8).

Synechococcus response to stirring

VBPO (Sync_2681) was the most upregulated protein with stirring in CC9311 after 4 hours and the second most upregulated after 24 hours (iTRAQ ratios of 2.71 and 8.29, respectively). The only protein with a greater change than VBPO after 24 hours of stirring was a conserved hypothetical, sync_1122 (up 8.493 in stirred CC9311). Proteins that were regulated in response to stirring across all treatments at both 4 hours and 24

hours were a beta-lactamase (sync_0349) and a ferritin (sync_0854). Other proteins uniquely upregulated in WT included a structural RTX toxin protein (sync_1217), a glutamyl tRNA reductase (sync_1686), and transcription related proteins, such as the subunits for DNA directed RNA polymerase.

Among the proteins down regulated in CC9311 after 24 hrs of stirring were an iron ABC transporter (sync_1545), a urea transporter (sync_2872), a hypothetical protein (sync_1097), and a DNA binding protein HU (sync_2191). The only proteins down regulated in both CC9311 and VMUT after 24 hr was a HlyD secretion protein (sync_1216). A protein annotated as a peroxiredoxin (sync_0689) also had a significant p-value and a ratio (0.822) close to the cut-off for being significantly down regulated.

Mutant reaction to stirring

Proteins uniquely upregulated in VMUT after 24 hours include a Clp protease (sync_2135; ratio: 1.207), a glycerol kinase (sync_0569, ratio: 1.204), and a conserved hypothetical (sync_2099, ratio:1.202). Only two proteins had an iTRAQ ratio below 0.8 after 24 hr in the mutant with a significant p-value; HisF, an imidazole glycerol phosphate synthase (sync_0176; ratio: 0.778) and the transporter Hlyd (sync_1216; ratio: 0.779). Two other proteins of interest that had a significant p-value and were close to an iTRAQ mass tag ratio of 0.8 in down-regulation were a preprotein translocase (sync_0086, ratio: 0.808) and a 2-isopropylmalate synthase (sync_0976, ratio: 0.804).

A broader perspective was taken for characterizing functional protein groups. Lists of regulated proteins were generated by taking all proteins with at least one peptide as well as an iTRAQ-ratio greater than 1.2 (upregulated proteins) or less than 0.8 (down regulated proteins). The GI accession numbers were then submitted to DAVID, an online

tool for grouping functionally related genes based on annotations (Huang *et al.*, 2009a, Huang *et al.*, 2009b). Categories of enriched functional groups are summarized in Table 3.10 and refer to results from the Functional Gene Categories tool, analyzed under high stringency. Protein functional groups with an Enrichment Score greater than 1.3 (corresponding to a $p \leq 0.05$) are considered to be significantly enriched in the list of genes.

After four hours of stirring in the wild type, several functional groups were enriched in upregulated proteins. The most enriched group annotated as having “peroxidase” functions included VBPO (sync_2681), a bacterioferritin comigratory protein (sync_2508), and hypothetical sync_0262. Other groups had metal ion binding (10 proteins including sync_0680, sync_2888, and sync_2861), iron binding (5 proteins) and a group of 5 thylakoid related proteins. After 24 hours of stirring, groups enriched in upregulated proteins included ion binding proteins (32 proteins), e- transport type proteins, transcription (DNA directed RNA polymerase genes), and 4 haemolysin (RTX) related proteins (sync_1039, sync_1217, sync_1260, sync_1129).

In the mutant, iron (8 proteins including sync_0854) and metal binding related (15 proteins) proteins were the only categories significantly enriched in proteins upregulated after four hours. Proteins upregulated in VMUT after 24 hours of stirring were enriched for proteins with cell wall related functions, including sync_2009, sync_0746, sync_2543, and sync_0734.

When the stirred CC9311 is compared to the stirred VMUT after 24 hours, cell wall and cell envelope related proteins as well as polysaccharide biosynthesis proteins

were significantly enriched in the mutant, including sync_0632 (MurE), sync_0150, sync_0162, and sync_2543, sync_0734.

Discussion

This study investigated the physiological function of vanadium-dependent bromoperoxidase in *Synechococcus* sp. CC9311. We found VBPO activity to be highly induced by physical agitation in the form of stirring or shaking. In growth experiments, VBPO activity was only found in stirred CC9311 cultures, and not in still cultures, though stirring did not affect the growth rate.

When the gene for VBPO (sync_2681) was selectively inactivated, stirring inhibited the growth of both VMUT and VMUT2 in initial growth curves (Figure 3.3 and Table 3.2). This striking phenotype was investigated further by monitoring VBPO activity under the following conditions, testing its role as an antioxidant and/or defense enzyme.

VBPO Induction Cues

Physical agitation from stirring or shaking caused a strong induction of VBPO activity. In response to stirring, VBPO activity increases rapidly over the first 48 hr (Figure 3.7). VBPO activity increases through the growth of a culture under constant stirring, becoming an abundant protein when visualized by SDS-PAGE (Figure 3.6) and quantified through iTRAQ, (Table 3.9). This indicates that the expression is not a short-term response (stress), but rather a response to a continuous cue.

Turbulence created by a rotational shaking plate has a low shear rate as calculated in Sahoo *et al.* (2003). Cultures in a flask had one-third VBPO activity after 4 hours of shaking at 120 rpm on a rotational shaking plate compared to cultures that were stirred at 200 rpm with a magnetic stir bar. Both of these conditions create turbulence in the liquid medium, though shaking in particular produces a very low laminar shear rate (0.028 s^{-1} , Sahoo *et al.*, 2003). It is hypothesized that particles less than 1 mm in length experience turbulent flows as laminar shear force (Guasto *et al.*, 2012). However, when cultures were incubated in Couette chambers used to apply a steady, laminar shear force, no VBPO activity was observed after 4 or 6 hours except for a small induction when a shear rate of 10 s^{-1} was applied. Along with the strong induction with shaking (low shear) this may suggest that turbulence, but not shear is an induction cue for VBPO.

The role of gas exchange was examined in order to determine whether the observed VBPO activity was resulting from a chemical change in the culture medium rather than the physical force. However, VBPO activity was present after four hours of stirring regardless of the presence of headspace. Eliminating the headspace prevents gas exchange, and therefore would prevent any major chemical shifts with the application of stirring, for example a decrease in oxygen supersaturation or an increase in CO_2 . Inversely, slow bubbling was used to increase gas exchange for the reasons described above, with a low shear (though shear rate for the bubbling was not estimated in this study). VBPO activity was not found in CC9311 that had been bubbling with lab air. These experiments suggest that the effects of gas exchange are not a likely cause of VBPO induction in *Synechococcus*.

VBPO and oxidative stress

VBPO reduces hydrogen peroxide to water as the initial step in the enzymatic reaction (Carter-Franklin & Butler, 2004). VBPO is thus hypothesized to act as an antioxidant, detoxifying metabolically produced or exogenous hydrogen peroxide (Manley, 2002). When hydrogen peroxide was added to still cultures of CC9311 at sublethal concentrations (25 μM), no VBPO activity induction was observed. The same was true for the oxidant, methyl viologen, which increases intracellular levels of superoxide (Krieger-Liszkay *et al.*, 2011).

This indicates that antioxidant activity may be ancillary and not a primary function of VBPO in *Synechococcus*. One consideration, however, is that VBPO activity is 3 times greater after four hours of stirring in the light compared to four hours of stirring in the dark. The same pattern was true for shaking flasks, indicating that photosynthesis may be important, but not required for the induction of VBPO. The energy requirement for the increased synthesis of VBPO is likely dependent on photosynthesis.

While increased oxidant concentrations did not induce VBPO activity, CC9311 was more resistant to hydrogen peroxide as a response to stirring. However, VMUT could resist H_2O_2 at the same concentrations as CC9311 when stirred. While the ability to withstand the H_2O_2 shock seems to be more related to preconditioning of a culture with stirring and not the presence of VBPO specifically, whatever secondary mutation allows the mutant to grow with stirring may also affect resistance to hydrogen peroxide.

The effects of hydrogen peroxide concentrations used in this study were comparable those in another marine cyanobacterium. *Synechococcus* WH7803 was found to recover after exposure to 25 μM H_2O_2 after preconditioning with highlight, but the

same concentration was ultimately toxic to cultures preconditioned to low light (Blot *et al.*, 2011). Methyl viologen concentrations as low as 1 μM were also found to be toxic to this strain over three days. This same study also found that the global transcription response as determined by microarray analysis was similar for both hydrogen peroxide and methyl viologen, and included an upregulation in PSII proteins, DNA repair proteins, chaperones (clpB_2377, clpP3, P4, and dnaK_1246), and several ROS detoxification proteins (sodC, thioredoxin, glutaredoxin and glutathione genes). Catalase, KatG, was only found to be upregulated under low light conditions in the presence of oxidants. In another study, cells of a freshwater cyanobacterium, *Synechococcus* sp. PCC 7942, remained viable 24 hours after exposure of up to 4.5-6.0 mM H_2O_2 (Perelman *et al.*, 2003), about three orders of magnitude greater than used in this study.

Proteins related to oxidative stress in the CC9311 genome based on annotations and specifically pertaining to H_2O_2 detoxification include glutathione peroxidase (sync_0096), thioredoxin peroxidase (sync_1322), and a putative peroxidase in the same genetic island (sync_2673) as VBPO. Thioredoxin peroxidase (sync_1322) was present (29 peptides after 4 hrs and 41 peptides after 24 hours), but it was not significantly regulated with stirring in either CC9311 or VMUT. Sync_0096 was also present in the iTRAQ data, but was not regulated with stirring in CC9311 or VMUT. The putative peroxidase, sync_2673 was not found in the iTRAQ data set. There are no putative catalases annotated in the CC9311 genome. Interestingly, an annotated peroxiredoxin (sync_0689) was slightly down regulated (0.822, p-value of 0.022) in CC9311 after 24 hrs of stirring. Peroxiredoxins can have peroxidase activity (Rhee *et al.*, 2001). As this protein was not significantly up- or downregulated in VMUT at any time point, it most

likely is not compensating for VBPO in the mutant. More work should be done to determine if VBPO is a tradeoff for sync_0689 in the stirred WT.

VBPO induction in response to bacteria

A marine bacterial assemblage, the PTB bacterial enrichment, induced VBPO activity 56-fold over control cultures in CC9311 over 24 hours (Table 3.3). No VBPO activity was observed in the negative controls, which included PTB bacterial enrichment incubated in SN medium as well as the PTB bacterial culture added to VMUT, indicating that CC9311 was the source of observed VBPO activity and not the PTB bacterial enrichment. Among the 19 clones isolated from the assemblage, none induced VBPO activity when co-cultured individually with CC9311 after 1 day or 7 days. Similarly, when all of the isolates are mixed and then added to CC9311, VBPO activity was not present. A neighbor joining analysis showed that PT-bacterial isolates were highly representative of the PTB assemblage seen in the clone library (Figure 3.12). Alpha- and gamma-proteobacteria were the two groups present in both the 16S rRNA clone library as well as the 19 PTB isolates. There was only one group, related to *Alteromonas* (BCw156 group), that was present in the 16S library but not represented in the isolates. There were three alpha-proteobacterial groups that were enriched in the isolates but not present in the 20 clones from the 16S library. This enrichment was likely due to alpha-proteobacteria preferentially growing on the nutrient rich media used for isolation. Six of the 19 isolates clustered with the 16S rRNA gene of *Alteromonas* S1080. The genome of a closely related (*Alteromonas* SN2, 99% identities of 16S rRNA gene) has an annotated nitrate reductase (accession AEF04544.1) which may explain the observed dominance of this

group when grown in F/4 media, used to maintain both the enrichment and the original source *Pteridomonas* culture. Induction of VBPO did not seem to be related to cell density, as the heterotrophic bacterial cultures as well as the PTB isolates were all added at approximately 1.0×10^6 cells ml⁻¹ at the start of each incubation.

VBPO in Acaryochloris marina

VBPO activity was detected in a cultures of *A. marina* and was greater in stirred cultures than in still cultures (Table 3.5). When gel-based VBPO activity assays were used, VBPO activity was observed in proteins separated under native conditions (Figure 3.10) but not with denaturing conditions (Figure 3.11).

VBPO is known to be a thermally stable protein (Krenn *et al.*, 1989), and the activity of VBPO is preserved in *Synechococcus* proteins under denaturing conditions (Johnson *et al.*, 2011). *Am*VBPO runs at an unexpectedly large size (220 kDa) similar to both the *Syn*VBPO and the *Co*VBPO standard. This could be the result of a protein complex or the result of the protein not fully denaturing in the conditions of the assay (Johnson *et al.*, 2011). *A. marina* has two genes predicted to be VBPO with a 2 kDa difference in size (68 kDa vs. 70 kDa). The resolution on either gel was not great enough to differentiate these proteins. It is unclear which, or if both genes are expressed and functional VBPOs.

Some strains of *A. marina* grow epiphytically on red algae (Chan *et al.*, 2007) which have multiple vanadium chloro- and bromo-peroxidases. Such a close ecological association may provide insights into gene function as well as gene origin. This physical proximity may have provided the opportunity for an exchange of VBPO from red algae to

A. marina, or cyanobacteria to red algae. While VBPO activity was detected in *A. marina* under similar conditions to CC9311 (stirring), the amount of VBPO specific activity was less than CC9311. While VBPO activity was detected under still conditions in *A. marina* in one trial, the strain was not axenic as obtained from the Roscoff culture collection.

iTRAQ proteomics

The use of iTRAQ in *Synechococcus* is a valuable molecular tool, quantifying a large portion of the proteome. Stirring elicits a strong induction of VBPO activity and was thus chosen as the condition to apply to cultures to investigate the role of VBPO in *Synechococcus*. In the two experiments, 37.6% and 33.6% the 2,944 predicted ORFs in the CC9311 genome were identified, comparable to the upper-end of proteome coverage in other prokaryotic studies. A recent iTRAQ study identified 19.6% of the theoretical proteome of *Synechocystis* PCC6803 as expressed proteins (Battchikova *et al.*, 2010). The same study summarized other bacterial proteomic studies, finding 13-27% proteome coverage. Only several genes were highly regulated with the application of stirring for 24 hours. VBPO was the most up-regulated gene after 4 hours and the second most up-regulated gene after 24 hours (iTRAQ ratios of 2.6 and 8.294, respectively). The most upregulated gene in CC9311 after 24 hours was sync_1122 (8.493) and was also upregulated in VMUT (2.361). Sync_1122 has a homologue in the draft genome *Synechococcus* WH8016 (84% protein identities, ZP_08956950), a closely related clade I strain of *Synechococcus* that lacks VBPO. Sync_1122 is characterized only as having two low-complexity repeat domains (MicrobesOnline).

The most upregulated protein with stirring found in both CC9311 and the mutant at both time points was a putative β -lactamase (sync_0349), a gene lacking homologues in other marine cyanobacteria. The closest homologue to sync_0349 is a beta-lactamase in *Myxococcus xanthus* DK1622 (accession YP_630373.1, 36.2% identities). The expression patterns of the homologue in *Myxococcus* are related to exposure to lactam antibiotics, and hypothesized to play a role in cell-wall restructuring (O'Connor & Zusman, 1999). This led to our testing of ampicillin on VBPO activity, but we found no effect.

Another protein that was significantly up-regulated across treatments was the ferritin sync_0854. This gene bears a 100% identities at the amino acid level to two other annotated ferritins (sync_1077 and sync_0687) in the genome of CC9311. While it is clear that there is a real increase in these peptides in stirred cultures compared to still cultures, it is not possible to determine which ferritin the peptides belonged to; as such, ProteinPilot allotted all (8) ferritin peptides to sync_0854 and not to the other two annotated genes, which created the ratio shown. In a previous experiment (Johnson *et al.*, 2011) proteins from CC9311 were separated via SDS-PAGE and a band showing VBPO activity was excised and sequenced. While the sequenced peptides were primarily from VBPO (sync_2681), a few peptides were from the ferritin, sync_1539 (Johnson *et al.*, 2011). Though sync_1539 has 47% identities to sync_0854 at the amino acid level, the peptides of sync_1539 detected using iTRAQ were not peptides that could have supported the ratios shown for sync_0854, making it unlikely that the findings from the gel experiment correlate to the iTRAQ results. Thus further analysis with quantitative RT-PCR is necessary to determine which ferritin, if not sync_0854, is upregulated with

the application of stirring. Because sync_0687 is next to a down regulated protein, sync_0677, it might be that this is the regulated ferritin.

Functional gene categories

VMUT2 (tag ratio 118/117 at 24 hr) had increased abundance of proteins related to cell wall synthesis and membrane related proteins after 24 hours of stirring (Table 3.9), but no apparent increase in expected stress related proteins such as heat shock proteins (hsp) or other chaperones such as GroEL or dnaK as predicted by proteomics studies on another cyanobacterium, *Synechocystis* sp. PCC 6803 (Castielli *et al.*, 2009). Cell wall related proteins were also significantly enriched in genes more abundant in stirred VMUT compared to stirred CC9311 after 24 hours (Mass tag ratio: 118/116). This is unlikely the result of kanamycin, which inhibits the ribosome processes, making an increase in translation-related proteins expected. Kanamycin would not explain the increase in cell wall related proteins.

There are a few caveats to consider in the functional gene category analysis using DAVID. The first is that the functional redundancy in gene annotations can cause a gene to appear in multiple categories, potentially leading to a bias for the enrichment of particular functions. The second consideration is that the gene lists used included proteins with only a single peptide hit. This was done intentionally to gain a broader perspective from the data set, however, this does mean that more scrutiny must be taken within each category for statistical significance. The final caveat is that hypothetical proteins that lack any annotations or known domains are not included in the analysis.

Genes in the HGT genetic islands were among the most highly regulated proteins detected in this study, however, expression of these genes within a single island varied dramatically. A large proportion, 23%, of all proteins identified in this study are annotated as hypothetical, similar to a previous iTRAQ study in *Synechocystis* finding 32% (Battchikova *et al.*, 2010).

General Discussion

Moderate stirring is a common culturing technique aimed at increasing gas exchange and does not affect the growth rate of CC9311 under the conditions tested. However, it has a dramatic effect on the expression of certain proteins as determined by quantitative proteomics. There are several known effects of fluid dynamics on bacteria. Bacterial response to small- scale turbulence can increase cell size and volume (Malits *et al.*, 2004, Malits & Weinbauer, 2009). In another study, there was a correlation between oxidative stress and the application of shear rates from 445-1482 s⁻¹ in *Bacillus subtilis* (Sahoo *et al.*, 2003, Sahoo *et al.*, 2006). One primary mechanism of prokaryotic mechanosensation is osmotically controlled, stretch-activated mechanosensitive ion channels (Martinac, 2004). There is a mechanosensitive ion channel (sync_2685) four ORFs downstream on the lagging strand from VBPO, but within the same HGT island. Sync_2685 was identified in the iTRAQ data sets, but did not have any differential expression patterns in response to stirring or in WT or the mutants.

It has been calculated that small particles (< 1.0 mm) experience a turbulent fluid environment as laminar shear based on Kolmogorov's eddy diffusivity predictions as summarized in a recent review (Guasto *et al.*, 2012). This review also discusses bacterial

response to shear as unlikely, citing two recent studies that did not find a bacterial response to shear stress applied in microfluidic chambers, though the body of knowledge of the effects of fluid dynamics on microorganisms is still growing. For example, mechanotransduction in bacteria results in biofilm formation in response to fluid shear (Weaver *et al.*, 2012). Gravity has also been proposed to serve as an induction cue in bacteria; microarray experiments characterized the response of *Staphylococcus aureus* to a low shear, simulated in microgravity conditions induced by a rotating wall chamber. Three strains showed a decrease in secreted proteins as well as a cell-wall stress protein (Nickerson *et al.*, 2003).

Allelopathy is an interaction in which one organism negatively impacts a competing organism through the use of chemicals, traditionally referred to in plant interactions (Ianora *et al.*, 2011). VBPO may play a role in allelopathic interactions in eukaryotic macroalgae. For example, it has been previously shown that the production of bromoform, a brominated product linked to VBPO, plays an allelopathic role in defense against epiphytic diatoms (Ohsawa *et al.*, 2001). This is based on the observation that live algae, which produce bromoform, could resist the growth of epiphytes compared to dead algae, which could not. Ohsawa *et al.* (2001) then showed that passing vaporized bromoform through a hydrophobic filter prevents the growth of epiphytes on the filter when submerged in natural seawater. It has also been shown that brominated products from algae have antibacterial effects (Weinberger *et al.*, 2007, Paul *et al.*, 2006). While the role of VBPO as an allelopathic enzyme in *Synechococcus* CC9311 was not shown in this study, future work should focus on this aspect of the enzyme using natural marine bacterial assemblages.

Conclusions

In this study, we found vanadium-dependent bromoperoxidase activity in *Synechococcus* CC9311 was rapidly and significantly induced in response to stirring or shaking of cultures, but not laminar shear or oxidative stress. We also found VBPO activity in CC9311 after exposure of to a bacterial assemblage, but not individual strains isolated from that enrichment, suggesting an ecological role for this enzyme. It is still not clear if VBPO is induced by the same mechanism under stirring or exposure to the bacterial assemblage. The use of iTRAQ proteomics showed significant upregulation of a beta-lactamase with stirring as well, with homologues that have functions relating to cell wall restructuring. This is further supported by an enrichment of cell wall related proteins in the stirred mutant, found by bioinformatics analysis. Our results indicate that VBPO may play a role in responding to cell wall stress as well as to interactions with heterotrophic bacteria. It does not appear to function as an antioxidant enzyme.

Acknowledgements

This research was funded by National Science Foundation grant IOS-1021421 to B.P and B.B and OCE-0648175 to B.P. and B.B. We would like to thank for M. Latz for advice and equipment and thank you to M. Ghassemian at the UCSD Biomolecular/Proteomics Mass Spectrometry Facility for help with the iTRAQ analysis.

Table 3.1: List of primers used in the construction and verification of the insertional gene inactivation for VMUT and VMUT2, as well as the universal primers used with the PTB enrichment.

Name	Sequence	Use
VBF	5' - CATCACGCCAGAGCAAGGCT	VMUT construct, PCR
VBR	5' - GAACTTTTGGTAGCGCACGGCC	VMUT construct, PCR
VBPO Verif F	5' - CAGCAGCAATCAACTCGACGC	VMUT genotyping
VBPO Verif R	5' - AGCGACTGATTGTGATTGCG	VMUT genotyping
9311 RPOC F	5' -CCCTTACTGCCAGCAATCTC	PCR Control
9311 RPOC R	5' - TGAAAGGGATYCCCAGTTATGT	PCR Control
pBR322 Forward a	5' - TAGGCGTATCACGAGGCC	VMUT genotyping
pBR322 Reverse a	5' - GGTGCCTGACTGCGTTAG	VMUT genotyping
VBPO Verif 2F	5' - CATCGGCAATGCCAGTCC	VMUT genotyping
27F	5' - AGAGTTTGATMTGGCTCAG	16S library
1492R	5' - TACGGYTACCTTGTTACGACTT	16S library

Table 3.2: Growth rate constants (k , day⁻¹) of CC9311 and VMUT (shaded) and CC9311 and VMUT2 (not shaded) under still and stirred conditions.

	Trial 1	Trial 2	Trial 3	Trial 4
9311 Still	-	0.295	0.538	0.554
9311 Stir	0.370	0.433	0.543	0.477
VMUT Still	-	0.428	0.552	0.451
VMUT Stir	0.000	0.066	0.014	0.486
9311 Still	0.606	0.628	0.514	0.658
9311 Stir	0.648	0.563	0.412	0.658
VMUT2 Still	0.232	0.534	0.606	0.632
VMUT2 Stir	0.064	0.218	0.573	0.653
VMUT2 Stir (Revived)	-	-	-	0.678
VMUT2 Still (Revived)	-	-	-	0.625

- Treatment not measured in that experiment

Table 3.3: VBPO activities measured in *Synechococcus* sp. CC9311 after exposure to different conditions and stresses.

Treatment	Specific activity $\mu\text{mol dibromothymol blue min}^{-1} \text{mg}^{-1}$	Stir $\mu\text{mol dibromothymol blue min}^{-1} \text{mg}^{-1}$	Still $\mu\text{mol dibromothymol blue min}^{-1} \text{mg}^{-1}$	VBPO Induction
<u>Physical Stress</u>				
Stirring, Light	0.0319 ± 0.0021	0.0319 ± 0.0021	0.00098 ± 0.0001	Yes
Stirring, Dark	0.0083 ± 0.0005	0.0319 ± 0.0021	0.00098 ± 0.0001	Yes
Shaking, Light	0.0079 ± 0.0001	0.0319 ± 0.0021	0.00098 ± 0.0001	Yes
Shaking, Dark	0.0029 ± 0.00009	0.0319 ± 0.0021	0.00098 ± 0.0001	Yes
Still, Dark	0.0009 ± 0.00014	0.0319 ± 0.0021	0.00098 ± 0.0001	No
Shear rate (s⁻¹)				
10	0.00174 ± 0.0002	0.00732 ± 0.0006	0.00109 ± 0.00012	Yes*
50	0.00147 ± 0.000216	0.00732 ± 0.0006	0.00109 ± 0.00012	No*
100	0.00002 ± 0.00002	0.003 ± 0.0002	0.0001 ± 0.00007	No
1000	0.00041 ± 0.00008	0.012 ± 0.0005	0.0005 ± 0.001	No*
<u>Gas exchange</u>				
Bubbling	0.0015 ± 0.0013	0.03451 ± 0.001	0.00227 ± 0.0019	No
Stir with headspace	0.0597 ± 0.0020	0.0597 ± 0.0020	0.0030 ± 0.0005	Yes*
Stir no headspace	0.0512 ± 0.0015	0.0597 ± 0.0020	0.0030 ± 0.0005	Yes*
Still no headspace	0.0025 ± 0.0004	0.0597 ± 0.0020	0.0030 ± 0.0005	No*
<u>Oxidative Stress</u>				
H ₂ O ₂ (25 μM)	0.0019 ± 0.0001	0.216 ± 0.030	0.0025 ± 0.0001	No*
Methyl Viologen (0.10 μM)	0.00028 ± 0.000004	0.00586 ± 0.0002	0.00061 ± 0.00003	No*
<u>Cell Wall Stress</u>				
Hypoosmotic shock (50% SW), (6hr still)	NS	0.015 ± 0.0015	NS	No
Hypoosmotic shock (50% SW), (6hr stir)	0.0009 ± 0.0005	0.015 ± 0.0015	NS	Yes

Table 3.3: continued

Treatment	Specific activity $\mu\text{mol dibromothymol blue min}^{-1} \text{mg}^{-1}$	Stir $\mu\text{mol dibromothymol blue min}^{-1} \text{mg}^{-1}$	Still $\mu\text{mol dibromothymol blue min}^{-1} \text{mg}^{-1}$	VBPO Induction
Hyperosmotic shock (125% SW), (6 hr still)	NS	0.015 \pm 0.0015	NS	No
Hyperosmotic shock (125% SW), (6 hr stir)	0.0129 \pm 0.0011	0.015 \pm 0.0015	NS	Yes
Ampicillin (10 $\mu\text{g/ml}$)	0.0006 \pm 0.0008	0.0131 \pm 0.001	NS	No*
Broken <i>Synechococcus</i>	NS	0.0131 \pm 0.001	NS	No*
Cell Contact (24hrs)				
<i>Synechococcus</i> sp. CC9605	0.003 \pm 0.0001	0.223 \pm 0.006	0.003 \pm 0.0002	No
<i>Silicibacter</i> TrichCH4B 24 hrs	0.001 \pm 0.0001	0.016 \pm 0.001	0.00096 \pm 0.0002	No*
<i>Alteromonas</i> TW-7	NS	0.085 \pm 0.004	0.0015 \pm 0.0003	No
Marine Bacterium TW-6	0.0014	0.085 \pm 0.004	0.0015 \pm 0.0003	No
<i>Pteridomonas</i>	0.0494 \pm 0.007	0.085 \pm 0.004	0.0015 \pm 0.0003	Yes
<i>Pteridomonas</i> 2.0 μm	0.0703 \pm 0.0177	0.085 \pm 0.004	0.0015 \pm 0.0003	Yes
<i>Pteridomonas</i> 0.2 μm	0.0017 \pm 0.0020	0.085 \pm 0.004	0.0015 \pm 0.0003	No
PT-Bacteria	0.0729 \pm 0.013	0.085 \pm 0.004	0.0015 \pm 0.0003	Yes
9311+ 1:5 dilution of PT-bacteria	0.0901 \pm 0.019	0.085 \pm 0.004	0.0015 \pm 0.0003	Yes
9311 +1:20 dilution of PT-Bacteria	0.0376 \pm 0.007	0.085 \pm 0.004	0.0015 \pm 0.0003	Yes
9311 +1:100 dilution of PT-Bacteria	0.0078 \pm 0.0010	0.085 \pm 0.004	0.0015 \pm 0.0003	Yes
9311 + PT-Bacteria supernatant	0.0824 \pm 0.0277	0.085 \pm 0.004	0.0015 \pm 0.0003	Yes
9311 + PT-Bacteria supernatant, 0.2 μm filtrate	NS	0.085 \pm 0.004	0.0015 \pm 0.0003	No
VMUT2, Stirring	NS	0.085 \pm 0.004	0.0015 \pm 0.0003	No
VMUT2 + PT-Bacteria	NS	0.085 \pm 0.004	0.0015 \pm 0.0003	No
SN + PT-Bacteria	NS	0.085 \pm 0.004	0.0015 \pm 0.0003	No

NS

*

VBPO activity is not significant; measured activity was less than 3 standard deviations above the no protein control
 * Insufficient No Protein controls in the VBPO assay for determining significance. Induction based on t-test with still control ($p < 0.05$).

Table 3.4: VBPO specific activity in CC9311 proteins after 24 hour exposure to different grazer cultures.

Treatment	Specific Activity	CC9311 Stir	CC9311 Still	VBPO Induction?
	μmol dibromothymol blue $\text{min}^{-1} \text{mg}^{-1}$	μmol dibromothymol blue $\text{min}^{-1} \text{mg}^{-1}$	μmol dibromothymol blue $\text{min}^{-1} \text{mg}^{-1}$	
<i>Goniomonas</i>	0.006 ± 0.0003	0.144 ± 0.001	NS	Yes
<i>Goniomonas</i> , 2.0 μm filtrate	0.005 ± 0.0002	0.144 ± 0.001	NS	Yes
<i>Pteridomonas</i>	0.011 ± 0.0005	0.144 ± 0.001	NS	Yes
<i>Pteridomonas</i> , 2.0 μm filtrate	0.022 ± 0.0002	0.144 ± 0.001	NS	Yes
<i>Paraphysomonas</i>	NS	0.144 ± 0.001	NS	No
Cercozoan	NS	0.144 ± 0.001	NS	No
<i>Oxyrrhis marina</i>	0.002 ± 0.00008	0.144 ± 0.001	NS	Yes
Choanoflagellate	NS	0.144 ± 0.001	NS	No

NS Not significant; the measured VBPO activity was less than 3 standard deviations above the no protein control.

Table 3.5: Specific VBPO activities of *Acaryochloris marina* cultures.

	VBPO Activity	
	$\mu\text{mol dibromothymol blue min}^{-1} \text{mg}^{-1}$	
	Still	Stir
Trial 1	NS	0.063 ± 0.0060
Trial 2	0.003 ± 0.0002	0.012 ± 0.0005

NS Not Significant, VBPO activity was less than the negative (no protein) control

Table 3.6: Numbers of peptide spectra and significant proteins from the two iTRAQ experiments.

	Experiment 1 (4 hrs)	Experiment 2 (24 hrs)
<u>Total spectra</u>	102,888 (17,408)	55,234 (36,444)
<u>Proteins</u>		
>1 peptide	1293	1173
>2 peptides	1108	989
Pval < 0.05	30	73

Table 3.7: Characteristics of colonies isolated from the PTB enrichment culture, including VBPO activity of CC9311 after 24 hr co-culturing experiment.

PTB #	Top 16S rRNA BLAST hit	% Identities	Alignment length	Isolation Media	Growth 2216/2 (OD600, 24 hrs)	Growth in F/4 + barley	VBPO Activity (μmol dibromothymol blue $\text{min}^{-1} \text{mg}^{-1}$)	Motility	Size	Pigment
1	<i>Alteromonas</i> sp. S1080	99.6	800	2216	0.318	++	0.001 ± 0.0006	No	Ovoid 1.5x2	
2	<i>Alteromonas</i> sp. S1080	98.6	727	2216	0.304	++	0.0001 ± 0.0009	No	Rod 1.5x2	
3	<i>Erythrobacter</i> sp. UST081027-248	99.2	923	2216	0.085	+	0.001 ± 0.001	No	Cocci 1.0 x 1.0	Red
4	<i>Alteromonas</i> sp. S1080	100.0	769	SN agar	0.221	++	NS	No	Cocci 2.0x2.0	
5	<i>Alteromonas</i> sp. S1080	99.7	913	SN agar	0.212	+	0.0002 ± 0.0005	No	Cocci 1x1	
6	<i>Alteromonas</i> sp. S1080	99.7	927	SN agar	0.244	++	0.0002	No	Cocci 2x2	
7	<i>Sulfitobacter</i> sp. RO2	97.2	994	SWC	0.264	+	NS	No	Varied Rods 1x1-7	
8	<i>Alteromonas</i> sp. Cv1	95.7	461	SWC	0.352	++	NS	No	Cocci 2x2	
9	<i>Alteromonas</i> sp. S1080	99.7	864	SWC/10	0.228	++	NS	No	Rod 1x2	
10	<i>Sulfitobacter</i> sp. RO2	97.5	982	SWC/10	0.454	+	NS	Yes	Rod 1x1.5	
11	<i>Sulfitobacter</i> sp. RO2	98.8	851	SN agar (pour plating)	0.317	--	NS	No	Bulbous rod 1.5x2-7	
12	<i>Erythrobacter</i> sp. UST081027-248	99.0	891	SN agar (pour plating)	0.208	+	NS	No	Cocci 1.5x1.5	Red

Table 3.7: continued

PTB #	Top 16S rRNA BLAST hit	% Identities	Alignment length	Isolation Media	Growth 2216/2 (OD600)	Growth in F/4 + barley	VBPO Activity (μmol dibromothymol blue $\text{min}^{-1} \text{mg}^{-1}$)	Motility	Size	Pigment
13	<i>Ruegeria pelagica</i>	99.4	818	SN agar (pour plating)	0.470	+	0.0003	Yes	Cocci 1.5x1.5	
14	<i>Sulfitobacter</i> sp. CB 2047	99.5	964	SN agar (pour plating)	0.381	++	NS	No	Cocci/chain 2.5	
15	<i>Ruegeria pelagica</i>	88.8	507	SN agar (pour plating)	0.583	+	NS	Yes	Rod 1x1.5	
16	Bacterium RCC 1927	99.1	779	2216	0.113	--	NS	No	Rod, small 0.8x1.5 (chains too)	Purple
17	Bacterium RCC 1927	98.3	586	SWC	0.570	--	NS	Yes	Ovoid 1x1.5	
18	<i>Ruegeria</i> sp. EDA3	99.0	698	SWC	0.620	--	NS	Yes	Cocci 1x1	
19	Bacterium RCC 1927	98.4	703	2216	0.121	--	NS	No	1x1.5	

- ++ Culture was densely turbid after six days growth
- + Culture was slightly turbid after six days growth in F/4 + barley
- Media was visually clear after six days growth, but cells were visible under the microscope
- NS Not significant, VBPO activity was lower than the limits of detection as determined by a no protein control

Table 3.8: Isobaric iTRAQ mass tags used and VBPO specific activities of each treatment in the iTRAQ proteomic experiments

Culture, Treatment	Cell Fraction	Trial 1 4 hrs iTRAQ Mass tag	Trial 1 4 hrs VBPO Activity	Trial 2 24 hrs iTRAQ Mass tag	Trial 2 24 hrs VBPO Activity
CC9311, Still	Proteins	114	0.003 ± 0.00023	113	0.00019 ± 0.0007
CC9311, Stir	Proteins	115	0.030 ± 0.001	114	0.1352 ± 0.009
VMUT, Still	Proteins	116	0.001 ± 0.00003	-	NS
VMUT, Stir	Proteins	117	0.001 ± 0.000	-	NS
CC9311, Still	Broken cells	-	-	115	0.00014 ± 0.00002
CC9311, Stir	Broken cells	-	-	116	0.0667 ± 0.008
VMUT2, Still	Broken cells	-	-	117	NS
VMUT2 Stir	Broken cells	-	-	118	NS

- Indicates that the sample was not taken or measured in that trial.

NS Not significant, VBPO activity was lower than the limits of detection; lower than the no protein control

Table 3.9: Proteins identified with a significant iTRAQ ratio ($p \leq 0.05$) in at least two treatments. Sorted by descending order of iTRAQ ratio (stir divided by still) from WT after 24 hrs.

Locus_tag	Name	Peptides 4 hrs	Peptides 24 hrs	CC9311 4hrs	PVal	CC9311 24 hrs	PVal	VMUT 4 hrs	PVal	VMUT2 24 hrs	PVal
sync_1122	hypothetical protein sync_1122	3	4	0.680		8.493	0.007	1.825		2.361	0.089
sync_2681	vanadium-dependent bromoperoxidase 2	23	63	2.771	0.000	8.294	0.000	1.117	0.477	1.141	0.015
sync_0349	beta-lactamase, putative	11	31	2.043	0.001	4.530	0.000	3.377	0.000	3.016	0.000
sync_2357	DNA-directed RNA polymerase subunit gamma	23	31	0.871	0.016	1.838	0.000	1.193	0.012	1.031	0.531
sync_0854	ferritin family protein	6	8	1.311	0.150	1.737	0.004	1.361	0.232	1.711	0.002
sync_2356	DNA-directed RNA polymerase subunit beta'	59	77	0.883	0.014	1.578	0.000	1.185	0.000	1.026	0.580
sync_0414	DNA-directed RNA polymerase subunit alpha	17	28	0.889	0.050	1.556	0.000	1.203	0.006	0.995	0.924
sync_0480	Hpt domain-containing protein	11	12	0.944	0.672	1.484	0.011	1.078	0.591	1.066	0.622
sync_2358	DNA-directed RNA polymerase subunit beta	41	48	0.913	0.610	1.484	0.000	1.260	0.000	0.956	0.163
sync_1686	glutamyl-tRNA reductase	9	10	1.067	0.449	1.416	0.013	0.953	0.364	1.169	0.066
sync_0411	50S ribosomal protein L13	9	16	0.936	0.329	1.406	0.003	0.945	0.404	1.095	0.210
sync_0383	30S ribosomal protein S7	18	25	0.982	0.924	1.336	0.046	0.958	0.564	1.085	0.437
sync_1217	structural toxin protein RtxA	16	11	1.127	0.099	1.333	0.015	1.229	0.044	1.050	0.698
sync_2939	excinuclease ABC subunit A	10	17	0.970	0.552	1.328	0.000	1.260	0.017	0.877	0.032
sync_2910	bifunctional aconitate hydratase 2/2-methylisocitrate dehydratase	14	11	1.078	0.226	1.289	0.003	0.990	0.819	1.131	0.186
sync_0273	phosphoglucomutase/phosphomannomutase family protein	16	8	0.972	0.576	1.256	0.033	1.074	0.224	1.085	0.325
sync_0973	DNA gyrase subunit A	7	17	0.936	0.287	1.252	0.005	1.041	0.508	0.981	0.680
sync_1234	PvdS	4	11	0.854	0.044	1.247	0.051	1.037	0.566	1.099	0.466
sync_2898	ferredoxin-nitrite reductase	33	34	1.190	0.002	1.223	0.039	1.054	0.384	0.961	0.417
sync_2371	transcription elongation factor NusA	3	20	0.839	0.018	1.195	0.157	0.962	0.507	0.940	0.597

Table 3.9: Continued

Locus_tag	Name	Peptides 4 hrs	Peptides 24 hrs	CC9311 4hrs	PVal	CC9311 24 hrs	PVal	VMUT 4 hrs	PVal	VMUT2 24 hrs	PVal
sync_0766	signal recognition particle protein	6	13	1.031	0.590	1.191	0.024	0.987	0.810	0.925	0.401
sync_2282	chaperonin GroEL	126	97	1.091	0.014	1.172	0.085	0.996	0.908	1.024	0.700
sync_0652	GTP-binding protein LepA	6	16	1.033	0.581	1.167	0.020	0.972	0.612	0.986	0.809
sync_1282	geranylgeranyl reductase	12	13	1.245	0.036	1.157	0.130	1.032	0.732	1.121	0.134
sync_0437	50S ribosomal protein L3	14	13	0.897	0.029	1.104	0.284	1.005	0.909	1.098	0.061
sync_2135	chaperonin GroEL	56	74	1.107	0.086	1.103	0.042	1.001	0.985	1.109	0.011
sync_1897	ATP-dependent Clp protease, Hsp 100, ATP-binding subunit ClpB	27	26	1.141	0.562	1.090	0.284	1.057	0.414	1.207	0.037
sync_0387	ferredoxin-dependent glutamate synthase, Fd-GOGAT	37	36	1.042	0.290	1.052	0.442	1.009	0.766	1.123	0.007
sync_0011	signal recognition particle-docking protein FtsY	14	10	1.099	0.044	1.034	0.549	1.019	0.800	0.981	0.810
sync_1309	acetazolamide conferring resistance protein Zam	10	19	0.903	0.192	1.026	0.672	1.107	0.584	0.895	0.026
sync_1051	superfamily II DNA/RNA helicase	6	10	0.998	0.973	1.024	0.824	0.959	0.615	0.819	0.035
sync_1253	glutamine synthetase	24	34	0.890	0.017	1.018	0.828	0.989	0.798	1.012	0.757
sync_1967	ribulose bisophosphate carboxylase	32	55	0.864	0.001	1.015	0.870	1.004	0.928	0.923	0.179
sync_0029	glyceraldehyde-3-phosphate dehydrogenase, type I	34	27	1.008	0.850	1.014	0.904	1.025	0.751	0.878	0.014
sync_2686	hypothetical protein sync_2686	12	4	1.061	0.652	1.009	0.950	1.181	0.049	0.946	0.511
sync_1993	ribosomal protein S1	23	12	1.121	0.026	0.999	0.993	1.034	0.549	1.082	0.425
sync_0569	glycerol kinase	11	9	1.016	0.753	0.961	0.525	0.943	0.479	1.204	0.021
sync_2671	sensory box/GGDEF family protein	9	12	0.975	0.793	0.961	0.787	1.053	0.770	1.151	0.048
sync_1975	protochlorophyllide reductase iron-sulfur ATP-binding protein	4	6	1.281	0.025	0.958	0.819	1.170	0.067	1.018	0.840
sync_1027	putative Clp protease, ATP-binding subunit ClpC	31	36	1.106	0.006	0.951	0.374	1.077	0.107	0.883	0.041
sync_0086	preprotein translocase subunit SecA	26	31	0.992	0.799	0.940	0.361	0.988	0.726	0.808	0.000

Table 3.9: Continued

Locus_tag	Name	Peptides 4 hrs	Peptides 24 hrs	CC9311 4hrs	PVal	CC9311 24 hrs	PVal	VMUT 4 hrs	PVal	VMUT2 24 hrs	PVal
sync_0731	cell division protein FtsZ	25	37	1.132	0.018	0.934	0.311	0.981	0.677	1.023	0.710
sync_0976	2-isopropylmalate synthase	19	17	0.979	0.762	0.924	0.518	0.998	0.981	0.804	0.007
sync_1280	sulfite reductase subunit beta	16	11	0.898	0.093	0.921	0.817	1.308	0.001	0.912	0.288
sync_2099	hypothetical protein sync_2099	11	11	1.055	0.596	0.901	0.528	1.239	0.128	1.202	0.016
sync_0354	sulfate adenylyltransferase	22	14	1.026	0.535	0.900	0.196	0.933	0.108	1.192	0.020
sync_0130	transketolase	82	67	1.007	0.845	0.894	0.023	0.956	0.325	1.029	0.566
sync_2505	protein phosphatase 2C	90	131	0.859	0.021	0.894	0.066	1.021	0.713	1.001	0.989
sync_1265	ribonucleotide reductase (class II)	27	15	0.893	0.014	0.887	0.170	0.977	0.702	1.083	0.093
sync_0176	imidazole glycerol phosphate synthase subunit hisF	7	6	1.058	0.312	0.884	0.347	1.055	0.332	0.778	0.025
sync_0258	enoyl-(acyl carrier protein) reductase	19	31	1.035	0.607	0.877	0.168	1.193	0.021	1.006	0.907
sync_2488	phycobilisome rod-core linker polypeptide cpcG1	18	31	1.038	0.452	0.854	0.007	1.048	0.430	0.996	0.943
sync_1931	glutathione reductase	43	29	0.984	0.734	0.853	0.034	0.975	0.654	1.051	0.352
sync_2362	histidinol dehydrogenase	16	14	1.128	0.031	0.839	0.333	0.943	0.335	0.958	0.494
sync_1356	hypothetical protein sync_1356	10	16	1.075	0.951	0.824	0.016	1.222	0.221	0.987	0.847
sync_0393	photosystem I P700 chlorophyll a apoprotein A1	11	22	1.229	0.816	0.824	0.013	1.270	0.274	0.947	0.436
sync_0689	peroxiredoxin 2 family protein	39	34	0.963	0.450	0.822	0.021	0.994	0.909	1.061	0.395
sync_0394	photosystem I P700 chlorophyll a apoprotein A2	12	16	1.019	0.768	0.822	0.364	1.032	0.618	0.886	0.037
sync_1986	GTP cyclohydrolase I	9	6	0.952	0.615	0.797	0.049	0.887	0.194	1.115	0.258
sync_0028	UDP-N-acetylmuramate--alanine ligase	7	8	1.038	0.701	0.796	0.018	0.986	0.843	0.821	0.220
sync_1545	ABC-type Fe ³⁺ transport system periplasmic component	12	12	0.941	0.244	0.791	0.015	1.045	0.397	0.943	0.400
sync_2788	glycine dehydrogenase	12	4	0.980	0.749	0.775	0.044	0.975	0.685	1.040	0.825
sync_2436	hypothetical protein sync_2436	2	6	0.899	0.237	0.773	0.032	1.039	0.648	1.070	0.405

Table 3.9: Continued

Locus_tag	Name	Peptides 4 hrs	Peptides 24 hrs	CC9311 4hrs	PVal	CC9311 24 hrs	PVal	VMUT 4 hrs	PVal	VMUT2 24 hrs	PVal
sync_2503	RND family efflux transporter MFP subunit	8	12	0.904	0.218	0.759	0.038	1.001	0.989	0.817	0.011
sync_2872	urea ABC transporter, periplasmic urea-binding protein	97	102	0.987	0.775	0.753	0.018	1.077	0.181	0.898	0.018
sync_1216	HlyD family secretion protein	15	15	0.874	0.016	0.746	0.004	0.908	0.163	0.779	0.001
sync_1097	hypothetical protein sync_1097	4	11	1.174	0.385	0.744	0.014	1.016	0.879	1.135	0.421
sync_0463	photosystem I reaction center subunit II	30	39	1.067	0.508	0.739	0.037	0.978	0.675	0.984	0.754
sync_0090	translation initiation factor IF-3	6	8	0.908	0.575	0.667	0.007	1.007	0.935	0.951	0.665
sync_2191	DNA-binding protein HU	7	22	0.983	0.836	0.663	0.006	1.036	0.682	1.004	0.989
sync_0681	ferrous iron transport protein B	4			0.787	0.021		1.049	0.575		

BOLD numbers have a p-value ≤ 0.05 and have an iTRAQ ratio that is < 0.8 or > 1.2

Table 3.10: List of functional gene categories enriched in iTRAQ experiments determined by DAVID (*see methods*).

UPREGULATED GENES

CC9311		VMUT		VMUT		Stirred after 24 hrs			
4 hrs		Stirred 24 hrs		4 hrs		24 hrs		MUTANT/CC9311	
Score	Annotation	Score	Annotation	Score	Annotation	Score	Annotation	Score	Annotation
1.84*	Peroxidase/antioxidant	2.05	ion binding	2.59	metal binding	1.67	Peptidoglycan biogenesis	1.49	Polysaccharide biosynthesis
1.81	Metal binding	1.77	e- transport	2.42	iron binding	0.87	cell wall / envelope	1.44	Cell envelope
1.36	Iron Binding	1.72	transcription	1.07	ferredoxin	0.56	RNA binding	0.98	Cell wall biosynthesis
1.33	Thylakoid	1.44	haemolysin (RTX)	0.90	transcription	0.43	RNA modification	0.74	Vit. B binding
0.74	Photosynthesis	0.89	translation	0.43	DNA repair / stress	0.32	metal ion binding	0.58	metal/ cation binding
0.46	e-transport	0.81	light harvesting	0.27	e- transport	0.19	amino acid biosynthesis	0.34	phosphorylation

DOWN REGULATED

<u>Score</u>	<u>Annotation</u>	<u>Score</u>	<u>Annotation</u>	<u>Score</u>	<u>Annotation</u>	<u>Score</u>	<u>Annotation</u>	<u>Score</u>	<u>Annotation</u>
		1.46	cell wall synthesis	0.62	Cation Binding	0.77	organic acid biosynthesis	1.96	haemolysin-type calcium-binding (rtx)
-	-	0.96	redox / homeostasis			0.69	photosynthesis	0.65	polysaccharide biosynthesis

* Gene functional groups shown in **bold** are considered to be significantly enriched, having an Enrichment Score that is greater than or equal to 1.3.

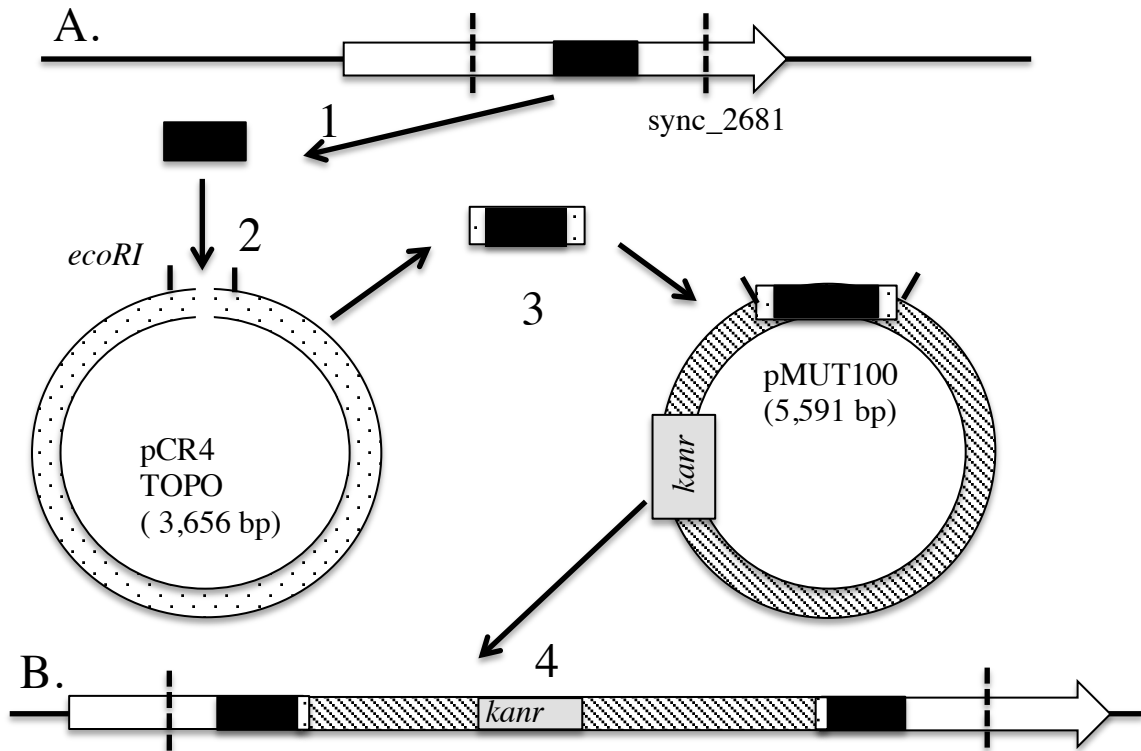


Figure 3.1: A diagram of the insertional gene inactivation of VBPO (*sync_2681*) in *Synechococcus* CC9311 (shown in A) to form the VMUT genotype (shown in B). Steps: 1. PCR amplification of gene fragment, 2. Clone into TOPO vector to form pTOP2681, 3. Excise new fragment with *EcoRI* and cloned into pMUT100 to form pVBR1, 4. Conjugation into CC9311 and homologous recombination from VMUT genotype. The vertical, dashed lines represent the primers used to verify the mutant genotype, VBPO verif long F / R, see Table 1.

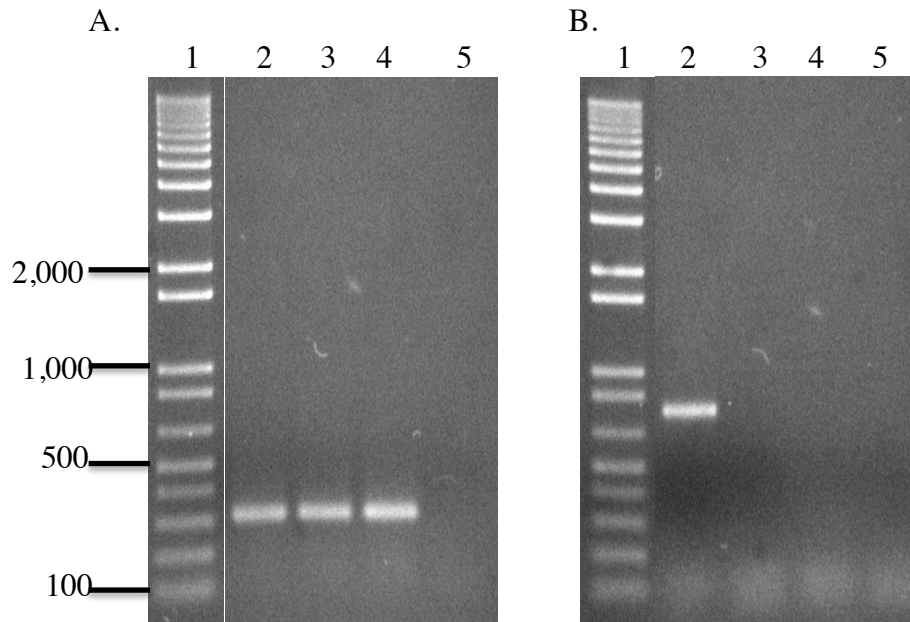


Figure 3.2: Verification of the mutant genotype; a 1% agarose gel showing PCR products from boiling DNA extraction of stock cultures using A) RPOC1 primers (303 bp) and B) verification primers (750 bp). Lanes left to right: 1) 1 Kb Plus Ladder (bp); 2) CC9311; 3) VMUT; 4) VMUT2; 5) no DNA control.

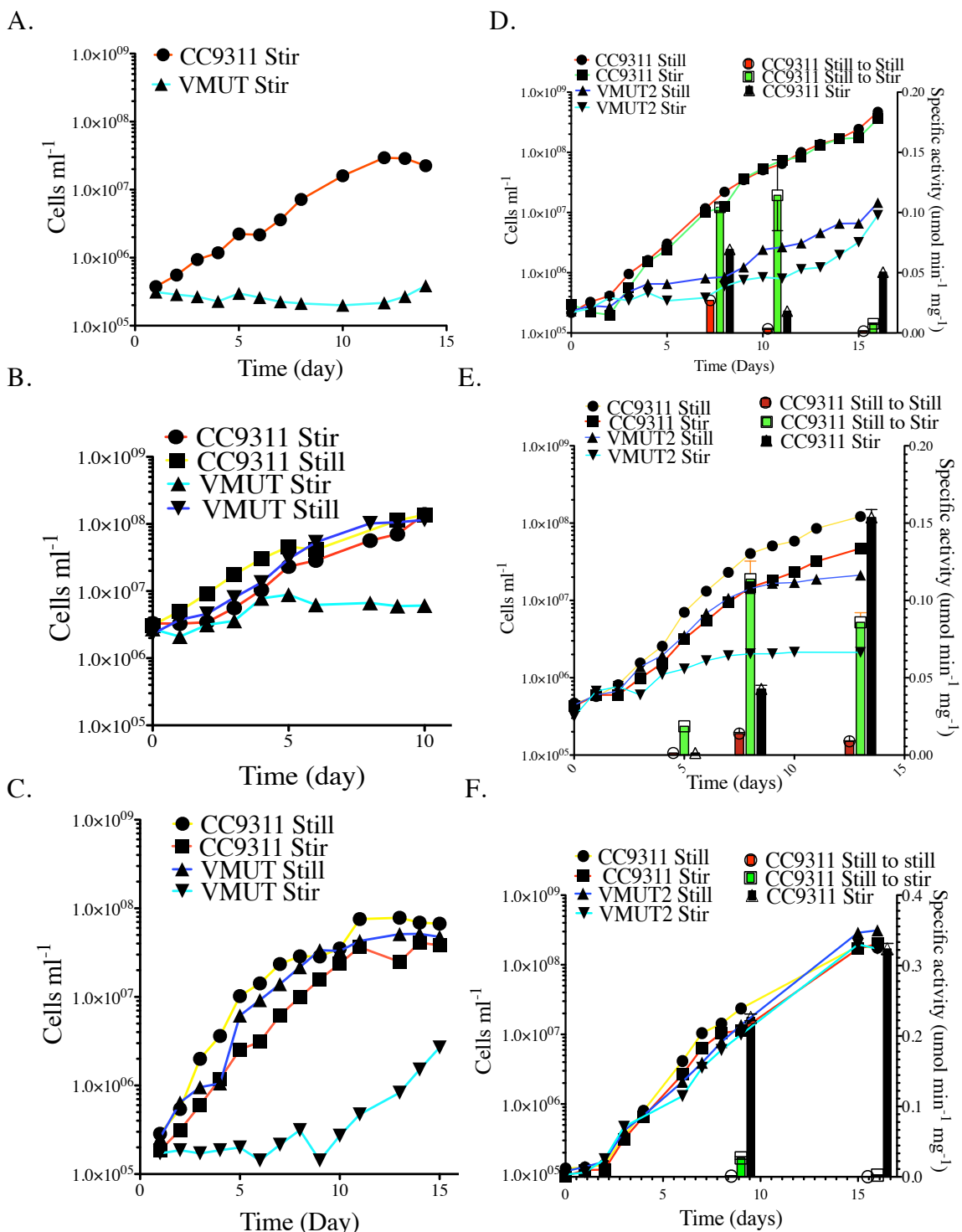


Figure 3.3: Growth curves showing the cell counts (lines) comparing the growth of CC9311 and the original mutant, VMUT, under stirred and still conditions over the first three growth curves (A-C) as well as CC9311 and VMUT2 (D-F). VBPO specific activities (bars) are also shown comparing CC9311 to VMUT2 (D-F) over three growth curves.

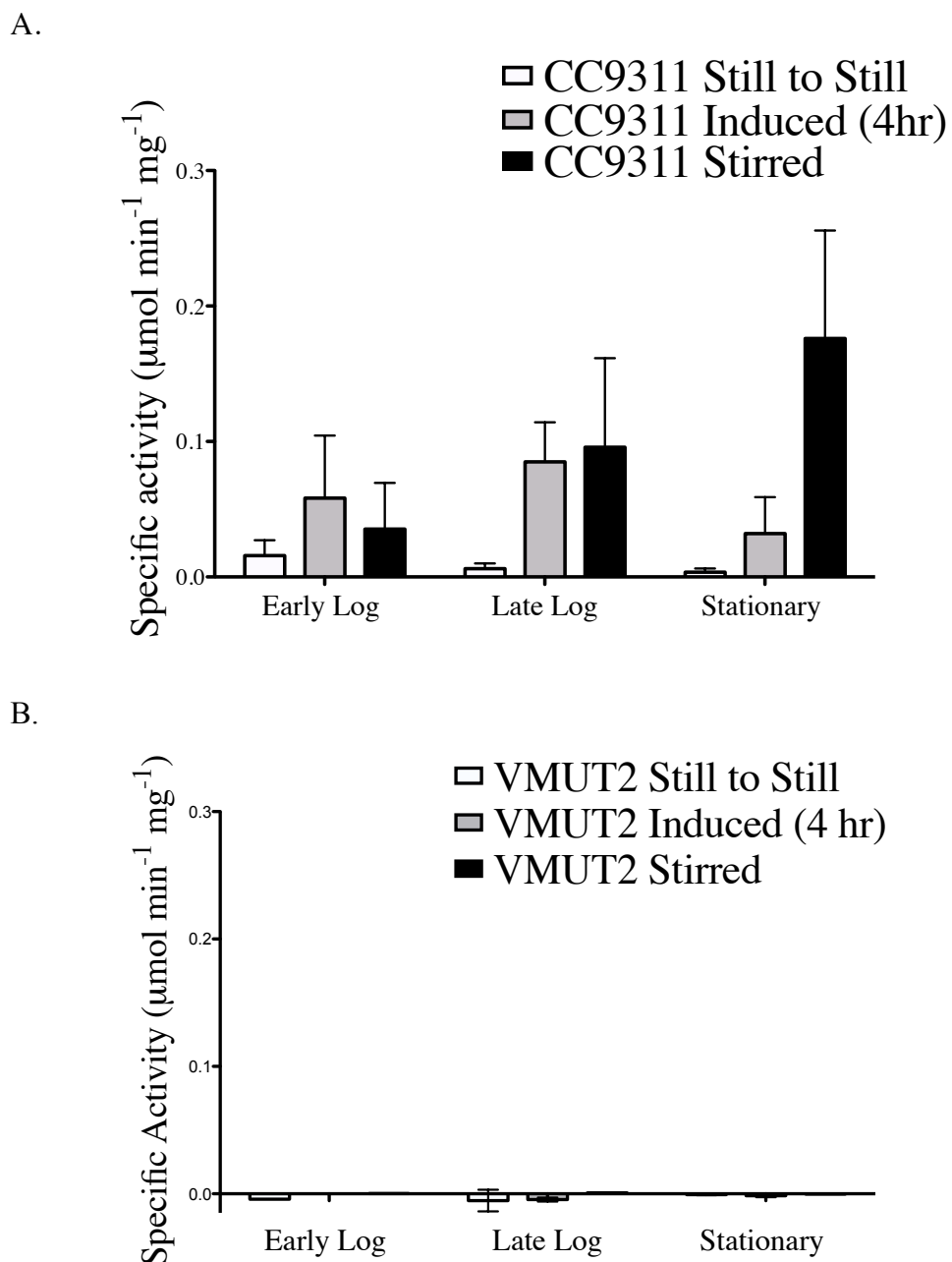


Figure 3.4: VBPO specific activity of proteins extracted from cultures of A) CC9311 and B) VMUT2 at different phases of growth. VBPO activities of biological triplicates are shown from cultures grown under still conditions (white bars), cultures grown under still conditions and subjected to a short term (4 hr) period of stirring (grey bars), and cultures grown with stirring from inoculation (black bars).

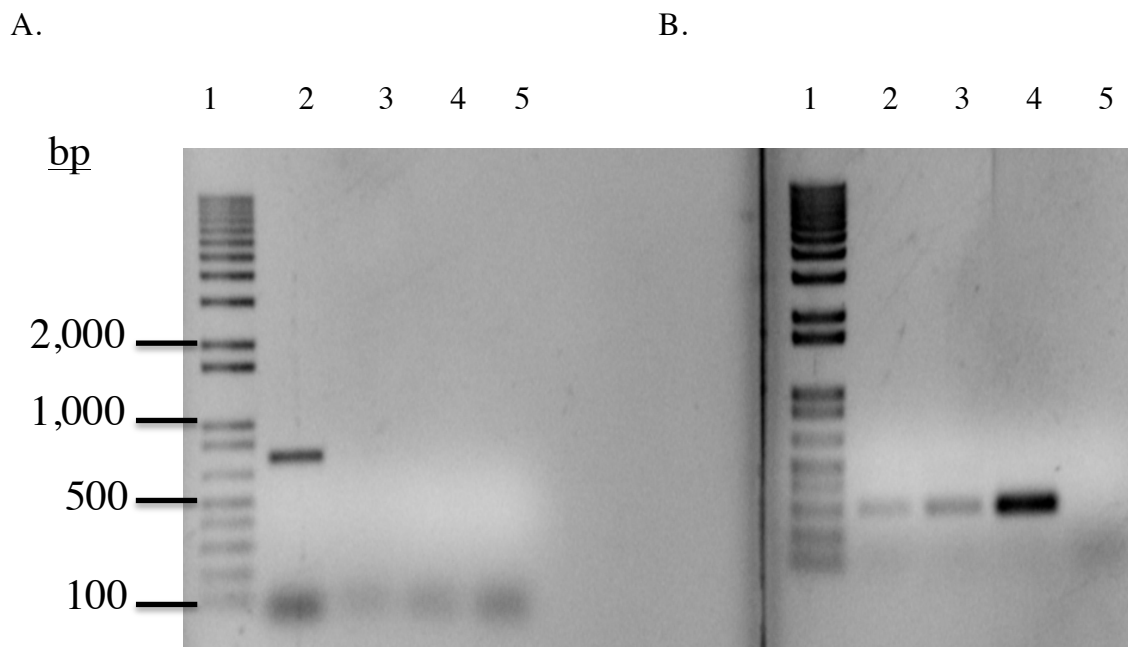


Figure 3.5: Genotype of VMUT after disappearance of stir-sensitive phenotype. PCR products from boiling DNA extraction shown on 1% agarose gels. Panel A: verifications primers (750 bp) lanes left to right: 1) 1 Kb Plus Ladder (bp); 2) CC9311; 3) VMUT stir; 4) VMUT still; 5) no DNA control. Panel B: RPOC1 primers (303 bp) lanes left to right: 1) 1 Kb Plus Ladder (bp); 2) CC9311; 3) VMUT stir; 4) VMUT still; 5) no DNA control.

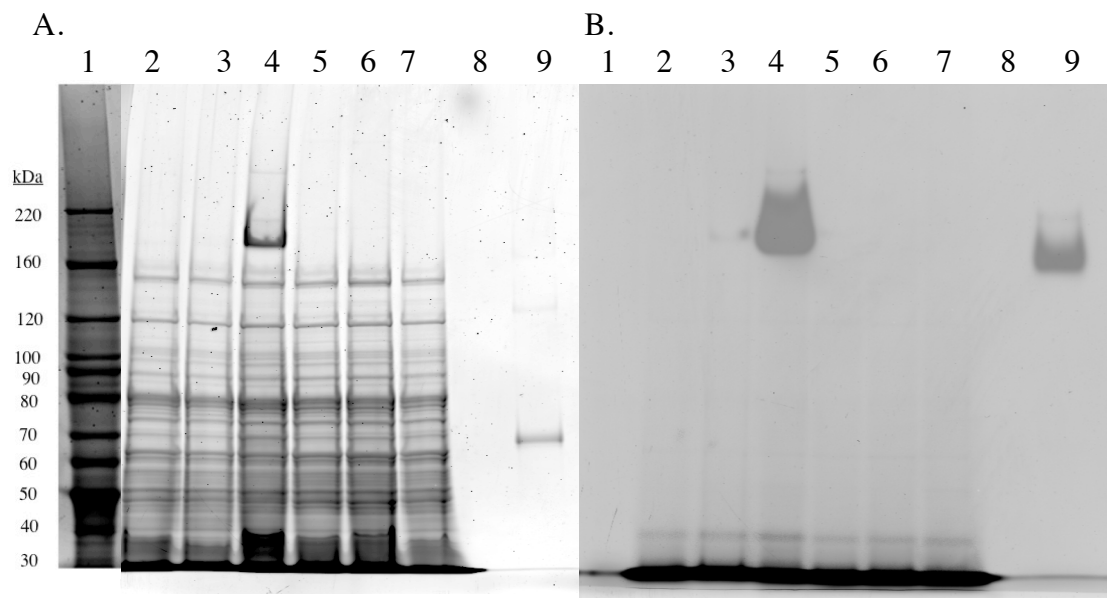


Figure 3.6: Duplicate SDS-PAGE of proteins extracted from CC9311 and VMUT2 in stationary phase; grown still, grown still with only four hours of stirring, or grown with constant stirring. Each lane was loaded with 55 μg protein and stained with A) sypro ruby or B) phenol-red in the presence of Na_3VO_4 , KBr , and H_2O_2 for VBPO activity. Lanes left to right: 1) Benchmark protein ladder (Life Technologies; note: the ladder shown is from a representative gel superimposed in lane 1), 2) 9311 still to still, 3) 9311 induced (4hrs), 4) 9311 stir, 5) VMUT2 still to still, 6) VMUT2 still to stir 7) VMUT2 stir 8) blank 9) *Corallina officinalis* (Co) VBPO, 0.01 U.

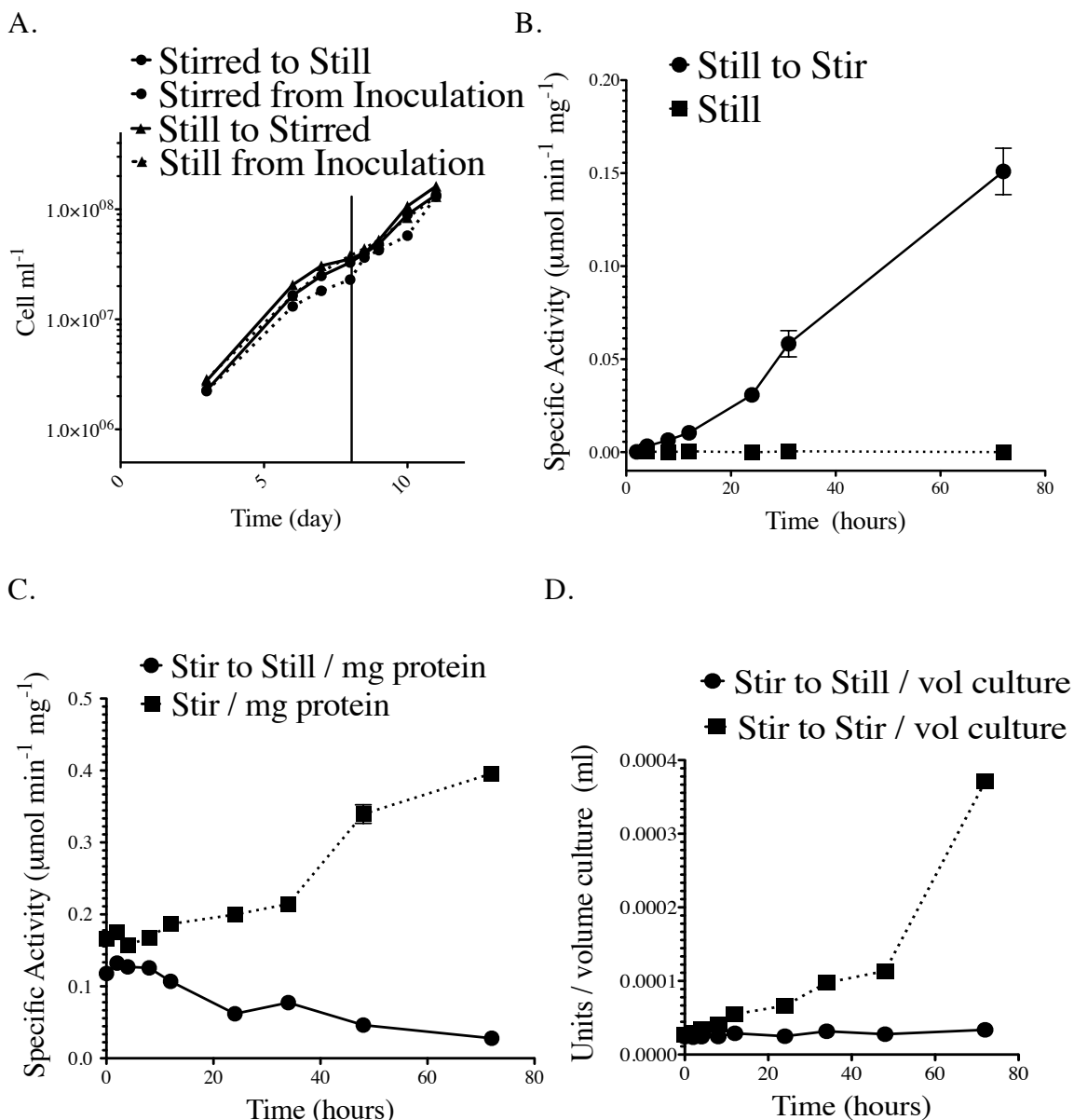


Figure 3.7: Induction and persistence of VBPO with stirring. A) Cell counts from cultures of CC9311 used to test the induction of VBPO with stirring over time. Vertical solid line shows when stirring was either initiated or halted in cultures. Growth rates of the cultures after the vertical line are 0.56 d^{-1} for the culture that was stirred from inoculation; 0.46 d^{-1} for the culture in which stirring was halted; 0.42 d^{-1} for the culture grown still from inoculation; and 0.50 d^{-1} for the culture in which stirring was initiated. B) Specific VBPO activities ($\mu\text{mol dibromothymol blue min}^{-1} \text{ mg}^{-1}$) after stirring was applied to a culture grown still from inoculation. C) Specific VBPO activity ($\mu\text{mol dibromothymol blue min}^{-1} \text{ mg}^{-1}$) after stirring is halted in a culture grown with stirring from inoculation. D) Units ($\mu\text{mol dibromothymol blue min}^{-1}$) of VBPO activity after stirring is halted in a culture grown with stirring from inoculation, normalized to the culture volume (the specific activities of these data are also shown in graph C).

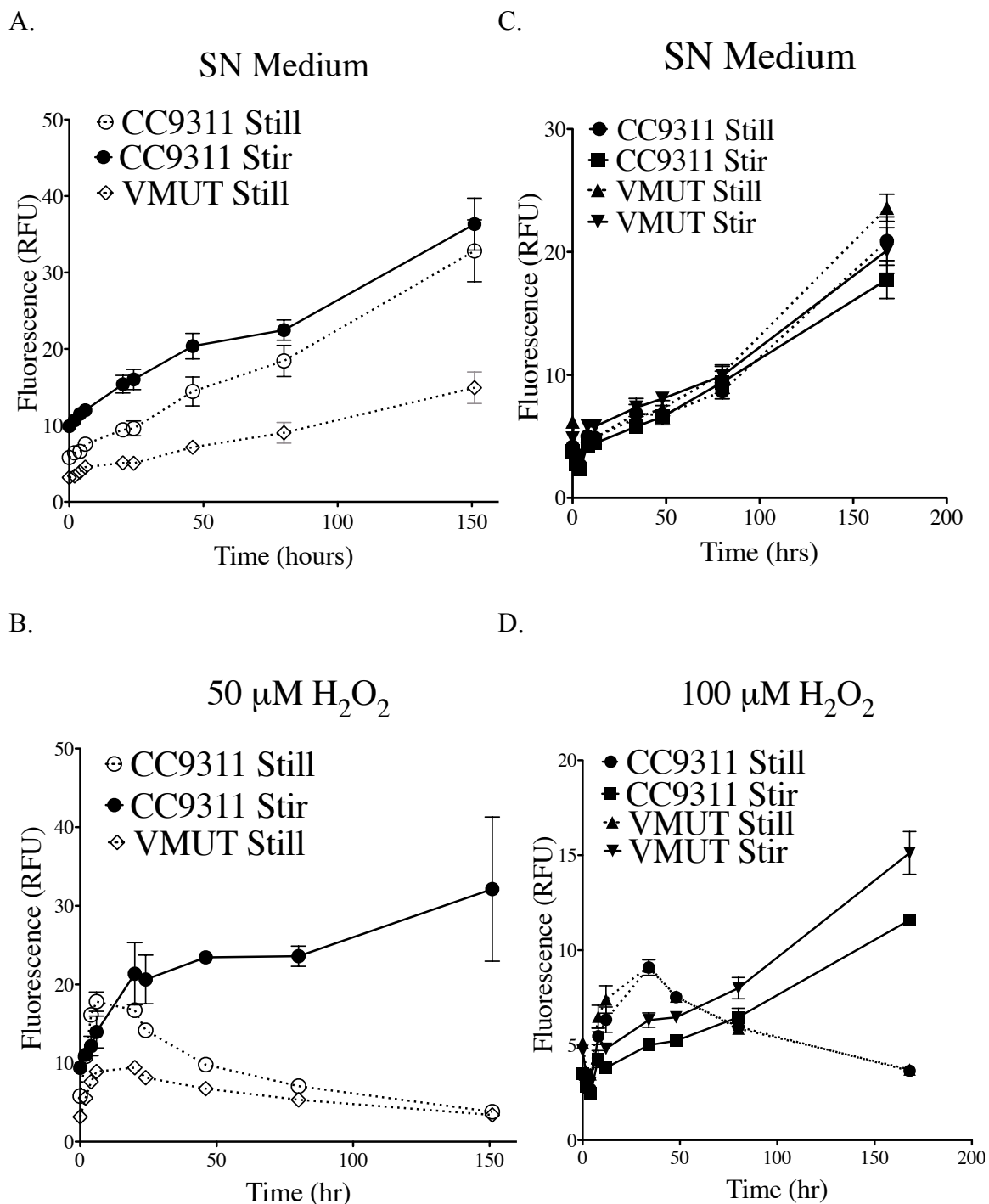
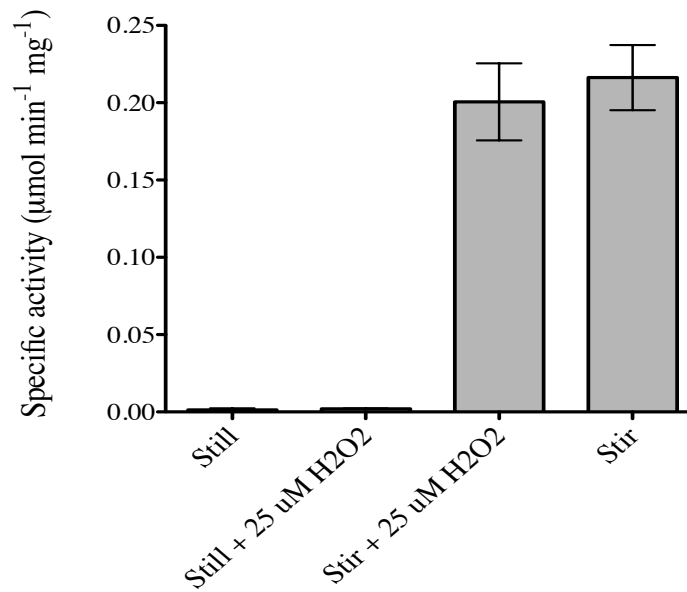


Figure 3.8: VBPO and cell resistance to hydrogen peroxide. Phycoerythrin autofluorescence of CC9311 and VMUT cultures after the addition of hydrogen peroxide. Solid lines represent cultures that have been preconditioned with stirring while dotted lines represent cultures that have been grown still from inoculation. A) Trial 1, no H_2O_2 controls; B) Trial 1, cultures with $50 \mu\text{M}$ H_2O_2 ; C) Trial 2, no H_2O_2 controls; D) Trial 2; $100 \mu\text{M}$ H_2O_2 added.

A.



B.

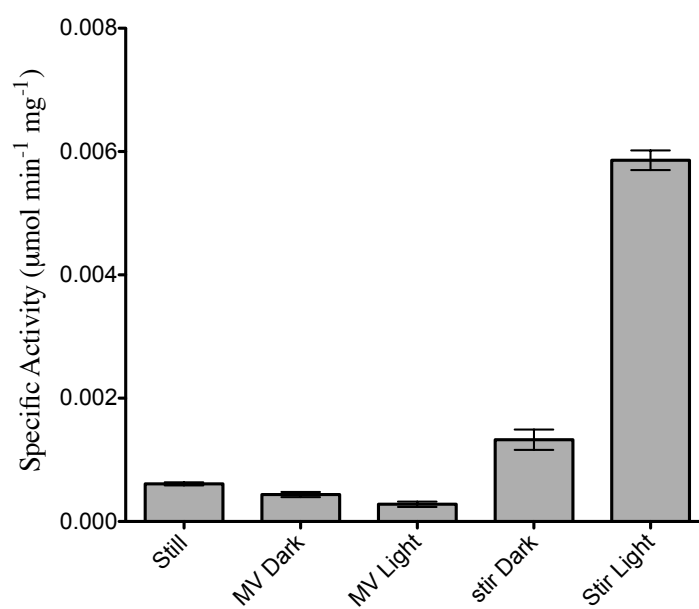


Figure 3.9: VBPO specific activities of CC9311 cultures exposed to A) 25 μM hydrogen peroxide and B) 0.1 μM methyl viologen (MV).

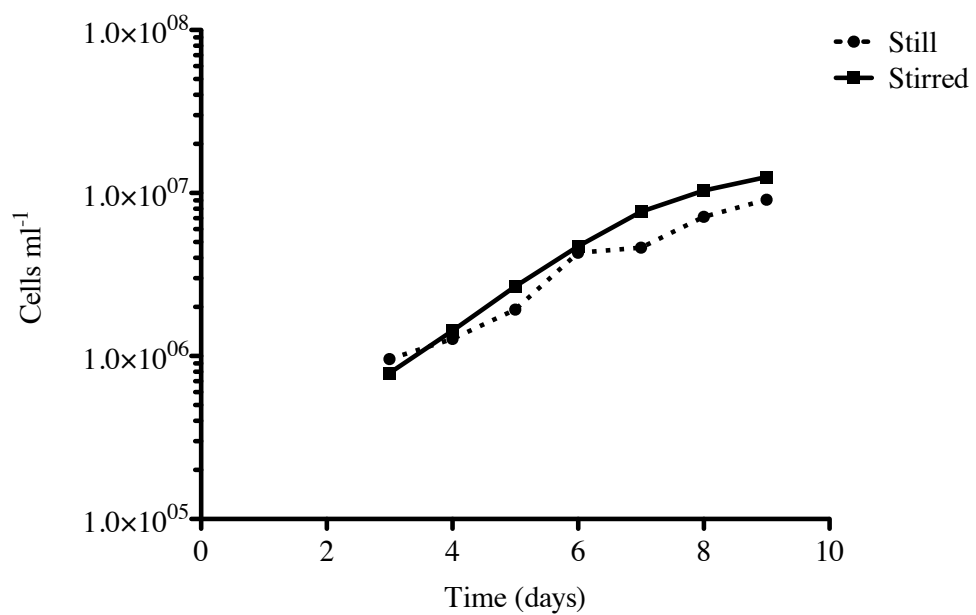


Figure 3.10: Cell counts of *Acaryochloris marina* cultures tested for VBPO activity (trial 2).

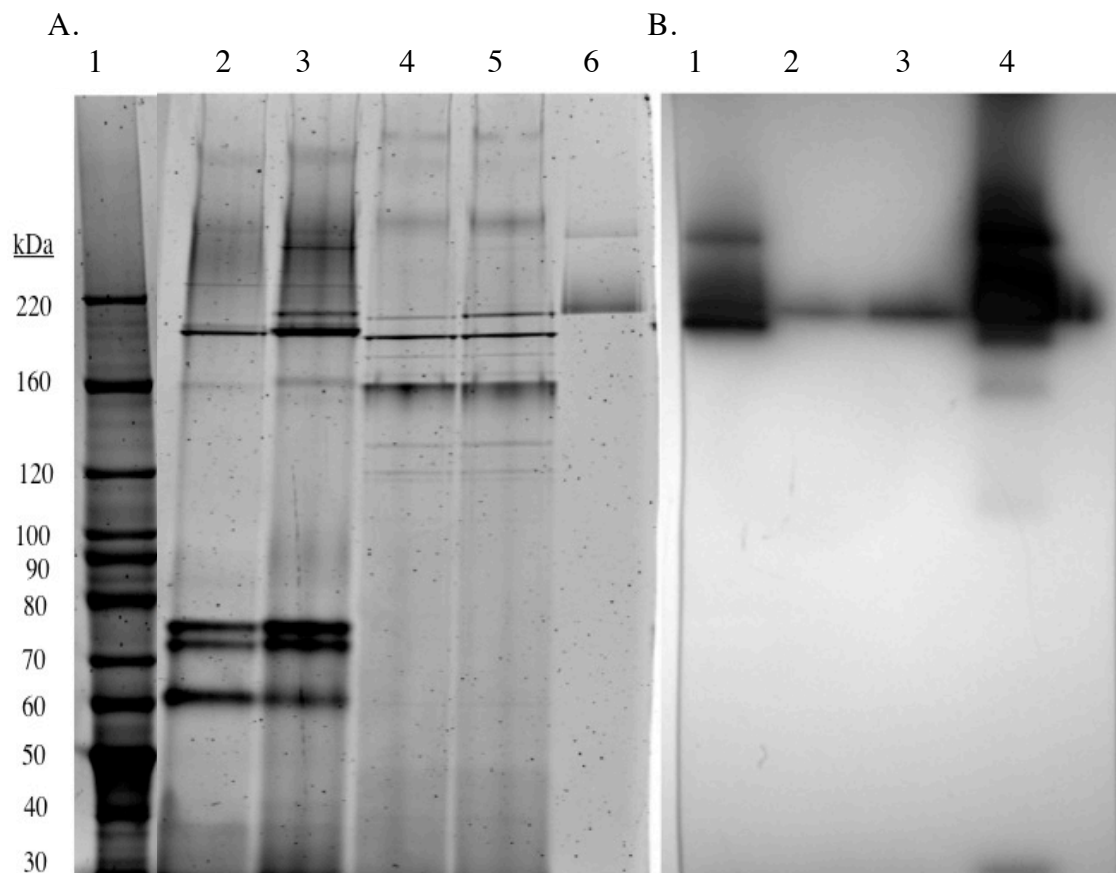


Figure 3.11: Native PAGE Gel of *Synechococcus* sp. CC9311 and *Acaryochloris marina* proteins, 21 μg protein per lane, from still and stirred cultures. Gel in panel A was stained with Sypro Ruby for total proteins, Gel in panel B was stained with phenol red for VBPO activity. Lanes left to right A) 1. Benchmark Protein ladder; 2. CC9311, still; 3. CC9311, stirred; 4. *A. marina*, still; 5. *A. marina*, stirred; 6. Co VBPO; B) 1. CC9311, stirred; 2. *A. marina*, still; 3. *A. marina*, stirred; 4. Co VBPO.

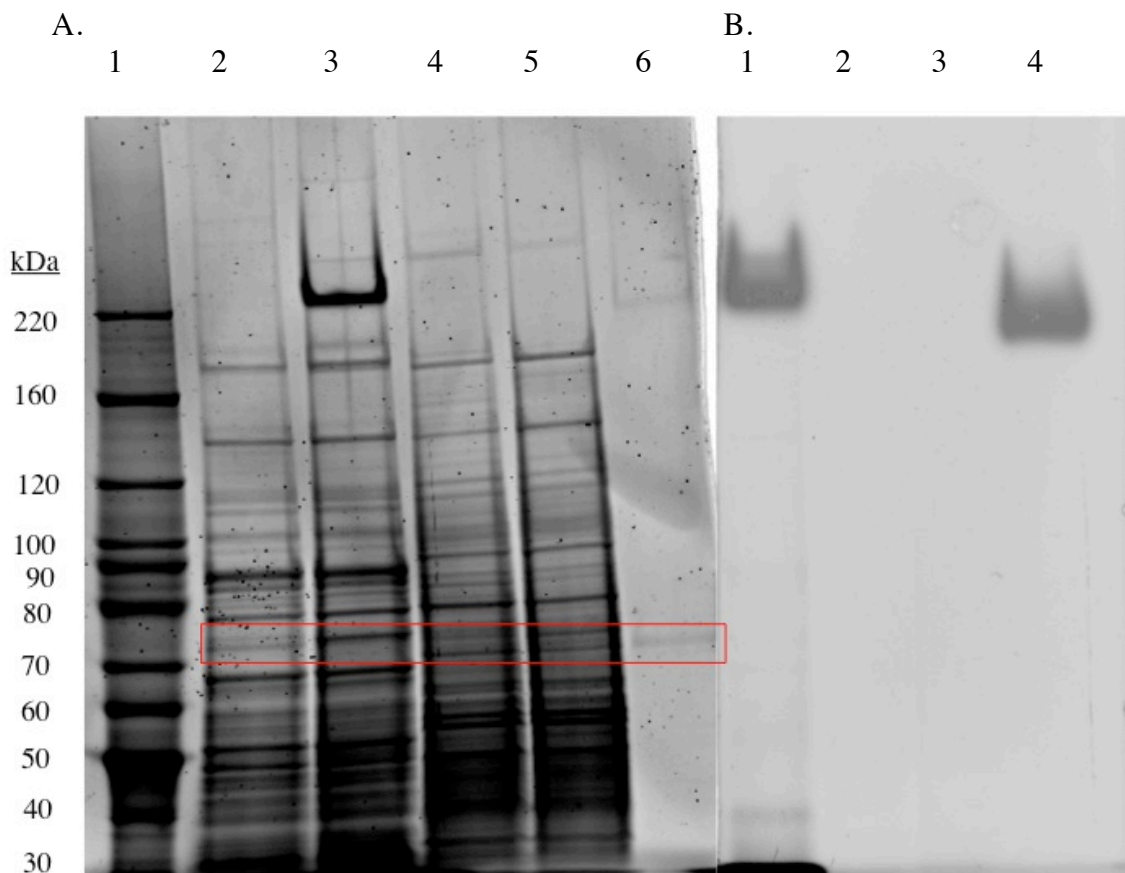


Figure 3.12: SDS-PAGE of *Synechococcus* CC9311 and *Acaryochloris marina* proteins, 26.5 μg protein per lane. Gel in panel A was stained with Sypro Ruby for total proteins, Gel in panel B was stained with phenol red for VBPO activity. Lanes left to right A) 1. Benchmark Protein ladder; 2. CC9311, still; 3. CC9311, stirred; 4. *A. marina*, still; 5. *A. marina*, stirred; 6. *C. officinalis* VBPO; B) 1. CC9311, stirred; 2. *A. marina*, still; 3. *A. marina*, stirred; 4. *Co* VBPO. Bold-lined box shows the denatured *Corallina officinalis* band in the control lane and the corresponding bands in each sample.

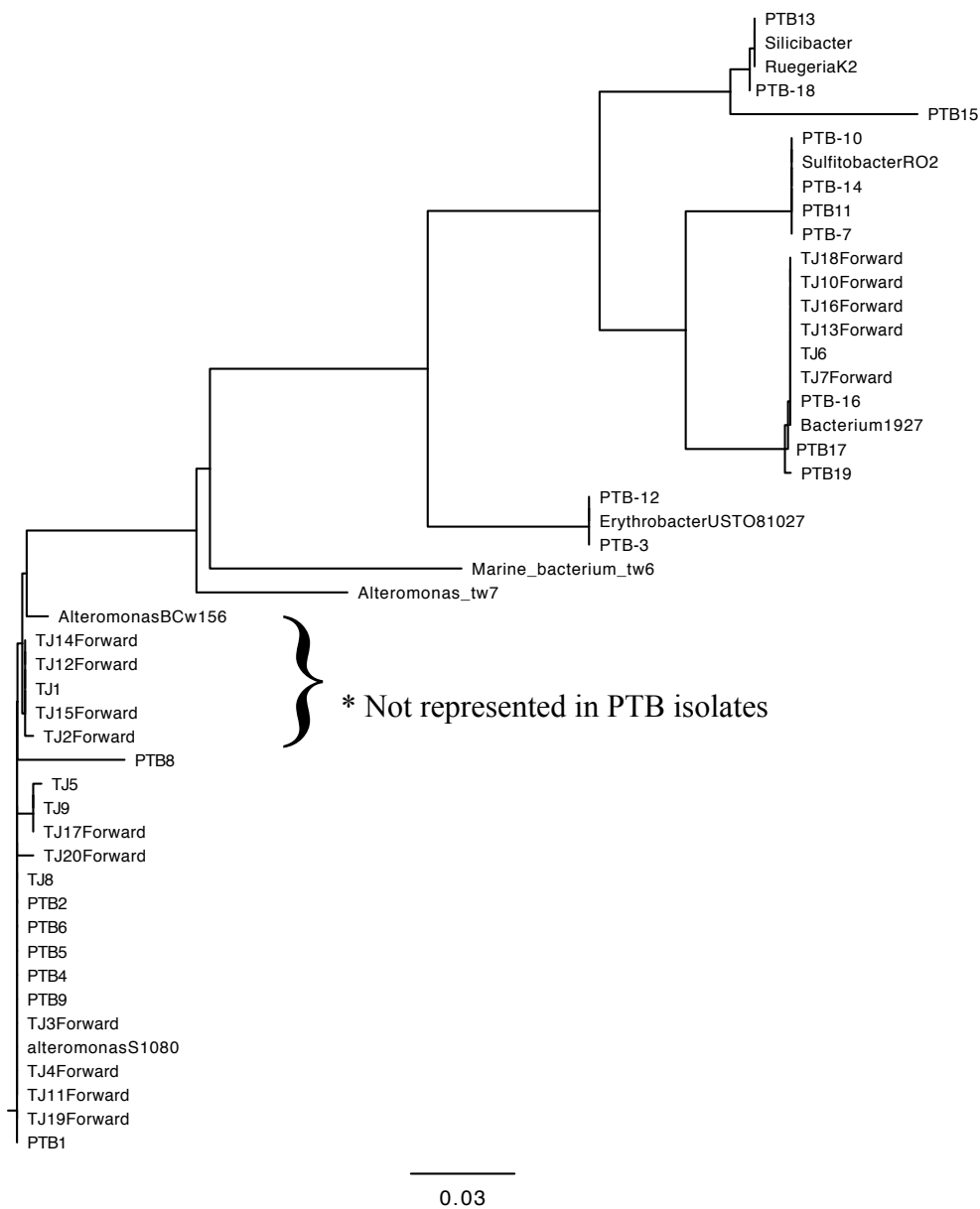


Figure 3.13: Neighbor-joining tree showing the 16S gene library constructed of the bacterial assemblage that induces VBPO in *Synechococcus* CC9311, the 19 isolates, as well as known sequences. TJ# refers to a clone from the 16S rRNA gene library and PTB# refers to a strain isolated from the *Pteridomonas* enrichment.

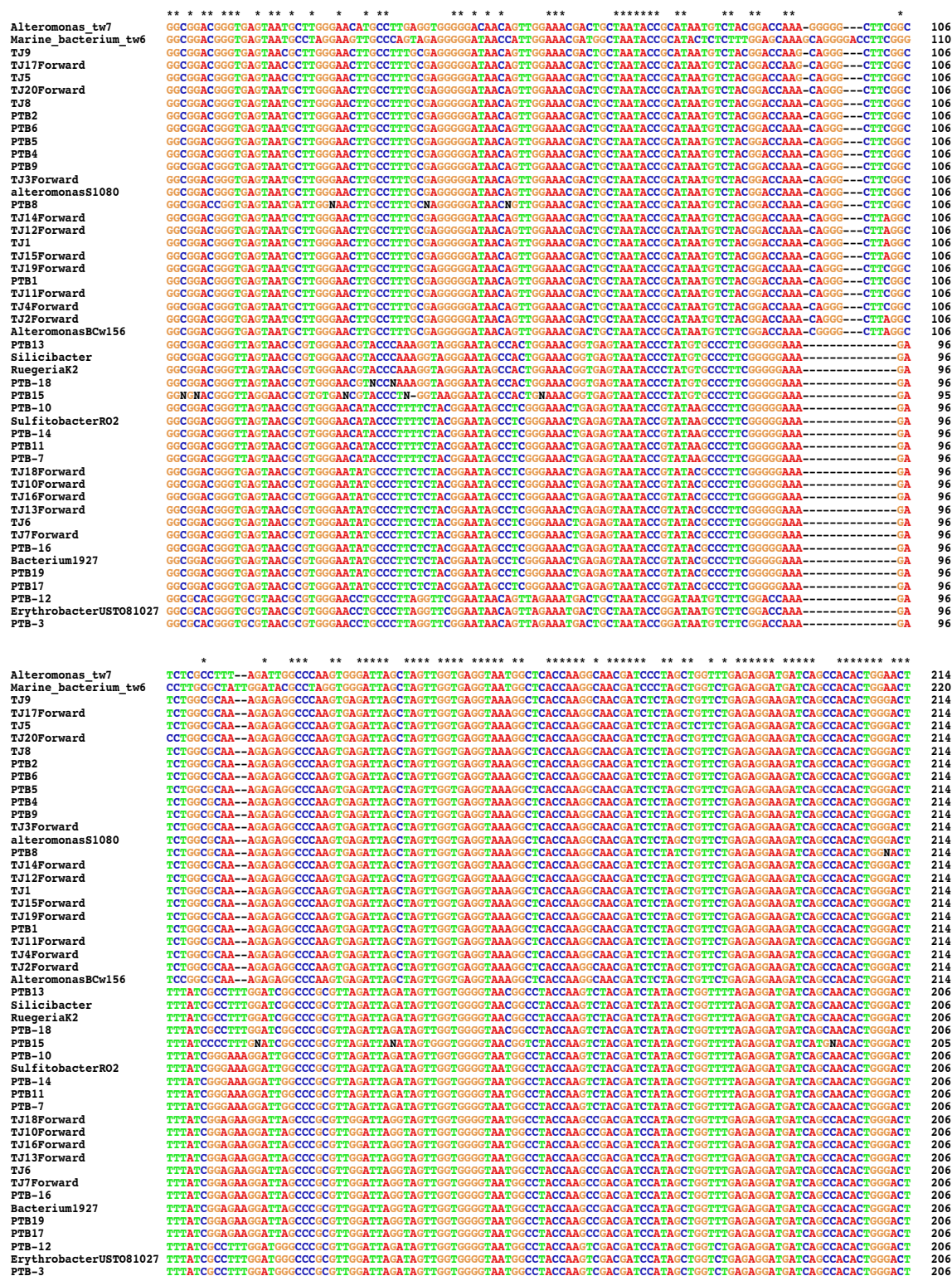


Figure 3.14: Alignment of the 421 bp fragment of the 16s rDNA genes from the PTB enrichment clone library (TJ#), 19 isolated strains (PTB#) and known sequences.

References

- Altschul, S. F., Madden, T. L., Schaffer, A. A., Zhang, J., Zhang, Z., Miller, W. & Lipman, D. J. 1997. Gapped BLAST and PSI-BLAST: a new generation of protein database search programs. *Nucleic Acids Research* 25:3389-402.
- Avrani, S., Wurtzel, O., Sharon, I., Sorek, R. & Lindell, D. 2011. Genomic island variability facilitates *Prochlorococcus*-virus coexistence. *Nature* 474:604-08.
- Battchikova, N., Vainonen, J. P., Vorontsova, N., Keranen, M., Carmel, D. & Aro, E. M. 2010. Dynamic changes in the proteome of *Synechocystis* 6803 in response to CO₂ limitation revealed by quantitative proteomics. *Journal of Proteome Research* 9:5896-912.
- Bernhardt, P., Okino, T., Winter, J. M., Miyanaga, A. & Moore, B. S. 2011. A stereoselective vanadium-dependent chloroperoxidase in bacterial antibiotic biosynthesis. *Journal of the American Chemical Society* 133:4268-70.
- Bidle, K. D. & Azam, F. 2001. Bacterial control of silicon regeneration from diatom detritus: Significance of bacterial ectohydrolases and species identity. *Limnology and Oceanography* 46:1606-23.
- Blot, N., Mella-Flores, D., Six, C., Le Corguille, G., Boutte, C., Peyrat, A., Monnier, A., Ratin, M., Gourvil, P., Campbell, D. A. & Garczarek, L. 2011. Light history influences the response of the marine cyanobacterium *Synechococcus* sp. WH7803 to oxidative stress. *Plant Physiology* 156:1934-54.
- Brahamsha, B. 1996. A genetic manipulation system for oceanic cyanobacteria of the genus *Synechococcus*. *Applied and Environmental Microbiology* 62:1747-51.
- Butler, A. & Carter-Franklin, J. N. 2004. The role of vanadium bromoperoxidase in the biosynthesis of halogenated marine natural products. *Natural Product Reports* 21:180-88.
- Carter, J. N., Beatty, K. E., Simpson, M. T. & Butler, A. 2002. Reactivity of recombinant and mutant vanadium bromoperoxidase from the red alga *Corallina officinalis*. *Journal of Inorganic Biochemistry* 91:59-69.
- Carter-Franklin, J. N. & Butler, A. 2004. Vanadium bromoperoxidase-catalyzed biosynthesis of halogenated marine natural products. *Journal of the American Chemical Society* 126:15060-66.
- Castielli, O., De la Cerda, B., Navarro, J. A., Hervas, M. & De la Rosa, M. A. 2009. Proteomic analyses of the response of cyanobacteria to different stress conditions. *Febs Letters* 583:1753-58.

- Chan, Y. W., Nenninger, A., Clokie, S. J. H., Mann, N. H., Scanlan, D. J., Whitworth, A. L. & Clokie, M. R. J. 2007. Pigment composition and adaptation in free-living and symbiotic strains of *Acaryochloris marina*. *Fems Microbiology Ecology* 61:65-73.
- Chenna, R., Sugawara, H., T, K., Lopez, R., Gibson, T., Higgins, D. G. & J.D, T. 2003. Multiple sequence alignment with the Clustal series of programs. *Nucleic Acids Research*, pp. 3497-500.
- Dufresne, A., Ostrowski, M., Scanlan, D. J., Garczarek, L., Mazard, S., Palenik, B. P., Paulsen, I. T., de Marsac, N. T., Wincker, P., Dossat, C., Ferriera, S., Johnson, J., Post, A. F., Hess, W. R. & Partensky, F. 2008a. Unraveling the genomic mosaic of a ubiquitous genus of marine cyanobacteria. *Genome Biology* 9.
- Guasto, J. S., Rusconi, R. & Stocker, R. 2012. Fluid mechanics of planktonic microorganisms. In: Davis, S. H. & Moin, P. [Eds.] *Annual Review of Fluid Mechanics, Vol 44*. Annual Reviews, Palo Alto, pp. 373-400.
- Guillard, R. R. & Ryther, J. H. 1962. Studies of marine planktonic diatoms 1. *Cyclotella nana hustedt*, and *Detonula confervacea* (cleve) gran. *Canadian Journal of Microbiology* 8:229-&.
- Huang, D. W., Sherman, B. T. & Lempicki, R. A. 2009a. Bioinformatics enrichment tools: paths toward the comprehensive functional analysis of large gene lists. *Nucleic Acids Research* 37:1-13.
- Huang, D. W., Sherman, B. T. & Lempicki, R. A. 2009b. Systematic and integrative analysis of large gene lists using DAVID bioinformatics resources. *Nature Protocols* 4:44-57.
- Huang, S. J., Wilhelm, S. W., Harvey, H. R., Taylor, K., Jiao, N. Z. & Chen, F. 2012. Novel lineages of *Prochlorococcus* and *Synechococcus* in the global oceans. *ISME Journal* 6:285-97.
- Ianora, A., Bentley, M. G., Caldwell, G. S., Casotti, R., Cembella, A. D., Engstrom-Ost, J., Halsband, C., Sonnenschein, E., Legrand, C., Llewellyn, C. A., Paldaviciene, A., Pilkaityte, R., Pohnert, G., Razinkovas, A., Romano, G., Tillmann, U. & Vaiciute, D. 2011. The relevance of marine chemical ecology to plankton and ecosystem function: an emerging field. *Marine Drugs* 9:1625-48.
- Jardillier, L., Zubkov, M. V., Pearman, J. & Scanlan, D. J. 2010. Significant CO₂ fixation by small prymnesiophytes in the subtropical and tropical northeast Atlantic Ocean. *ISME Journal* 4:1180-92.

- Johnson, T. L., Palenik, B. & Brahmsha, B. 2011. Characterization of a functional vanadium-dependent bromoperoxidase in the marine cyanobacterium *Synechococcus* sp. CC9311. *Journal of Phycology* 47:792-801.
- Juhl, A. R., Velazquez, V. & Latz, M. I. 2000. Effect of growth conditions on flow-induced inhibition of population growth of a red-tide dinoflagellate. *Limnology and Oceanography* 45:905-15.
- Kamenarska, Z., Taniguchi, T., Ohsawa, N., Hiraoka, M. & Itoh, N. 2007. A vanadium-dependent bromoperoxidase in the marine red alga *Kappaphycus alvarezii* (Doty) Doty displays clear substrate specificity. *Phytochemistry* 68:1358-66.
- Krenn, B., Izumi, Y., Yamada, H. & Wever, R. 1989. A comparison of different (vanadium) bromoperoxidases - the bromoperoxidase from *Corallina pilulifera* is also vanadium enzyme. *Biochemica et Biophysica ACTA* 998:63-68.
- Krieger-Liszkay, A., Kos, P. B. & Hideg, E. 2011. Superoxide anion radicals generated by methylviologen in photosystem I damage photosystem II. *Physiologia Plantarum* 142:17-25.
- Latz, M. I., Case, J. F. & Gran, R. L. 1994. Excitation of bioluminescence by laminar fluid shear associated with simple couette-flow. *Limnology and Oceanography* 39:1424-39.
- Li, W. K. W. 1994. Primary production of prochlorophytes, cyanobacteria, and eukaryotic ultraphytoplankton - measurements from flow cytometric sorting. *Limnology and Oceanography* 39:169-75.
- Malits, A., Peters, F., Bayer-Giraldi, M., Marrase, C., Zoppini, A., Guadayol, O. & Alcaraz, M. 2004. Effects of small-scale turbulence on bacteria: A matter of size. *Microbial Ecology* 48:287-99.
- Malits, A. & Weinbauer, M. G. 2009. Effect of turbulence and viruses on prokaryotic cell size, production and diversity. *Aquatic Microbial Ecology* 54:243-54.
- Manley, S. L. 2002. Phyto-genesis of halomethanes: A product of selection or a metabolic accident? *Biogeochemistry* 60:163-80.
- Martinac, B. 2004. Mechanosensitive ion channels: molecules of mechanotransduction. *Journal of Cell Science* 117:2449-60.
- Moore, C. A. & Okuda, R. K. 1996. Bromoperoxidase activity in 94 species of marine algae. *Journal of Natural Toxins* 5:295-305.

- Nickerson, C. A., Ott, C. M., Wilson, J. W., Ramamurthy, R., LeBlanc, C. L., Bentrup, K. H. Z., Hammond, T. & Pierson, D. L. 2003. Low-shear modeled microgravity: a global environmental regulatory signal affecting bacterial gene expression, physiology, and pathogenesis. *Journal of Microbiological Methods* 54:1-11.
- O'Connor, K. A. & Zusman, D. R. 1999. Induction of beta-lactamase influences the course of development in *Myxococcus xanthus*. *Journal of Bacteriology* 181:6319-31.
- Ohkubo, S., Miyashita, H., Murakami, A., Takeyama, H., Tsuchiya, T. & Mimuro, M. 2006. Molecular detection of epiphytic *Acaryochloris* spp. on marine macroalgae. *Applied and Environmental Microbiology* 72:7912-15.
- Ohsawa, N., Ogata, Y., Okada, N. & Itoh, N. 2001. Physiological function of bromoperoxidase in the red marine alga, *Corallina pilulifera*: production of bromoform as an allelochemical and the simultaneous elimination of hydrogen peroxide. *Phytochemistry* 58:683-92.
- Palenik, B., Ren, Q., Dupont, C., Myers, G., Heidelberg, J., Badger, J., Madupu, R., Nelson, W., Brinkac, L., Dodson, R., Durkin, A., Daugherty, S., Sullivan, S., Khouri, H., Mohamoud, Y., Halpin, R. & Paulsen, I. 2006. Genome sequence of *Synechococcus* CC9311: Insights into adaptation to a coastal environment. *Proceedings of the National Academy of Sciences of the United States of America* 103:13555-59.
- Paul, N. A., de Nys, R. & Steinberg, P. D. 2006. Chemical defence against bacteria in the red alga *Asparagopsis armata*: linking structure with function. *Marine Ecology-Progress Series* 306:87-101.
- Penno, S., Lindell, D., & Post, A. F. 2006. Diversity of *Synechococcus* and *Prochlorococcus* populations determined from DNA sequences of the N-regulatory gene ntcA. *Environmental Microbiology* 8:1200-11.
- Perelman, A., Uzan, A., Hacoen, D. & Schwarz, R. 2003. Oxidative stress in *Synechococcus* sp. strain PCC 7942: Various mechanisms for H₂O₂ detoxification with different physiological roles. *Journal of Bacteriology* 185:3654-60.
- Rambaut, A. 1996. Se-Align: Sequence Alignment Editor.
<http://tree.bio.ed.ac.uk/software/seal/>.
- Rambaut, A. 2008. FigTree. 1.2 ed. <http://tree.bio.ed.ac.uk/software/FigTree/>.
- Rhee, S. G., Kang, S. W., Chang, T. S., Jeong, W. & Kim, K. 2001. Peroxiredoxin, a novel family of peroxidases. *Iubmb Life* 52:35-41.

- Roe, K. L., Barbeau, K., Mann, E. L. & Haygood, M. G. 2012. Acquisition of iron by *Trichodesmium* and associated bacteria in culture. *Environmental Microbiology* **14**:1681-95.
- Ross, P. L., Huang, Y. L. N., Marchese, J. N., Williamson, B., Parker, K., Hattan, S., Khainovski, N., Pillai, S., Dey, S., Daniels, S., Purkayastha, S., Juhasz, P., Martin, S., Bartlett-Jones, M., He, F., Jacobson, A. & Pappin, D. J. 2004. Multiplexed protein quantitation in *Saccharomyces cerevisiae* using amine-reactive isobaric tagging reagents. *Molecular & Cellular Proteomics* **3**:1154-69.
- Ruby, E. G. & Neilson, K. H. 1978. Seasonal changes in species composition of luminous bacteria in nearshore seawater. *Limnology and Oceanography* **23**:530-33.
- Sahoo, S., Rao, K. K. & Suraishkumar, G. K. 2006. Reactive oxygen species induced by shear stress mediate cell death in *Bacillus subtilis*. *Biotechnology and Bioengineering* **94**:118-27.
- Sahoo, S., Verma, R. K., Suresh, A. K., Rao, K. K., Bellare, J. & Suraishkumar, G. K. 2003. Macro-level and genetic-level responses of *Bacillus subtilis* to shear stress. *Biotechnology Progress* **19**:1689-96.
- Shiller, A. M. & Mao, L. J. 1999. Dissolved vanadium on the Louisiana Shelf: effect of oxygen depletion. *Continental Shelf Research* **19**:1007-20.
- Stuart, R. K., Dupont, C. L., Johnson, D. A., Paulsen, I. T. & Palenik, B. 2009. Coastal strains of marine *Synechococcus* species exhibit increased tolerance to copper shock and a distinctive transcriptional response relative to those of open-ocean strains. *Applied and Environmental Microbiology* **75**:5047-57.
- Stuart, R. K., Brahamsha, B., Busby, K., Palenik, B. 2013. Genomic island genes in a coastal marine *Synechococcus* strain confer enhanced tolerance to copper and oxidative stress. *The ISME Journal*. 1-11. DOI 10.1038/ismej.2012.175.
- Swingley, W. D., Chen, M., Cheung, P. C., Conrad, A. L., Dejesa, L. C., Hao, J., Honchak, B. M., Karbach, L. E., Kurdoglu, A., Lahiri, S., Mastrian, S. D., Miyashita, H., Page, L., Ramakrishna, P., Satoh, S., Sattley, W. M., Shimada, Y., Taylor, H. L., Tomo, T., Tsuchiya, T., Wang, Z. T., Raymond, J., Mimuro, M., Blankenship, R. E. & Touchman, J. W. 2008. Niche adaptation and genome expansion in the chlorophyll d-producing cyanobacterium *Acaryochloris marina*. *Proceedings of the National Academy of Sciences of the United States of America* **105**:2005-10.
- Waterbury, J. B. & Willey, J. M. 1988. Isolation and growth of the marine planktonic cyanobacteria. *Methods in Enzymology* **167**:100-05.

- Weaver, W. M., Milisavljevic, V., Miller, J. F. & Di Carlo, D. 2012. Fluid flow induces biofilm formation in *Staphylococcus epidermidis* polysaccharide intracellular adhesin-positive clinical isolates. *Applied and Environmental Microbiology* 78:5890-96.
- Weinberger, F., Coquempot, B., Forner, S., Morin, P., Kloareg, B. & Potin, P. 2007. Different regulation of haloperoxidation during agar oligosaccharide-activated defence mechanisms in two related red algae, *Gracilaria* sp and *Gracilaria chilensis*. *Journal of Experimental Botany* 58:4365-72.
- Winter, J. M. & Moore, B. S. 2009. Exploring the chemistry and biology of vanadium-dependent haloperoxidases. *Journal of Biological Chemistry* 284:18577-81.

Chapter 3, in part, is currently being prepared for submission for publication of the material by Johnson, Todd; Paz-Yepes, Javier; Palenik, Brian; and Bianca, Brahamsha. The dissertation author was the primary investigator and will be first author of this chapter.

Chapter 4

Halomethane production by vanadium-dependent bromoperoxidase in marine

Synechococcus

Abstract

Vanadium-dependent bromoperoxidase (VBPO) has been suggested to produce halogenated methanes in eukaryotic macro- and microalgae, but this activity has not been studied in marine prokaryotes. This study measured halomethane production in two strains of *Synechococcus*; one with VBPO (strain CC9311) and one without VBPO (strain WH8102). A mutant strain of CC9311, VMUT, in which the gene for VBPO is disrupted, was also tested. A suite of halomethanes was measured in the headspace above cultures as well as in the culture medium with a purge-and-trap method.

Monohalomethanes were the most consistently produced molecules among the three strains tested. Additionally, CC9311 produced 382.4 ± 28.0 molecules cell⁻¹ day⁻¹ of bromoform (CHBr₃) when VBPO activity was detected and only 13.9 ± 5.6 molecules cell⁻¹ day⁻¹ when VBPO activity was not detected. No production was seen by VMUT or WH8102. These data show that bromoform (CHBr₃) production rates are dramatically increased with or exclusive to the presence of VBPO, supporting its involvement in bromoform synthesis. We have also seen evidence of chloroform production in both CC9311 and WH8102 and dichloromethane production synthesis in CC9311. This study thus provides evidence that marine *Synechococcus* can be a natural source of marine bromoform, which contributes to ozone depletion in the stratosphere.

Introduction

Halomethanes are naturally and anthropogenically derived small molecules that transport halogen species to the upper stratosphere and can contribute to ozone degradation (Law & Sturges, 2010). There is a need to establish and quantify known sources and sinks of atmospheric bromine as only about two thirds of stratospheric levels can be accounted for by tropospheric concentrations of methyl bromide and bromine containing halons (Montzka & Reimann, 2010). This has generated interest in determining additional natural sources of halogenated methanes. Longer lived halomethanes, such as methyl bromide have both natural and anthropogenic sources and are thought to contribute greatly to stratospheric halide concentrations because they degrade slowly and can more easily circulate to higher elevations (Quack & Wallace, 2003) unlike polyhalomethanes, which degrade more quickly in the atmosphere (Liang *et al.*, 2010). However, recently observed convection patterns and atmospheric measurements support the idea that very short lived halogenated substances (VSLS), such as the polyhalomethanes can be a source of stratospheric inorganic halides and may be an important link to understanding the gap between known sources of atmospheric bromine and the amount of inorganic bromine that reaches the stratosphere (Aschmann & Sinnhuber, 2012; Montzka & Reimann, 2010). Many areas of ocean surface water are saturated in halogenated methanes, and thus the ocean acts primarily as a source for halogenated methanes (Paul & Pohnert, 2011). The production of such halomethanes including iodinated, brominated, and chlorinated methanes, has long been attributed to eukaryotic macroalgae (Beissner *et al.*, 1981, Ohsawa *et al.*, 2001, Manley & Barbero, 2001). Eukaryotic macroalgae contribute greatly to marine-derived brominated methanes

but are primarily coastal. Marine phytoplankton are a potential source of marine-based halomethane production as they have a much broader distribution (Paul and Pohnert, 2011).

Some studies have focused on field data, correlating photosynthetic pigments to halomethane production. For example, Karlsson *et al.* (2008) found that the production of bromoform (CHBr_3) in seawater was correlated to a phytoplankton bloom dominated by the cyanobacterium *Pseudoanabaena* in the Baltic Sea. Other studies have found a significant correlation between CHBr_3 and chlorophyll in ocean transects (Kurihara *et al.*, 2012). From these studies, it has been suggested that bromoform could be related to bloom conditions of phytoplankton. Furthermore, while vanadium-dependent haloperoxidases help regulate the iodide and bromide concentrations in eukaryotic algae (Kupper *et al.*, 2008, Chance *et al.*, 2009), little is known about halide metabolism in bacteria, particularly in marine cyanobacteria. Literature primarily focuses on the potential of heterotrophic bacteria to degrade methyl halides in both laboratory (McAnulla *et al.*, 2001) and field studies (Cox *et al.*, 2012).

Halomethane production has been demonstrated in laboratory studies of marine eukaryotic phytoplankton (Scarratt & Moore, 1998, Moore *et al.*, 1996), but has not been well-characterized in marine cyanobacteria. These globally important organisms have a wide distribution and a substantial influence on marine biogeochemistry, reflected in their large contribution to marine based photosynthetic carbon fixation (Partensky *et al.*, 1999, Jardillier *et al.*, 2010). Cyanobacteria of the genera *Prochlorococcus* and *Synechococcus* have previously been found to produce CH_3I , CH_3Br , and CH_3Cl (Brownell *et al.*, 2010,

Scarratt & Moore, 1998). However, polyhalomethane production in a laboratory setting has not been previously tested in marine *Synechococcus*.

The gene for a predicted vanadium-dependent bromoperoxidase (VBPO) was recently found in the genome of *Synechococcus* sp. CC9311 (Palenik *et al.*, 2006) and characterized as a functional enzyme (Johnson *et al.*, 2011). Though VBPO genes are found in other cyanobacteria, it is not a universal cyanobacterial core gene. It appears to have been horizontally acquired by strain CC9311. VBPO has been implicated in the production of polyhalogenated methanes in eukaryotic macroalgae, thus the presence of a functional VBPO in CC9311 represents the genetic potential to produce brominated organic molecules.

In this study, halomethanes were collected from the headspace above cultures or by flushing “zero” air through cultures using a custom purge-and-trap system. Halomethane concentrations were then measured on a “Medusa” GC-MS, a specialized gas chromatographic system with mass spectrometric detection for the monitoring of trace levels of halogenated organics (Miller *et al.*, 2008).

The goal of this chapter was to test multiple strains of *Synechococcus* for the production of halomethanes and to determine if this production is linked to the presence of a vanadium-dependent bromoperoxidase. Halomethanes were measured in two strains of marine *Synechococcus* (CC9311 and WH8102), one of which (CC9311) contains a functional vanadium-dependent bromoperoxidase. A mutant strain of CC9311, VMUT, which lacks a functional VBPO (see Chapter 3) was also tested. Furthermore, these strains were tested under varied culture conditions in which VBPO is expressed at

different levels. This study provides the first evidence of bromoform production in marine *Synechococcus* and that the production is due to VBPO.

Materials and Methods

Cultures and growth conditions

Cultures of *Synechococcus* sp. CC9311, referred to as CC9311 (Palenik *et al.*, 2006), *Synechococcus* sp. WH8102, referred to as WH8102 (Palenik *et al.*, 2003) and *Synechococcus* sp. VMUT, referred to as VMUT (see Chapter 3) were grown in SN medium (Waterbury & Willey, 1988) supplemented with 250 nM sodium orthovanadate (Na_3VO_4). VMUT was grown under the same conditions with the addition of 20 $\mu\text{g ml}^{-1}$ kanamycin sulfate (Sigma-Aldrich, St. Louis, Missouri, USA). *Synechococcus* sp. VMUT was created through insertional gene-inactivation, where the ORF encoding VBPO (sync_2681) in CC9311 was disrupted through the insertion of pVBR1 through homologous recombination and thus lacks a functional VBPO. This inactivation is detailed in Chapter 3.

Cultures were inoculated in 1.5 L medium in 2.8 L flasks, and grown at 23°C with constant light (20 $\mu\text{mol photons m}^{-2} \text{sec}^{-1}$) to exponential growth ($1.0\text{-}5.0 \times 10^7 \text{ cell ml}^{-1}$). Portions of the cultures, as described for each experiment, were then sampled for cell concentration, VBPO activity, and halomethane production.

Cell counts

To determine cell concentrations, samples (1 ml) were taken from each culture, preserved in 0.25% glutaraldehyde (final concentration, Sigma-Aldrich), and stored at

-80°C until analysis. Cell counts were determined by flow cytometry (FACSort, Becton Dickinson, New Jersey, USA) as described in Chapter 3.

VBPO Specific Activity

To confirm the presence or absence of VBPO activity, proteins were extracted from portions of cultures used in this experiment and tested for VBPO activity using either the monochlorodimedone assay or the thymol blue assay, both described by Johnson *et al.* (2011). Briefly, cells were harvested by centrifugation at 13,175 xg for 10 min at 18°C. Cell pellets were resuspended in 100 mM 2-(*N*-morpholino)ethanesulfonic acid (MES, 99%, Acros Organics, Geel, Belgium) buffer, pH 7.0, and run through a French pressure cell, with three passes at 20,000 psi. Broken cells were centrifuged again at 6,275 xg for 10 min at 4°C. The clarified supernatant was used as the protein extract and tested for VBPO activity using either monochlorodimedone or thymol blue. VBPO activities were normalized to protein concentration and are shown as $\mu\text{mol monochlorodimedone min}^{-1} \text{mg}^{-1} \text{protein}$ or $\mu\text{mol dibromothymol blue min}^{-1} \text{mg}^{-1} \text{protein}$.

Headspace analysis

The headspace above cultures of *Synechococcus* WH8102 (which lacks a VBPO) and CC9311 (which has a VBPO) was sampled for halomethanes. Cell-free SN medium was also measured as a negative control for the method to determine the background concentrations from the medium. For each strain, a 1.5 L culture was grown to exponential growth as described above with constant stirring using a 5.0 cm magnetic stir bar at 200 rpm. Cell concentrations were determined in cultures at the start of each two-

hour incubation (Table 4.2) and were between $0.8 - 7.0 \times 10^7$ cells ml^{-1} . VBPO activity was tested in *Synechococcus* sp. CC9311 and WH8102 (Table 4.2), and only detected in CC9311 (trial 1, 0.284 ± 0.072 μmol monochlorodimedone $\text{min}^{-1} \text{mg}^{-1}$ protein; trial 2, 0.175 ± 0.032 μmol dibromothymol blue $\text{min}^{-1} \text{mg}^{-1}$ protein).

To sample the headspace, 100 ml of grown culture were transferred to a sterile 500 ml flask and sealed with a blue rubber stopper (No. 7, Fisher). A 1/16-inch stainless steel tube was connected to a tank of ultra-high purity grade (UHP) air (Airgas) on one end, and inserted through the stopper into the flask containing the culture on the other. A second stainless steel tube was inserted through the rubber stopper on one end and connected to an evacuated, 6 L stainless steel collection vessel (SilcoCan, Restek Corporation). The flask was flushed 10 times with the UHP zero air by over pressurizing the flask to 10 psi above ambient (determined by the pressure on the regulator attached to the zero air) then released via the outgoing stainless steel tubing to remove the lab air from the flask. After flushing, the outward stainless steel tube was connected to the closed collection vessel, sealing the system. After two hours, the headspace was sampled by over-pressurizing the flask with zero air to 15 psi, and then allowing the air to flow to the 6 L stainless steel collection vessel. This was repeated 11 times.

The stainless steel vessels were then connected to the “Medusa” GC/MS (see below) and halomethane concentrations were measured in 2.0 L air from each sample. Each vessel was measured on the GC/MS in triplicate with a blank between each sample to determine any background from the previous analysis. The flush gas (UHP zero air, Airgas) was also run in at least triplicates to determine the background concentrations of each molecule. Concentrations in the headspace were calculated based on the dilution

with the flush gas as determined by the pressures in the vessel before and after flushing. If present, the concentration from the blanks (from the “Medusa” GC/MS system and/or flush gas) was subtracted from the measured concentration before accounting for the dilution.

Halomethane concentrations in the liquid medium of each flask were calculated from the concentrations measured in the headspace using Henry’s Law. Dimensionless Henry’s constants (H_k) used in this study were established in previous literature (Table 4.1) for conditions comparable to this study, with seawater salinity (not measured in this study) and temperatures between 20-23°C.

The Henry’s constants used were originally determined in full salinity seawater, while the medium used in this study, SN medium, is composed of 75% seawater and 25% milliQ. However, extra nutrients are added that contribute to the total solute concentration of the medium, thus the Henry’s constants should still be appropriate for the SN medium.

Purge-and-trap experiment

In a second type of experiment, halomethanes were sampled in cultures of three strains of marine *Synechococcus* using a custom purge-and-trap system, depicted in Figure 4.1. VBPO activity was measured in proteins extracted immediately after halomethane sampling (Table 4.4) with only CC9311 showing VBPO activity under stirred conditions ($0.024 \pm 0.002 \mu\text{mol min}^{-1} \text{mg}^{-1}$). Cell counts were also followed through the growth of the cultures as well as at the beginning and the end of each 24 hour incubation (Figure 4.2). Over the 24 hour incubation period, all cultures experienced a

slight decrease in cell concentration, except for VMUT still, which continued exponential growth, and WH8102 stirred, which had a dramatic decrease in measured cell concentration (2.21×10^7 cells ml^{-1} to 4.53×10^6 cells ml^{-1}) over the 24 hours (Table 4.4).

For sampling halomethanes, serum bottles were prepared by acid washing, autoclaving, and sealing with a rubber septum and aluminum crimp. The empty bottles were then flushed with UHP zero air (Airgas) to 10 psi above ambient (1 atm) and then released through a second stainless steel tube 10 times per bottle, diluting lab air down to 1×10^{-10} . For each strain, cultures were grown in 1.5 L batches (without stirring), then three serum bottles (1 L, Bellco Glass) flushed with UHP zero air were injected with 400 ml of culture using a 60 ml syringe (Becton Dickinson) with a 22-gauge needle (Precision Glide, Becton Dickinson) under sterile conditions. One of the serum bottles was sampled immediately and is referred to as the time zero sample. The two remaining bottles were placed in a lighted incubator (23 °C with $20 \mu\text{mol photons m}^{-2} \text{s}^{-1}$ light). One was stirred with a magnetic stir plate (Fisher) at 200 rpm with a 2.5 cm stir bar to induce VBPO activity, while the other remained still (no induction of VBPO activity). Both were sampled after 24 hours.

To measure gas production, a 1/16-inch stainless steel tube connected to the UHP zero air tank was inserted through the rubber septum into the culture so that the tube was close to, but not touching the bottom. Air was flushed through the culture and into another stainless steel tube that connected the serum bottle to a 6 L stainless steel vessel (SilcoCan, Restek), which had been evacuated to 10 mTorr or less. Zero air was flushed through the culture until the vessel reached 30 psia (about 12 L of air). After a serum bottle was sampled, the 6 L vessel containing the sample was connected directly to the

UHP zero air tank and the pressure in the vessel was increased by an additional 10 psi, as the pressure in the vessel drives the injection of the sample into the “Medusa” GC/MS. All exact pressures were measured using a high precision pressure gauge (Paroscientific). All connections with the stainless steel tubing were created using either stainless steel Swagelok or VICI compression type fittings.

Purge efficiencies were calculated using an equation established by Ruiz-Brevia *et al.* (2009), where R_j is the purge efficiency as a % dissolved gas recovered from the media; F is the flow rate of flush gas; t is the time of flushing; V_G is the volume of gas in headspace, K_x is the inverse of the Henry’s constant (Henry’s constants given in Table 4.1), and V_L is the volume of culture (Equation 1). The flow rate (F) of the flush gas (zero air) and flush time (t) were not measured in this experiment. However, the exact volume of flush gas was used to replace the product of $F \times t$ (a volume), determined using the pressures in the tank before and after flushing.

Equation 1:

$$R_j (\%) = 100 \left(1 - \exp \left[\frac{-Ft}{V_G + K_x V_L} \right] \right)$$

Purge efficiencies (Table 4.5) were calculated (Equation 1) using published Henry’s constants and the volume of flush gas passed through the medium. Each 0.4 L culture was flushed with approximately 12.5 L of UHP zero air, precisely determined by measuring the pressure in the 6.0 L vessel before and after purging for each sample. Bromoform is the most soluble gas with a purge efficiency of $46.0 \pm 1.2\%$. Dibromomethane had a purge efficiency of $60.8 \pm 1.3\%$. All other gases tested had an estimated purge efficiency of around 90-99%.

Purge efficiencies were used to calculate the halomethane concentrations (pmol L^{-1}) in the three strains of *Synechococcus*, which were then normalized to the number of cells in the culture ($\text{pmol L}^{-1} \text{ cell}^{-1}$) before and after 24 hours with and without stirring. Due to a large decrease in the cell counts at 24 hours for WH8102 as well as cell concentrations ranging from $0.4 - 6.6 \times 10^7 \text{ cell ml}^{-1}$ at the time of sampling (Table 4.4), halomethane concentrations were normalized to the total number of cells in each sample at time zero. Production rates were calculated by subtracting the amount of halomethane (moles) present at time zero from the amount of halomethane (moles) present after 24 hrs. The difference was then normalized to the number of cells in each culture at time zero, using 5% error for the cell counts. As a second metric of production, rates were also normalized to the cell concentrations averaged between 0 and 24 hours of the incubation, taking into account the actual error of the measurement by using 1/2 of the difference of the cell concentrations at the two time points as uncertainty. Final uncertainties were calculated using standard propagation of error as guided by Taylor (1997) of the standard deviation of triplicate measurements.

GC-MS Analysis

Samples were analyzed on the “Medusa” GC/MS system described by Miller *et al.* (2008). Air samples (2.0 L) from each collection vessel were injected in triplicates into the “Medusa” system. In the system, gases are pre-concentrated in a cold trap at -165°C (HayeSep D, VICI), and helium carrier gas is used to reduce amounts of bulk gases. The most volatile analytes, carbon tetrafluoride (CF_4) and several remaining bulk gases, are transferred through a second, smaller diameter cold trap at -165°C (HayeSep D,

VICI), then separated on a custom pre-column (consisting of a combination of 40 mg 100/120 mesh molecular sieve 4 Å and 160 mg of 100/120 mesh HiSiv-3000), and then separated by a CP-PoraBOND Q column, before MSD detection (Agilent 5973/5975 quadrupole MSD). In a second injection step, all other less volatile gasses are cryofocused on the second trap to further reduce water and carbon dioxide, then they bypass the pre-column and are injected into the main column for mass spectrometric detection.

Results

Headspace experiment

Several halogenated methanes, including CH₃I, CH₃Br, CH₂Br₂, CHBr₃, CH₃Cl, CH₂Cl₂, and CHCl₃, were measured in the headspace above cultures of log-phase *Synechococcus* strains CC9311 and WH8102 after a two-hour incubation (trial one and trial two) as well as after a four-hour incubation (CC9311, trial 2). The concentration (pmol L⁻¹) of each halomethane was then calculated for the liquid phase of cell-free SN medium, WH8102, and CC9311 (Table 4.2). All compounds measured were above the flush gas concentrations except for CH₂Cl₂ in CC9311 in the first trial. Furthermore, concentrations of CH₃Cl and CH₂Cl₂ had very large uncertainties, partially due to large error associated with the Henry's constant used in the calculations. Concentrations were also determined relative to the SN-medium blank (SN medium values were subtracted from culture values) and normalized by the cell concentration at the time of the sampling (Table 4.3). While this is not a true production rate, it indicates whether or not a halomethane accumulated in a culture.

Methyl bromide was the only halomethane that was consistently and significantly above the SN medium control in both cultures for both trials (Table 4.3). More methyl bromide was detected in CC9311 ($9.36 \pm 2.74 \text{ pmol L}^{-1} \text{ cell}^{-1} \times 10^7$) than in WH8102 ($5.01 \pm 4.11 \text{ pmol L}^{-1} \text{ cell}^{-1} \times 10^7$) in trial one, while similar amounts ($0.66 \pm 0.45 \text{ pmol L}^{-1} \text{ cell}^{-1} \times 10^7$ and $0.77 \pm 0.32 \text{ pmol L}^{-1} \text{ cell}^{-1} \times 10^7$) were measured in trial two after the 2-hour incubations. Methyl iodide, similarly, was measured in all of the samples except WH8102 in the second trial.

Overall, more brominated and iodinated halomethanes (CH_3I , CH_3Br , CH_2Br_2 , and CHBr_3) were consistently above the SN blank in both trials for CC9311 compared to WH8102. The most abundant of these was bromoform in CC9311 (trial 1, $51.76 \pm 4.43 \text{ pmol L}^{-1} \text{ cell}^{-1} \times 10^7$; trial 2, $97.42 \pm 11.55 \text{ pmol L}^{-1} \text{ cell}^{-1} \times 10^7$), which was significantly greater than concentrations measured in WH8102 (trial 1, $13.89 \pm 2.57 \text{ pmol L}^{-1} \text{ cell}^{-1} \times 10^7$; trial 2, $-14.89 \pm 7.17 \text{ pmol L}^{-1} \text{ cell}^{-1} \times 10^7$) in both trials. Bromoform concentrations were less in the four hour incubation of CC9311 compared to the two hour incubation in the second trial (Table 4.3).

Chlorinated methanes were also detected. A large amount of dichloromethane was detected in the 4 hour incubation of CC9311 ($1256.09 \pm 957.69 \text{ pmol L}^{-1} \text{ cell}^{-1} \times 10^7$) but not detected in any other sample. Similarly, but due to large uncertainties, methyl chloride was only significantly different than the SN medium control in the four hour incubation of CC9311 in (Table 4.3). Chloroform (CHCl_3) concentrations were lower in the cultures compared to the SN-medium in trial 1. However, in trial 2, chloroform concentrations were greater than the medium for both CC9311 ($11.20 \pm 3.18 \text{ pmol L}^{-1} \text{ cell}^{-1} \times 10^7$) and WH8102 ($14.36 \pm 4.54 \text{ pmol L}^{-1} \text{ cell}^{-1} \times 10^7$) in the two-hour incubations

but not significantly different than the SN medium in the four hour incubation of CC9311 (Table 4.3).

Purge-and-trap experiment

The same suite of halomethanes were measured in cultures of *Synechococcus* under conditions that elicit the expression of a vanadium-dependent bromoperoxidase in CC9311 (stirring) and those that do not (still) over a 24-hour incubation. Overall, chloromethane concentrations were greater than those of bromo- and iodomethanes, with methyl chloride being the most abundant compound detected, having concentrations ranging from 77.86 ± 0.27 to 163.70 ± 0.56 pmol L⁻¹ (Table 4.6). Halomethane concentrations normalized to the total number of cells measured at the beginning of each 24-hour incubation gave the same abundance pattern and had uncertainties of 5% (Table 4.7).

Due to a decrease in cell counts (Figure 4.2) halomethane production rates for this experiment were normalized to both the total number of cells at the initial time point for each incubation (Table 4.8) as well as the averaged number of cells between the zero and 24 hour time points for each culture (Table 4.9).

When halomethane production rates are normalized to the total number of cells at the initial time point (Table 4.8), production of bromoform over the 24-hour incubation period was thirty times greater in CC9311 when VBPO activity was present (382.4 ± 28.0 molecules cell⁻¹ day⁻¹ under stirred conditions) compared to CC9311 with no detectable VBPO activity (13.9 ± 5.6 molecules cell⁻¹ day⁻¹ under still conditions). A similar amount of bromoform was produced in VMUT under stirred conditions (14.4 ± 5.8 molecules

cell⁻¹ day⁻¹) as compared to CC9311 under still conditions (13.9 ± 5.6 molecules cell⁻¹ day⁻¹). Bromoform production was not significantly detected in VMUT under still conditions or WH8102 under stirred conditions.

Two monohalomethanes, CH₃I and CH₃Cl, were produced in all samples analyzed by the purge-and-trap method. Methyl chloride (CH₃Cl) was the most abundant halomethane produced among all strains and conditions tested, with cultures producing 321.4 ± 110.1 to 838.8 ± 115.7 molecules cell⁻¹ day⁻¹ (Table 4.8). CC9311 produced more methyl chloride than the other two strains tested. Less methyl iodide production was observed compared to methyl chloride. In CC9311, more methyl iodide was produced under still conditions (55.4 ± 4.1 molecules cell⁻¹ day⁻¹) compared to stirred (7.1 ± 1.6 molecules cell⁻¹ day⁻¹), though a similar amount of CH₃I was produced in VMUT when stirred (6.0 ± 1.7 molecules cell⁻¹ day⁻¹) and still (4.3 ± 1.8 molecules cell⁻¹ day⁻¹) within error. Methyl iodide production in WH8102 when stirred (1.7 ± 1.3 molecules cell⁻¹ day⁻¹) was about four times less than CC9311 stirred.

Methyl bromide (CH₃Br) production was only detected for CC9311, and like methyl iodide, more was produced in the still culture (667.1 ± 39.7 molecules cell⁻¹ day⁻¹) compared to the stirred (437.5 ± 27.3 molecules cell⁻¹ day⁻¹). Methyl bromide was not significantly produced by VMUT or WH8102.

The other polyhalomethanes measured in this study were less common between strains than the monohalomethanes. Dichloromethane production was only observed in CC9311 when stirred (308.3 ± 94.8 molecules cell⁻¹ day⁻¹), but was not significantly different from zero in all other samples. Chloroform (CHCl₃) was measured in both CC9311 and WH8102 under stirred conditions, but showed a decrease in other samples.

Dibromomethane was only produced in CC9311 (2.96 ± 1.39 molecules cell⁻¹ day⁻¹) and VMUT (3.18 ± 1.7 molecules cell⁻¹ day⁻¹) under stirred conditions in relatively low amounts compared to other gasses that were produced.

Halomethane production rates were also normalized by the average number of cells between the 0 and 24 hour time points, taking into account one-half of the difference of the cell counts for the error (Table 4.9). With these more conservative error calculations, no gases were produced at significant rates by either VMUT or WH8102. However, CC9311 did produce significant amounts monohalomethanes (CH₃I, 81.4 ± 31.7 molecules cell⁻¹ day⁻¹; CH₃Br, 980.9 ± 321.0 molecules cell⁻¹ day⁻¹; and CH₃Cl, 1233.4 ± 933.8 molecules cell⁻¹ day⁻¹) under still conditions. When stirred, CC9311 produced two monohalomethanes (CH₃Br, 643.4 ± 220.6 molecules cell⁻¹ day⁻¹; and CH₃Cl, 1063.7 ± 889.8 molecules cell⁻¹ day⁻¹) as well as bromoform (CHBr₃, 562.3 ± 198.1 molecules cell⁻¹ day⁻¹) and dichloromethane (CH₂Cl₂; 453.4 ± 347.3 molecules cell⁻¹ day⁻¹). Neither dibromomethane nor chloroform production were significantly different from zero using this more conservative normalization.

Discussion

Halomethane production by Synechococcus with VBPO

This study was designed to test if marine *Synechococcus* produces detectable amounts of polyhalomethanes and if so, if the production of such molecules depends on the presence of vanadium-dependent bromoperoxidase. To test these hypotheses, we used *Synechococcus* sp. CC9311, which expresses a functional VBPO when cultures are grown stirred, but not when cultures are still (Johnson *et al.*, 2011; see Chapter 3). The

use of this expression pattern was an important control for this experiment, allowing the same organism to be tested under two conditions with very different VBPO activity. We also used a mutant of CC9311 (VMUT), which lacks a functional VBPO due to an insertional gene inactivation of *sync_2681*, the ORF encoding VBPO. This allowed for testing halomethane production under the same culture conditions as CC9311 to determine if VBPO or another physiological process is involved. The third strain tested was WH8102, a distantly related species of marine *Synechococcus*, which lacks a VBPO as indicated in the sequenced genome (Palenik *et al.*, 2003). WH8102 was also important for putting this study into context as it has been tested previously for methyl halide production (Brownell *et al.*, 2010).

Synechococcus CC9311 was found to produce much greater amounts of bromoform when VBPO was expressed (CC9311 stirred) compared to when VBPO was absent (CC9311 Still, VMUT, WH8102, Table 4.8). The presence of VBPO was confirmed by testing for VBPO specific activity in all cultures (Tables 4.2 and 4.4), showing that VBPO was only expressed in cultures of CC9311 that had been stirred. Previous work has shown that the observed VBPO activity in CC9311 is the result of the gene product of *sync_2681* (Johnson *et al.*, 2011). Thus, bromoform production is due to VBPO activity.

Beissner *et al.* (1979, 1981) incubated extracts from the alga *P. capitatus* containing bromoperoxidase activity with organic acid precursors, finding that alpha-ketoacids produced the most dibromomethane and bromoform. From these experiments, a metabolic pathway for the production of polyhalomethanes (Figure 4.3) was proposed and has been supported indirectly by other experiments (Weinberger *et al.*, 2007,

Abrahamsson *et al.*, 2003). Itoh and Shinya (1994) followed up on this pathway, finding that common organic acids such as pyruvate, 2-ketoglutarate, and oxaloacetate can also act as substrates for VBPO to produce bromoform. The experiments that attribute VBPO to polyhalomethane production used semi-purified proteins from eukaryotic algae extracts that have bromoperoxidase activity, while none use genetic approaches to directly link the gene product to halomethane production. The mechanism proposed by Beissner *et al.* (1981) explains the production of both dibromomethane (CH_2Br_2) and bromoform (CHBr_3), but not methyl bromide (CH_3Br).

In this study, methyl chloride was one of the most abundant molecules detected and produced by CC9311, VMUT, and WH8102 regardless of culture conditions (Table 4.6 and Table 4.8), which is consistent with previous findings. Brownell *et al.* (2010) found that *Prochlorococcus* produced 1.3 molecules $\text{cell}^{-1} \text{day}^{-1}$ of methyl bromide and that *Synechococcus* WH8102 produced slightly more. Though unable to normalize *Synechococcus* production rates by cell count, which makes a direct comparison difficult, they reported concentrations of 20 pmol L^{-1} of CH_3I , 10 pmol L^{-1} of CH_3Br , and 180 pmol L^{-1} of CH_3Cl instead. In trial 1 of the headspace analysis, our results show that WH8102 produced $4.73 \pm 1.58 \text{ pmol L}^{-1}$ of CH_3I , $12.76 \pm 2.41 \text{ pmol L}^{-1}$ of CH_3Br , and $384.83 \pm 559.96 \text{ pmol L}^{-1}$ of CH_3Cl , which is not significantly different than zero (Table 4.2). Unlike Brownell *et al.* (2010), we found higher concentrations of methyl bromide than methyl iodide. Our results also demonstrate that CC9311 produces more monohalomethanes than WH8102, except for chloroform, which was greater in WH8102 (Table 4.8).

Interestingly, more methyl bromide was produced in still cultures of CC9311, but was significantly decreased when the culture was stirred and VBPO was present (Table 4.8). This suggests that available bromide is being used by VBPO for bromoform production outcompeting methyl bromide production compared to “normal” conditions. However, more work is needed to validate this hypothesis.

Monohalomethane production is thought to be more ubiquitous in the marine environment and has been measured in macroalgae (Manley *et al.*, 1992, Kupper *et al.*, 2008), numerous phytoplankton (Manley *et al.*, 1992, Manley & de la Cuesta, 1997, Hill & Manley, 2009), cyanobacteria (Brownell *et al.*, 2010), and heterotrophic bacteria (Fujimori *et al.*, 2012). The production of monohalomethanes is generally associated with the activity of S-adenosyl methionine dependent halide methyltransferase activity (Toda & Itoh, 2011, Bayer *et al.*, 2009). However, neither *Synechococcus* WH8102 nor CC9311 have predicted methyl halide methyltransferase genes as indicated by a blastp search of a known bacterial SAM-dependent methyltransferase gene from *Synechococcus elongatus*, accession YP_172090 (Bayer *et al.*, 2009) against the NCBI database as well as Cyanobase (genome.microbedb.jp/cyanobase/). However, there are several other SAM-dependent methyltransferases (sync_2647, sync_1254, sync_1268, sync_2340) annotated in the *Synechococcus* CC9311 genome. Another consideration is that an uncharacterized hypothetical gene is involved in methyl halide production. It is unlikely that VBPO is involved in monohalomethane production in CC9311, as less production is seen in these compounds in stirred cultures where VBPO is present. However, more testing would be required to determine the exact genes involved in monohalomethane production in *Synechococcus*.

Results from this experiment show that much less bromoform is produced than what could theoretically be produced by CC9311 based on measured VBPO activity. In the purge-and-trap experiment, the VBPO activity (0.024 ± 0.002 μmol dibromothymol blue min^{-1} mg^{-1} protein after 24 hours stirring) would allow for a bromoform production rate of 1.32×10^{16} molecules min^{-1} , which over the 24 hours would produce 2.18×10^8 molecules cell^{-1} day^{-1} of bromoform. However, the measured bromoform production of 382.4 ± 28.0 molecules cell^{-1} day^{-1} (Table 4.8) is five orders of magnitude smaller. This might be an indication that VBPO is not operating at its full potential *in vivo*, potentially due to non-ideal conditions or substrates that are limited due to insufficient production of or slow transport into the cell. An alternate hypothesis is that other halogenated products are formed by VBPO, competing with the production of bromoform. There are different suggestions in the literature, arguing that the bromination reaction of the VBPO is nonspecific due to a potentially freely dispersing HOBr intermediate that then reacts with available electron-rich organic molecules in the cell (Martinez *et al.*, 2001). However, there are several examples of substrate specificity in the bromination step of the VBPO reaction, including the role of vanadium haloperoxidases in the synthesis of specific molecules (Kamenarska *et al.*, 2007, Butler & Carter-Franklin, 2004).

This study provides evidence that CC9311 and WH8102 may produce chloroform (CHCl_3) under stirred conditions. In trial 2 of the headspace experiment, both cultures showed an increase in chloroform compared to the SN-medium control (Table 4.3). Furthermore, both CC9311 and WH8102 showed chloroform production in the purge-and-trap experiment when normalized to the cell concentrations at the beginning of the incubation (Table 4.8). Conversely, chloroform concentrations decreased in cultures

grown under still conditions as well as the stirred mutant over 24 hours (Table 4.8). Chloroform concentrations were also less than the SN-medium control in the first trial of the headspace analysis (Table 4.3). However, no significant production of chloroform was observed when more conservative uncertainties for cell counts were used in production rate calculations (Table 4.9).

Data from this study also indicates that CC9311 may produce dichloromethane (CH_2Cl_2) when the culture is stirred. In the headspace analysis, CH_2Cl_2 was the most abundant molecule found, with $1256.09 \pm 957.69 \text{ pmol L}^{-1} \text{ cell}^{-1} \times 10^7$ in the four hour incubation of CC9311 (Table 4.3), though production was not measured in the first trial of the headspace or the 2 hour time point of the second trial of the headspace. In the purge-and-trap experiment, CH_2Cl_2 was produced in stirred CC9311, even using the most conservative error estimates (Table 4.9). It is important to note that both numbers have very large uncertainties in addition to inconsistent production between the two trials of the headspace experiment.

Due to high error and inconsistencies in this study, further experiments are necessary to determine if *Synechococcus* cultures can produce dichloromethane and/or chloroform. For dichloromethane a more robust Henry's constant would be critical and the uncertainty in the cell counts would need to be reduced.

Functions of halomethane production in Synechococcus

As discussed in Chapters 1 and 2, there are two supported hypotheses for the function of VBPO in photosynthetic organisms. One hypothesis is that VBPO detoxifies metabolically produced hydrogen peroxide (H_2O_2), a substrate of the enzyme (Figure

4.4), with the production of halomethanes being a secondary effect and perhaps a way to eliminate the HO-Br generated by the two-electron oxidation of halides in the VBPO reaction scheme. The second hypothesized function for VBPO is to produce brominated organic molecules that may serve as a chemical defense against organisms such as grazers and/or bacteria.

Experiments in Chapter 3 of this dissertation describe patterns of VBPO regulation in *Synechococcus* CC9311, finding induction of VBPO activity by physical agitation as well as the presence of a heterotrophic bacterial assemblage. The induction of VBPO activity in the presence of heterotrophic bacteria supports the idea that VBPO may act a defense mechanism. Eukaryotic algal production of bromoform has been identified as a defense against epiphytic diatoms (Ohsawa *et al.*, 2001) as well as heterotrophic bacteria (Paul *et al.*, 2006). While this study demonstrates the production of bromoform is dependent on the presence of VBPO, further testing would be required to determine if VBPO has an allelopathic effect on the specific bacterial assemblage that is responsible for its induction (See Chapter 3).

Experimental caveats

Although *Synechococcus* cultures were in logarithmic growth at the beginning of each experiment, cell counts for WH8102 dramatically decreased during the 24-hour incubation of the purge-and-trap experiment, as determined by flow-cytometry. Possible sources of error include cell lysis during the 24-hour incubation under possibly carbon dioxide limited air or that cells were clumped or stuck to the side of the flask. Production rates for this experiment were thus presented normalized by the cell concentration at the

beginning of each incubation as well as the average cell counts between the 0 and 24 hour time points. The latter, as more conservative measure, also uses one-half of the difference of the two cell counts as the error. Perhaps if the cultures were growing normally, different rates of halomethane production would have been observed, however our production pattern was similar to those seen previously.

The error associated with the chlorinated compounds was also very large in both experiments. This is partially due to the error from the Henry's constants (Table 4.1) used in the calculations for both methyl chloride (13%) as well as dichloromethane (70%). In the headspace experiments, another factor was the relatively high concentrations of these compounds in the SN medium. The measured concentrations for the blank and the cultures were similar, thus the media-subtracted concentrations retained large uncertainties through propagation of error.

Lastly, it is difficult to extrapolate measurements of halomethane production made in this study to halomethane contributions of *Synechococcus* on a global scale as VBPO is in a horizontally transferred region of the CC9311 genome and it is not ubiquitous in other strains of *Synechococcus*. However, *Synechococcus*-like VBPO genes are detectable in environmental water samples by PCR (See *Chapter 2*). More work is needed on the distribution of VBPO genes and functional VBPOs in environmental phytoplankton populations.

Conclusions

Our results indicate that bromoform is produced in *Synechococcus* sp. CC9311 by vanadium-dependent bromoperoxidase (VBPO). Our evidence was provided by the use

of a gene-inactivated mutant, known expression patterns of the enzyme, as well as the use of another strain of *Synechococcus* with a sequenced genome that lacks VBPO. This result expands the known potential of halomethane production in *Synechococcus* beyond monohalomethanes and provides a mechanism for bromoform production. The diverse potential for halomethane production between strains of *Synechococcus* is important when considering atmospheric bromine sources that are biogeochemically relevant on a global scale.

Acknowledgments

I would like to thank Jens Mühle and the entire laboratory of R.F. Weiss for providing equipment as well as tremendous support with equipment, experimental design, and operation of the “Medusa” GC/MS.

Table 4.1: Dimensionless Henry's constants (K_H) used in calculations for the headspace experiment as well as purge efficiency calculations for the purge-and-trap experiment.

Compound	Dimensionless Henry's Constant K_h	Reported Error (\pm)	Temperature $^{\circ}\text{C}$	Reference
CH_3I	0.2245	0.0054	20	Moore <i>et al.</i> , 1995
CH_3Br	0.24	0.01	22	Elliot and Rowland, 1993
CH_2Br_2	0.0336	0.0002	20	Moore <i>et al.</i> , 1995
CHBr_3	0.0217	0.0002	20	Moore <i>et al.</i> , 1995
CH_3Cl	0.388	0.0518	20	Moore, 2000
CH_2Cl_2	0.097	0.0683	20	Moore, 2000
CHCl_3	0.1446	0.0017	20	Moore <i>et al.</i> , 1995

Table 4.2: Cell concentrations (cells ml⁻¹), VBPO activity (trial 1: μmol monochlorodimedone min⁻¹ mg⁻¹; trial 2: μmol dibromothymol blue min⁻¹ mg⁻¹), and halomethane concentrations (pmol L⁻¹) measured in the headspace of *Synechococcus* cultures.

Treatment	Trial 1			Trial 2			
	SN Medium	WH8102	CC9311	SN Medium	WH8102	CC9311	CC9311
Incubation time (hrs)	2	2	2	2	2	2	4
Cell concentration (Cell ml ⁻¹)	--	8.0 x 10 ⁶	1.2 x 10 ⁷	--	4.6 x 10 ⁷	6.85 x 10 ⁷	6.85 x 10 ⁷
VBPO activity (μmol min ⁻¹ mg ⁻¹)	--	0.0009 ± 0.0009 [#]	0.284 ± 0.072 [#]	--	NS	0.175 ± 0.032	0.175 ± 0.032
CH₃I (pmol L ⁻¹)	1.87 ± 1.50	4.73 ± 1.58	24.39 ± 2.52	2.25 ± 0.15	1.96 ± 0.14	4.03 ± 0.28	4.67 ± 0.32
CH₃Br (pmol L ⁻¹)	8.74 ± 2.23	12.76 ± 2.41	18.10 ± 2.74	17.23 ± 1.32	20.28 ± 1.61	22.52 ± 1.73	24.53 ± 2.08
CH₂Br₂ (pmol L ⁻¹)	4.88 ± 0.55	7.27 ± 0.80	9.66 ± 0.78	32.59 ± 2.1	33.8 ± 2.18	41.29 ± 2.67	38.64 ± 2.85
CHBr₃ (pmol L ⁻¹)	11.26 ± 0.99	22.35 ± 1.72	63.02 ± 4.43	369.36 ± 24.34	300.54 ± 22.22	1037.19 ± 67.5	883.68 ± 58.32
CH₃Cl (pmol L ⁻¹)	362.49 ± 558.62	384.83 ± 559.96	552.52 ± 567.10	201.91 ± 30.11	231.73 ± 34.65	190.74 ± 28.48	289.3 ± 43.27
CH₂Cl₂ (pmol L ⁻¹)	262.55 ± 1164.8	211.27 ± 115.19	*	632.34 ± 447.11	439.58 ± 310.83	866.81 ± 613.09	9242.83 ± 6535.54
CHCl₃ (pmol L ⁻¹)	261.24 ± 40.14	151.90 ± 35.36	210.19 ± 37.96	185.35 ± 12.23	251.74 ± 16.72	262.13 ± 17.61	195.09 ± 12.88

- * Concentration could not be determined, the value was less than flush gas
- Not tested
- NS Not significant, VBPO activity was less than the no-protein (negative) control.
- # VBPO activity was not normalized to a no-protein control

Table 4.3: Halomethane concentrations ($\text{pmol L}^{-1} \text{ cell}^{-1} \times 10^7$) measured in the headspace above cultures of *Synechococcus*, with the blank value (SN medium) subtracted and normalized to cell concentration.

	Trial 1		Trial 2		
	WH8102 (2 hrs)	CC9311 (2 hrs)	WH8102 (2 hrs)	CC9311 (2 hrs)	CC9311 (4 hrs)
	$\text{pmol L}^{-1} \text{ cell}^{-1}$	$\text{pmol L}^{-1} \text{ cell}^{-1}$	$\text{pmol L}^{-1} \text{ cell}^{-1}$	$\text{pmol L}^{-1} \text{ cell}^{-1}$	$\text{pmol L}^{-1} \text{ cell}^{-1}$
CH₃I	3.57 ± 2.73	22.51 ± 2.52	-0.06 ± 0.04	0.26 ± 0.05	0.35 ± 0.05
CH₃Br	5.01 ± 4.11	9.36 ± 2.74	0.66 ± 0.45	0.77 ± 0.32	1.06 ± 0.36
CH₂Br₂	2.98 ± 1.22	4.78 ± 0.78	0.26 ± 0.66	1.27 ± 0.50	0.88 ± 0.52
CHBr₃	13.89 ± 2.57	51.76 ± 4.43	-14.89 ± 7.17	97.42 ± 11.55	75.03 ± 9.95
CH₃Cl	27.91 ± 988.52	190.03 ± 567.10	6.45 ± 9.94	-1.63 ± 6.05	12.75 ± 7.72
CH₂Cl₂	-64.09 ± 2050.26	*	-41.71 ± 117.83	34.2 ± 110.71	1256.09 ± 957.69
CHCl₃	-136.60 ± 67.20	-51.05 ± 37.96	14.36 ± 4.54	11.20 ± 3.18	1.42 ± 2.59

Note: Numbers in grey are not significantly different than zero

* The concentration could not be determined as the measured value was below that of the flush gas.

Table 4.4: Cell concentrations and VBPO activities measured in cultures used in the purge-and-trap experiment.

Treatment	Condition	Incubation time (hours)	Cell Concentrations (Cells⁻¹ ml⁻¹)	VBPO Activity (μmol dibromothymol blue min⁻¹ mg⁻¹)
CC9311	Still	0	5.30×10^7	NS
CC9311	Still	24	2.36×10^7	NS
CC9311	Stir	24	3.15×10^7	0.024 ± 0.002
VMUT	Still	0	4.00×10^7	NS
VMUT	Still	24	6.61×10^7	NS
VMUT	Stir	24	3.09×10^7	NS
WH8102	Still	0	2.21×10^7	NS
WH8102	Stir	24	4.53×10^6	NS

NS Not significant, VBPO activity was below the limits of detection (less than three standard deviations from the no protein control).

Table 4.5: Purge efficiencies (percent recovered) by compound from the purge-and-trap experiment.

Sample	CH ₃ I	CH ₃ Br	CH ₂ Br ₂	CHBr ₃	CH ₃ Cl	CH ₂ Cl ₂	CHCl ₃
CC9311 (0 hrs)	99.6 ± 0.0	99.7 ± 0.1	64.5 ± 0.5	49.4 ± 0.5	100.0 ± 0.0	93.6 ± 10.8	97.9 ± 0.1
CC9311 Still (24 hrs)	99.5 ± 0.1	99.6 ± 0.1	64.0 ± 0.5	48.9 ± 0.5	100.0 ± 0.0	93.3 ± 11.1	97.7 ± 0.1
CC9311 Stir (24 hrs)	99.6 ± 0.0	99.7 ± 0.1	64.5 ± 0.5	49.4 ± 0.5	100.0 ± 0.0	93.6 ± 10.8	97.9 ± 0.1
VMUT (0 hrs)	99.6 ± 0.0	99.7 ± 0.1	65.9 ± 0.5	50.7 ± 0.5	100.0 ± 0.0	94.2 ± 10.2	98.2 ± 0.1
VMUT Still (24 hrs)	99.6 ± 0.0	99.7 ± 0.1	65.5 ± 0.5	50.3 ± 0.5	100.0 ± 0.0	94.0 ± 10.3	98.1 ± 0.1
VMUT Stir (24 hrs)	99.4 ± 0.1	99.5 ± 0.1	62.0 ± 0.5	47.0 ± 0.5	99.9 ± 0.0	92.3 ± 12.2	97.2 ± 0.1
WH8102 (0 hrs)	99.5 ± 0.1	99.6 ± 0.1	63.9 ± 0.5	48.8 ± 0.5	100.0 ± 0.0	93.3 ± 11.2	97.7 ± 0.1
WH8102 Stir (24 hrs)	99.6 ± 0.0	99.7 ± 0.1	65.8 ± 0.5	50.6 ± 0.5	100.0 ± 0.0	94.2 ± 10.2	98.1 ± 0.1

Table 4.6: Halomethane concentrations (pmol L⁻¹) of each bottle measured in the purge-and-trap experiment.

Sample	CH ₃ I	CH ₃ Br	CH ₂ Br ₂	CHBr ₃	CH ₃ Cl	CH ₂ Cl ₂	CHCl ₃
CC9311 (0 hrs)	1.33 ± 0.01	5.30 ± 0.02	1.30 ± 0.01	5.39 ± 0.02	89.91 ± 0.33	30.14 ± 0.57	36.92 ± 0.16
CC9311 still (24 hrs)	6.20 ± 0.03	63.99 ± 0.22	1.29 ± 0.01	6.62 ± 0.03	163.70 ± 0.56	29.23 ± 0.57	20.42 ± 0.07
CC9311 stir (24 hrs)	1.95 ± 0.01	43.80 ± 0.15	1.57 ± 0.01	39.03 ± 0.24	153.55 ± 0.54	57.26 ± 1.09	47.96 ± 0.18
VMUT (0 hrs)	1.25 ± 0.01	6.02 ± 0.02	1.27 ± 0.01	4.36 ± 0.02	83.84 ± 0.28	42.20 ± 0.75	30.69 ± 0.10
VMUT still (24 hrs)	1.54 ± 0.01	6.08 ± 0.02	1.25 ± 0.01	4.41 ± 0.02	105.21 ± 0.36	41.43 ± 0.76	25.63 ± 0.11
VMUT stir (24 hrs)	1.65 ± 0.01	6.38 ± 0.02	1.49 ± 0.01	5.32 ± 0.02	106.91 ± 0.38	41.53 ± 0.89	26.41 ± 0.12
WH8102 (0 hrs)	0.53 ± 0.00	3.55 ± 0.01	1.24 ± 0.01	4.22 ± 0.02	77.86 ± 0.27	29.43 ± 0.57	39.69 ± 0.15
WH8102 stir (24 hrs)	0.59 ± 0.00	3.58 ± 0.01	1.21 ± 0.01	4.07 ± 0.02	92.89 ± 0.32	29.08 ± 0.51	51.43 ± 0.19

Table 4.7: Halomethane concentrations ($\text{pmol L}^{-1} \text{cell}^{-1} \times 10^9$) measured in *Synechococcus* cultures in the purge-and-trap experiment, normalized by cell concentrations at time zero.

Culture		Time (hr)	CH_3I	CH_3Br	CH_2Br_2	CHBr_3	CH_3Cl	CH_2Cl_2	CHCl_3
CC9311	Still	0	0.09 ± 0.03	0.37 ± 0.11	0.09 ± 0.03	0.37 ± 0.11	6.24 ± 1.86	2.09 ± 0.63	2.56 ± 0.76
CC9311	Still	24	0.43 ± 0.13	4.44 ± 1.33	0.09 ± 0.03	0.46 ± 0.14	11.36 ± 3.39	2.03 ± 0.61	1.42 ± 0.42
CC9311	Stir	24	0.14 ± 0.04	3.04 ± 0.91	0.11 ± 0.03	2.71 ± 0.81	10.65 ± 3.18	3.97 ± 1.19	3.33 ± 0.99
VMUT	Still	0	0.07 ± 0.03	0.33 ± 0.13	0.07 ± 0.03	0.24 ± 0.09	4.59 ± 1.77	2.31 ± 0.89	1.68 ± 0.65
VMUT	Still	24	0.08 ± 0.03	0.33 ± 0.13	0.07 ± 0.03	0.24 ± 0.09	5.76 ± 2.22	2.27 ± 0.88	1.40 ± 0.54
VMUT	Stir	24	0.09 ± 0.03	0.35 ± 0.13	0.08 ± 0.03	0.29 ± 0.11	5.85 ± 2.26	2.27 ± 0.88	1.45 ± 0.56
WH8102	Still	0	0.10 ± 0.07	0.67 ± 0.44	0.23 ± 0.15	0.79 ± 0.52	14.62 ± 9.65	5.52 ± 3.65	7.45 ± 4.92
WH8102	Stir	24	0.11 ± 0.07	0.67 ± 0.44	0.23 ± 0.15	0.76 ± 0.50	17.44 ± 11.51	5.46 ± 3.60	9.66 ± 6.37

Table 4.8: Production rates (molecules cell⁻¹ day⁻¹) of halomethanes in two strains of *Synechococcus* and a VBPO-gene inactivated mutant from the purge-and-trap experiment, normalized to cell concentrations at time zero.

Sample	CH ₃ I	CH ₃ Br	CH ₂ Br ₂	CHBr ₃	CH ₃ Cl	CH ₂ Cl ₂	CHCl ₃
CC9311 Still	55.4 ± 4.1	667.1 ± 39.7	-0.21 ± 1.28	13.9 ± 5.6	838.8 ± 115.7	-10.3 ± 62.1	-187.6 ± 27.0
CC9311 Stir	7.1 ± 1.6	437.5 ± 27.3	2.96 ± 1.39	382.4 ± 28.0	723.4 ± 110.8	308.3 ± 94.8	125.5 ± 38.4
VMUT Still	4.3 ± 1.8	1.0 ± 7.0	-0.36 ± 1.58	0.8 ± 5.2	321.4 ± 110.1	-11.7 ± 109.5	-76.2 ± 33.3
VMUT Stir	6.0 ± 1.7	5.5 ± 7.2	3.18 ± 1.7	14.4 ± 5.8	347.0 ± 111.4	-10.1 ± 117.8	-64.5 ± 33.8
WH8102 Stir	1.7 ± 1.3	0.8 ± 7.5	-0.76 ± 2.84	-4.2 ± 9.0	408.7 ± 179.2	-9.4 ± 142.7	319.4 ± 97.7

Note: Numbers in grey are not significantly different than zero.

Table 4.9: Production rates (molecules cell⁻¹ day⁻¹) of halomethanes in two strains of *Synechococcus* and a VBPO-gene inactivated mutant from the purge-and-trap experiment, normalized by the averaged cell concentrations between time 0 and 24 hours.

Sample	CH ₃ I	CH ₃ Br	CH ₂ Br ₂	CHBr ₃	CH ₃ Cl	CH ₂ Cl ₂	CHCl ₃
CC9311 Still	81.4 ± 31.7	980.9 ± 321.0	-0.3 ± 9.2	20.5 ± 42.8	1233.4 ± 933.8	-15.2 ± 225.7	-275.8 ± 211.2
CC9311 Stir	10.4 ± 11.8	643.4 ± 220.6	4.4 ± 10.2	562.3 ± 198.1	1063.7 ± 889.8	453.4 ± 347.3	184.5 ± 302.9
VMUT Still	3.8 ± 20.1	0.9 ± 43.6	-0.3 ± 9.1	0.7 ± 31.6	281.8 ± 684.9	-10.2 ± 313.1	-66.8 ± 203.6
VMUT Stir	5.3 ± 10.6	4.8 ± 44.7	2.8 ± 10.0	12.6 ± 35.0	304.2 ± 691.7	-8.9 ± 315.8	-56.5 ± 206.2
WH8102 Stir	2.8 ± 23.9	1.4 ± 150.4	-1.3 ± 51.7	-7.0 ± 175.2	679.7 ± 3619.4	-15.6 ± 1253.8	531.1 ± 1940.2

Note: Numbers in grey are not significantly different than zero.

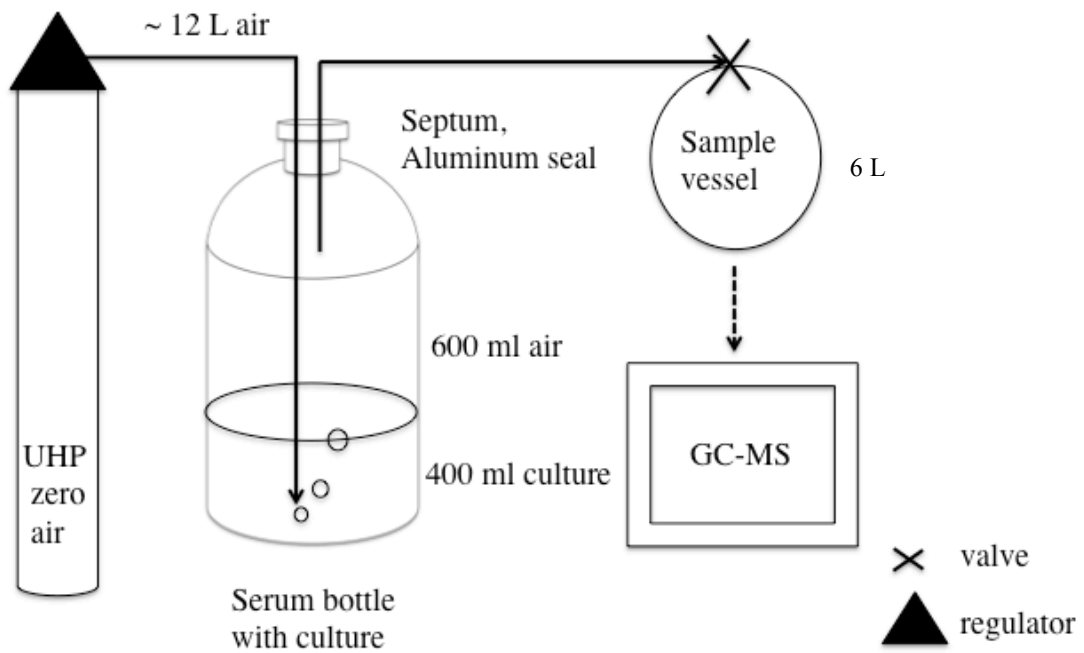


Figure 4.1: Experimental design used to measure halomethane production in *Synechococcus* cultures.

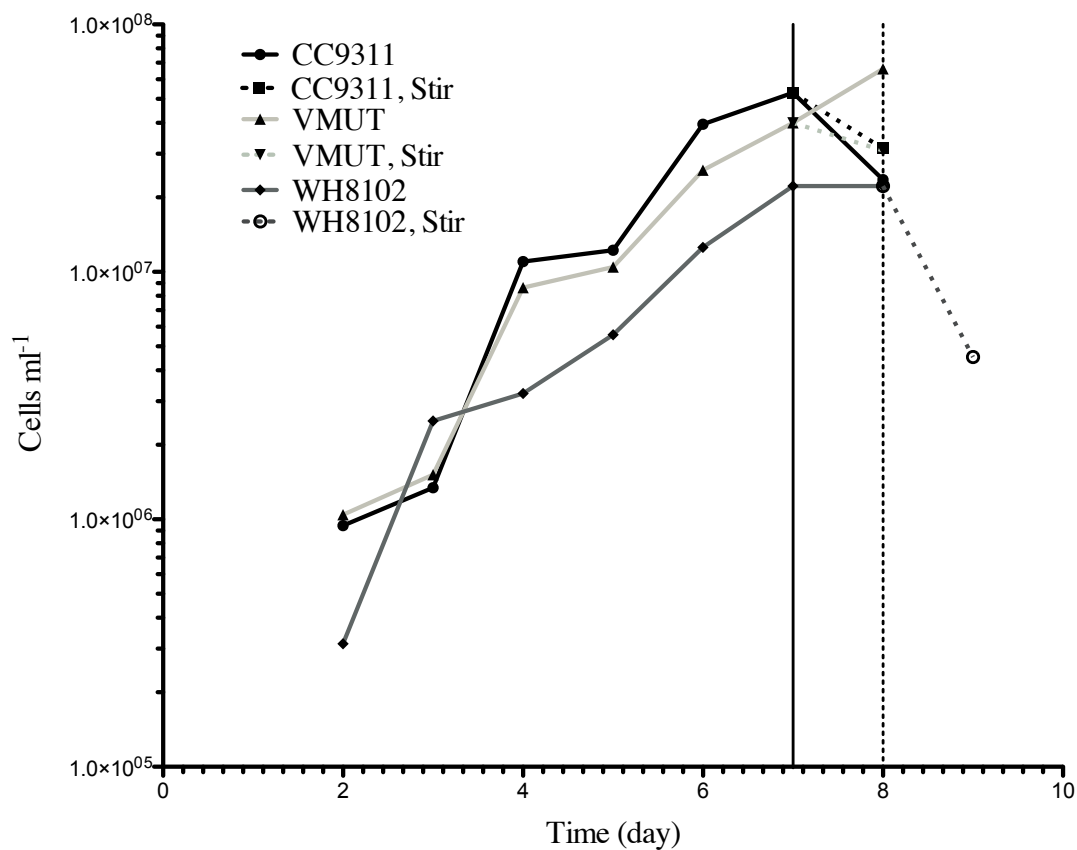


Figure 4.2: Cell concentrations of cultures (1.5 L) used in the purge-and-trap experiment (solid lines days 2-7). Vertical solid line at day seven indicates when CC9311 (Black) and VMUT2 (light grey) cultures were split and sealed in a serum bottle for 24 hrs with (dotted) and without (dotted) stirring. The vertical dotted line at day 8 indicates when WH8102 (dark grey) was sealed in a serum bottle for 24 hrs. Cell concentrations were determined by flow cytometry and shown in Cells ml^{-1} .

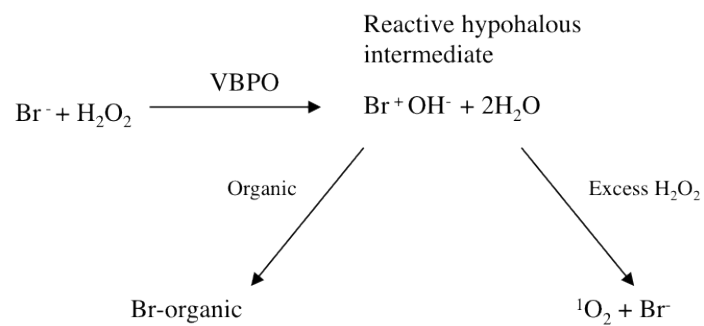


Figure 4.4: Reaction scheme for vanadium-dependent bromoperoxidase determined for VBPO in the red algae, *Corallina officinalis*. This figure is adapted from Carter *et al.* (2002).

References

- Abrahamsson, K., Choo, K. S., Pedersen, M., Johansson, G. & Snoeijs, P. 2003. Effects of temperature on the production of hydrogen peroxide and volatile halocarbons by brackish-water algae. *Phytochemistry* 64:725-34.
- Aschmann, J. & Sinnhuber, B. M. 2012. Contribution of very short-lived substances to stratospheric bromine loading: uncertainties and constraints. *Atmos. Chem. Phys. Discuss.* 12:302833-30326.
- Bayer, T. S., Widmaier, D. M., Temme, K., Mirsky, E. A., Santi, D. V. & Voigt, C. A. 2009. Synthesis of methyl halides from biomass using engineered microbes. *Journal of the American Chemical Society* 131:6508-15.
- Beissner, R. S., Guilford, W. J., Coates, R. M. & Hager, L. P. 1981. Synthesis of brominated heptanones and bromoform by a bromoperoxidase of marine origin. *Biochemistry* 20:3724-31.
- Brownell, D. K., Moore, R. M. & Cullen, J. J. 2010. Production of methyl halides by *Prochlorococcus* and *Synechococcus*. *Global Biogeochemical Cycles* 24.
- Butler, A. & Carter-Franklin, J. N. 2004. The role of vanadium bromoperoxidase in the biosynthesis of halogenated marine natural products. *Natural Product Reports* 21:180-88.
- Chance, R., Baker, A. R., Kupper, F. C., Hughes, C., Kloareg, B. & Malin, G. 2009. Release and transformations of inorganic iodine by marine macroalgae. *Estuarine Coastal and Shelf Science* 82:406-14.
- Cox, M. J., Schafer, H., Nightingale, P. D., McDonald, I. R. & Murrell, J. C. 2012. Diversity of methyl halide-degrading microorganisms in oceanic and coastal waters. *Fems Microbiology Letters* 334:111-18.
- Fujimori, T., Yoneyama, Y., Taniai, G., Kurihara, M., Tamegai, H. & Hashimoto, S. 2012. Methyl halide production by cultures of marine proteobacteria *Erythrobacter* and *Pseudomonas* and isolated bacteria from brackish water. *Limnology and Oceanography* 57:154-62.
- Hill, V. L. & Manley, S. L. 2009. Release of reactive bromine and iodine from diatoms and its possible role in halogen transfer in polar and tropical oceans. *Limnology and Oceanography* 54:812-22.
- Itoh, N. & Shinya, M. 1994. Seasonal evolution of bromomethanes from Coralline algae (*Corallinaceae*) and its effect on the atmospheric ozone. *Marine Chemistry* 45:95-103.

- Jardillier, L., Zubkov, M. V., Pearman, J. & Scanlan, D. J. 2010. Significant CO₂ fixation by small prymnesiophytes in the subtropical and tropical northeast Atlantic Ocean. *Isme Journal* 4:1180-92.
- Johnson, T. L., Palenik, B. & Brahamsha, B. 2011. Characterization of a functional vanadium-dependent bromoperoxidase in the marine cyanobacterium *Synechococcus* sp. CC9311. *Journal of Phycology* 47:792-801.
- Kamenarska, Z., Taniguchi, T., Ohsawa, N., Hiraoka, M. & Itoh, N. 2007. A vanadium-dependent bromoperoxidase in the marine red alga *Kappaphycus alvarezii* (Doty) Doty displays clear substrate specificity. *Phytochemistry* 68:1358-66.
- Karlsson, A., Auer, N., Schulz-Bull, D. & Abrahamsson, K. 2008. Cyanobacterial blooms in the Baltic - A source of halocarbons. *Marine Chemistry* 110:129-39.
- Kupper, F. C., Carpenter, L. J., McFiggans, G. B., Palmer, C. J., Waite, T. J., Boneberg, E. M., Woitsch, S., Weiller, M., Abela, R., Grolimund, D., Potin, P., Butler, A., Luther, G. W., Kroneck, P. M. H., Meyer-Klaucke, W. & Feiters, M. C. 2008. Iodide accumulation provides kelp with an inorganic antioxidant impacting atmospheric chemistry. *Proceedings of the National Academy of Sciences of the United States of America* 105:6954-58.
- Kurihara, M., Iseda, M., Ioriya, T., Horimoto, N., Kanda, J., Ishimaru, T., Yamaguchi, Y. & Hashimoto, S. 2012. Brominated methane compounds and isoprene in surface seawater of Sagami Bay: Concentrations, fluxes, and relationships with phytoplankton assemblages. *Marine Chemistry* 134:71-79.
- Law, K. S. & Sturges, W. T. 2010. Chapter 2: Halogenated very short-lived substances. Scientific Assessment of Ozone Depletion: 2010. World Meteorological Organization.
- Liang, Q., Stolarski, R. S., Kawa, S. R., Nielsen, J. E., Douglass, A. R., Rodriguez, J. M., Blake, D. R., Atlas, E. L. & Ott, L. E. 2010. Finding the missing stratospheric Br_y: a global modeling study of CHBr₃ and CH₂Br₂. *Atmospheric Chemistry and Physics* 10:2269-86.
- Lin, C. Y. & Manley, S. L. 2012. Bromoform production from seawater treated with bromoperoxidase. *Limnology and Oceanography* 57:1857-66.
- Manley, S. L. & Barbero, P. E. 2001. Physiological constraints on bromoform (CHBr₃) production by *Ulva lactuca* (Chlorophyta). *Limnology and Oceanography* 46:1392-99.

- Manley, S. L. & delaCuesta, J. L. 1997. Methyl iodide production from marine phytoplankton cultures. *Limnology and Oceanography* 42:142-47.
- Manley, S. L., Goodwin, K. & North, W. J. 1992. Laboratory production of bromoform, methylene bromide, and methyl iodide by a macroalgae and distribution in nearshore Southern California waters. *Limnology and Oceanography* 37:1652-59.
- Martinez, J. S., Carroll, G. L., Tschirret-Guth, R. A., Altenhoff, G., Little, R. D. & Butler, A. 2001. On the regiospecificity of vanadium bromoperoxidase. *Journal of the American Chemical Society* 123:3289-94.
- McAnulla, C., Woodall, C. A., McDonald, I. R., Studer, A., Vuilleumier, S., Leisinger, T. & Murrell, J. C. 2001. Chloromethane utilization gene cluster from *Hyphomicrobium chloromethanicum* strain CM2(T) and development of functional gene probes to detect halomethane-degrading bacteria. *Applied and Environmental Microbiology* 67:307-16.
- Miller, B. R., Weiss, R. F., Salameh, P. K., Tanhua, T., Grealley, B. R., Muhle, J. & Simmonds, P. G. 2008. Medusa: A sample preconcentration and GC/MS detector system for in situ measurements of atmospheric trace halocarbons, hydrocarbons, and sulfur compounds. *Analytical Chemistry* 80:1536-45.
- Montzka, S. A. & Reimann, S. 2010. Chapter 1: Ozone-depleting substances (ODSs) and related chemicals. Scientific Assessment of Ozone Depletion: 2010. World Meteorological Organization.
- Moore, R. M., Geen, C. E. & Tait, V. K. 1995. Determination of Henry Law constants for a suite of naturally-occurring halogenated methanes in seawater. *Chemosphere* 30:1183-91.
- Moore, R. M., Webb, M., Tokarczyk, R. & Wever, R. 1996. Bromoperoxidase and iodoperoxidase enzymes and production of halogenated methanes in marine diatom cultures. *Journal of Geophysical Research-Oceans* 101:20899-908.
- Ohsawa, N., Ogata, Y., Okada, N. & Itoh, N. 2001. Physiological function of bromoperoxidase in the red marine alga, *Corallina pilulifera*: production of bromoform as an allelochemical and the simultaneous elimination of hydrogen peroxide. *Phytochemistry* 58:683-92.
- Palenik, B., Brahamsha, B., Larimer, F., Land, M., Hauser, L., Chain, P., Lamerdin, J., Regala, W., Allen, E., McCarren, J., Paulsen, I., Dufresne, A., Partensky, F., Webb, E. & Waterbury, J. 2003. The genome of a motile marine *Synechococcus*. *Nature*. 424:1037-42.

- Palenik, B., Ren, Q., Dupont, C., Myers, G., Heidelberg, J., Badger, J., Madupu, R., Nelson, W., Brinkac, L., Dodson, R., Durkin, A., Daugherty, S., Sullivan, S., Khouri, H., Mohamoud, Y., Halpin, R. & Paulsen, I. 2006. Genome sequence of *Synechococcus* CC9311: Insights into adaptation to a coastal environment. *Proceedings of the National Academy of Sciences of the United States of America* 103:13555-59.
- Partensky, F., Hess, W. R. & Vaultot, D. 1999. *Prochlorococcus*, a marine photosynthetic prokaryote of global significance. *Microbiology and Molecular Biology Reviews* 63:106.
- Paul, C. & Pohnert, G. 2011. Production and role of volatile halogenated compounds from marine algae. *Natural Product Reports* 28:186-95.
- Paul, N. A., de Nys, R. & Steinberg, P. D. 2006. Chemical defence against bacteria in the red alga *Asparagopsis armata*: linking structure with function. *Marine Ecology-Progress Series* 306:87-101.
- Quack, B. & Wallace, D. W. R. 2003. Air-sea flux of bromoform: Controls, rates, and implications. *Global Biogeochemical Cycles* 17.
- Ruiz-Bevia, F., Fernandez-Torres, M. J. & Blasco-Alemany, M. P. 2009. Purge efficiency in the determination of trihalomethanes in water by purge-and-trap gas chromatography. *Analytica Chimica Acta* 632:304-14.
- Scarratt, M. G. & Moore, R. M. 1998. Production of methyl bromide and methyl chloride in laboratory cultures of marine phytoplankton II. *Marine Chemistry* 59:311-20.
- Taylor, J.R.. 1997. An introduction to error analysis: the study of uncertainties in physical measurements. University Science Books. Sausalito, CA.
- Toda, H. & Itoh, N. 2011. Isolation and characterization of a gene encoding a S-adenosyl-L-methionine-dependent halide/thiol methyltransferase (HTMT) from the marine diatom *Phaeodactylum tricorutum*: Biogenic mechanism of CH₃I emissions in oceans. *Phytochemistry* 72:337-43.
- Waterbury, J. B. & Willey, J. M. 1988. Isolation and growth of the marine planktonic cyanobacteria. *Methods in Enzymology* 167:100-05.
- Weinberger, F., Coquempot, B., Forner, S., Morin, P., Kloareg, B. & Potin, P. 2007. Different regulation of haloperoxidation during agar oligosaccharide-activated defence mechanisms in two related red algae, *Gracilaria* sp and *Gracilaria chilensis*. *Journal of Experimental Botany* 58:4365-72.

Chapter 4, in part, is currently being prepared for submission for publication of the material by Johnson, Todd; Mühle, Jens; Palenik, Brian; and Brahamsha, Bianca. The dissertation author was the primary investigator and will be first author of this paper.

Chapter 5: Conclusions

This work shows the first characterization of a vanadium-dependent bromoperoxidase (VBPO) in a cyanobacterium and provides insight into the functionality, role, and products of the enzyme in *Synechococcus* sp. CC9311. While a vanadium-dependent chloroperoxidase has been characterized in a heterotrophic bacterium (Bernhardt *et al.*, 2011), previous studies on vanadium-dependent haloperoxidases have focused almost exclusively on VBPO in eukaryotic marine macro- and microalgae (Winter & Moore, 2009). While this dissertation begins to understand the implications of cyanobacterial vanadium-dependent bromoperoxidases, there are still questions surrounding the utility for and applications of VBPO in *Synechococcus*.

This research was initiated upon the annotation of a hypothetical gene as a VBPO in the *Synechococcus* CC9311 genome, followed up with VBPO activity being found in protein extracts of *Synechococcus* CC9311. Research presented in this dissertation shows that the observed VBPO activity is the result of a single protein as determined by separating CC9311 proteins via SDS-PAGE, staining for VBPO activity using phenol red, and sequencing the only band with VBPO activity. Use of different halides *in vitro* also demonstrates that VBPO in CC9311 oxidizes bromide and iodide, but not chloride.

This research also aimed to address the genetic potential and activity of VBPO in other cyanobacteria. The first aspect of this was showing that other cyanobacteria have the genetic potential for VBPO activity through the use of PCR probes to screen closely related (Clade I) strains of *Synechococcus* finding VBPO gene in *Synechococcus* WH8020 and through mining sequence databases, finding annotated VBPO genes in

other strains of cyanobacteria. This research also detected VBPO genes in environmental water samples using degenerate PCR primers specific to *Synechococcus* VBPO, though it is not possible to say to which organisms the genes belonged. To follow up on the genetic potential of this gene in other cyanobacteria, VBPO activity was observed in *Synechococcus* WH8020 (Chapter 2) and *Acaryochloris marina* (Chapter 3), showing that while VBPO genes are not ubiquitous in cyanobacteria or even marine *Synechococcus*, VBPO is active in at least some species.

Another major focus of this research was to determine the function of VBPO in *Synechococcus*. VBPO is differentially expressed in cultures of *Synechococcus* with conditions that involve physical agitation. We establish that stirring and shaking induces VBPO activity regardless of gas exchange, light, osmotic stress, or oxidative stress. Furthermore, when isolated laminar shear force (shear rates of 50-1000 s⁻¹) were applied to *Synechococcus* CC9311, no VBPO activity was observed. Using a mutant lacking a functional VBPO, quantitative proteomics was employed to determine if other proteins are regulated with or any physiological processes that may be affected by stirring. The results show that VBPO is the second most upregulated protein, with stirring in CC9311 along with a beta-lactamase (sync_0349) and a hypothetical protein (sync_1122). When the mutant lacking VBPO was exposed to stirring, there was a slight enrichment in cell wall biosynthesis related proteins (Chapter 3).

VBPO is also likely involved in the bacteria-bacteria interaction between *Synechococcus* and a specific heterotrophic bacterial assemblage. This was found by measuring VBPO activity in *Synechococcus* after exposure to the bacterial fraction (0.2 – 2.0 µm filtrates) of a culture of *Pteridomonas*, a consumer of *Synechococcus*. Follow up

experiments showed that heterotrophic bacterial strains isolated from this culture do not individually induce VBPO activity in *Synechococcus*. While VBPO is clearly not a response of *Synechococcus* to exposure to all heterotrophic bacteria or cell contact, there was a strong response to this specific alpha- and gamma- proteobacterial dominated assemblage.

The third goal addressed in this research was the potential for VBPO in *Synechococcus* to produce brominated organic molecules. This dissertation provides the first reports of bromoform production by a marine *Synechococcus* linked to the presence of VBPO. This was confirmed through the inactivation of VBPO, which resulted in the elimination of bromoform production (Chapter 4). Furthermore, another strain of *Synechococcus* WH8102, which lacks VBPO, produced much less bromoform.

In future work, it would be important to link bromoform production to the ecology of *Synechococcus*, identifying any effects on other organisms. A focus should be taken on looking at the allelopathic role that VBPO has on other bacteria, particularly the bacterial assemblage known to induce the production of VBPO in *Synechococcus*. A vital aspect of this would be to show that the production of brominated molecules, such as bromoform, provides a competitive advantage to *Synechococcus*, such as preventing the growth of surrounding heterotrophic bacteria as one example.

Another question that is currently gaining more attention is how bacteria experience the physical environment in which they reside. Being in a liquid environment, aquatic bacteria are continuously exposed to fluid motion. While fluid dynamics predicts that “particles” the size of a bacterium ($\sim 1 \mu\text{m}$) experience turbulence as shear (Guasto *et al.*, 2012), results in this study suggest that *Synechococcus* experience shear and

turbulence differently under the conditions tested (Chapter 3). The field of mechano-microbiology may offer answers to what bacteria actually feel and experience a liquid media and offer insights on how we should approach the study of planktonic marine bacteria.

References

- Bernhardt, P., Okino, T., Winter, J. M., Miyanaga, A. & Moore, B. S. 2011. A stereoselective vanadium-dependent chloroperoxidase in bacterial antibiotic biosynthesis. *Journal of the American Chemical Society* **133**:4268-70.
- Guasto, J. S., Rusconi, R. & Stocker, R. 2012. Fluid mechanics of planktonic microorganisms. *In*: Davis, S. H. & Moin, P. [Eds.] *Annual Review of Fluid Mechanics*, Annual Reviews, Palo Alto, **44**:373-400.
- Winter, J. M. & Moore, B. S. 2009. Exploring the chemistry and biology of vanadium-dependent haloperoxidases. *Journal of Biological Chemistry* **284**:18577-81.

Appendix 1

All proteins detected in the iTRAQ proteomic experiments described in Chapter 3. The table includes genes in horizontally transferred islands defined by Dufresne *et al.*, (2009). The number of peptides detected for each protein are shown along with the iTRAQ mass tag ratios and associated p-values.

Appendix 1

Locus _tag	Name	HGT Island	Other HGT	Peptides (95%)		CC9311 4 hrs Protein		CC9311 24 hrs Protein		CC9311 24 hrs Broken Cells		VMUT 4 hrs Protein		VMUT 24 hours Broken Cell	
				4 hr	24 hr	115: 114	PVal	114: 113	PVal	116: 115	PVal	117: 116	PVal	118: 117	PVal
sync_0001	DNA polymerase III subunit beta			14	19	0.979	0.670	1.081	0.282	0.978	0.774	0.989	0.821	1.028	0.765
sync_0002	hypothetical protein sync_0002			2	1	1.093	0.433	0.948	0.891	1.021	0.968	0.909	0.368	1.005	0.980
sync_0003	phosphoribosylformylglycinamidin e synthase II			27	16	1.007	0.838	1.034	0.386	0.986	0.803	0.979	0.533	0.940	0.147
sync_0004	amidophosphoribosyltransferase			8	13	1.106	0.337	1.079	0.315	1.026	0.793	0.989	0.895	1.129	0.119
sync_0005	DNA gyrase subunit A			3	9	0.966	0.726	1.083	0.484	0.891	0.152	1.094	0.488	0.999	0.988
sync_0006	TPR repeat-containing protein			9	8	1.038	0.962	1.103	0.285	0.896	0.559	1.090	0.456	0.898	0.572
sync_0008	hypothetical protein sync_0008			8	7	0.944	0.718	0.798	0.286	0.997	0.981	1.063	0.488	0.812	0.310
sync_0009	hypothetical protein sync_0009				3			0.930	0.406	0.884	0.566			0.915	0.663
sync_0010	transcription antitermination protein NusB			6	8	1.050	0.557	1.092	0.375	1.050	0.685	1.039	0.633	1.138	0.126
sync_0011	signal recognition particle-docking protein FtsY			14	10	1.099	0.044	1.034	0.549	0.980	0.874	1.019	0.800	0.981	0.810
sync_0013	argininosuccinate lyase			9	5	1.056	0.636	1.177	0.460	0.850	0.561	0.952	0.445	1.042	0.769
sync_0014	RNA recognition motif-containing protein			10	15	0.913	0.698	0.529		1.096		0.893	0.402	0.867	
sync_0016	methionine-R-sulfoxide reductase			1		0.995						1.730			
sync_0017	hypothetical protein sync_0017			1		0.963						1.085			
sync_0020	twitching motility protein			4	4	0.926	0.464	0.745	0.368	0.871	0.399	1.059	0.438	0.951	0.754
sync_0021	type IV pilus assembly protein PilB			7	3	1.047	0.729	1.041	0.864	1.171	0.284	1.080	0.507	1.254	0.117
sync_0022	co-chaperone GrpE			20	16	1.048	0.799	1.196	0.469	1.216	0.182	0.983	0.919	1.102	0.560
sync_0023	DnaJ protein			1	4	1.111	0.719	1.072	0.686	0.996	0.959	1.171	0.321	1.037	0.760
sync_0024	hypothetical protein sync_0024			1		1.103	0.504					1.061	0.656		
sync_0026	hypothetical protein sync_0026			7	8	1.019	0.852	0.663	0.309	0.983	0.927	1.146	0.386	0.988	0.942
sync_0027	UDP-N- acetylenolpyruvoylglucosamine reductase			5	2	0.985	0.906	0.903	0.742	1.108	0.516	1.002	0.990	0.907	0.607

sync_0028	UDP-N-acetylmuramate--alanine ligase	7	8	1.038	0.701	0.796	0.018	0.821	0.202	0.986	0.843	0.821	0.220
sync_0029	glyceraldehyde-3-phosphate dehydrogenase, type I	34	27	1.008	0.850	1.014	0.904	0.979	0.634	1.025	0.751	0.878	0.014
sync_0031	peptidyl-prolyl cis-trans isomerase, cyclophilin-type	8	11	1.135	0.823	0.954	0.644	1.075	0.654	1.158	0.258	0.935	0.582
sync_0032	elongation factor P	10	7	0.844	0.350	0.717	0.605	0.792	0.640	0.979	0.875	0.860	0.204
sync_0033	acetyl-CoA carboxylase, biotin carboxyl carrier protein	2	12	1.029	0.822	0.871	0.724	0.967	0.931	0.942	0.655	0.857	0.597
sync_0034	4-hydroxythreonine-4-phosphate dehydrogenase	3		1.011	0.929					0.881	0.424		
sync_0035	NAD dependent epimerase/dehydratase	2	1	0.849		1.152		1.077		1.061		1.097	
sync_0039	penicillin amidase	1		2.079						1.540			
sync_0041	methyl-accepting chemotaxis protein	2	2	0.993	0.957	1.015	0.947	0.655	0.356	1.125	0.527	1.182	0.352
sync_0042	hypothetical protein sync_0042	2		0.822						0.942			
sync_0043	hypothetical protein sync_0043	2	1	0.989	0.938	1.078		1.625		1.181	0.342	1.103	
sync_0045	soluble hydrogenase, tritium exchange subunit, putative	14	11	1.082	0.532	1.068	0.780	1.278	0.108	0.915	0.198	1.041	0.594
sync_0047	bifunctional GMP synthase/glutamine amidotransferase protein	11	11	1.011	0.873	1.016	0.871	0.974	0.857	0.957	0.421	0.993	0.952
sync_0049	hypothetical protein sync_0049	3		0.928	0.455					0.913	0.591		
sync_0050	hypothetical protein sync_0050	2		1.198						1.229			
sync_0051	putative penicillin-binding protein	5	2	0.913	0.313	0.943	0.875	0.999	0.993	0.966	0.550	1.022	0.966
sync_0052	glycosyl transferase, group 1 family protein		4			1.095	0.445	0.922	0.333			1.002	0.988
sync_0053	sulfolipid biosynthesis protein SqdB	23	17	0.960	0.357	1.044	0.614	1.001	0.993	0.957	0.330	0.968	0.680
sync_0055	thiazole synthase	4	4	0.985	0.869	0.940	0.472	0.912	0.302	0.978	0.815	1.091	0.345
sync_0056	hypothetical protein sync_0056	3	8	0.969	0.880	1.032	0.684	1.080	0.354	1.052	0.706	1.067	0.426

sync_0057	putative photosystem I assembly related protein Ycf37	2	4	1.580	0.807	1.059	0.940	1.071	0.590	1.644	0.465	0.912	0.632
sync_0058	50S ribosomal protein L20		7			1.335		1.323				1.757	
sync_0059	50S ribosomal protein L35		2			1.097		0.921				1.058	
sync_0060	SpoIID/LytB domain-containing protein	2	3	1.074	0.510	0.780	0.221	1.027	0.779	0.970	0.766	0.950	0.596
sync_0061	glycosyl transferase, group 2 family protein	2	2	0.877	0.420	1.345	0.209	0.886	0.729	0.955	0.731	1.126	0.451
sync_0062	DNA polymerase III, subunits gamma and tau	2		1.049	0.742					0.967	0.905		
sync_0064	ATP-dependent protease ATP-binding subunit	2	3	0.994	0.951	0.907	0.682	0.987	0.917	0.991	0.923	0.908	0.382
sync_0065	ATP-dependent Clp protease, proteolytic subunit ClpP	6	4	1.021	0.867	0.935	0.520	0.944	0.598	1.060	0.548	1.045	0.664
sync_0066	trigger factor	19	37	1.000	0.989	1.057	0.351	1.040	0.509	1.021	0.656	0.988	0.766
sync_0067	aspartate-semialdehyde dehydrogenase	9	4	0.960	0.860	1.104	0.527	1.057	0.403	0.972	0.900	1.117	0.114
sync_0068	dihydrodipicolinate synthase	20	12	1.007	0.933	1.036	0.872	0.965	0.775	0.940	0.490	0.952	0.475
sync_0069	metallo-beta-lactamase family protein	25	15	0.953	0.577	1.121	0.139	0.916	0.138	1.045	0.481	0.978	0.792
sync_0072	hypothetical protein sync_0072	2		0.943	0.688					0.921	0.593		
sync_0074	excinuclease ABC subunit B	2	2	1.076	0.599	0.986	0.977	0.924	0.855	1.092	0.540	0.983	0.910
sync_0075	aspartate kinase	4	4	1.082	0.575	1.447		0.903		1.021	0.872	0.929	
sync_0076	curli production assembly/transport component CsgG subfamily protein	2	1	1.158	0.528	1.430		1.261		0.920	0.586	1.250	
sync_0079	DNA mismatch repair protein	2		1.065	0.559					1.036	0.706		
sync_0081	riboflavin synthase subunit beta	7	12	0.964	0.641	0.976	0.804	0.738	0.038	0.947	0.497	0.977	0.824
sync_0083	glyoxalase family protein family	2		1.412						0.678			
sync_0084	hypothetical protein sync_0084		1			1.185		0.803				0.747	
sync_0085	glycosyl transferase, group 1 family protein	1		0.982						0.816			

sync_0086	preprotein translocase subunit SecA	26	31	0.992	0.799	0.940	0.361	0.852	0.009	0.988	0.726	0.808	0.000
sync_0087	serine O-acetyltransferase		1			0.935	0.622	1.191	0.330			1.126	0.598
sync_0088	transcriptional regulator, GntR family protein	5	6	0.927	0.592	0.848	0.497	0.865	0.636	1.143	0.197	0.814	0.297
sync_0090	translation initiation factor IF-3	6	8	0.908	0.575	0.667	0.007	1.119	0.342	1.007	0.935	0.951	0.665
sync_0092	DNA gyrase subunit B	26	15	1.045	0.212	1.069	0.405	0.868	0.302	1.082	0.218	0.952	0.422
sync_0096	glutathione peroxidase	16	9	1.001	0.990	0.953	0.750	1.071	0.786	0.926	0.331	1.063	0.831
sync_0097	magnesium transporter	1		0.988						1.038			
sync_0098	Type II alternative RNA polymerase sigma factor, sigma-70 family protein	1		0.750						0.872			
sync_0100	acriflavin resistance protein acrF	4	7	1.098	0.325	0.885	0.302	0.716	0.007	0.974	0.732	0.915	0.278
sync_0101	RND family efflux transporter MFP subunit		2			0.774	0.707	1.029	0.920			0.976	0.847
sync_0102	putative A/G-specific adenine glycosylase	1		0.767						1.274			
sync_0103	sugar kinase, ribokinase family protein	9	6	1.051	0.346	1.061	0.462	1.016	0.871	0.983	0.867	0.946	0.429
sync_0105	putative glutamine synthetase	4	1	1.050	0.754	0.819		0.993		0.869	0.577	1.865	
sync_0107	hypothetical protein sync_0107	1		1.204						1.059			
sync_0108	S-adenosyl-L-homocysteine hydrolase	30	13	1.003	0.955	0.841	0.282	1.036	0.662	0.934	0.124	0.943	0.484
sync_0109	hypothetical protein sync_0109	2	3	0.944	0.665	1.315	0.334	0.723	0.523	0.870	0.396	1.234	0.292
sync_0110	single-strand DNA-binding protein	6	5	0.963	0.815	1.082	0.585	0.798	0.512	1.093	0.552	1.000	0.997
sync_0111	rod shape determining protein	15	25	1.049	0.933	1.043	0.728	1.032	0.792	1.183	0.313	0.923	0.288
sync_0112	cell shape-determining protein	2		0.825	0.303					0.942	0.655		
sync_0114	solute-binding family I protein	3	4	1.019	0.836	0.837	0.530	0.913	0.549	0.900	0.592	0.939	0.761
sync_0115	two-component response regulator	4	2	0.832	0.300	1.021		1.337		0.942	0.573	0.984	
sync_0116	lysyl-tRNA synthetase	6	12	0.982	0.792	1.025	0.801	1.127	0.177	0.951	0.472	0.989	0.914

sync_0117	hypothetical protein sync_0117		16	3	1.122	0.451	1.083		0.890		0.955	0.856	0.856	
sync_0118	hypothetical protein sync_0118			1			0.925	0.446	0.998	0.983			1.060	0.487
sync_0119	hypothetical protein sync_0119		6	7	1.092	0.566	1.337	0.285	0.778	0.102	0.877	0.446	0.730	0.219
sync_0122	serine/threonine protein kinase		9	6	0.988	0.891	1.061	0.490	1.019	0.836	1.121	0.236	0.953	0.449
sync_0124	Holliday junction DNA helicase B		2		1.089	0.546					0.993	0.983		
sync_0125	TPR repeat-containing protein		2		1.199						0.806			
sync_0126	peptidase, M20D family protein		5	2	1.084	0.492	1.531		0.756		1.056	0.388	0.939	
sync_0128	CotB mutant		5	2	0.983	0.812	1.007		0.692		0.941	0.409	0.920	
sync_0129	thiamine biosynthesis protein ThiC		25	19	1.085	0.188	0.952	0.515	0.885	0.159	0.963	0.563	0.952	0.398
sync_0130	transketolase		82	67	1.007	0.845	0.894	0.023	1.050	0.593	0.956	0.325	1.029	0.566
sync_0131	3-oxoacyl-[acyl-carrier-protein] synthase II		22	14	0.991	0.898	0.827	0.453	0.943	0.526	1.002	0.969	0.980	0.795
sync_0133	photosystem I subunit VII		12	14	0.953	0.550	0.964	0.771	0.818	0.024	0.970	0.702	1.005	0.940
sync_0134	D-fructose-6-phosphate amidotransferase		12	10	1.043	0.578	0.971	0.803	1.015	0.916	1.039	0.458	1.007	0.932
sync_0145	GDP-L-fucose synthetase	ISL1	5	2	1.064	0.925	1.087		0.978		1.080	0.548	1.116	
sync_0146	GDP-mannose 4,6-dehydratase	ISL1	1	2	0.961		0.987		0.452		0.966		0.620	
sync_0150	chain length determinant protein family protein	ISL1	1	7	1.106	0.512	1.194	0.593	0.945	0.561	1.049	0.725	0.918	0.588
sync_0157	hypothetical protein sync_0157	ISL1	2		1.010	0.938					1.108	0.613		
sync_0159	dTDP-glucose 4-6-dehydratase-like protein	ISL1	7	1	0.979	0.673	1.199	0.661	1.064	0.779	0.978	0.783	1.048	0.819
sync_0160	mannose-1-phosphate guanylyltransferase/mannose-6-phosphate isomerase	ISL1	9	6	1.057	0.614	1.399	0.054	1.064	0.502	0.958	0.506	1.050	0.756
sync_0162	chain length determinant protein family protein	ISL1	3	4	1.101	0.425	0.811	0.558	0.799	0.392	1.012	0.880	1.024	0.825
sync_0169	UDP-N-acetylglucosamine 2-epimerase	ISL1	4	3	0.927	0.367	1.465		0.870		1.007	0.930	1.030	

sync_0170	CMP-N-acetylneuraminic acid synthetase	ISL1	YES	3		0.923	0.567					1.032	0.802		
sync_0172	imidazole glycerol phosphate synthase, glutamine amidotransferase subunit	ISL1	YES	2	4	1.059	0.828	2.360	0.366	0.584	0.651	1.079	0.491	0.991	0.973
sync_0174	N-acetylneuraminic acid condensing enzyme	ISL1	YES	16	13	0.931	0.275	1.004	0.977	0.971	0.876	0.984	0.766	1.008	0.925
sync_0175	hypothetical protein sync_0175	ISL1	YES	6		1.086	0.392					0.878	0.441		
sync_0176	imidazole glycerol phosphate synthase subunit hisF	ISL1	YES	7	6	1.058	0.312	0.884	0.347	0.866	0.092	1.055	0.332	0.778	0.025
sync_0177	hypothetical protein sync_0177	ISL1	YES	38	29	1.002	0.981	0.933	0.600	1.042	0.388	1.006	0.960	1.029	0.577
sync_0178	asparagine synthase (glutamine-hydrolyzing)	ISL1	YES	18	18	0.938	0.186	1.092	0.293	1.064	0.559	0.981	0.687	0.971	0.753
sync_0179	DegT/DnrJ/EryC1/StrS aminotransferase family protein	ISL1	YES	6	7	1.043	0.603	0.671	0.267	1.213	0.076	1.130	0.194	1.059	0.798
sync_0181	NeuB family protein	ISL1	YES	12	9	0.966	0.552	1.133	0.265	1.005	0.980	1.053	0.388	1.030	0.641
sync_0182	posttranslational flagellin modification protein B	ISL1	YES	6	3	0.996	0.949	0.847	0.700	1.150	0.610	1.016	0.825	0.810	0.123
sync_0183	undecaprenyl-phosphate glucosyltransferase	ISL1			3			0.935	0.918	0.783	0.489			0.916	0.660
sync_0184	hypothetical protein sync_0184	ISL1	YES	3	2	0.925	0.957	1.136	0.425	0.849	0.620	0.988	0.938	0.985	0.902
sync_0185	hypothetical protein sync_0185	ISL1	YES	2		0.933	0.536					0.969	0.748		
sync_0186	hypothetical protein sync_0186	ISL1			4			1.185		1.345				1.224	
sync_0187	short chain dehydrogenase	ISL1		20	21	0.975	0.688	1.065	0.761	1.071	0.192	0.979	0.760	1.117	0.126
sync_0192	putative nucleotide sugar epimerase/dehydratase	ISL1		8	13	0.927	0.369	1.093	0.298	1.075	0.201	0.976	0.621	0.957	0.445
sync_0195	16S rRNA-processing protein			4	2	0.990	0.943	0.978		0.920		1.017	0.839	0.925	
sync_0196	hypothetical protein sync_0196			2	7	0.948	0.700	0.926	0.405	1.060	0.754	1.131	0.647	0.953	0.661
sync_0202	large conductance mechanosensitive channel protein			7	4	0.994	0.948	2.031		1.119		1.028	0.778	0.915	
sync_0205	phosphorylase			70	37	0.988	0.952	0.998	0.974	1.051	0.580	1.018	0.708	1.045	0.441

sync_0206	transporter, monovalent cation:proton antiporter-2 (CPA2) family protein	3		1.073	0.617					0.993	0.955		
sync_0208	hydrolase, alpha/beta fold family protein	3	2	1.085	0.283	1.117	0.808	0.786	0.158	1.001	0.993	0.879	0.644
sync_0209	aldose 1-epimerase subfamily protein	14	7	0.997	0.949	0.855	0.531	1.010	0.946	1.010	0.832	1.057	0.359
sync_0210	glycolate oxidase chain	3		0.960	0.971					1.023	0.925		
sync_0213	Fe-S oxidoreductase		1			1.070		1.152				0.932	
sync_0214	isocitrate dehydrogenase	28	17	1.040	0.319	1.030	0.686	1.060	0.392	1.048	0.411	1.010	0.809
sync_0216	Heme oxygenase	11	10	1.091	0.320	1.016	0.852	1.042	0.494	0.974	0.745	1.087	0.425
sync_0217	hypothetical protein sync_0217	2	8	0.825	0.186	1.071	0.564	1.002	0.976	1.104	0.452	1.029	0.716
sync_0219	ATP-binding ABC transporter family protein	3	5	0.942	0.550	1.297	0.073	1.045	0.720	1.002	0.983	1.003	0.965
sync_0220	glycosyl transferase family protein	3	2	0.869	0.536	1.167	0.478	1.094	0.719	0.990	0.937	1.254	0.266
sync_0222	glycosyl transferase, group 1 family protein	3	7	0.970	0.733	1.006	0.962	1.112	0.777	0.922	0.336	1.146	0.400
sync_0224	hypothetical protein sync_0224	3	2	0.918	0.626	0.911		2.357		0.989	0.934	2.159	
sync_0225	hypothetical protein sync_0225	1		0.610						1.227			
sync_0226	hypothetical protein sync_0226	7	8	0.986	0.850	1.380	0.056	0.870	0.095	0.976	0.743	1.024	0.854
sync_0227	ATP-dependent DNA helicase PcrA	7	5	1.132	0.156	1.053	0.840	0.903	0.492	1.069	0.211	0.813	0.287
sync_0229	hypothetical protein sync_0229		1			1.039		0.968				0.916	
sync_0231	UDP-glucose 4-epimerase	10	6	0.997	0.981	0.817	0.438	0.893	0.286	0.922	0.178	1.002	0.993
sync_0232	histidyl-tRNA synthetase	12	5	1.000	0.999	1.084	0.569	0.844	0.340	1.032	0.779	0.830	0.313
sync_0233	UDP-glucose dehydrogenase	9	11	1.104	0.106	0.892	0.059	0.979	0.769	0.980	0.715	0.895	0.131
sync_0234	WbnF	10	9	1.026	0.774	1.022	0.920	0.788	0.042	0.978	0.779	0.912	0.467
sync_0236	photosystem II reaction center protein J		2			0.367	0.358	1.239	0.284			0.950	0.707
sync_0237	photosystem II reaction center L	2		1.008						0.980			

sync_0238	cytochrome b559 subunit beta		1			1.293		0.949			1.066			
sync_0240	Ycf48-like protein	8	10	0.987	0.919	1.030	0.775	0.851	0.202	1.005	0.943	0.977	0.878	
sync_0241	rubredoxin	4	7	0.898	0.500	1.000	0.999	1.152	0.396	0.972	0.833	1.249	0.216	
sync_0243	NADH dehydrogenase subunit B	7	5	1.296	0.439	1.693		1.007		1.163	0.380	1.213		
sync_0244	NADH dehydrogenase subunit J		4			0.927	0.604	0.918	0.569			0.995	0.989	
sync_0245	hypothetical protein sync_0245	1	1	0.930	0.464	1.416		0.872		1.131	0.271	1.131		
sync_0247	ABC transporter	5	3	0.914	0.241	0.895	0.341	1.007	0.979	0.965	0.611	1.002	0.990	
sync_0248	magnesium chelatase, ATPase subunit D	1	3	0.945	0.607	0.828	0.331	1.112	0.432	1.029	0.741	1.149	0.232	
sync_0250	NUDIX hydrolase	1		0.914						0.888				
sync_0251	NUDIX hydrolase	4		0.901	0.357					0.901	0.401			
sync_0252	deoxyribodipyrimidine photolyase		1			1.002		0.978				0.921		
sync_0253	DegT/DnrJ/EryC1/StrS aminotransferase family protein	3	3	0.942	0.449	1.637	0.449	0.994	0.968	0.922	0.486	1.128	0.524	
sync_0254	thioredoxin family protein	2	1	0.994	0.962	0.737		0.759		0.941	0.880	1.088		
sync_0258	enoyl-(acyl carrier protein) reductase	19	31	1.035	0.607	0.877	0.168	0.991	0.852	1.193	0.021	1.006	0.907	
sync_0260	imidazoleglycerol-phosphate dehydratase	3	1	0.982	0.824	0.979	0.865	0.857	0.363	0.966	0.676	0.880	0.420	
sync_0262	hypothetical protein sync_0262	1	2	1.250	0.953	1.243		1.880		2.193	0.357	1.906		
sync_0263	two component sensor histidine kinase, putative	YES	7	9	0.908	0.130	0.985	0.934	0.919	0.514	0.955	0.443	0.954	0.545
sync_0264	AraC family transcriptional regulator			2		1.159	0.672	0.829	0.331			0.992	0.967	
sync_0265	two-component response regulator	YES	5	3	0.938	0.402	1.008	0.954	0.843	0.437	1.114	0.183	1.152	0.497
sync_0266	hypothetical protein sync_0266			3		0.727	0.517	1.018	0.913			1.125	0.766	
sync_0269	putative sarcosine oxidase	11	12	1.113	0.116	0.952	0.563	1.241	0.129	1.009	0.886	1.091	0.533	
sync_0270	leucine dehydrogenase	5		0.873	0.133					0.844	0.212			

sync_0271	hypothetical protein sync_0271	15	16	0.979	0.978	0.961	0.718	0.992	0.937	1.021	0.872	0.935	0.505
sync_0272	non-canonical purine NTP pyrophosphatase	2	2	1.050	0.717	0.566		0.986		1.113	0.485	0.905	
sync_0273	phosphoglucomutase/phosphomanomutase family protein	16	8	0.972	0.576	1.256	0.033	1.202	0.189	1.074	0.224	1.085	0.325
sync_0275	glycine cleavage T-protein (aminomethyl transferase) superfamily protein	2	2	1.028	0.933	1.255	0.267	1.028	0.916	0.830	0.318	1.175	0.355
sync_0276	orotate phosphoribosyltransferase	5	3	1.320	0.142	1.129	0.599	0.944	0.687	0.964	0.590	1.408	0.568
sync_0279	hypothetical protein sync_0279		4			1.030	0.933	0.877	0.859			0.721	0.190
sync_0280	dehydrogenase	5	2	0.939	0.672	1.022	0.966	1.044	0.745	1.089	0.683	1.019	0.954
sync_0282	glycosyl transferase WecB/TagA/CpsF family protein		3			1.136	0.332	1.096	0.326			1.211	0.355
sync_0284	queuine tRNA-ribosyltransferase	2	1	0.979	0.867	0.959	0.793	0.902	0.496	0.973	0.908	1.039	0.801
sync_0286	two-component sensor histidine kinase	2		0.875	0.600					1.037	0.781		
sync_0289	bifunctional phosphoribosylaminoimidazolecarboxamide formyltransferase/IMP cyclohydrolase	17	16	1.014	0.758	1.108	0.467	1.137	0.281	1.056	0.279	1.101	0.123
sync_0290	hypothetical protein sync_0290		1			0.738		1.144				0.757	
sync_0292	4-hydroxy-3-methylbut-2-enyl diphosphate reductase	10	6	0.958	0.499	1.047	0.702	1.032	0.911	0.986	0.845	1.036	0.710
sync_0293	ammonium transporter	9	11	0.937		1.117	0.776	0.605	0.136	1.038		0.792	0.587
sync_0296	cytochrome c oxidase subunit Va	2		1.267	0.352					0.884	0.448		
sync_0297	hypothetical protein sync_0297	5	3	0.993	0.966	0.936	0.533	0.727	0.487	1.067	0.644	0.922	0.460
sync_0300	serine hydroxymethyltransferase	32	28	1.003	0.928	1.027	0.761	1.068	0.430	0.987	0.755	1.078	0.091

sync_0301	glycosyl transferase, group 4 family protein	2	1	0.949		1.194		0.964		1.104		0.768	
sync_0302	CinA-like protein	3	3	0.967	0.792	1.053	0.855	0.818	0.132	0.881	0.423	0.799	0.544
sync_0303	isopropylmalate isomerase large subunit	11	3	1.097	0.328	1.234	0.358	1.146	0.403	1.004	0.952	0.907	0.514
sync_0304	3-isopropylmalate dehydratase, small subunit	4		1.004	0.963					0.867	0.240		
sync_0305	pentapeptide repeat-containing protein	3		1.029	0.871					1.332	0.425		
sync_0308	glycoside hydrolase family protein	6		1.006	0.918					0.889	0.317		
sync_0310	photosystem II reaction center protein H	2	5	0.843		0.979		0.945		1.080		1.124	
sync_0311	twin-arginine translocation protein TatA	2	1	0.995	0.966	1.114	0.479	0.917	0.556	1.007	0.972	1.099	0.527
sync_0312	peptidyl-tRNA hydrolase	7	3	1.086	0.218	1.133	0.430	1.001	0.994	0.910	0.167	1.046	0.728
sync_0315	hypothetical protein sync_0315	2	5	0.891	0.241	0.880	0.510	0.969	0.695	0.966	0.679	1.041	0.710
sync_0316	nitrogen-responsive regulatory protein	10	14	0.972	0.964	0.887	0.219	0.983	0.762	1.136	0.342	1.024	0.680
sync_0317	ribonuclease PH	6	3	1.014	0.829	0.992	0.952	0.887	0.681	0.965	0.588	0.852	0.373
sync_0319	deoxycytidine triphosphate deaminase		1			0.852		1.468				1.319	
sync_0320	thymidylate synthase, flavin-dependent	12	7	1.076	0.439	0.757	0.159	0.954	0.511	0.990	0.847	0.967	0.636
sync_0321	thioredoxin	1		1.075						0.955			
sync_0325	phosphotransferase superclass	3	1	1.004	0.963	1.258		0.867		0.878	0.250	1.189	
sync_0326	BadF/BadG/BcrA/BcrD family ATPase	1		1.210						1.036			
sync_0329	hypothetical protein sync_0329	4		0.866	0.230					1.086	0.628		
sync_0333	isoleucyl-tRNA synthetase	16	9	0.998	0.955	0.946	0.737	1.028	0.783	0.957	0.290	0.979	0.813
sync_0334	hypothetical protein sync_0334	2		1.041	0.692					1.090	0.499		
sync_0337	aspartyl/glutamyl-tRNA amidotransferase subunit C	6	5	1.062	0.444	0.975	0.739	0.973	0.726	0.970	0.756	0.939	0.439

sync_0338	creatininase	4	2	1.063	0.450	0.889		0.947		0.966	0.660	1.037	
sync_0343	aspartate carbamoyltransferase catalytic subunit	5	1	1.048	0.554	1.011	0.928	1.131	0.737	1.019	0.810	1.320	0.218
sync_0344	NADH dehydrogenase	13	10	1.080	0.875	1.047	0.712	0.826	0.013	1.114	0.349	0.912	0.272
sync_0346	hypothetical protein sync_0346		2			0.916	0.914	0.998	0.997			0.958	0.837
sync_0349	beta-lactamase, putative	11	31	2.043	0.001	4.530	0.000	5.608	0.000	3.377	0.000	3.016	0.000
sync_0351	hypothetical protein sync_0351		1			2.511		1.032				1.543	
sync_0352	phosphopantothencysteine decarboxylase/phosphopantothenate--cysteine ligase	1		0.803						1.120			
sync_0353	photosystem II manganese-stabilizing protein	26	29	1.034	0.486	0.914	0.230	0.899	0.298	0.992	0.862	0.923	0.174
sync_0354	sulfate adenyltransferase	22	14	1.026	0.535	0.900	0.196	1.044	0.574	0.933	0.108	1.192	0.020
sync_0355	cell division protein FtsH	14	19	0.997	0.943	0.995	0.917	0.943	0.247	1.034	0.422	0.917	0.246
sync_0356	2-dehydro-3-deoxyphosphogluconate aldolase/4-hydroxy-2-oxoglutarate aldolase	1	1	1.113		1.200		1.070		1.124		1.030	
sync_0357	hypothetical protein sync_0357	5	9	0.854	0.111	0.744	0.487	0.723	0.061	1.024	0.755	0.926	0.454
sync_0358	chorismate synthase	10	6	0.968	0.572	0.752	0.321	0.814	0.113	1.070	0.263	0.871	0.235
sync_0359	cupin superfamily protein	4	2	1.047	0.640	1.213	0.436	1.187	0.554	0.882	0.143	0.903	0.421
sync_0361	glycosidase	4	4	1.093	0.246	1.229		1.156		1.032	0.660	0.971	
sync_0362	mannosyl-3-phosphoglycerate phosphatase	3	3	0.947	0.683	0.712	0.201	0.850	0.328	0.883	0.553	0.971	0.831
sync_0363	redox protein	1	1	1.259		0.574		0.776		0.485		0.897	
sync_0369	radical SAM domain-containing protein	2		0.959	0.893					1.094	0.613		
sync_0371	ATP-dependent Clp protease adaptor protein ClpS	1	1	1.043	0.763	1.055	0.699	0.914	0.818	0.854	0.499	0.848	0.359
sync_0372	L,L-diaminopimelate aminotransferase	26	20	1.057	0.276	0.997	0.986	1.086	0.502	0.964	0.379	1.064	0.477
sync_0374	ribonuclease, Rne/Rng family protein	12	19	0.864	0.107	0.966	0.706	0.974	0.639	1.086	0.339	0.941	0.204

sync_0377	prephenate dehydratase	6	3	1.055	0.554	1.229		0.736		1.052	0.477	0.798	
sync_0379	ATP-dependent protease La	3		1.027	0.839					0.952	0.713		
sync_0380	30S ribosomal protein S10	6	13	0.971	0.612	1.028	0.748	1.009	0.911	1.016	0.780	0.953	0.710
sync_0381	elongation factor Tu	81	86	1.102	0.314	0.888	0.454	0.964	0.448	1.057	0.537	1.002	0.990
sync_0382	elongation factor G	58	47	0.974	0.375	0.998	0.974	1.023	0.682	0.983	0.556	0.974	0.647
sync_0383	30S ribosomal protein S7	18	25	0.982	0.924	1.336	0.046	1.013	0.940	0.958	0.564	1.085	0.437
sync_0384	30S ribosomal protein S12	4	6	0.931	0.606	1.115	0.604	1.045	0.638	1.033	0.803	0.998	0.990
sync_0385	hypothetical protein sync_0385		1			0.883		1.603				1.361	
sync_0386	hypothetical protein sync_0386	5	7	0.998	0.969	1.033	0.889	0.931	0.764	1.107	0.302	0.892	0.324
sync_0387	ferredoxin-dependent glutamate synthase, Fd-GOGAT	37	36	1.042	0.290	1.052	0.442	1.038	0.485	1.009	0.766	1.123	0.007
sync_0392	hypothetical protein sync_0392	11	7	0.984	0.980	0.668	0.351	0.891	0.442	1.106	0.468	0.925	0.301
sync_0393	photosystem I P700 chlorophyll a apoprotein A1	11	22	1.229	0.816	0.824	0.013	0.984	0.764	1.270	0.274	0.947	0.436
sync_0394	photosystem I P700 chlorophyll a apoprotein A2	12	16	1.019	0.768	0.822	0.364	1.061	0.381	1.032	0.618	0.886	0.037
sync_0398	photosystem I reaction center protein subunit XI	10	9	1.030	0.921	1.369	0.170	1.033	0.812	0.968	0.768	1.040	0.645
sync_0400	hypothetical protein sync_0400	4	3	0.932	0.410	0.980	0.915	1.069	0.526	0.935	0.422	1.085	0.750
sync_0403	Beta-lactamase superfamily protein	2		1.048	0.717					0.953	0.797		
sync_0406	alanine racemase	1		1.299						0.853			
sync_0408	peptide chain release factor 1	1	1	1.327		1.178	0.641	1.050	0.825	1.964		1.011	0.930
sync_0409	50S ribosomal protein L31	4	1	1.025	0.797	1.145		1.157		1.081	0.452	0.951	
sync_0410	30S ribosomal protein S9	13	14	0.911	0.491	0.835	0.177	1.273	0.014	0.941	0.477	0.972	0.764
sync_0411	50S ribosomal protein L13	9	16	0.936	0.329	1.406	0.003	0.972	0.668	0.945	0.404	1.095	0.210
sync_0413	50S ribosomal protein L17	5	8	0.921	0.255	1.198	0.332	1.209	0.029	1.019	0.774	1.049	0.473
sync_0414	DNA-directed RNA polymerase subunit alpha	17	28	0.889	0.050	1.556	0.000	1.025	0.620	1.203	0.006	0.995	0.924
sync_0415	30S ribosomal protein S11	4	7	1.115	0.673	1.083	0.693	1.108	0.338	0.911	0.597	1.022	0.812

sync_0416	30S ribosomal protein S13	5	7	1.078	0.316	1.038	0.652	1.000	0.995	0.964	0.697	1.015	0.825
sync_0417	50S ribosomal protein L36	2	1	0.806		1.054		0.974		1.164		0.971	
sync_0418	adenylate kinase	7	9	1.003	0.985	1.019	0.882	1.428	0.507	0.982	0.894	1.073	0.817
sync_0419	preprotein translocase subunit SecY	3		0.913	0.410					1.008	0.941		
sync_0420	50S ribosomal protein L15	12	14	0.908	0.111	1.026	0.768	1.112	0.405	0.927	0.175	0.954	0.591
sync_0421	30S ribosomal protein S5	11	22	0.958	0.560	0.883	0.491	1.155	0.022	1.030	0.697	1.005	0.917
sync_0422	50S ribosomal protein L18	6	6	1.050	0.741	1.127	0.288	1.238	0.497	1.091	0.463	0.997	0.980
sync_0423	50S ribosomal protein L6	8	11	1.004	0.956	1.122	0.515	1.146	0.275	0.995	0.947	0.982	0.854
sync_0424	30S ribosomal protein S8	10	9	0.955	0.636	1.137	0.440	1.155	0.186	0.958	0.770	1.145	0.138
sync_0425	50S ribosomal protein L5	8	16	0.893	0.150	0.933	0.505	1.152	0.109	0.957	0.528	1.025	0.622
sync_0426	50S ribosomal protein L24	6	4	0.979	0.772	1.050	0.600	1.145	0.160	0.962	0.598	0.985	0.845
sync_0427	50S ribosomal protein L14	10	11	0.993	0.965	1.226	0.426	1.082	0.490	0.977	0.806	1.222	0.489
sync_0428	30S ribosomal protein S17	3	7	0.927	0.456	1.105	0.423	1.126	0.415	0.882	0.267	1.051	0.485
sync_0429	50S ribosomal protein L29		10			1.017	0.957	0.995	0.968			1.080	0.436
sync_0430	50S ribosomal protein L16	8	7	0.901	0.640	1.432	0.248	0.947	0.708	1.103	0.657	1.144	0.485
sync_0431	30S ribosomal protein S3	17	17	0.963	0.427	1.134	0.097	1.145	0.025	0.940	0.202	0.904	0.066
sync_0432	50S ribosomal protein L22	4	4	0.717		0.840	0.336	1.080	0.596	0.937		0.913	0.543
sync_0433	30S ribosomal protein S19	4	5	0.737		1.182	0.280	1.167	0.229	0.886		1.219	0.289
sync_0434	50S ribosomal protein L2	5	8	0.963	0.715	1.187	0.246	1.136	0.101	0.940	0.481	0.997	0.966
sync_0435	50S ribosomal protein L23	7	9	1.044	0.541	1.057	0.730	1.104	0.530	0.966	0.624	0.977	0.749
sync_0436	50S ribosomal protein L4	7	14	1.035	0.560	1.126	0.492	1.040	0.764	1.111	0.290	1.009	0.944
sync_0437	50S ribosomal protein L3	14	13	0.897	0.029	1.104	0.284	1.213	0.033	1.005	0.909	1.098	0.061
sync_0438	hypothetical protein sync_0438	3	4	1.065	0.471	0.791	0.184	0.852	0.135	1.025	0.759	0.886	0.225
sync_0443	recombinase A	5	10	1.169	0.469	1.066	0.682	1.361	0.154	0.911	0.394	1.154	0.342
sync_0445	hypothetical protein sync_0445		2			1.719		0.736				1.162	
sync_0447	arogenate dehydrogenase	3	2	1.000	0.998	1.137	0.425	0.984	0.925	1.026	0.782	1.087	0.559
sync_0450	hypothetical protein sync_0450	6	3	1.089	0.323	1.081	0.687	0.828	0.097	1.057	0.501	0.796	0.050

sync_0452	putative molybdopterin biosynthesis protein MoeB		4	5	1.149	0.588	0.718		0.740		0.993	0.974	1.368	
sync_0455	glutamate decarboxylase		16	17	0.969	0.747	0.983	0.847	1.070	0.408	0.921	0.347	1.030	0.522
sync_0460	phosphoenolpyruvate carboxylase		23	31	1.024	0.571	1.103	0.298	0.981	0.828	0.951	0.242	1.024	0.659
sync_0461	putative glutamate--cysteine ligase		8	7	1.052	0.430	0.992	0.958	0.962	0.707	1.062	0.700	1.037	0.752
sync_0462	putative anthranilate synthase component I		7	4	1.067	0.523	1.074	0.582	1.144	0.637	0.955	0.595	1.023	0.886
sync_0463	photosystem I reaction center subunit II		30	39	1.067	0.508	0.739	0.037	0.819	0.147	0.978	0.675	0.984	0.754
sync_0466	ATPase		5	5	0.849	0.143	0.918	0.467	1.050	0.499	1.118	0.218	0.984	0.909
sync_0467	coproporphyrinogen III oxidase		7	9	1.106	0.159	1.102	0.244	0.986	0.850	0.917	0.214	0.935	0.435
sync_0468	N-acetylmuramoyl-L-alanine amidase		4	2	1.068	0.375	0.751	0.265	0.956	0.694	1.189	0.059	0.858	0.132
sync_0471	3'-5' exonuclease family protein		7	6	1.037	0.629	1.071	0.594	0.826	0.391	1.046	0.554	0.941	0.539
sync_0472	hypothetical protein sync_0472		3	3	0.962	0.675	1.690	0.133	0.963	0.955	0.979	0.797	0.969	0.806
sync_0473	hypothetical protein sync_0473			1			0.857		1.067				0.895	
sync_0480	Hpt domain-containing protein	ISL2	11	12	0.944	0.672	1.484	0.011	0.885	0.582	1.078	0.591	1.066	0.622
sync_0481	phosphoribosylaminoimidazole synthetase	ISL2	6	2	0.862	0.218	1.151		0.946		1.138	0.256	0.998	
sync_0483	bifunctional pantoate ligase/cytidylate kinase	ISL2	5	3	1.020	0.909	1.066	0.738	0.975	0.910	0.983	0.873	0.936	0.727
sync_0486	phycocyanin alpha subunit phycocyanobilin lyase, CpcE subunit	ISL2		1	0.752						0.965			
sync_0487	hypothetical protein sync_0487	ISL2		1			0.856		0.742				0.841	
sync_0488	phycocyanin, alpha subunit	ISL2	70	10	0.970	0.740	0.956	0.803	0.936	0.533	0.988	0.876	1.019	0.730
sync_0489	phycocyanin, beta subunit	ISL2	75	13	0.945	0.401	0.987	0.877	1.034	0.827	1.011	0.869	1.109	0.138
sync_0490	phycoerythrobilin:ferredoxin oxidoreductase	ISL2	5	2	0.948	0.527	1.072	0.511	0.937	0.895	0.996	0.963	0.993	0.978
sync_0491	dihydrobiliverdin:ferredoxin oxidoreductase	ISL2	9	7	1.012	0.910	0.967	0.822	0.973	0.767	0.917	0.460	0.962	0.584

sync_0492	hypothetical protein sync_0492	ISL2		6	3	0.824	0.092	0.942	0.731	1.133	0.493	0.956	0.754	0.923	0.583
sync_0493	hypothetical protein sync_0493	ISL2		5	7	1.013	0.914	1.090	0.722	0.976	0.850	1.029	0.819	1.305	0.226
sync_0495	C-phycoerythrin class I beta chain	ISL2		74	11 3	0.904	0.220	0.919	0.417	1.027	0.836	0.942	0.407	1.030	0.835
sync_0496	C-phycoerythrin class I alpha chain	ISL2		66	18 2	0.937	0.260	0.921	0.710	0.987	0.894	1.006	0.920	1.066	0.452
sync_0497	bilin biosynthesis protein mpeV	ISL2	YES	2	1	0.994	0.961	1.011		1.187		1.093	0.538	0.881	
sync_0498	hypothetical protein sync_0498	ISL2		4	4	1.086	0.628	0.842		0.921		0.924	0.499	1.049	
sync_0499	bilin biosynthesis protein cpeY	ISL2	YES	2	1	0.933	0.398	0.750		1.222		0.964	0.639	0.779	
sync_0500	bilin biosynthesis protein cpeZ	ISL2	YES	4	8	1.198	0.443	1.112	0.334	1.143	0.430	0.873	0.285	1.043	0.752
sync_0501	bilin biosynthesis protein mpeU	ISL2	YES	10	6	0.946	0.576	1.035	0.913	0.981	0.940	1.041	0.488	1.204	0.424
sync_0502	phycoerythrin class II gamma chain, linker polypeptide	ISL2	YES	23	41	0.961	0.473	1.003	0.985	1.036	0.607	0.995	0.929	1.060	0.197
sync_0504	C-phycoerythrin class II alpha chain	ISL2		15 0	31 0	0.926	0.267	0.865	0.420	1.048	0.655	1.038	0.584	1.077	0.202
sync_0505	C-phycoerythrin class II beta chain	ISL2		14 6	22 7	0.915	0.221	0.895	0.431	1.011	0.919	0.982	0.793	0.979	0.842
sync_0506	CpeY protein	ISL2		11	11	1.127	0.809	1.052	0.592	0.980	0.908	1.093	0.360	1.108	0.140
sync_0507	hypothetical protein sync_0507	ISL2	YES	4	4	0.963	0.767	1.263	0.376	0.739	0.172	1.025	0.847	0.911	0.723
sync_0508	hypothetical protein sync_0508	ISL2		3	2	0.999	0.989	0.836	0.159	0.950	0.782	1.018	0.848	1.026	0.806
sync_0509	hypothetical protein sync_0509	ISL2	YES	3		1.075	0.490					0.966	0.724		
sync_0510	phycoerythrin linker protein CpeS	ISL2		8	13	0.975	0.696	0.996	0.976	1.073	0.694	0.979	0.742	1.162	0.181
sync_0511	phycobilisome linker polypeptide	ISL2	YES	21	33	1.032	0.537	1.085	0.507	1.021	0.638	1.054	0.343	1.039	0.524
sync_0512	phycobilisome linker polypeptide	ISL2		72	12 9	0.961	0.294	0.919	0.195	1.024	0.675	1.004	0.913	1.061	0.142
sync_0513	phycobilisome linker polypeptide	ISL2		15	46	1.002	0.977	1.007	0.931	0.930	0.236	1.034	0.679	0.962	0.300
sync_0514	pentapeptide repeat-containing protein	ISL2		6	6	1.039	0.555	1.161	0.287	0.968	0.840	0.989	0.877	0.996	0.950
sync_0515	phycobilisome rod-core linker polypeptide (L-RC 28.5)	ISL2		13	28	1.005	0.964	1.005	0.915	1.072	0.574	1.005	0.929	1.008	0.929

sync_0516	phycobilisome linker polypeptide	ISL2	YES	35	40	0.938	0.345	0.906	0.385	0.968	0.654	0.945	0.633	1.050	0.529
sync_0518	hypothetical protein sync_0518	ISL2		4	4	1.076	0.714	1.054	0.775	0.807	0.250	0.972	0.723	0.776	0.274
sync_0519	hypothetical protein sync_0519	ISL2		1		1.067						0.917			
sync_0520	hypothetical protein sync_0520	ISL2		1		1.200						1.004			
sync_0526	hypothetical protein sync_0526			3		0.951	0.704					0.924	0.571		
sync_0528	carbohydrate kinase, FGGY family protein			1		0.948	0.804					0.978	0.861		
sync_0529	S-adenosylmethionine synthetase			34	22	0.937	0.174	0.897	0.239	1.172	0.068	0.946	0.238	0.991	0.910
sync_0531	30S ribosomal protein S1			30	17	1.040	0.467	1.103	0.303	1.099	0.447	1.105	0.326	1.149	0.065
sync_0532	transcriptional regulator NrdR			3	5	0.973	0.926	1.385	0.584	0.826	0.226	1.024	0.917	1.141	0.851
sync_0534	photosystem II P680 chlorophyll A apoprotein			18	43	1.045	0.394	0.934	0.585	1.074	0.246	0.957	0.477	0.930	0.305
sync_0535	ferredoxin (2Fe-2S)			2		1.074	0.675					1.222	0.572		
sync_0537	universal stress protein family protein			14	13	1.052	0.425	0.965	0.641	1.085	0.244	1.079	0.501	1.058	0.404
sync_0544	cell division topological specificity factor MinE			3	7	1.002	0.980	1.446	0.071	0.964	0.644	1.012	0.902	1.052	0.686
sync_0545	septum site-determining protein MinD			10	19	1.128	0.463	0.986	0.806	0.953	0.435	1.114	0.292	0.955	0.489
sync_0546	septum site-determining protein MinC			3		1.070	0.644					1.036	0.832		
sync_0548	carboxyl-terminal processing proteinase			9	9	0.982	0.818	1.024	0.817	1.064	0.620	1.086	0.423	1.125	0.469
sync_0549	cytochrome b6			5	5	0.891	0.467	1.088	0.425	0.937	0.525	0.950	0.737	0.753	0.079
sync_0550	cytochrome b6-f complex subunit IV				1			1.364	0.434	0.997	0.976			1.130	0.724
sync_0551	neutral invertase like protein			2	4	0.938	0.763	1.535	0.224	0.849	0.359	0.991	0.945	0.662	0.383
sync_0562	photosystem I reaction center subunit IV			12	13	1.293	0.240	0.957		0.992		0.966	0.816	0.691	
sync_0565	LysM domain-containing protein			1		1.355						1.290			

sync_0566	NAD-dependent aldehyde dehydrogenase		6	9	1.015	0.983	0.891	0.310	1.043	0.834	1.135	0.452	0.917	0.392
sync_0567	trehalose synthase	ISL3		4			0.977	0.858	1.018	0.890			0.933	0.859
sync_0568	glycerol dehydrogenase-like protein	ISL3	8	6	1.038	0.644	1.111	0.464	1.084	0.651	0.912	0.262	1.054	0.782
sync_0569	glycerol kinase	ISL3	11	9	1.016	0.753	0.961	0.525	0.959	0.598	0.943	0.479	1.204	0.021
sync_0573	putative two-component hybrid sensor and regulator	ISL3	4	2	0.978	0.913	0.842	0.752	1.076	0.642	1.012	0.908	1.086	0.689
sync_0578	3-dehydroquinate dehydratase	ISL3		1			0.923		1.272				0.235	
sync_0579	tRNA-(ms[2]io[6]A)-hydroxylase	ISL3	1		1.096						0.776			
sync_0586	DNA-binding response regulator	ISL3	2		0.818						1.066			
sync_0590	precorrin-2 C20-methyltransferase		1		0.912						0.956			
sync_0596	GTP-binding protein EngA			2			0.974	0.936	0.728	0.262			0.876	0.411
sync_0598	hypothetical protein sync_0598		5	7	1.128	0.372	0.852	0.441	1.167	0.135	0.883	0.290	1.011	0.892
sync_0599	hypothetical protein sync_0599		3	3	0.887	0.281	1.219	0.562	0.900	0.250	0.860	0.208	0.866	0.540
sync_0601	pyrroline-5-carboxylate reductase		2		1.014	0.918					0.929	0.462		
sync_0602	glycosyl transferases group 1		2		1.081	0.576					1.060	0.665		
sync_0605	deoxyribose-phosphate aldolase		1	1	1.015		0.801		1.039		1.238		0.894	
sync_0606	ribosomal subunit interface protein		9	16	1.159	0.842	0.989	0.940	0.874	0.301	1.023	0.885	0.991	0.916
sync_0608	long-chain acyl-CoA synthetase		4	6	0.916	0.481	1.036	0.728	0.994	0.919	1.079	0.563	1.038	0.740
sync_0616	hypothetical protein sync_0616		13	8	0.989	0.869	1.144	0.265	0.960	0.635	1.011	0.900	1.120	0.153
sync_0617	branched-chain alpha-keto acid dehydrogenase subunit E2		30	21	0.956	0.904	1.049	0.685	0.973	0.781	1.028	0.849	0.961	0.564
sync_0619	S-adenosylmethionine:tRNA ribosyltransferase-isomerase(queuosine biosynthesis protein queA)		8	5	1.020	0.693	1.128	0.397	0.932	0.475	0.961	0.593	1.162	0.205

sync_0620	cysteine synthase A		81	70	0.938	0.188	0.982	0.878	1.030	0.472	0.972	0.551	1.000	0.991
sync_0622	cystathionine gamma-synthase		2		0.995	0.966					0.962	0.779		
sync_0623	cystathionine beta-lyase/cystathionine gamma-synthase		1	2	1.069		1.128	0.789	1.065	0.835	0.920		0.936	0.776
sync_0627	hypothetical protein sync_0627		1	1	1.076		1.237		1.428		0.897		1.155	
sync_0629	30S ribosomal protein S4		6	12	0.992	0.890	1.270	0.089	1.118	0.112	0.913	0.154	0.988	0.824
sync_0631	ribonucleotide reductase (class II)			3			0.895		1.115				1.099	
sync_0632	UDP-N-acetylmuramoylalanyl-D-glutamate--2,6-diaminopimelate ligase		3	2	1.182	0.725	0.767		0.561		1.035	0.789	1.070	
sync_0633	calcium/proton exchanger	ISL4	2		1.005	0.970					0.982	0.912		
sync_0634	hydrophobic amino acid ABC transporter periplasmic amino acid-binding protein	ISL4	4	6	0.952	0.595	0.654	0.291	0.960	0.749	1.002	0.985	1.116	0.466
sync_0636	L-cysteine/cystine lyase-like protein	ISL4	4		1.058	0.559					0.918	0.402		
sync_0642	hypothetical protein sync_0642	ISL4	1		0.888						0.859			
sync_0647	NifU domain-containing protein	ISL4	11	9	1.002	0.986	1.251	0.353	0.976	0.925	1.056	0.753	0.627	0.186
sync_0648	malate:quinone oxidoreductase	ISL4		1			0.918		1.473				0.919	
sync_0652	GTP-binding protein LepA	ISL4	6	16	1.033	0.581	1.167	0.020	1.054	0.646	0.972	0.612	0.986	0.809
sync_0662	hypothetical protein sync_0662	ISL4	3	4	0.668	0.155	1.054	0.880	0.944	0.564	0.966	0.889	0.981	0.840
sync_0675	sensor histidine kinase	ISL4	1	2	0.967		0.680		0.806		1.243		1.040	
sync_0680	Ferritin	ISL4	1		1.251						0.991			
sync_0681	ferrous iron transport protein B	ISL4	YES	4		0.787	0.021				1.049	0.575		
sync_0682	ferrous iron transport protein A	ISL4		1			0.641	0.139	0.980	0.870			1.131	0.431
sync_0689	peroxiredoxin 2 family protein	ISL4	39	34	0.963	0.450	0.822	0.021	1.086	0.378	0.994	0.909	1.061	0.395
sync_0692	hypothetical protein sync_0692		1		0.919						0.927			
sync_0694	sun protein		2		1.043	0.742					1.088	0.576		

sync_0695	membrane carboxypeptidase (penicillin-binding protein)		7	8	1.009	0.897	0.932	0.519	0.984	0.885	1.072	0.307	0.912	0.314
sync_0697	hypothetical protein sync_0697		3	2	0.960	0.688	1.011	0.964	0.932	0.780	1.030	0.767	0.996	0.977
sync_0698	imidazole glycerol phosphate synthase subunit HisF		3	4	0.922	0.241	1.332	0.427	0.952	0.634	0.899	0.144	1.265	0.129
sync_0700	ubiquinone/menaquinone biosynthesis methyltransferase UbiE		1	1	0.829		0.637		0.857		0.964		1.140	
sync_0702	hypothetical protein sync_0702	ISL5	1		1.005						1.036			
sync_0705	hypothetical protein sync_0705	ISL5		1			1.140		1.101				0.771	
sync_0706	sensor histidine kinase	ISL5	3	1	1.060	0.582	1.146		1.795		0.935	0.771	1.287	
sync_0707	DNA-binding response regulator	ISL5	3	3	1.139	0.418	0.938	0.659	1.136	0.448	0.815	0.287	1.156	0.545
sync_0714	putative lipoprotein	ISL5	1		0.771						0.910			
sync_0717	glycyl-tRNA synthetase subunit alpha		5	2	1.022	0.813	0.831	0.546	1.160	0.642	0.926	0.498	0.953	0.732
sync_0722	hypothetical protein sync_0722		3	2	1.075		0.866		1.461		0.971		1.145	
sync_0725	ketol-acid reductoisomerase		35	34	1.032	0.530	0.917	0.530	1.120	0.328	1.013	0.795	0.963	0.695
sync_0726	ATP-dependent Clp protease proteolytic subunit		6	11	1.160	0.130	0.770	0.056	0.988	0.918	0.912	0.228	0.914	0.357
sync_0727	ATP-dependent Clp protease-like protein		8	6	1.043	0.631	0.813	0.071	1.065	0.565	0.972	0.746	0.804	0.063
sync_0728	PIN/TRAM domain-containing protein		2	3	1.015	0.920	1.076	0.727	0.906	0.410	1.113	0.358	0.995	0.954
sync_0730	3-methyl-2-oxobutanoate hydroxymethyltransferase		1		1.015						0.949			
sync_0731	cell division protein FtsZ		25	37	1.132	0.018	0.934	0.311	0.914	0.190	0.981	0.677	1.023	0.710
sync_0732	hypothetical protein sync_0732		1	1	0.882	0.430	0.979	0.940	0.861	0.373	0.912	0.528	1.085	0.564
sync_0733	hypothetical protein sync_0733		4	3	0.953	0.620	0.859		0.837		1.009	0.925	1.026	
sync_0734	D-alanine--D-alanine ligase		4	2	1.075	0.598	1.470		0.713		0.958	0.717	1.214	
sync_0735	tRNA-i(6)A37 thiotransferase enzyme MiaB		2		0.814	0.468					1.314	0.477		
sync_0736	muconate cycloisomerase		1	1	1.038		1.245	0.362	0.943	0.826	1.081		0.771	0.236

sync_0737	hypothetical protein sync_0737	1		0.974						0.814			
sync_0744	acetylornithine aminotransferase	5	4	0.992	0.933	1.212	0.156	1.062	0.714	0.962	0.566	0.990	0.890
sync_0746	UDP-N-acetylglucosamine 1-carboxyvinyltransferase	3	2	0.977	0.808	1.166		2.089		0.942	0.713	1.416	
sync_0748	4Fe-4S iron sulfur cluster binding protein	5	9	1.076	0.502	0.820	0.174	0.926	0.388	1.152	0.239	0.894	0.237
sync_0749	RNA methyltransferase, TrmH family protein	1		0.814	0.311					1.044	0.764		
sync_0750	dihydrolipoamide dehydrogenase	21	22	0.962	0.607	1.023	0.661	0.972	0.556	1.013	0.887	0.985	0.776
sync_0751	indole-3-glycerol-phosphate synthase	6	7	0.912	0.288	1.007	0.969	1.266	0.113	0.944	0.480	1.050	0.605
sync_0753	hydrogenase accessory protein		1			0.629		0.356				2.468	
sync_0755	superoxide dismutase, Ni	11	12	1.020	0.797	1.223	0.122	1.036	0.605	1.023	0.804	0.928	0.446
sync_0756	FKBP-type peptidyl-prolyl cis-trans isomerase	9	9	1.052	0.473	0.807	0.444	1.202	0.315	1.007	0.923	0.960	0.873
sync_0757	hypothetical protein sync_0757	5	11	1.024	0.763	1.376	0.064	0.991	0.932	1.107	0.244	0.936	0.513
sync_0759	tRNA (5-methylaminomethyl-2-thiouridylate)-methyltransferase		1			0.770		4.007				3.651	
sync_0760	carbohydrate kinase family protein	2	1	0.987	0.971	1.079		1.218		0.881	0.565	1.141	
sync_0761	Type II alternative RNA polymerase sigma factor, sigma-70 family protein	3	1	0.928	0.593	19.576		1.019		0.963	0.937	0.947	
sync_0764	pyruvate dehydrogenase E1 alpha subunit	12	10	1.078	0.597	1.011	0.891	1.195	0.183	0.941	0.591	1.035	0.608
sync_0765	DnaJ domain-containing protein	10	21	1.004	0.941	1.051	0.356	0.932	0.156	0.962	0.743	0.917	0.188
sync_0766	signal recognition particle protein	6	13	1.031	0.590	1.191	0.024	1.064	0.611	0.987	0.810	0.925	0.401
sync_0767	30S ribosomal protein S16	4	8	0.849	0.186	1.239	0.116	0.926	0.301	0.937	0.516	0.870	0.617
sync_0769	hypothetical protein sync_0769	3	3	1.158	0.799	0.555		0.782		1.194	0.342	0.668	

sync_0770	hypothetical protein sync_0770		2		0.991	0.926					1.053	0.599		
sync_0771	hypothetical protein sync_0771		2		0.958	0.751					1.009	0.943		
sync_0772	alpha-acetolactate decarboxylase		1		1.086						0.952			
sync_0773	GTP-binding protein Era			3			1.043	0.656	1.137	0.446			0.990	0.933
sync_0781	2C-methyl-D-erythritol 2,4-cyclodiphosphate synthase	ISL6		3		1.099	0.378				0.809	0.131		
sync_0785	hypothetical protein sync_0785			3			0.895	0.732	1.017	0.903			0.856	0.389
sync_0788	hypothetical protein sync_0788		1	2	1.011	0.935	1.356	0.200	1.202	0.440	0.951	0.723	1.477	0.158
sync_0791	thiamine-phosphate pyrophosphorylase		4	1	1.051	0.472	1.333		1.024		1.062	0.391	0.909	
sync_0793	riboflavin biosynthesis protein RibF			2		1.099	0.659				0.988	0.942		
sync_0795	acid phosphatase SurE		6	4	1.050	0.772	0.939	0.570	0.934	0.700	1.122	0.400	0.898	0.315
sync_0796	phenylalanyl-tRNA synthetase, alpha subunit		6	6	0.818	0.134	1.394	0.275	0.897	0.667	1.031	0.748	0.998	0.979
sync_0797	hypothetical protein sync_0797		6	5	1.065	0.686	0.912	0.673	0.992	0.946	0.898	0.245	1.248	0.170
sync_0804	ABC1 family protein		3	1	1.095	0.402	0.917	0.575	1.010	0.921	1.063	0.464	0.905	0.376
sync_0805	zeta-carotene desaturase		4		0.899	0.486					1.101	0.365		
sync_0806	inorganic polyphosphate/ATP-NAD kinase		5	1	1.080	0.603	1.061		0.944		0.983	0.874	1.507	
sync_0818	hypothetical protein sync_0818	ISL7	9	5	0.942	0.418	0.914	0.382	1.161	0.132	0.965	0.774	0.944	0.630
sync_0820	hypothetical protein sync_0820		4	1	1.072	0.406	0.603		0.557		0.889	0.200	1.067	
sync_0821	riboflavin biosynthesis protein RibD			5		0.907	0.271				0.862	0.199		
sync_0822	alcohol dehydrogenase			2		0.993	0.972				0.862	0.135		
sync_0825	cell division protein FtsH3		24	25	1.033	0.490	0.943	0.299	0.975	0.742	1.070	0.168	0.946	0.328
sync_0826	ornithine carbamoyltransferase		11	12	1.031	0.720	0.962	0.587	0.962	0.776	1.024	0.781	1.050	0.804
sync_0827	carboxylesterase			1			1.230		1.072				1.123	
sync_0828	hypothetical protein sync_0828		4	3	0.928		0.760	0.751	0.624	0.132	0.854		1.001	0.997
sync_0829	hypothetical protein sync_0829		1	1	1.014		0.954		0.838		1.060		1.017	

sync_0830	hypothetical protein sync_0830		7	2	1.167	0.443	0.822	0.305	0.940	0.650	1.105	0.478	1.007	0.958
sync_0831	LexA repressor		1		0.861						0.832			
sync_0836	hypothetical protein sync_0836	ISL8		1					2.359		1.261			0.704
sync_0838	hypothetical protein sync_0838	ISL8	1	1	0.945				1.011		1.033		0.854	1.154
sync_0845	hypothetical protein sync_0845	ISL8	2		1.064	0.709					0.939	0.639		
sync_0850	hypothetical protein sync_0850	ISL8		1					1.078		0.899			1.262
sync_0854	ferritin	ISL8	6	8	1.311	0.150	1.737	0.004	1.403	0.006	1.361	0.232	1.711	0.002
sync_0855	hypothetical protein sync_0855	ISL8		2					0.803		0.979			1.106
sync_0856	gluconolactonase precursor	ISL8	11	8	0.994	0.920	0.943	0.395	1.024	0.788	0.944	0.355	1.054	0.495
sync_0861	mandelate racemase/muconate lactonizing protein	ISL8	3	5	1.184	0.508	1.013	0.859	1.101	0.447	0.840	0.373	1.205	0.114
sync_0865	hypothetical protein sync_0865	ISL8	1		1.001						0.928			
sync_0868	hypothetical protein sync_0868	ISL8	3	1	0.969	0.776	0.667	0.157	0.795	0.264	1.025	0.924	1.073	0.616
sync_0870	SAP domain-containing protein	ISL8		2					1.053	0.725	1.103	0.504		0.906
sync_0872	glyceraldehyde-3-phosphate dehydrogenase, type I	ISL8	6	4	1.088	0.352	1.082	0.810	1.258	0.263	1.006	0.939	0.949	0.805
sync_0873	hypothetical protein sync_0873	ISL8	2		0.918	0.594					0.989	0.937		
sync_0874	photosystem I reaction center subunit psaK (photosystem I subunit X)	ISL8		3					2.350		0.987			0.906
sync_0890	hypothetical protein sync_0890		1		1.050						1.091			
sync_0896	photosystem II 44 kDa subunit reaction center protein		13	16	0.952	0.475	1.207	0.250	1.037	0.759	0.999	0.993	0.961	0.711
sync_0898	photosystem I assembly protein Ycf4		3	4	0.957	0.611	1.213	0.604	0.912	0.561	0.977	0.915	0.875	0.660
sync_0899	peptidyl-prolyl cis-trans isomerase, cyclophilin-type		7	8	1.052	0.960	0.851	0.219	0.841	0.019	1.072	0.798	0.996	0.937
sync_0900	acetolactate synthase 3 regulatory subunit		5	8	0.994	0.958	0.878	0.558	1.000	0.997	1.044	0.740	0.801	0.474
sync_0904	3-beta hydroxysteroid dehydrogenase/isomerase family protein		8	9	0.947	0.736	0.927	0.667	0.912	0.612	0.983	0.908	0.853	0.284

sync_0905	hypothetical protein sync_0905		1	2	0.879		0.917	0.771	1.924	0.106	0.936		1.161	0.397
sync_0906	methyltransferase		1	1	0.912		0.803		0.981		0.964		0.995	
sync_0909	translation initiation factor IF-1		6	5	0.955	0.729	0.864	0.586	1.039	0.898	1.134	0.492	0.930	0.648
sync_0910	thioredoxin-disulfide reductase		14	12	1.165	0.209	0.795	0.140	1.094	0.497	0.933	0.731	1.003	0.985
sync_0915	NAD/NADP transhydrogenase alpha subunit		24	23	1.040	0.365	1.054	0.668	0.884	0.086	0.943	0.513	0.946	0.329
sync_0917	NAD/NADP transhydrogenase beta subunit		16	4	1.059	0.786	1.326	0.538	1.116	0.742	1.077	0.566	1.235	0.219
sync_0920	1-deoxy-D-xylulose 5-phosphate reductoisomerase		6	5	0.919	0.352	1.153	0.054	1.099	0.485	0.991	0.934	1.079	0.618
sync_0921	Na+-dependent transporter of the SNF family protein		1	2	0.928		1.054		1.386		1.164		1.198	
sync_0923	hypothetical protein sync_0923		3	3	0.973	0.902	0.647		1.123		1.016	0.897	0.586	
sync_0924	cysteinyI-tRNA synthetase		14	7	0.935	0.343	1.240	0.088	1.064	0.635	1.061	0.326	0.878	0.125
sync_0928	DNA polymerase I		5	5	1.024	0.869	1.056	0.816	0.972	0.823	0.946	0.595	0.934	0.622
sync_0930	translation-associated GTPase		10	12	1.083	0.257	1.082	0.450	0.945	0.624	1.052	0.382	0.998	0.976
sync_0934	hypothetical protein sync_0934		2	2	0.992	0.958	0.801	0.657	1.294	0.241	1.185	0.413	1.177	0.596
sync_0935	hypothetical protein sync_0935		3	1	1.167	0.232	0.926		0.526		1.074	0.651	1.165	
sync_0936	transporter, major facilitator family protein		1		0.892						1.073			
sync_0937	hypothetical protein sync_0937			1			1.038	0.770	0.973	0.826			1.191	0.476
sync_0939	ABC transporter substrate-binding protein		1	4	1.019		1.108	0.348	0.954	0.804	0.695		1.106	0.356
sync_0941	homoserine dehydrogenase		13	14	1.117	0.341	0.935	0.605	0.914	0.399	0.974	0.843	0.935	0.538
sync_0948	carbonic anhydrase	ISL9	2		0.943	0.661					0.964	0.833		
sync_0950	hypothetical protein sync_0950	ISL9	16	53	0.890	0.194	0.899	0.361	0.876	0.212	1.077	0.368	0.871	0.066
sync_0954	hypothetical protein sync_0954	ISL9		1			0.859		1.135				0.831	
sync_0955	hypothetical protein sync_0955	ISL9	3		0.934	0.504					0.851	0.253		
sync_0956	hypothetical protein sync_0956	ISL9	19	5	0.932	0.300	0.948	0.704	0.929	0.612	0.958	0.604	1.063	0.684
sync_0957	hypothetical protein sync_0957	ISL9	2		1.025	0.852					0.996	0.975		

sync_0962	magnesium chelatase, ATPase subunit I	16	21	1.186	0.158	1.058	0.721	1.044	0.803	0.947	0.359	1.023	0.922
sync_0963	hypothetical protein sync_0963	8	5	1.026	0.696	1.059	0.530	0.967	0.607	1.011	0.896	1.057	0.477
sync_0964	carboxylesterase, beta-lactamase family protein	6	9	0.984	0.863	0.919	0.430	1.020	0.784	1.009	0.921	0.928	0.352
sync_0969	imidazole glycerol phosphate synthase, glutamine amidotransferase subunit		1			1.270		1.097				0.928	
sync_0970	thioredoxin	18	24	0.933	0.402	0.899	0.136	0.907	0.539	0.978	0.777	0.953	0.606
sync_0971	inositol-5-monophosphate dehydrogenase	31	28	1.028	0.951	0.817	0.198	0.883	0.100	1.011	0.926	1.033	0.463
sync_0972	hypothetical protein sync_0972	3	4	0.881	0.431	0.874	0.405	1.007	0.958	0.915	0.678	0.850	0.407
sync_0973	DNA gyrase subunit A	7	17	0.936	0.287	1.252	0.005	0.925	0.162	1.041	0.508	0.981	0.680
sync_0975	hypothetical protein sync_0975	3		1.045	0.975					1.234	0.540		
sync_0976	2-isopropylmalate synthase	19	17	0.979	0.762	0.924	0.518	0.859	0.067	0.998	0.981	0.804	0.007
sync_0980	ferredoxin	2	2	0.845		0.726		0.869		1.413		0.990	
sync_0982	hypothetical protein sync_0982	4		1.052	0.763					0.901	0.348		
sync_0989	HDIG domain-containing protein	5	5	0.964	0.605	0.975	0.842	1.652	0.124	0.955	0.691	1.011	0.928
sync_0990	putative FOLD bifunctional protein	8	2	1.031	0.645	0.822		1.152		1.103	0.383	1.120	
sync_0991	geranylgeranyl diphosphate synthase	6	5	1.040	0.576	1.059	0.664	0.954	0.801	0.962	0.583	1.201	0.316
sync_0997	hypothetical protein sync_0997		1			1.954		1.178				0.776	
sync_0998	EntD	5	3	0.972		1.046	0.878	0.886	0.436	1.042		0.906	0.608
sync_0999	acylphosphatase		1			1.074		1.789				1.501	
sync_1000	cobyrinic acid a,c-diamide synthase	3		0.940	0.646					0.945	0.770		
sync_1001	glucose 6-phosphate dehydrogenase effector OpcA	7	8	0.948	0.528	1.192	0.477	1.101	0.487	0.957	0.592	1.074	0.615
sync_1002	glucose-6-phosphate 1-dehydrogenase	23	32	1.090	0.239	0.947	0.302	1.052	0.295	0.999	0.982	1.075	0.137
sync_1003	ferredoxin--NADP reductase	50	37	0.946	0.236	1.002	0.987	1.025	0.822	1.021	0.802	0.978	0.804

sync_1006	adaptive-response sensory kinase	4	1	1.171	0.230	1.101		1.307		0.794	0.760	1.017	
sync_1007	hypothetical protein sync_1007		1			0.844		0.926				1.084	
sync_1008	cAMP phosphodiesterases class-II	8	11	1.171	0.315	0.769	0.085	0.991	0.949	1.416	0.152	0.932	0.480
sync_1009	aminopeptidase N	7	8	0.964	0.520	1.011	0.916	0.882	0.239	0.959	0.466	1.002	0.985
sync_1010	hypothetical protein sync_1010		1			1.095		0.979				1.016	
sync_1011	ribose-phosphate pyrophosphokinase	9	3	0.999	0.995	0.921	0.752	0.766	0.169	1.161	0.439	1.229	0.135
sync_1013	LytR-membrane bound transcriptional regulator		4			1.470	0.342	1.238	0.445			1.081	0.808
sync_1014	hypothetical protein sync_1014	1		1.020						0.694			
sync_1015	4-alpha-glucanotransferase	3	3	0.879	0.302	0.801	0.270	1.031	0.810	0.944	0.652	0.963	0.938
sync_1016	helix-hairpin-helix DNA-binding motif-containing protein	3	3	1.094	0.831	1.086	0.680	0.825	0.140	1.006	0.982	1.034	0.725
sync_1019	hypothetical protein sync_1019	2	1	0.901	0.511	0.833		0.819		1.050	0.730	0.970	
sync_1020	hypothetical protein sync_1020	1		0.873						1.087			
sync_1022	Orn/Lys/Arg decarboxylase family protein		1			0.493		1.278				0.895	
sync_1024	hypothetical protein sync_1024	4	1	1.122	0.933	0.823	0.302	1.061	0.657	1.257	0.471	1.051	0.723
sync_1026	glycerol dehydrogenase family protein	4		0.948	0.743					1.028	0.795		
sync_1027	putative Clp protease, ATP-binding subunit ClpC	31	36	1.106	0.006	0.951	0.374	0.889	0.063	1.077	0.107	0.883	0.041
sync_1029	diaminopimelate decarboxylase	16	18	0.963	0.527	0.901	0.406	1.065	0.378	0.949	0.414	1.055	0.580
sync_1030	hypothetical protein sync_1030	1	3	0.832		1.107		0.889		1.112		1.517	
sync_1031	undecaprenyl diphosphate synthase	4	3	0.994	0.941	1.145	0.699	1.084	0.456	1.062	0.415	0.934	0.803
sync_1035	glutathione S-transferase domain-containing protein	1		0.885						0.988			
sync_1038	recombination protein RecR		4			0.811		1.152				0.516	
sync_1039	PsbP		2			1.465	0.167	0.813	0.289			0.969	0.809

sync_1044	putative cell envelope-related function transcriptional attenuator		4	4	0.931	0.351	0.995	0.992	0.820	0.372	0.842	0.114	1.093	0.473	
sync_1045	transporter, monovalent cation:proton antiporter-2 (CPA2) family protein		5	5	0.950	0.525	1.077	0.405	0.973	0.740	1.009	0.936	1.143	0.180	
sync_1046	ABC transporter, multidrug efflux family protein		1	3	0.896		0.906	0.845	1.059	0.911	1.148		0.852	0.832	
sync_1048	putative RNA-binding protein		25	17	0.897	0.319	1.003	0.977	1.013	0.883	0.944	0.574	1.002	0.986	
sync_1051	superfamily II DNA/RNA helicase		6	10	0.998	0.973	1.024	0.824	1.130	0.168	0.959	0.615	0.819	0.035	
sync_1070	intracellular protease/amidase, ThiJ/PfpL family protein	ISL10	2	2	0.803	0.505	0.850	0.357	1.052	0.715	1.139	0.456	1.075	0.619	
sync_1071	hypothetical protein sync_1071	ISL10	3	8	0.912		0.906	0.787	1.074	0.783	0.909		1.023	0.950	
sync_1073	putative lipoprotein	ISL10		2			0.811	0.301	1.081	0.575			1.317	0.489	
sync_1074	hypothetical protein sync_1074	ISL10	4	2	0.926		0.827		0.980		0.945		0.939		
sync_1078	isochorismatase family protein	ISL10	YES	14	13	1.044	0.602	0.705	0.221	0.881	0.737	0.975	0.828	0.824	0.488
sync_1079	sensory box histidine kinase/response regulator	ISL10	YES	2	2	1.011	0.909	0.985	0.899	1.174	0.078	0.965	0.702	1.320	0.099
sync_1080	hypothetical protein sync_1080	ISL10	YES	2	4	1.153		0.523		1.067		0.813		1.956	
sync_1081	metallothionein-related protein	ISL10	YES	6	2	1.071	0.467	0.706		0.961		1.194	0.122	0.927	
sync_1082	hypothetical protein sync_1082	ISL10		2	0.953						1.112				
sync_1097	hypothetical protein sync_1097	ISL10		4	11	1.174	0.385	0.744	0.014	0.863	0.198	1.016	0.879	1.135	0.421
sync_1098	hypothetical protein sync_1098	ISL10		6	5	0.917	0.257	0.950	0.789	0.892	0.568	1.189	0.058	0.944	0.490
sync_1106	hypothetical protein sync_1106	ISL10		1		0.925					0.928				
sync_1114	cupin domain-containing protein	ISL10		10	2	1.019	0.844	0.852	0.639	0.908	0.513	1.037	0.707	0.812	0.286
sync_1116	DNA-binding response regulator	ISL10		2		1.115	0.636				1.385	0.263			
sync_1122	hypothetical protein sync_1122	ISL10		3	4	0.680		8.493	0.007	7.425	0.058	1.825		2.361	0.089
sync_1125	choloylglycine hydrolase	ISL10		6	3	0.907	0.415	0.990	0.958	1.067	0.780	1.067	0.514	1.056	0.574

sync_1129	type I secretion target GGXGXDXXX repeat-containing protein	ISL10		4					1.936	2.727				1.718
sync_1132	hypothetical protein sync_1132	ISL10		1					0.765					0.793
sync_1133	histidine protein kinase; sensor protein	ISL10		5		0.509			1.051				0.450	0.945
sync_1134	response regulator receiver domain-containing protein	ISL10		1					1.130					0.933
sync_1137	photosystem II protein Y	ISL10		2					1.324	1.153				0.864
sync_1140	carotenoid isomerase	ISL10		2	1	0.648			0.941	0.839			0.724	1.124
sync_1145	two-component response regulator	ISL10		9	10	0.846		0.643	1.010	0.939	0.617		0.953	0.913
														0.420
sync_1147	glutaredoxin-like protein	ISL10		3	6	0.633		0.433	1.142	0.924	0.692		0.935	0.731
														0.062
sync_1148	BolA family protein	ISL10		5					1.570	0.705				1.169
sync_1149	hypothetical protein sync_1149	ISL10		11	20	0.979		0.572	1.002	0.919	0.975		0.680	1.105
														0.281
sync_1150	phospholipid and glycerol acyltransferase	ISL10		3				0.178	0.709	0.812	0.591			0.944
														0.665
sync_1151	pyridoxal phosphate biosynthetic protein PdxJ	ISL10		6	9	0.991		0.732	1.001	0.959	0.383		0.970	1.081
														0.285
sync_1152	hypothetical protein sync_1152	ISL10		3	4				0.921	0.886				0.877
														0.934
sync_1159	nucleoside 2- deoxyribosyltransferase	ISL10		1					0.876					1.185
sync_1160	hypothetical protein sync_1160	ISL10		1					0.848					0.922
sync_1161	glutathione S-transferase	ISL10		4	2	0.636		0.444	1.071	0.845	0.253		0.612	0.864
														0.427
sync_1165	hypothetical protein sync_1165			2	5	0.689		0.411	1.197	0.877	0.866		0.505	1.122
														0.453
sync_1167	transcriptional regulator, Fur family protein			2				0.455	1.380	0.987	0.977			1.122
														0.552
sync_1169	hypothetical protein sync_1169			2	4	0.560			0.922	1.066			0.404	1.006
sync_1171	glucosylglycerol 3-phosphatase			12	2	0.892		0.251	0.989	0.671	0.228		0.723	1.040
														0.760
sync_1173	hypothetical protein sync_1173			6	1	0.663		0.430	0.944	1.132	0.584		0.575	0.853
														0.573
sync_1174	RecF/RecN/SMC domain- containing protein			4		0.565			0.931				0.826	1.021

sync_1175	DNA repair exonuclease			1		1.046	0.651				0.916	0.654			
sync_1178	transglycosylase SLT domain-containing protein			6	1	0.977	0.703	1.098	0.666	1.365	0.308	0.965	0.561	1.064	0.461
sync_1179	hypothetical protein sync_1179			15	10	0.915	0.215	0.951	0.712	1.018	0.849	0.958	0.527	0.976	0.681
sync_1180	O-acetylhomoserine sulfhydrylase			18	26	1.037	0.748	0.959	0.296	0.894	0.054	1.128	0.246	0.949	0.407
sync_1181	homoserine O-succinyltransferase			3	5	0.990	0.954	0.842	0.238	1.228	0.075	1.058	0.571	1.115	0.671
sync_1186	polar amino acid ABC transporter ATP-binding protein			5		0.984						0.987			
sync_1188	hypothetical protein sync_1188			1		1.201						1.031			
sync_1190	polar amino acid ABC transporter periplasmic amino acid-binding protein			7	3	1.068	0.416	1.055	0.726	0.823	0.127	0.977	0.692	1.085	0.310
sync_1191	Sulfate permease				3			0.945	0.729	0.944	0.498			0.942	0.693
sync_1194	oxidoreductase				3			0.540		1.039				1.075	
sync_1195	sirohydrochlorin cobaltochelataase			8	8	1.027	0.780	1.227	0.252	1.003	0.979	0.989	0.909	0.861	0.213
sync_1200	L-asparaginase, thermolabile			10	8	1.073	0.530	0.722	0.214	1.193	0.630	1.031	0.681	0.834	0.572
sync_1203	hypothetical protein sync_1203			3	3	1.054	0.586	0.741	0.071	0.785	0.232	1.038	0.722	0.918	0.410
sync_1204	carbamoyl phosphate synthase large subunit			25	26	1.062	0.305	1.082	0.369	0.988	0.787	0.950	0.314	1.047	0.351
sync_1205	hypothetical protein sync_1205			11	10	0.890	0.454	0.940	0.685	1.080	0.227	0.919	0.455	1.051	0.565
sync_1206	Sodium:alanine symporter family protein			4	3	1.085	0.676	1.236	0.513	0.921	0.423	1.056	0.679	0.971	0.855
sync_1207	hypothetical protein sync_1207			4	5	1.006	0.963	1.010	0.981	0.963	0.707	1.170	0.358	0.973	0.791
sync_1208	ABC transporter, permease/ATP-binding protein			8	5	1.006	0.955	1.435	0.155	0.794	0.081	1.041	0.443	0.976	0.785
sync_1210	triosephosphate isomerase			4	5	1.014	0.880	1.062	0.653	1.012	0.966	0.888	0.278	1.006	0.963
sync_1211	dihydropteroate synthase			1		0.969						0.945			
sync_1213	hypothetical protein sync_1213	ISL11	YES	1		1.341						0.901			
sync_1214	ABC transporter RzcB, putative	ISL11	YES	6	7	0.878	0.290	1.090	0.782	0.855	0.137	0.924	0.706	0.859	0.291

sync_1215	ABC transporter ATP-binding protein	ISL11	YES	8	6	0.851	0.071	0.996	0.949	0.990	0.922	0.902	0.278	1.009	0.930
sync_1216	HlyD family secretion protein	ISL11	YES	15	15	0.874	0.016	0.746	0.004	0.803	0.012	0.908	0.163	0.779	0.001
sync_1217	structural toxin protein RtxA	ISL11	YES	16	11	1.127	0.099	1.333	0.015	1.520	0.021	1.229	0.044	1.050	0.698
sync_1220	magnesium chelatase			3	4	0.996	0.977	1.238	0.345	1.202	0.280	1.367	0.488	0.986	0.883
sync_1221	dihydrodipicolinate reductase			13	11	0.954	0.452	0.948	0.788	0.994	0.969	0.945	0.534	1.010	0.930
sync_1222	hypothetical protein sync_1222				2			1.034	0.875	0.708	0.183			0.767	0.232
sync_1226	adenine phosphoribosyltransferase			8	11	0.999		1.048	0.628	1.214	0.103	0.968		1.186	0.098
sync_1227	hypothetical protein sync_1227				4			1.296	0.299	0.788	0.674			1.010	0.943
sync_1228	hypothetical protein sync_1228			4	4	0.955	0.659	0.884	0.526	0.853	0.587	0.937	0.539	0.705	0.249
sync_1232	two-component response regulator			17	8	1.057	0.679	0.976	0.860	1.042	0.758	1.115	0.503	1.114	0.233
sync_1234	PvdS			4	11	0.854	0.044	1.247	0.051	1.210	0.206	1.037	0.566	1.099	0.466
sync_1241	hypothetical protein sync_1241	ISL12		4	2	0.930	0.605	0.869		1.178		0.944	0.804	0.909	
sync_1244	oxidoreductase, short-chain dehydrogenase/reductase family protein	ISL12		3	2	0.954	0.723	0.686		1.045		1.056	0.688	0.809	
sync_1245	carbamoyl-phosphate synthase L chain	ISL12			1			0.630		1.082				0.924	
sync_1251	hypothetical protein sync_1251	ISL12		3		1.072	0.701					0.947	0.609		
sync_1252	nuclease-like protein	ISL12		4		1.103	0.351					0.979	0.822		
sync_1253	glutamine synthetase	ISL12		24	34	0.890	0.017	1.018	0.828	0.999	0.982	0.989	0.798	1.012	0.757
sync_1257	hypothetical protein sync_1257	ISL12	YES	3	4	0.979	0.879	1.147	0.417	1.061	0.679	0.979	0.877	1.079	0.450
sync_1258	putative nuclease	ISL12		2	1	1.074	0.601	0.931	0.763	0.829	0.336	1.166	0.479	0.943	0.845
sync_1260	type I secretion target GGXGXDXXX repeat-containing protein	ISL12			4			1.332	0.719	2.507	0.212			1.141	0.784
sync_1265	ribonucleotide reductase (class II)	ISL12		27	15	0.893	0.014	0.887	0.170	1.014	0.861	0.977	0.702	1.083	0.093
sync_1269	peptide chain release factor 3			7	5	0.980	0.897	1.173	0.482	1.136	0.428	0.982	0.944	0.951	0.702
sync_1271	chaperone			2	4	1.136		1.143	0.584	0.951	0.849	1.132		1.168	0.393

sync_1272	chaperonin HSP33	2	2	1.071		1.281		1.038		0.808		0.875	
sync_1273	ABC transporter, ATP-binding protein		1			1.439		1.290				1.081	
sync_1274	hypothetical protein sync_1274		1			0.975		0.724				0.806	
sync_1275	30S ribosomal protein S2	11	14	0.946	0.342	1.201	0.067	0.992	0.937	0.956	0.528	1.042	0.619
sync_1276	elongation factor Ts	16	18	0.935	0.312	1.027	0.707	1.051	0.411	0.990	0.874	0.983	0.745
sync_1277	hypothetical protein sync_1277		1	0.561						1.070			
sync_1280	sulfite reductase subunit beta	16	11	0.898	0.093	0.921	0.817	1.011	0.892	1.308	0.001	0.912	0.288
sync_1281	glycyl-tRNA synthetase, beta subunit	17	19	0.967	0.594	0.985	0.829	1.078	0.252	0.963	0.425	1.038	0.380
sync_1282	geranylgeranyl reductase	12	13	1.245	0.036	1.157	0.130	1.037	0.529	1.032	0.732	1.121	0.134
sync_1285	GTP-binding protein TypA	16	19	1.000	0.997	0.897	0.129	0.991	0.937	1.007	0.922	0.898	0.154
sync_1286	hypothetical protein sync_1286		1			0.956		0.894				0.999	
sync_1287	hypothetical protein sync_1287		1			0.914	0.712	1.184	0.338			1.039	0.809
sync_1288	ABC transporter ATP-binding protein	2	4	0.876	0.409	0.924	0.435	1.120	0.387	1.004	0.974	0.939	0.521
sync_1289	putative membrane protein, YjgP/YjgQ family protein	3		0.880	0.425					1.117	0.479		
sync_1290	cytochrome c assembly protein		1	1.925						1.010			
sync_1293	chaperone protein dnaK2 (heat shock protein 70-2) (heat shock 70 kdaprotein 2) (HSP70-2)	11		0.992	0.958					1.721	0.051		
sync_1294	hypothetical protein sync_1294	3	4	0.939	0.677	0.996	0.980	0.916	0.379	0.962	0.790	1.109	0.531
sync_1299	hypothetical protein sync_1299		1			1.049		1.570				1.494	
sync_1300	DNA and RNA helicase	2	2	0.852		1.212	0.565	1.018	0.865	0.882		0.994	0.940
sync_1301	methionyl-tRNA formyltransferase		1	1.467						0.830			
sync_1302	tldD/pmbA family protein	17	9	1.012	0.811	1.032	0.818	1.015	0.904	0.910	0.078	1.061	0.347
sync_1303	TldD protein	11	9	1.079	0.187	0.960	0.615	1.266	0.074	0.908	0.132	0.998	0.983
sync_1304	magnesium-protoporphyrin IX monomethyl ester cyclase	5	2	1.118	0.213	1.056	0.854	1.062	0.656	1.011	0.921	0.943	0.665

sync_1305	hypothetical protein sync_1305		3				1.003		0.903				1.074
sync_1307	hypothetical protein sync_1307		1				1.188		1.036				1.129
sync_1308	aromatic acid decarboxylase	6	5	0.994	0.937	1.220	0.690	0.894	0.359	1.002	0.987	1.155	0.597
sync_1309	acetazolamide conferring resistance protein Zam	10	19	0.903	0.192	1.026	0.672	0.994	0.925	1.107	0.584	0.895	0.026
sync_1316	phosphatase/phosphohexomutase of HAD family protein	2		1.148	0.484					1.524	0.228		
sync_1319	50S ribosomal protein L32		2			1.029	0.824	1.155	0.391			0.931	0.612
sync_1320	cell division protein FtsH4	11	12	0.971	0.541	0.991	0.923	1.165	0.721	1.010	0.875	0.855	0.237
sync_1321	hypothetical protein sync_1321	1		0.920						1.064			
sync_1322	thioredoxin peroxidase	29	41	1.008	0.910	0.944	0.853	0.977	0.881	1.008	0.920	0.998	0.981
sync_1326	rRNA methylase	1		0.991	0.921					0.979	0.822		
sync_1328	proton extrusion protein PcxA	7	5	0.955	0.535	0.867	0.414	1.040	0.726	0.959	0.444	1.037	0.794
sync_1329	hypothetical protein sync_1329	8	10	0.986	0.847	1.027	0.738	0.821	0.094	0.945	0.477	0.880	0.141
sync_1330	hypothetical protein sync_1330	10	9	0.991	0.926	1.194	0.342	0.803	0.420	1.127	0.425	1.048	0.623
sync_1331	hypothetical protein sync_1331	1		1.066						0.993			
sync_1332	hypothetical protein sync_1332		3			0.913	0.626	1.072	0.626			0.958	0.757
sync_1333	methionyl-tRNA synthetase	10	9	0.995	0.917	0.962	0.707	0.930	0.504	1.042	0.421	0.998	0.992
sync_1336	exoribonuclease, VacB/RNB family protein	2		0.971	0.831					0.996	0.965		
sync_1337	30S ribosomal protein S18	3	7	0.896	0.471	1.081	0.769	0.969	0.701	0.950	0.702	1.045	0.589
sync_1338	50S ribosomal protein L33	1	1	0.971	0.815	1.025	0.847	0.893	0.457	0.968	0.797	0.915	0.537
sync_1339	phenylalanyl-tRNA synthetase, beta subunit	19	16	0.995	0.912	1.017	0.831	1.023	0.801	1.046	0.534	0.919	0.311
sync_1341	allophycocyanin alpha, B subunit	6	12	0.977	0.866	0.795	0.186	0.956	0.499	0.999	0.989	0.906	0.288
sync_1342	DnaJ domain-containing protein	1		0.863						1.082			
sync_1344	hypothetical protein sync_1344	3		0.878	0.449					1.092	0.568		
sync_1350	hypothetical protein sync_1350		2			1.101		0.967				1.232	
sync_1352	hypothetical protein sync_1352	5	3	1.150		0.648		0.986		0.963		0.728	

sync_1353	methionine synthase	8	4	1.000	1.000	1.052	0.767	1.202	0.162	0.960	0.635	0.938	0.666
sync_1354	branched-chain amino acid aminotransferase	11	16	0.977	0.770	0.899	0.478	1.039	0.537	0.992	0.916	1.000	0.994
sync_1356	hypothetical protein sync_1356	10	16	1.075	0.951	0.824	0.016	0.848	0.217	1.222	0.221	0.987	0.847
sync_1359	deoxyribodipyrimidine photolyase family protein	7	3	0.897	0.259	1.623	0.250	1.165	0.668	0.982	0.918	0.837	0.469
sync_1362	pantetheine-phosphate adenylyltransferase	2		1.082	0.575					1.028	0.828		
sync_1363	hypothetical protein sync_1363	17	8	1.038	0.940	1.057	0.561	0.853	0.128	1.056	0.825	0.902	0.377
sync_1364	D-alanyl-D-alanine carboxypeptidase	5	3	1.132	0.337	0.927	0.414	1.150	0.191	0.971	0.725	0.882	0.335
sync_1365	hypothetical protein sync_1365	5	8	1.014	0.882	0.802	0.274	0.976	0.787	0.875	0.241	1.001	0.989
sync_1366	hypothetical protein sync_1366	3	3	0.933		1.068		0.876		1.041		0.862	
sync_1368	diaminopimelate epimerase	19	12	1.042	0.657	1.032	0.683	0.991	0.891	0.894	0.235	1.025	0.855
sync_1374	hypothetical protein sync_1374	2		0.885						0.986			
sync_1375	leucyl-tRNA synthetase	11	8	1.013	0.826	0.898	0.267	0.800	0.142	0.995	0.958	1.020	0.889
sync_1376	glucose-6-phosphate isomerase	22	26	1.026	0.572	0.936	0.259	0.988	0.878	1.020	0.693	1.007	0.933
sync_1378	N-acetylmuramoyl-L-alanine amidase	5	1	0.868	0.102	0.884	0.507	1.123	0.643	1.095	0.510	1.048	0.734
sync_1379	PDZ domain-containing protein	8	3	0.978	0.970	0.963	0.770	0.965	0.713	1.076	0.597	1.050	0.611
sync_1381	phosphoribosylglycinamide formyltransferase		1			1.136		1.378				0.785	
sync_1382	N-acetyl-gamma-glutamyl-phosphate reductase	9	10	0.987	0.831	0.851	0.100	1.172	0.346	1.034	0.755	1.049	0.790
sync_1383	bifunctional 3,4-dihydroxy-2-butanone 4-phosphate synthase/GTP cyclohydrolase II protein	10	5	1.065	0.339	1.126	0.538	0.987	0.939	1.024	0.621	0.953	0.644
sync_1384	peptidylprolyl cis-trans isomerase, cyclophilin-type	33	17	0.945	0.611	0.829	0.211	0.817	0.036	0.983	0.876	1.023	0.752
sync_1385	methylthioadenosine phosphorylase	5	2	0.958	0.652	0.780		0.854		0.898	0.348	1.020	

sync_1386	N-acetylmuramic acid-6-phosphate etherase		5	5	0.909	0.387	0.993	0.960	0.955	0.638	0.914	0.247	0.923	0.506
sync_1387	hypothetical protein sync_1387		1	2	0.983		0.918	0.490	1.127	0.362	1.083		0.909	0.286
sync_1389	chaperone protein DnaK		11	14	0.947	0.515	1.056	0.459	0.950	0.606	1.080	0.111	0.912	0.214
sync_1390	phosphate ABC transporter, permease protein PstC		1	1	0.854		1.317		0.980		1.178		1.196	
sync_1392	phosphate ABC transporter, ATP- binding protein		9	7	1.020	0.752	0.946	0.583	1.061	0.563	0.950	0.407	0.977	0.813
sync_1394	ferredoxin, 2Fe-2S			1			1.104		1.180				1.239	
sync_1395	inositol-1-monophosphatase		7	7	1.154	0.611	0.951	0.702	0.585	0.466	0.949	0.671	0.831	0.312
sync_1396	ATP phosphoribosyltransferase regulatory subunit		9	9	0.984	0.797	0.950	0.386	1.084	0.437	1.002	0.970	1.003	0.963
sync_1398	heat shock protein 90		22	23	0.966	0.368	1.035	0.513	1.062	0.332	0.994	0.869	1.039	0.466
sync_1399	50S ribosomal protein L28		2	4	0.939	0.446	1.057	0.659	1.161	0.101	1.012	0.876	1.177	0.066
sync_1401	glucosylglycerol-phosphate synthase		9	5	0.968	0.590	0.875	0.430	1.059	0.647	0.930	0.256	1.028	0.853
sync_1405	ABC transporter for sugars, ATP binding protein	YES	4	1	0.917	0.550	0.864	0.631	0.956	0.727	0.965	0.786	0.857	0.364
sync_1410	1-deoxy-D-xylulose-5-phosphate synthase		3	4	1.033	0.913	0.856	0.362	0.925	0.650	0.840	0.334	0.979	0.886
sync_1411	threonine dehydratase		8	8	0.960	0.461	1.057	0.507	1.088	0.496	1.010	0.881	1.067	0.487
sync_1412	segregation and condensation protein B		5	5	1.007	0.941	0.889		1.150		1.104	0.205	0.704	
sync_1414	MazG family pyrophosphatase		3	1	1.080	0.579	1.111		1.096		0.970	0.809	1.033	
sync_1415	pyruvate kinase		20	24	1.080	0.086	0.942	0.186	1.052	0.525	0.995	0.910	0.921	0.056
sync_1416	macrolide ABC transporter, permease protein			3			5.273		1.491				1.213	
sync_1417	metalloprotease, ATP-dependent, FtsH family protein		15	21	0.991	0.875	1.049	0.641	0.871	0.007	0.946	0.261	0.900	0.221
sync_1418	ATP-dependent Clp protease proteolytic subunit		13	10	1.055	0.526	1.044	0.702	1.037	0.762	1.012	0.884	1.013	0.915
sync_1419	ThfI-like protein		7	12	1.036	0.711	1.035	0.830	0.891	0.577	0.921	0.422	1.151	0.632
sync_1420	hypothetical protein sync_1420		4	2	1.169	0.967	1.037	0.781	1.277	0.263	1.403	0.682	1.335	0.464

sync_1423	ATP-dependent Clp protease adaptor		1		1.277						0.910				
sync_1424	transporter, major facilitator family protein		1			1.616		1.003				1.191			
sync_1428	phosphoribosylaminoimidazole carboxylase ATPase subunit		3	4	0.908	0.636	0.987		1.357		1.089	0.701	1.040		
sync_1430	3-dehydroquinase synthase		5	9	1.009	0.923	0.872	0.152	1.017	0.821	0.935	0.514	1.196	0.080	
sync_1432	hypothetical protein sync_1432		1		1.324						1.288				
sync_1433	endolysin		9	11	1.057	0.465	0.957	0.623	0.949	0.579	1.009	0.901	1.016	0.894	
sync_1434	hypothetical protein sync_1434		2		0.825	0.515					0.994	0.979			
sync_1436	quinolinate synthetase		2		1.070	0.505					1.017	0.896			
sync_1440	hypothetical protein sync_1440	YES	1		0.889	0.446					0.805	0.491			
sync_1445	hypothetical protein sync_1445	ISL13	YES	7	2	0.889	0.448	0.807		1.334		1.021	0.866	1.360	
sync_1447	hypothetical protein sync_1447	ISL13	YES	1	2	0.979	0.872	0.709		0.445		0.920	0.573	0.681	
sync_1448	SPFH domain-containing protein	ISL13		3	5	1.226	0.319	0.973	0.741	1.054	0.374	0.998	0.981	1.056	0.547
sync_1449	SPFH domain-containing protein	ISL13		4	12	0.970	0.694	1.100	0.428	1.015	0.922	1.029	0.709	1.090	0.232
sync_1455	Short-chain dehydrogenase/reductase	ISL13		4				1.017	0.900	1.047	0.722			1.067	0.631
sync_1460	chalcone synthase	ISL13		2		1.093	0.627					0.818	0.131		
sync_1462	putative esterase/lipase/thioesterase	ISL13		1		1.089	0.983					1.613	0.330		
sync_1463	D-isomer specific 2-hydroxyacid dehydrogenase family protein	ISL13		2		0.969	0.734					1.061	0.546		
sync_1467	endoglucanase	ISL13		5				1.132	0.427	1.156	0.354			1.033	0.827
sync_1469	hypothetical protein sync_1469	ISL13		2	1	0.983	0.903	0.954		0.837		1.013	0.957	0.710	
sync_1470	hypothetical protein sync_1470	ISL13		1	2	1.580		0.708		0.926		0.915		0.946	
sync_1471	feruloyl-CoA synthetase	ISL13		2		1.077	0.474					0.989	0.934		
sync_1478	hypothetical protein sync_1478	ISL13		3		0.789						0.849			

sync_1483	ABC transporter ATP-binding protein	ISL13		4	1	0.922	0.426	1.223	0.404	1.141	0.700	1.003	0.972	1.093	0.712
sync_1489	multicopper oxidase	ISL13		9	7	1.054	0.954	1.126	0.715	0.962	0.902	1.098	0.714	0.793	0.195
sync_1490	4-methyl-5(B-hydroxyethyl)-thiazole monophosphate biosynthesis enzyme	ISL13		1	2	0.867		1.160		0.758		1.159		1.175	
sync_1491	indolepyruvate decarboxylase	ISL13		10	8	1.043	0.594	0.763	0.323	1.024	0.901	1.037	0.772	0.929	0.383
sync_1493	hypothetical protein sync_1493	ISL13		2		1.019	0.959					1.045	0.736		
sync_1501	porin	ISL13			22			1.352	0.621	2.161	0.723			1.159	0.860
sync_1509	hypothetical protein sync_1509	ISL13		2		0.899	0.570					0.864	0.392		
sync_1510	cation efflux system protein czcA-1	ISL13			3			0.890		0.846				0.905	
sync_1512	GGDEF/EAL domain-containing protein	ISL13	YES	21	18	0.967	0.483	1.148	0.118	1.054	0.523	1.104	0.058	1.050	0.690
sync_1513	putative lipoprotein	ISL13			3			0.832		0.938				0.963	
sync_1514	GGDEF domain-containing protein	ISL13	YES	2		1.033						1.011			
sync_1516	hydrolase CocE/NonD family protein subfamily	ISL13	YES	15	24	1.039	0.519	0.886	0.410	1.245	0.018	0.940	0.303	0.916	0.295
sync_1525	signal peptidase I			2		0.995						0.882			
sync_1527	naphthoate synthase			4		0.902	0.153					0.747	0.138		
sync_1528	protein erfK/srfK precursor			3	1	0.932	0.517	1.006		0.917		0.994	0.942	0.798	
sync_1529	glycogen synthase			3	7	0.949	0.510	1.078	0.470	1.104	0.245	0.952	0.593	1.022	0.830
sync_1531	UDP-N-acetylmuramoyl-tripeptide--D-alanyl-D-alanine ligase			2		0.951	0.784					1.002	0.985		
sync_1533	UDP-N-acetylglucosamine pyrophosphorylase, putative			10	7	1.042	0.605	1.081	0.252	0.945	0.384	1.066	0.584	1.067	0.331
sync_1534	hypothetical protein sync_1534			5	2	0.902	0.323	0.845	0.339	1.326	0.248	0.988	0.889	1.065	0.638
sync_1537	3-phosphoshikimate 1-carboxyvinyltransferase			7	3	1.049	0.465	0.977	0.923	0.997	0.984	0.890	0.108	1.053	0.596
sync_1539	ferritin			23	20	0.945	0.588	1.012	0.934	0.795	0.121	1.041	0.637	0.915	0.426

sync_1540	regulatory proteins, Crp family protein		2		0.657	0.147				0.728	0.557			
sync_1542	porin		24	28	0.860	0.230	0.742	0.199	0.893	0.301	1.010	0.922	0.977	0.859
sync_1544	putative hydroxylase		4		0.947	0.540					0.990	0.896		
sync_1545	ABC-type Fe ³⁺ transport system periplasmic component		12	12	0.941	0.244	0.791	0.015	1.000	1.000	1.045	0.397	0.943	0.400
sync_1546	3-octaprenyl-4-hydroxybenzoate carboxy-lyase		7	7	0.962	0.552	0.944	0.598	0.933	0.694	0.975	0.690	1.109	0.193
sync_1547	2-phosphosulfolactate phosphatase		5	3	0.943	0.532	0.900	0.736	1.358	0.204	0.996	0.954	1.006	0.964
sync_1548	nitrilase		11	9	1.046	0.665	0.935	0.605	1.027	0.796	0.885	0.147	1.064	0.844
sync_1549	cell wall hydrolase/autolysin		2	3	0.912	0.580	0.901	0.178	1.034	0.626	1.173	0.356	0.990	0.881
sync_1550	glutamate racemase		3		0.928	0.590					1.084	0.713		
sync_1551	solaneyl diphosphate synthase		6		0.845	0.108					0.961	0.817		
sync_1552	HAD family hydrolase		3	1	1.064	0.644	0.948	0.687	1.037	0.805	0.863	0.484	0.978	0.860
sync_1553	acetate--CoA ligase		31	32	1.007	0.864	1.017	0.765	1.024	0.690	1.010	0.798	1.000	0.996
sync_1554	hypothetical protein sync_1554		12	5	0.987	0.890	0.971	0.785	0.844	0.079	1.016	0.929	1.109	0.305
sync_1555	hypothetical protein sync_1555		2	1	1.123		1.111		1.006		1.033		0.952	
sync_1556	bacterioferritin comigratory protein		4	5	0.951	0.876	0.964	0.812	1.088	0.560	0.995	0.953	0.971	0.873
sync_1557	DNA polymerase III, epsilon subunit		1		0.911						0.837			
sync_1561	signal peptidase II			1			0.759		0.615				0.784	
sync_1562	penicillin-binding protein		4	1	0.998	0.990	0.772		0.885		1.171	0.445	1.041	
sync_1563	GTP-binding protein		2		1.030	0.767					0.903	0.368		
sync_1564	pyridoxal-dependent decarboxylase family protein		1		1.226						1.154			
sync_1566	serine:pyruvate/alanine:glyoxylate aminotransferase		13	8	0.928	0.449	0.959	0.701	1.124	0.178	0.993	0.914	0.994	0.933
sync_1567	allophycocyanin, beta subunit		11	20	1.000	0.997	0.975	0.870	1.098	0.342	1.040	0.487	1.130	0.296
sync_1569	glutamine synthetase, type I	ISL14	13 6	10 3	0.994	0.875	0.890	0.148	1.041	0.586	0.992	0.830	0.984	0.756

sync_1574	SAP domain-containing protein	ISL14	11	6	1.062	0.573	0.868	0.395	0.795	0.266	0.993	0.980	1.088	0.636
sync_1576	methyltransferase, UbiE/COQ5 family protein		2	3	0.952	0.563	1.028	0.865	1.283	0.474	0.983	0.842	1.023	0.816
sync_1577	copper binding proteins, plastocyanin		2		0.899						1.019			
sync_1579	hypothetical protein sync_1579		1	1	1.002	0.989	1.495		1.274		0.933	0.635	0.893	
sync_1581	GUN4-like family protein		2	2	1.042	0.667	0.940		0.785		0.957	0.780	1.040	
sync_1583	photosystem II reaction center protein Psb28		9	6	1.095		0.830	0.161	1.095	0.398	0.728		0.946	0.722
sync_1586	flavin reductase-like domain-containing protein		11	18	1.051	0.721	1.088	0.495	0.934	0.509	0.883	0.449	1.025	0.698
sync_1588	preprotein translocase subunit SecF		5	5	0.932	0.513	1.052	0.761	1.000	1.000	0.974	0.793	0.984	0.886
sync_1589	preprotein translocase subunit SecD		4	13	1.002	0.980	0.999	0.997	1.043	0.647	1.000	0.998	0.975	0.838
sync_1590	pyruvate dehydrogenase E1 beta subunit		12	13	0.998	0.980	0.999	0.997	1.019	0.871	0.932	0.362	1.100	0.284
sync_1593	4-diphosphocytidyl-2C-methyl-D-erythritol kinase		1	2	1.269		1.489	0.155	1.240	0.275	1.565		1.006	0.959
sync_1597	hypothetical protein sync_1597		3	2	1.053	0.610	1.106	0.900	0.764	0.776	0.947	0.598	1.300	0.236
sync_1598	pentapeptide repeat-containing protein		7	6	0.958	0.704	0.937	0.511	0.829	0.149	1.099	0.510	0.930	0.468
sync_1600	hypothetical protein sync_1600			2			1.024		0.784				1.207	
sync_1602	hypothetical protein sync_1602		4	2	1.134		0.798	0.359	1.286	0.689	0.842		1.264	0.289
sync_1604	GAF domain-containing protein		3	1	0.966	0.772	0.991		1.274		1.024	0.806	1.586	
sync_1608	FAD-dependent monooxygenase, putative			5			1.016	0.964	1.001	0.993			1.000	1.000
sync_1615	hypothetical protein sync_1615			1			0.650	0.603	1.012	0.968			1.091	0.580
sync_1622	hypothetical protein sync_1622	ISL15	15	9	0.998	0.979	1.103	0.765	0.845	0.282	0.972	0.701	1.119	0.291
sync_1628	30S ribosomal protein S15		2	3	1.038	0.812	1.255	0.326	1.122	0.337	1.168	0.430	1.101	0.550
sync_1631	glutamyl-tRNA(Gln) amidotransferase, A subunit		13	8	0.995	0.917	0.948	0.563	0.961	0.683	0.933	0.222	0.964	0.580

sync_1632	hypothetical protein sync_1632	4	4	1.124	0.729	0.771	0.243	0.924	0.580	0.973	0.914	0.995	0.969
sync_1633	RNA methyltransferase	2	3	0.838		1.130	0.449	1.007	0.986	1.075		0.980	0.928
sync_1635	STAS domain-containing protein	2	2	1.081	0.456	1.025	0.844	0.945	0.813	1.003	0.972	1.177	0.348
sync_1636	carbamoyl phosphate synthase small subunit	5	1	1.017	0.929	0.996	0.988	0.799	0.295	1.072	0.761	1.005	0.972
sync_1637	anthranilate phosphoribosyltransferase	5	5	1.024		1.079	0.775	0.943	0.670	1.000		0.822	0.304
sync_1638	heavy metal ABC transporter (HMT) family permease/ATP-binding protein	2	3	1.025	0.847	0.995	0.979	1.262	0.395	1.003	0.979	1.047	0.754
sync_1640	methionine-S-sulfoxide reductase	8	4	0.995	0.946	0.702	0.177	0.975	0.843	1.014	0.936	0.845	0.723
sync_1646	hypothetical protein sync_1646	6	5	1.045	0.763	1.028	0.954	0.980	0.854	1.035	0.640	0.983	0.868
sync_1651	peptidase, M16B family protein	3	2	1.086	0.559	1.039		1.171		0.824	0.304	0.878	
sync_1654	hypothetical protein sync_1654		2			0.640		0.958				1.001	
sync_1656	phycocyanobilin:ferredoxin oxidoreductase	3	1	0.741		1.290		1.045		0.428		1.410	
sync_1657	ABC transporter		1			0.942		1.198				0.930	
sync_1659	ABC transporter, ATP-binding component	2		0.972						1.159			
sync_1661	glycosyl transferase, group 2 family protein		2			1.096	0.529	1.315	0.227			1.044	0.875
sync_1663	hypothetical protein sync_1663	4	5	0.878		1.002		1.078		0.965		1.193	
sync_1670	ABC-type phosphate/phosphonate transport system periplasmic component	4	6	1.134	0.126	0.790	0.107	0.954	0.737	1.102	0.213	0.907	0.257
sync_1671	aspartate aminotransferase	13	10	0.953	0.357	0.994	0.949	1.090	0.537	1.067	0.375	0.969	0.750
sync_1674	4-hydroxy-3-methylbut-2-en-1-yl diphosphate synthase	5	5	1.035	0.664	1.450	0.728	1.300	0.614	1.234	0.275	1.153	0.424
sync_1675	C-terminal processing peptidase	20	17	1.094	0.865	0.906	0.243	1.027	0.599	1.087	0.544	1.042	0.412

sync_1679	transcription-repair coupling factor		1			1.451	0.510	0.477	0.483			0.736	0.758
sync_1682	hypothetical protein sync_1682		1			0.860		0.846				0.779	
sync_1683	ribulose-phosphate 3-epimerase	20	13	0.915	0.327	1.016	0.931	0.728	0.619	0.934	0.691	0.980	0.834
sync_1684	ribulose-phosphate 3-epimerase	20	6	0.818	0.487	0.865	0.222	0.820	0.371	0.931	0.799	0.912	0.699
sync_1685	fructose 1,6-bisphosphatase II	34	27	1.030	0.583	0.894	0.228	1.096	0.291	1.003	0.959	0.940	0.226
sync_1686	glutamyl-tRNA reductase	9	10	1.067	0.449	1.416	0.013	0.980	0.846	0.953	0.364	1.169	0.066
sync_1687	glucose-1-phosphate adenylyltransferase	18	30	0.986	0.771	0.891	0.233	1.043	0.497	0.928	0.292	1.074	0.263
sync_1688	6-phosphogluconate dehydrogenase	53	28	0.952	0.320	0.834	0.180	0.922	0.313	0.963	0.450	0.967	0.560
sync_1689	6-phosphogluconolactonase	13	13	1.150	0.075	1.049	0.559	1.066	0.546	1.070	0.486	0.941	0.495
sync_1690	hypothetical protein sync_1690	1	1	1.060	0.702	0.868		0.954		1.028	0.856	0.960	
sync_1692	dihydroxy-acid dehydratase	17	13	1.110	0.162	1.140	0.185	1.260	0.061	1.044	0.502	1.106	0.195
sync_1693	hypothetical protein sync_1693	5	6	0.935	0.485	1.240	0.214	0.841	0.095	0.972	0.760	0.961	0.689
sync_1695	pentapeptide repeat-containing protein		4			0.908	0.572	1.087	0.662			0.905	0.643
sync_1696	cobalamin biosynthesis protein CobW	5	8	1.065	0.465	1.071	0.804	0.922	0.569	0.854	0.152	0.908	0.514
sync_1700	phosphoribosylformylglycinamide synthase, PurS protein	2	6	0.924	0.445	1.009	0.951	0.931	0.620	0.936	0.512	0.905	0.377
sync_1701	phosphoribosylformylglycinamide synthase I	6	4	1.064	0.403	0.909	0.365	0.938	0.563	1.038	0.552	1.022	0.814
sync_1702	hypothetical protein sync_1702	2		1.202	0.407					1.147	0.425		
sync_1703	fructose-1,6-bisphosphate aldolase	21	29	0.999	0.981	1.025	0.701	1.243	0.056	1.005	0.924	1.122	0.108
sync_1704	fructose-bisphosphate aldolase class-I	13	11	1.018	0.691	0.877	0.074	1.019	0.797	0.959	0.355	0.954	0.456
sync_1705	oxidoreductase, NAD-binding	9	5	0.963	0.659	0.991	0.911	0.985	0.828	0.931	0.571	1.022	0.819
sync_1706	hypothetical protein sync_1706	1		1.010						0.849			
sync_1707	acetyl-CoA carboxylase subunit beta	2	6	0.936	0.644	0.735	0.297	0.987	0.887	0.926	0.597	0.938	0.520
sync_1711	phosphoribulokinase	11	19	0.997	0.969	0.942	0.663	1.064	0.620	0.974	0.707	0.908	0.393

sync_1712	3-isopropylmalate dehydrogenase	8	7	0.988	0.934	1.171	0.102	1.075	0.462	1.002	0.985	1.059	0.665
sync_1713	UDP-3-O-[3-hydroxymyristoyl] glucosamine N-acyltransferase	3	2	1.014	0.951	1.290		0.965		0.977	0.943	0.867	
sync_1718	hypothetical protein sync_1718	1		85.574						3.256			
sync_1719	hypothetical protein sync_1719	5	6	0.957	0.784	1.036	0.913	1.109	0.630	1.062	0.473	0.920	0.467
sync_1720	hypothetical protein sync_1720		4			0.816	0.342	1.012	0.941			0.904	0.819
sync_1723	1-(5-phosphoribosyl)-5-[(5-phosphoribosylamino)methylidene amino] imidazole-4-carboxamide isomerase	4	9	0.986	0.876	0.986	0.857	0.951	0.622	0.868	0.581	0.986	0.856
sync_1724	nucleotide sugar epimerase	7	9	1.034	0.731	0.836	0.077	1.040	0.455	1.000	0.998	1.035	0.511
sync_1726	CBS domain-containing protein	7	12	0.941	0.605	0.936	0.794	1.075	0.671	1.022	0.747	1.130	0.446
sync_1727	hypothetical protein sync_1727	15	12	1.006	0.929	1.008	0.910	0.956	0.456	0.985	0.823	1.000	0.997
sync_1728	ATP synthase	6	4	0.969	0.625	0.967	0.771	1.047	0.738	1.080	0.259	0.977	0.832
sync_1729	hypothetical protein sync_1729	3	2	1.083		1.220		0.895		0.936		1.139	
sync_1734	GIC family ligand gated channel		2			1.260		0.868				1.022	
sync_1735	CopG family protein	1		1.516						1.197			
sync_1736	glutaredoxin domain/DNA-binding domain-containing protein	2	4	1.032	0.806	0.989	0.934	1.081	0.393	0.982	0.886	0.914	0.374
sync_1737	hypothetical protein sync_1737		5			0.666		0.840				0.859	
sync_1741	hypothetical protein sync_1741	1		0.919						1.125			
sync_1742	cytochrome c, class IC:cytochrome c, class I		6			0.813	0.481	1.219	0.542			1.130	0.434
sync_1750	hypothetical protein sync_1750		2			1.351	0.568	0.988	0.967			1.120	0.456
sync_1752	putative permease	1		0.877						1.009			
sync_1755	hypothetical protein sync_1755	2	2	1.232	0.290	1.074		0.934		1.040	0.767	1.097	
sync_1771	copper/zinc superoxide dismutase	2		0.868						1.144			
sync_1779	hypothetical protein sync_1779	1	1	0.916		0.911		1.185		0.909		2.141	
sync_1780	transcriptional regulator	9	30	0.984	0.842	0.712	0.058	1.011	0.888	0.967	0.686	0.908	0.305

sync_1781	hypothetical protein sync_1781	5	4	0.788		1.383		0.491		1.070		1.106	
sync_1794	hypothetical protein sync_1794	4		1.017	0.890					1.142	0.268		
sync_1795	hypothetical protein sync_1795		1			1.125	0.477	1.100	0.534			1.042	0.761
sync_1798	transporter, stomatin/podocin/band 7/nephrin.2/SPFH (stomatin) family protein	9	15	0.968	0.615	0.941	0.663	0.814	0.009	1.005	0.943	0.977	0.695
sync_1803	carotenoid binding protein	14	3	1.064	0.889	1.093	0.556	0.808	0.291	1.083	0.497	1.022	0.872
sync_1808	hypothetical protein sync_1808	3	1	1.379	0.615	1.266		0.649		0.844	0.565	0.914	
sync_1810	hypothetical protein sync_1810	4		1.006						1.042			
sync_1813	acetyltransferase	1		1.689						1.172			
sync_1815	hypothetical protein sync_1815	1	2	1.056		1.139		1.173		0.988		0.812	
sync_1817	transcriptional regulator	4	2	0.925	0.387	1.006	0.959	1.097	0.519	1.012	0.891	1.000	0.999
sync_1819	DnaJ domain-containing protein		2			0.963	0.870	1.025	0.847			0.975	0.842
sync_1820	hypothetical protein sync_1820		1			1.054		0.918				1.048	
sync_1821	hypothetical protein sync_1821	3	1	1.190	0.330	1.047		0.993		1.028	0.830	1.139	
sync_1830	enzyme of the cupin superfamily protein		2			0.275		1.090				1.286	
sync_1832	hypothetical protein sync_1832	1	2	1.032		0.998	0.989	0.782	0.275	0.943		1.125	0.550
sync_1835	aldehyde dehydrogenase family protein	6	3	1.027	0.765	0.881	0.284	0.917	0.493	0.947	0.656	0.898	0.236
sync_1836	NAD dependent epimerase/dehydratase	5	3	0.985	0.869	1.105	0.427	0.990	0.948	1.045	0.494	0.977	0.835
sync_1839	hypothetical protein sync_1839	3	2	0.951		1.043	0.874	0.954	0.809	0.989		1.132	0.509
sync_1844	carotenoid isomerase, putative	1	3	1.041		0.893	0.642	1.072	0.609	0.957		1.049	0.811
sync_1845	hypothetical protein sync_1845	4	6	0.886	0.548	1.556	0.155	0.761	0.451	0.974	0.836	1.100	0.380
sync_1848	hypothetical protein sync_1848	1	5	1.136	0.893	0.585	0.282	0.869	0.298	1.041	0.851	0.894	0.310
sync_1849	hypothetical protein sync_1849		1			0.847		1.100				0.966	
sync_1850	endonuclease III	1		1.209						0.907			
sync_1852	hypothetical protein sync_1852	2		1.110						1.079			

sync_1853	hypothetical protein sync_1853	1	1	0.963		0.666		1.029		0.931		0.918	
sync_1857	Ser/Thr protein phosphatase family protein	6	2	1.170	0.218	0.595		1.014		1.015	0.936	1.082	
sync_1858	photosystem q(b) protein	6	13	1.361		1.704	0.394	1.043	0.770	1.167		1.288	0.514
sync_1861	cation efflux system protein	2	1	0.870		1.201		1.340		1.201		0.792	
sync_1862	hypothetical protein sync_1862	5	8	0.885		1.341	0.195	1.160	0.214	1.089		1.090	0.743
sync_1863	tryptophanyl-tRNA synthetase	9	4	0.947	0.664	1.034	0.732	1.166	0.213	1.014	0.882	0.995	0.978
sync_1866	threonyl-tRNA synthetase	9	7	1.005	0.943	1.397	0.178	1.300	0.254	1.040	0.524	1.068	0.539
sync_1868	glucokinase	7	6	1.000	1.000	0.881	0.233	1.194	0.078	1.099	0.666	0.817	0.070
sync_1869	homoserine kinase	9	5	1.046	0.520	0.853	0.120	1.094	0.578	0.962	0.576	1.001	0.989
sync_1870	NAD(P)H-quinone oxidoreductase subunit 4		1			1.255	0.394	0.748	0.215			1.193	0.740
sync_1871	phosphofructokinase	20	8	0.952	0.282	1.162	0.152	1.017	0.885	0.986	0.735	1.003	0.956
sync_1872	arginine repressor domain-containing protein	1		1.091	0.544					1.119	0.582		
sync_1877	dihydroneopterin aldolase	1		0.889						0.945			
sync_1878	gamma-glutamyl phosphate reductase	12	10	1.115	0.198	1.050	0.647	1.011	0.949	0.934	0.290	1.054	0.768
sync_1883	hypothetical protein sync_1883	4	5	1.045		0.900	0.481	1.081	0.584	1.070		1.199	0.318
sync_1884	S15 family X-Pro dipeptidyl-peptidase	1		0.906	0.862					1.152	0.820		
sync_1886	glycogen branching enzyme	15	9	1.088	0.346	0.992	0.910	1.080	0.196	0.977	0.691	1.086	0.152
sync_1887	uroporphyrinogen decarboxylase	16	19	0.974	0.602	1.010	0.923	0.953	0.529	0.954	0.370	1.015	0.766
sync_1888	NAD dependent epimerase/dehydratase	1	5	0.906		1.193	0.219	0.801	0.170	0.918		0.984	0.931
sync_1889	plastocyanin	16	17	1.027		0.808	0.119	0.975	0.911	0.976		1.088	0.461
sync_1897	ATP-dependent Clp protease, Hsp 100, ATP-binding subunit ClpB	27	26	1.141	0.562	1.090	0.284	1.109	0.204	1.057	0.414	1.207	0.037
sync_1898	hypothetical protein sync_1898	1		1.468						0.816			

sync_1899	bifunctional phosphoribosyl-AMP cyclohydrolase/phosphoribosyl- ATP pyrophosphatase protein	5		1.085	0.956				1.167	0.621			
sync_1900	hypothetical protein sync_1900	2	2	1.151		0.981	0.938	1.099	0.618	1.199		0.964	0.777
sync_1902	type II alternative RNA polymerase sigma factor	1	3	1.176	0.936	1.112	0.695	0.922	0.772	1.322	0.452	0.789	0.333
sync_1905	hypothetical protein sync_1905	7		1.089	0.710					1.020	0.877		
sync_1906	hypothetical protein sync_1906	2	1	0.985	0.965	0.488		0.849		1.065	0.799	1.674	
sync_1909	YciI-like protein	5		1.016	0.931					0.909	0.368		
sync_1910	tryptophan synthase subunit alpha	8	6	0.955	0.651	1.007	0.950	1.012	0.871	0.950	0.618	1.300	0.168
sync_1911	hypothetical protein sync_1911		1			1.096		0.932				0.776	
sync_1914	hypothetical protein sync_1914	9	4	0.989	0.825	0.855	0.214	1.199	0.450	0.922	0.284	0.984	0.926
sync_1915	dehydrogenase subunit-like protein	2		0.931	0.501					1.048	0.655		
sync_1917	hypothetical protein sync_1917	4	3	0.945	0.550	0.980	0.934	1.233	0.128	0.995	0.959	1.365	0.110
sync_1918	glucose 1-dehydrogenase	13	12	0.953	0.458	0.984	0.872	1.014	0.821	1.071	0.301	0.990	0.843
sync_1920	gluconolactonase precursor	4	1	1.024	0.852	1.454		0.985		0.830	0.356	0.942	
sync_1921	hypothetical protein sync_1921		1			1.020		1.007				0.905	
sync_1922	dihydroorotase	5		0.855	0.408					1.080	0.632		
sync_1923	sulfate transporter, sulfate permease (SulP) family protein		4			1.166	0.625	1.203	0.316			1.303	0.238
sync_1926	hypothetical protein sync_1926		2			1.308		1.157				1.372	
sync_1927	cytochrome c oxidase subunit II	3		1.003	0.975					1.000	0.999		
sync_1930	dehydrogenase subunit-like protein	10	6	0.992	0.906	0.762	0.088	1.070	0.848	0.977	0.873	1.129	0.616
sync_1931	glutathione reductase	43	29	0.984	0.734	0.853	0.034	1.004	0.940	0.975	0.654	1.051	0.352
sync_1932	hypothetical protein sync_1932	2	3	0.864	0.215	0.863	0.601	1.175	0.186	0.845	0.175	0.998	0.992
sync_1933	chromosomal replication initiation protein	3	5	1.180	0.479	0.967	0.660	0.881	0.295	1.137	0.624	1.020	0.901

sync_1934	peptidase, S1C (protease Do) family protein			8	13	0.940	0.302	1.011	0.948	0.888	0.247	0.972	0.675	0.925	0.301
sync_1939	ABC transporter, permease/ATP-binding protein			4	3	0.963	0.622	1.186	0.670	1.074	0.670	0.913	0.254	0.861	0.602
sync_1940	ATP phosphoribosyltransferase catalytic subunit			2		0.952	0.746					0.889	0.450		
sync_1942	ABC transporter ATP-binding protein			2	7	0.944	0.376	1.062	0.463	0.919	0.484	0.942	0.350	1.064	0.456
sync_1943	putative endoribonuclease L-PSP			5	3	0.962	0.761	0.832	0.202	0.986	0.894	1.073	0.608	0.921	0.701
sync_1944	hypothetical protein sync_1944			1		0.669						1.037			
sync_1945	cbbX protein	ISL16			1			0.752		0.989				1.103	
sync_1946	pterin-4 alpha-carbinolamine dehydratase-like protein	ISL16		2	5	1.066	0.370	1.077	0.629	1.104	0.265	1.015	0.831	1.099	0.182
sync_1950	flavodoxin FldA	ISL16	YES	3		0.994	0.970					0.949	0.897		
sync_1953	ferredoxin	ISL16	YES	2		1.141						1.326			
sync_1957	CO2 hydration protein		YES	5	4	0.957	0.623	0.880	0.283	0.844	0.350	0.974	0.736	1.021	0.919
sync_1959	NAD(P)H-quinone oxidoreductase subunit F			1	1	0.942	0.656	0.735	0.520	1.048	0.735	0.972	0.841	0.989	0.952
sync_1960	carbon dioxide concentrating mechanism protein CcmK			6	11	0.935	0.628	1.008		0.974		1.015	0.909	0.742	
sync_1963	carboxysome peptide A				1			0.939		1.239				0.869	
sync_1964	carboxysome shell protein CsoS3			2	7	0.905	0.804	1.045	0.659	1.055	0.459	1.485	0.199	0.858	0.082
sync_1965	hypothetical protein sync_1965			8	27	0.865	0.185	1.168	0.115	0.922	0.203	1.070	0.356	0.905	0.054
sync_1966	ribulose bisphosphate carboxylase, small subunit			7	10	0.958	0.755	1.367	0.424	0.951	0.704	0.961	0.773	0.935	0.623
sync_1967	ribulose bisophosphate carboxylase			32	55	0.864	0.001	1.015	0.870	1.025	0.527	1.004	0.928	0.923	0.179
sync_1968	carbon dioxide concentrating mechanism protein ccmK			16	40	0.877	0.253	1.070	0.413	1.561	0.243	1.162	0.306	1.130	0.594
sync_1971	hypothetical protein sync_1971			1	3	1.211		2.093		2.013		1.213		1.183	
sync_1972	putative lipoprotein			16	24	1.017	0.790	0.989	0.906	0.883	0.077	1.012	0.849	0.909	0.088

sync_1973	light-independent protochlorophyllide reductase subunit N	14	12	1.075	0.640	1.076	0.534	0.834	0.056	1.037	0.770	0.954	0.697
sync_1974	light-independent protochlorophyllide reductase subunit B	6	4	1.156	0.188	1.103	0.650	1.053	0.665	1.031	0.724	0.873	0.526
sync_1975	protochlorophyllide reductase iron- sulfur ATP-binding protein	4	6	1.281	0.025	0.958	0.819	1.142	0.331	1.170	0.067	1.018	0.840
sync_1976	protochlorophyllide oxidoreductase	1	6	1.023		0.952	0.830	0.975	0.795	0.980		1.034	0.750
sync_1979	hypothetical protein sync_1979	1		1.146						1.217			
sync_1983	peptidase, M50B family protein		2			1.110	0.518	0.941	0.553			0.844	0.462
sync_1984	N-(5'phosphoribosyl)anthranilate isomerase	1		0.875						1.074			
sync_1985	hypothetical protein sync_1985	12	7	1.104	0.111	0.910	0.253	0.969	0.594	1.064	0.259	1.044	0.513
sync_1986	GTP cyclohydrolase I	9	6	0.952	0.615	0.797	0.049	0.825	0.124	0.887	0.194	1.115	0.258
sync_1987	short chain dehydrogenase	1	2	1.038	0.780	1.350		0.745		0.843	0.420	0.931	
sync_1988	acetyl-CoA carboxylase carboxyltransferase subunit alpha	3	5	0.983	0.903	0.907	0.311	1.017	0.928	1.028	0.914	0.919	0.492
sync_1989	dehydrogenase	7	3	0.916	0.172	0.470	0.317	0.870	0.652	0.923	0.203	1.281	0.336
sync_1990	hypothetical protein sync_1990	5	3	1.117	0.518	1.855	0.121	1.342	0.242	1.110	0.533	1.292	0.463
sync_1993	ribosomal protein S1	23	12	1.121	0.026	0.999	0.993	1.024	0.870	1.034	0.549	1.082	0.425
sync_1994	hypothetical protein sync_1994	8		1.053	0.421					0.955	0.669		
sync_1995	hypothetical protein sync_1995	3		1.017	0.894					1.006	0.970		
sync_1996	uncharacterized FAD-dependent dehydrogenase	2		0.999	0.996					0.999	0.993		
sync_1998	thermonuclease-like protein	2		0.943	0.665					0.989	0.931		
sync_1999	acetolactate synthase 3 catalytic subunit	7	14	1.074	0.294	1.048	0.719	0.891	0.504	0.995	0.962	1.126	0.358
sync_2000	ferrochelatase	12	7	1.044	0.541	0.936	0.642	0.901	0.197	1.018	0.845	0.915	0.260

sync_2003	cob(I)alamin adenosyltransferase	3	9	0.969	0.736	0.933	0.613	1.053	0.821	1.067	0.507	1.138	0.219
sync_2004	uridylate kinase	5	8	0.979		0.868	0.431	0.902	0.718	1.210		0.751	0.237
sync_2005	ribosome recycling factor	11	9	0.947	0.942	0.900	0.317	0.973	0.775	1.007	0.967	1.049	0.850
sync_2008	transaldolase/EF-hand domain-containing protein	31	27	1.001	0.991	0.996	0.975	0.891	0.182	0.989	0.856	1.030	0.706
sync_2009	cell division protein FtsI/penicillin-binding protein 2	3	1	0.934	0.624	0.946		0.698		1.151	0.631	1.272	
sync_2011	CAAX amino terminal protease family protein	5	6	0.997	0.962	1.024	0.843	0.859	0.235	0.999	0.989	1.102	0.607
sync_2012	alpha-ribazole-5-P phosphatase	11	11	1.073	0.307	1.065	0.631	0.895	0.449	0.920	0.326	0.954	0.680
sync_2014	Signal peptidase I	5	6	0.915	0.393	1.010	0.950	0.755	0.169	1.012	0.896	1.148	0.261
sync_2015	hypothetical protein sync_2015	1	2	1.197		1.068	0.436	0.982	0.819	0.841		1.145	0.157
sync_2016	arsenate reductase	2	4	0.838		1.029	0.882	1.135	0.202	1.278		0.997	0.968
sync_2017	iron-sulfur cluster-binding protein	10	20	1.105	0.446	0.823	0.116	1.043	0.534	1.089	0.268	1.000	1.000
sync_2018	inorganic pyrophosphatase	5		1.023	0.855					1.239	0.276		
sync_2021	prolyl-tRNA synthetase	18	17	1.000	0.998	0.908	0.388	1.120	0.287	1.001	0.994	1.077	0.408
sync_2022	photosystem II Psb27 protein		1			0.784		1.209				0.845	
sync_2023	adenylosuccinate synthetase	27	22	1.010	0.796	1.011	0.820	1.026	0.762	0.964	0.355	0.936	0.353
sync_2024	carbohydrate kinase	16	12	0.983	0.794	1.053	0.711	0.955	0.775	1.022	0.876	1.085	0.289
sync_2026	single-stranded DNA-binding protein	11	4	1.048	0.840	1.128	0.282	1.048	0.806	0.775	0.391	1.223	0.134
sync_2027	hypothetical protein sync_2027	2	4	1.164	0.367	1.381	0.205	1.095	0.418	1.086	0.556	1.075	0.502
sync_2028	hypothetical protein sync_2028	2		1.024	0.853					1.126	0.445		
sync_2029	acetylglutamate kinase	4	1	1.035	0.690	0.817	0.298	1.021	0.873	0.881	0.313	0.993	0.969
sync_2030	hypothetical protein sync_2030	1		0.937						0.843			
sync_2032	RNA polymerase sigma factor RpoD	4	6	0.889	0.140	1.100	0.410	1.017	0.871	0.971	0.676	1.000	0.998
sync_2034	hypothetical protein sync_2034	2	1	0.982		1.457		0.803		0.921		0.558	

sync_2036	porphobilinogen deaminase		19	20	1.059	0.288	0.890	0.056	1.007	0.953	0.952	0.494	0.949	0.473
sync_2039	inorganic pyrophosphatase		13	12	1.033	0.655	0.996	0.978	0.960	0.543	0.956	0.515	1.011	0.927
sync_2040	carboxypeptidase Taq		7	6	1.087	0.930	1.000	0.999	0.932	0.541	1.100	0.898	0.935	0.398
sync_2044	putative pterin-4a-carbinolamine dehydratase		4	2	1.057	0.856	1.102		0.998		0.981	0.828	0.945	
sync_2045	putative cobalamin biosynthesis protein CobW		4	4	0.965	0.603	1.238	0.866	1.123	0.673	0.926	0.293	1.345	0.292
sync_2051	hypothetical protein sync_2051			1			1.119	0.470	1.109	0.496			1.209	0.310
sync_2053	hypothetical protein sync_2053		6	8	1.136	0.089	1.104	0.309	1.065	0.608	1.053	0.511	1.018	0.859
sync_2055	hypothetical protein sync_2055		5	2	1.178	0.423	0.829		0.917		0.923	0.576	1.032	
sync_2058	glutamate-1-semialdehyde aminotransferase		39	30	0.952	0.372	1.008	0.949	0.933	0.317	1.038	0.569	0.999	0.983
sync_2060	hypothetical protein sync_2060	ISL17	2	1	0.914	0.531	0.755		1.118		0.965	0.781	1.140	
sync_2061	nucleotide-binding protein	ISL17	15	13	1.014	0.816	1.038	0.601	1.052	0.434	1.053	0.642	0.998	0.989
sync_2062	hypothetical protein sync_2062	ISL17	4	4	0.931	0.510	1.126	0.391	1.039	0.697	0.914	0.486	1.031	0.783
sync_2063	hypothetical protein sync_2063	ISL17	11		0.867	0.515					0.414	0.433		
sync_2064	hypothetical protein sync_2064	ISL17	1	1	0.968		0.683		0.988		1.148		0.697	
sync_2077	hypothetical protein sync_2077	ISL17	3	2	0.950	0.735	0.976	0.796	1.154	0.328	0.973	0.863	1.051	0.609
sync_2080	aldehyde dehydrogenase family protein	ISL17	3	2	1.156	0.300	0.784		0.635		0.920	0.419	1.077	
sync_2084	hypothetical protein sync_2084		5	3	0.960	0.612	1.066	0.637	0.940	0.875	1.101	0.278	0.886	0.438
sync_2087	3'-phosphoadenosine-5'-phosphosulfate (PAPS) 3'-phosphatase		11	7	1.032	0.767	0.784	0.146	0.901	0.847	1.037	0.742	1.074	0.865
sync_2088	polynucleotide phosphorylase/polyadenylase		49	82	0.946	0.104	1.040	0.565	1.020	0.742	0.994	0.853	0.960	0.373
sync_2089	30S ribosomal protein S14		1	9	1.040		1.099	0.392	1.002	0.987	1.094		1.072	0.398
sync_2090	membrane-associated zinc metalloprotease, putative		3	2	1.079	0.446	0.862		1.163		1.008	0.928	0.598	
sync_2091	seryl-tRNA synthetase		22	16	0.988	0.805	0.859	0.066	0.989	0.869	0.985	0.847	1.057	0.618
sync_2093	ATPase, AAA family protein		4	2	1.022	0.825	0.977	0.910	0.892	0.653	0.915	0.407	0.989	0.932

sync_2095	putative inner membrane protein translocase component YidC	9	4	1.045	0.691	1.272	0.248	0.830	0.311	0.969	0.821	0.951	0.807
sync_2096	hypothetical protein sync_2096	2	2	1.109	0.540	0.953		0.682		1.040	0.770	0.998	
sync_2099	hypothetical protein sync_2099	11	11	1.055	0.596	0.901	0.528	1.328	0.002	1.239	0.128	1.202	0.016
sync_2101	signal peptide peptidase SppA (protease IV)	7	9	1.012	0.925	1.052	0.520	1.015	0.857	0.952	0.674	0.996	0.954
sync_2106	pspA/IM30 family protein	9	10	1.165	0.085	1.169	0.335	1.010	0.881	1.143	0.273	0.933	0.343
sync_2107	thioredoxin	5	6	0.999	0.994	1.116	0.811	1.021	0.909	1.068	0.651	1.044	0.858
sync_2111	DNA-binding response regulator	6	7	1.030	0.732	1.062	0.709	1.154	0.226	0.857	0.428	1.158	0.094
sync_2113	NAD(P)H-quinone oxidoreductase subunit 2	2		1.175	0.363					1.070	0.690		
sync_2114	DNA topoisomerase I	11	16	0.998	0.990	1.084	0.343	1.055	0.642	0.968	0.516	1.028	0.678
sync_2116	hypothetical protein sync_2116	1		1.097	0.535					0.855	0.658		
sync_2117	hypothetical protein sync_2117		1			0.765		1.307				0.756	
sync_2121	hypothetical protein sync_2121		2			1.236	0.327	0.971	0.921			1.121	0.556
sync_2124	transcriptional regulator	4	3	0.878	0.250	0.969	0.658	1.025	0.848	1.547	0.081	1.043	0.561
sync_2126	cytochrome c oxidase subunit I	3		1.020	0.876					0.856	0.367		
sync_2127	cytochrome c oxidase, subunit II	3		1.310						1.018			
sync_2130	drug exporter ABC transporter ATP-binding protein	11	5	0.969	0.814	1.207	0.441	1.036	0.901	1.002	0.987	0.935	0.593
sync_2131	ABC-type multidrug transport system permease component		1			0.924		1.015				0.597	
sync_2133	N-acetylmannosamine-6-phosphate 2-epimerase	1	1	1.133		1.419	0.277	0.848	0.344	1.052		1.251	0.282
sync_2135	chaperonin GroEL	56	74	1.107	0.086	1.103	0.042	1.011	0.795	1.001	0.985	1.109	0.011
sync_2137	3-oxoacyl-(acyl-carrier-protein) reductase	9	19	1.056	0.666	0.942	0.653	0.918	0.141	1.017	0.838	1.022	0.723
sync_2138	potassium transporter, voltage-gated ion channel (VIC) family protein	1		0.944						1.350			

sync_2139	hypothetical protein sync_2139		7	5	0.831	0.142	0.888	0.143	1.020	0.778	1.022	0.790	0.931	0.334
sync_2140	2-C-methyl-D-erythritol 4-phosphate cytidyltransferase		3	2	0.901	0.614	0.900	0.489	1.028	0.905	0.986	0.922	1.226	0.300
sync_2141	hypothetical protein sync_2141		1	1	1.129		0.907		0.859		1.127		1.108	
sync_2143	exopolyphosphatase		1		0.516						1.374			
sync_2144	hypothetical protein sync_2144		15	8	1.054	0.843	0.984	0.960	1.025	0.893	0.983	0.912	1.107	0.309
sync_2146	precorrin-4 C11-methyltransferase		5	6	0.893	0.296	1.416	0.051	0.995	0.953	1.037	0.779	1.122	0.379
sync_2148	apocytochrome f		6	11	1.136	0.341	0.805	0.123	0.837	0.595	1.026	0.797	0.816	0.141
sync_2149	cytochrome b6-f complex iron-sulfur subunit		6	5	0.896	0.330	1.205	0.818	1.052	0.950	1.028	0.812	0.949	0.948
sync_2150	hypothetical protein sync_2150		1	1	0.878		1.317		0.917		1.095		1.843	
sync_2153	guanylate kinase, putative		5		0.953	0.714					1.059	0.669		
sync_2155	photosystem I reaction center subunit III		4	8	1.000	0.999	0.782	0.256	0.991	0.947	1.155	0.570	0.954	0.829
sync_2157	high light inducible protein-related protein		3		0.972	0.840					1.006	0.988		
sync_2158	twitching mobility protein PilT		5	2	1.023	0.905	0.941	0.664	1.313	0.406	1.200	0.302	0.875	0.429
sync_2159	UDP-N-acetylglucosamine 2-epimerase		16	19	1.063	0.316	0.942	0.668	0.972	0.863	1.023	0.627	0.989	0.896
sync_2163	glutamyl-tRNA synthetase		6	8	0.946	0.649	0.903	0.530	0.956	0.642	0.964	0.876	1.111	0.309
sync_2166	hypothetical protein sync_2166		2	7	0.956		1.050	0.819	0.972	0.830	0.985		1.138	0.547
sync_2168	50S ribosomal protein L19		9	18	0.967	0.701	1.155	0.218	1.007	0.918	0.959	0.480	1.095	0.177
sync_2170	methionine aminopeptidase		13	7	0.962	0.659	0.756	0.372	0.936	0.591	0.896	0.258	1.064	0.402
sync_2172	phosphotransacetylase domain-containing protein		10	8	1.033	0.654	1.096	0.227	0.936	0.368	1.099	0.470	1.175	0.093
sync_2173	hypothetical protein sync_2173		3	7	0.911	0.691	0.977	0.820	1.035	0.846	0.843	0.473	1.113	0.357
sync_2187	hypothetical protein sync_2187	ISL18	1		0.799						0.937			
sync_2189	hypothetical protein sync_2189	ISL18	3		0.874	0.476					1.184	0.352		
sync_2191	DNA-binding protein HU		7	22	0.983	0.836	0.663	0.006	1.120	0.333	1.036	0.682	1.004	0.989
sync_2193	glycogen debranching protein		5	3	1.128	0.868	1.310	0.275	1.041	0.815	1.162	0.162	1.102	0.373

sync_2198	hypothetical protein sync_2198		7	8	0.951	0.464	1.066	0.816	0.946	0.757	0.930	0.297	1.043	0.579
sync_2199	hypothetical protein sync_2199		2	2	1.015	0.918	1.126		0.817		1.099	0.561	0.947	
sync_2200	orotidine 5'-phosphate decarboxylase		3	4	1.011	0.925	1.111		0.815		1.007	0.945	0.733	
sync_2202	hypothetical protein sync_2202			2			1.208		1.082				1.033	
sync_2203	tyrosyl-tRNA synthetase		7	6	1.050	0.669	0.938	0.888	0.923	0.761	0.965	0.651	0.870	0.411
sync_2204	hypothetical protein sync_2204		4	4	0.948	0.531	1.515		1.062		1.062	0.596	1.108	
sync_2208	leucyl aminopeptidase		8	5	1.038	0.575	1.034	0.724	0.988	0.927	1.076	0.605	1.036	0.674
sync_2210	peptide methionine sulfoxide reductase MsrA		4	3	1.013	0.877	0.862	0.290	0.840	0.300	0.919	0.350	1.064	0.572
sync_2211	lipid-A-disaccharide synthase		1	2	1.295		0.732	0.204	0.999	0.992	0.970		0.629	0.367
sync_2212	UDP-N-acetylglucosamine acyltransferase		6	3	1.058	0.442	1.254	0.262	0.989	0.975	1.103	0.215	0.953	0.717
sync_2213	(3R)-hydroxymyristoyl-ACP dehydratase			2			1.010	0.941	0.775	0.244			0.917	0.542
sync_2214	UDP-3-O-[3-hydroxymyristoyl] N-acetylglucosamine deacetylase			2			1.173		1.197				0.811	
sync_2215	membrane protein, OMP85 family protein		12	24	0.927	0.083	0.974	0.768	1.022	0.840	0.988	0.766	1.047	0.528
sync_2216	phosphoribosylaminoimidazole-succinocarboxamide synthase		4	2	1.060	0.581	0.998	0.998	1.062	0.498	0.961	0.619	0.963	0.775
sync_2217	hypothetical protein sync_2217		1	2	0.863		0.844	0.397	1.201	0.334	1.290		1.095	0.498
sync_2218	phosphoribosylamine--glycine ligase		8	9	1.013	0.842	1.021	0.876	0.888	0.656	0.967	0.604	0.923	0.630
sync_2219	sensory box histidine kinase		3	4	1.051	0.723	1.110	0.181	1.102	0.208	0.939	0.641	1.015	0.886
sync_2220	circadian clock protein KaiC		31	19	1.045	0.391	0.973	0.644	1.091	0.349	0.999	0.981	1.132	0.186
sync_2221	circadian clock protein KaiB		6	5	1.022	0.750	1.380	0.427	0.713	0.265	0.972	0.682	1.012	0.886
sync_2222	circadian clock protein KaiA		7	6	1.064	0.390	1.033	0.831	1.238	0.125	0.988	0.862	1.052	0.850
sync_2223	50S ribosomal protein L21		9	5	1.094		1.145	0.242	1.178	0.186	1.161		1.231	0.578
sync_2224	50S ribosomal protein L27		5	8	1.017	0.854	1.065	0.624	0.938	0.708	0.984	0.857	1.049	0.602
sync_2236	hypothetical protein sync_2236	ISL19		3			1.014		0.721				1.094	

sync_2237	cupin domain-containing protein	ISL19	2		1.057	0.696				1.383	0.190			
sync_2245	hydantoinase/oxoprolinase:hydantoinase B/oxoprolinase		1		1.137	0.439				0.973	0.916			
sync_2246	glucosamine-6-phosphate isomerase		1		0.944					0.826				
sync_2249	ribonuclease Z (RNase Z) (tRNA 3 endonuclease)		1		0.860					1.211				
sync_2250	cytochrome c-550		10	11	0.931	0.476	1.118	0.468	0.951	0.706	1.001	0.992	0.592	0.416
sync_2251	phycobilisome linker polypeptide		1	12	1.047		1.037	0.638	0.967	0.601	1.012		1.027	0.556
sync_2252	hypothetical protein sync_2252		7	4	1.056	0.507	0.695	0.060	0.888	0.482	1.021	0.867	1.262	0.444
sync_2254	ferredoxin		24	27	1.195	0.782	0.852	0.396	0.885	0.784	0.779	0.472	0.894	0.546
sync_2256	D-3-phosphoglycerate dehydrogenase		26	24	1.033	0.469	1.082	0.342	1.045	0.332	1.006	0.884	0.973	0.547
sync_2257	hypothetical protein sync_2257		2	2	1.040	0.760	0.982	0.886	0.835	0.319	0.939	0.643	0.942	0.654
sync_2258	S4 domain-containing protein		2		1.141						1.076			
sync_2265	hypothetical protein sync_2265		2	3	1.095	0.750	0.909	0.400	1.008	0.952	1.124	0.871	1.119	0.684
sync_2269	DNA-directed RNA polymerase subunit omega		2	1	0.853		1.350		1.116		1.139		0.992	
sync_2272	hypothetical protein sync_2272		1	1	0.934		1.141		1.220		1.296		1.062	
sync_2274	ferredoxin-thioredoxin reductase variable chain			2			0.786		1.152				0.777	
sync_2275	pyrimidine regulatory protein PyrR		6	7	1.004	0.975	1.223	0.301	1.221	0.435	1.033	0.688	1.214	0.278
sync_2276	phosphoglyceromutase		20	10	1.006	0.893	1.063	0.755	1.096	0.410	0.954	0.403	1.127	0.441
sync_2282	chaperonin GroEL		12	97	1.091	0.014	1.172	0.085	0.990	0.894	0.996	0.908	1.024	0.700
sync_2283	co-chaperonin GroES		24	25	0.968	0.548	0.970	0.584	1.181	0.026	0.976	0.644	1.073	0.191
sync_2284	F0F1 ATP synthase subunit beta		30	57	1.018	0.866	1.027	0.790	0.938	0.301	1.000	0.999	0.991	0.858
sync_2285	F0F1 ATP synthase subunit epsilon		1	2	1.043	0.744	0.900	0.519	1.103	0.578	0.995	0.968	1.008	0.955

sync_2286	hypothetical protein sync_2286	12	10	0.992	0.901	1.169	0.456	1.126	0.114	0.959	0.514	0.996	0.948
sync_2287	putative fructose-6-phosphate aldolase	2		1.043	0.754					0.851	0.578		
sync_2288	HAD superfamily phosphatase	7	4	1.124	0.393	0.989	0.933	1.078	0.804	0.857	0.354	0.973	0.767
sync_2290	peptidase, M24B family protein	7	3	0.978	0.717	0.884	0.560	0.946	0.591	0.963	0.688	1.042	0.674
sync_2291	SBC domain-containing protein	1	2	0.731		0.937		0.792		1.134		0.975	
sync_2294	NAD+ synthetase		2			0.954		0.975				0.868	
sync_2295	alanine dehydrogenase	7	5	1.100	0.355	0.807	0.305	0.884	0.408	0.987	0.880	0.968	0.681
sync_2308	hypothetical protein sync_2308		1			0.848	0.474	0.956	0.683			1.023	0.867
sync_2310	ferredoxin, 2Fe-2S	5		1.002	0.993					1.170	0.805		
sync_2312	F0F1 ATP synthase subunit gamma	8	12	1.010	0.921	1.119	0.130	1.045	0.779	1.088	0.377	0.936	0.428
sync_2313	F0F1 ATP synthase subunit alpha	27	37	0.952	0.256	1.011	0.943	0.953	0.551	1.044	0.316	0.986	0.827
sync_2314	F0F1 ATP synthase subunit delta	4	5	0.944	0.478	1.154	0.148	0.941	0.665	0.984	0.836	0.931	0.584
sync_2315	F0F1 ATP synthase subunit B	5	8	1.084	0.285	0.926	0.502	0.825	0.031	0.990	0.885	0.974	0.814
sync_2316	F0F1 ATP synthase subunit B'	2	6	1.097	0.546	0.813	0.284	0.947	0.572	1.099	0.538	0.917	0.200
sync_2320	methyltransferase	2	4	0.935		0.597		1.171		0.798		1.562	
sync_2321	anchor polypeptide LCM	53	10	1.055	0.715	1.024	0.610	0.936	0.144	1.032	0.487	0.965	0.267
sync_2323	allophycocyanin, alpha subunit	36	57	0.957	0.450	1.005	0.927	0.961	0.619	1.048	0.428	1.084	0.193
sync_2324	allophycocyanin, beta subunit	45	71	0.967	0.588	1.083	0.671	1.028	0.875	1.018	0.754	1.023	0.860
sync_2325	phycobilisome linker polypeptide		5			0.856	0.578	0.877	0.423			0.950	0.667
sync_2328	ResB-like protein required for cytochrome c biosynthesis		2			1.333	0.281	1.269	0.324			1.042	0.749
sync_2331	nitrogen regulatory protein P-II	14	19	0.971	0.693	0.968	0.929	0.950	0.710	1.027	0.718	1.059	0.517
sync_2334	adenylosuccinate lyase	11	20	0.963	0.537	1.091	0.512	1.095	0.151	0.951	0.412	1.033	0.526
sync_2336	fumarate hydratase		7			1.105	0.397	1.002	0.984			0.939	0.723
sync_2337	superfamily II RNA helicase	4	2	0.866	0.235	0.790	0.595	0.918	0.810	1.097	0.273	0.833	0.317

sync_2338	8-amino-7-oxononanoate synthase	1		1.088	0.551				0.832	0.332			
sync_2341	dethiobiotin synthetase	1	1	0.982	0.887	0.764		0.640		1.041	0.762	0.621	
sync_2343	adenosylmethionine-8-amino-7-oxononanoate transaminase	2		0.938	0.544					0.938	0.452		
sync_2344	hypothetical protein sync_2344		1			1.434		1.220				0.941	
sync_2349	hypothetical protein sync_2349	3	3	0.930	0.816	0.920	0.792	0.895	0.648	0.928	0.755	1.006	0.979
sync_2351	HEAT repeat-containing protein	5	6	0.994	0.945	1.137	0.166	1.070	0.744	1.029	0.829	1.027	0.886
sync_2356	DNA-directed RNA polymerase subunit beta'	59	77	0.883	0.014	1.578	0.000	1.070	0.288	1.185	0.000	1.026	0.580
sync_2357	DNA-directed RNA polymerase subunit gamma	23	31	0.871	0.016	1.838	0.000	1.017	0.876	1.193	0.012	1.031	0.531
sync_2358	DNA-directed RNA polymerase subunit beta	41	48	0.913	0.610	1.484	0.000	1.053	0.254	1.260	0.000	0.956	0.163
sync_2360	hydrolase, TatD family protein	1		0.825						0.800			
sync_2361	30S ribosomal protein S20	5	7	0.887	0.731	0.986	0.899	1.100	0.285	0.912	0.557	0.951	0.571
sync_2362	histidinol dehydrogenase	16	14	1.128	0.031	0.839	0.333	0.921	0.419	0.943	0.335	0.958	0.494
sync_2363	ribose 5-phosphate isomerase A	13	16	1.055	0.410	0.945	0.662	1.036	0.573	1.005	0.938	1.028	0.801
sync_2364	Serine proteases, trypsin family protein	6	4	1.012	0.885	0.890	0.481	0.749	0.316	1.053	0.524	0.829	0.328
sync_2366	ABC transporter solute-binding protein	13	30	1.035	0.623	0.831	0.117	1.177	0.179	0.997	0.966	1.016	0.874
sync_2369	putative lipoprotein	13	10	1.145	0.109	0.994	0.944	1.036	0.617	1.032	0.655	0.965	0.583
sync_2370	hypothetical protein sync_2370	1		0.844						0.727			
sync_2371	transcription elongation factor NusA	3	20	0.839	0.018	1.195	0.157	0.896	0.313	0.962	0.507	0.940	0.597
sync_2373	translation initiation factor IF-2	26	33	0.955	0.235	0.891	0.155	1.056	0.193	1.050	0.212	0.952	0.328
sync_2374	hypothetical protein sync_2374	1		1.230						1.101			
sync_2382	2,5-dichloro-2,5-cyclohexadiene-1,4-diol dehydrogenase(2,5-ddol dehydrogenase)	2	1	0.940	0.718	0.928		0.983		1.024	0.947	1.091	

sync_2386	putative lipoprotein		1			1.256		1.168				1.024		
sync_2387	hypothetical protein sync_2387		3	1	1.126		1.441	1.777		1.184		1.659		
sync_2388	hypothetical protein sync_2388		17		1.197	0.333				0.987	0.955			
sync_2389	aspartoacylase		1		1.238					1.350				
sync_2390	glutathione S-transferase		1		0.912	0.609				1.032	0.737			
sync_2391	hypothetical protein sync_2391		1	1	1.081		1.334	0.738		0.865		0.694		
sync_2393	CP12 domain-containing protein		1	1	1.352		0.878	0.439	1.494	0.385	0.961	0.980	0.907	
sync_2394	GTPase ObgE			2			1.236		0.880			0.603		
sync_2395	iron ABC transporter ATP-binding protein		5	6	0.914	0.185	1.090	0.505	1.022	0.763	0.952	0.461	1.018	0.807
sync_2396	MutS2 family protein		2		0.971	0.756					1.057	0.494		
sync_2398	delta-aminolevulinic acid dehydratase		20	17	1.091	0.079	0.927	0.565	1.182	0.312	0.943	0.227	1.127	0.110
sync_2399	DnaJ3 protein		4	1	0.918	0.315	1.208	0.311	1.143	0.409	1.223	0.065	1.300	0.232
sync_2400	hypothetical protein sync_2400		6	7	1.054	0.466	0.987	0.946	0.936	0.436	1.089	0.268	0.902	0.401
sync_2411	hypothetical protein sync_2411	ISL21		1			0.875		0.780				0.930	
sync_2424	cytochrome P450	ISL21		4			0.893	0.458	0.803	0.417			1.046	0.726
sync_2430	hypothetical protein sync_2430	ISL21	9	4	0.885	0.206	0.819	0.667	1.335	0.341	0.897	0.240	1.072	0.832
sync_2431	hypothetical protein sync_2431	ISL21	5	3	1.050	0.628	0.972	0.849	0.921	0.343	1.116	0.197	0.975	0.864
sync_2434	hypothetical protein sync_2434	ISL21	3	3	0.954	0.642	0.783	0.109	0.981	0.910	0.948	0.846	1.137	0.281
sync_2436	hypothetical protein sync_2436	ISL21	2	6	0.899	0.237	0.773	0.032	1.039	0.802	1.039	0.648	1.070	0.405
sync_2444	hypothetical protein sync_2444	ISL21		3			1.517	0.151	1.039	0.903			1.073	0.612
sync_2446	hypothetical protein sync_2446	ISL21		2			0.888		1.415				1.434	
sync_2450	RNA methylase family protein		7		0.959	0.650					1.101	0.191		
sync_2451	hypothetical protein sync_2451		2	1	1.124	0.644	0.750		0.639		0.933	0.547	0.839	
sync_2452	hypothetical protein sync_2452		4	5	1.055	0.589	0.945	0.879	1.009	0.959	0.966	0.797	0.783	0.101
sync_2454	chromosome segregation protein SMC		6		0.976	0.666					0.973	0.629		

sync_2455	PRC-barrel domain-containing protein	11	7	1.082	0.575	0.884	0.363	1.142	0.353	0.993	0.917	1.114	0.166
sync_2457	hypothetical protein sync_2457		2			0.357		0.906				1.547	
sync_2459	acetyl-CoA carboxylase biotin carboxylase subunit	10	4	0.987	0.863	1.053	0.763	1.219	0.712	1.023	0.702	1.037	0.895
sync_2462	hypothetical protein sync_2462	4	4	0.963	0.752	0.955	0.685	0.872	0.412	1.027	0.808	0.902	0.639
sync_2465	high light inducible protein	2	1	0.943	0.659	0.959		0.663		0.934	0.614	0.991	
sync_2466	peroxisomal fatty acyl CoA ABC transporter ATP-binding protein	10	6	0.970	0.939	0.986	0.960	0.793	0.152	0.966	0.753	1.016	0.850
sync_2467	histidine triad family protein	1	4	1.221	0.462	0.921	0.581	1.052	0.723	0.798	0.699	0.962	0.890
sync_2470	30S ribosomal protein S21	2	6	1.010		0.907	0.843	1.320	0.364	0.937		1.111	0.358
sync_2471	hypothetical protein sync_2471	12	11	1.118	0.121	1.014	0.927	1.054	0.478	1.047	0.480	1.044	0.740
sync_2473	peptide deformylase	1	1	1.098		0.733		1.050		1.175		1.026	
sync_2474	peptidase, S9C (acylaminoacyl-peptidase) family protein	5		0.956	0.519					0.905	0.191		
sync_2475	L-fucose phosphate aldolase	1		1.107						1.322			
sync_2476	methylthioribose-1-phosphate isomerase	8	5	1.014	0.840	1.106	0.522	0.896	0.203	1.001	0.983	0.834	0.350
sync_2480	cysteine desulfurase, SufS family protein	9	4	0.912	0.096	0.978	0.775	0.892	0.205	0.978	0.663	1.118	0.214
sync_2481	FeS assembly protein SufD	10	5	0.994	0.911	0.874	0.663	1.110	0.608	0.982	0.834	0.961	0.842
sync_2482	FeS assembly ATPase SufC	11	11	1.080	0.247	0.870	0.122	0.916	0.534	1.030	0.802	0.853	0.164
sync_2483	cysteine desulfurase activator complex subunit SufB	14	5	1.013	0.815	0.703	0.175	0.912	0.446	0.949	0.282	0.950	0.618
sync_2484	ferredoxin thioredoxin reductase, catalytic beta chain	8	4	0.917	0.212	1.064	0.526	0.888	0.284	0.980	0.790	1.005	0.956
sync_2486	hypothetical protein sync_2486	1		0.993						0.881			
sync_2487	hypothetical protein sync_2487	8	4	1.004	0.956	0.877	0.411	1.047	0.883	0.999	0.994	1.117	0.792
sync_2488	phycobilisome rod-core linker polypeptide cpcG1	18	31	1.038	0.452	0.854	0.007	1.015	0.861	1.048	0.430	0.996	0.943
sync_2489	hypothetical protein sync_2489	18	8	0.987	0.903	0.991	0.960	1.063	0.490	1.047	0.451	1.058	0.665

sync_2496	hypothetical protein sync_2496	5	4	1.029	0.716	0.915	0.694	1.147	0.411	1.091	0.383	0.947	0.697
sync_2500	phosphoglucomutase	25	28	1.008	0.846	1.135	0.166	1.096	0.406	0.968	0.456	1.084	0.063
sync_2502	RND multidrug efflux transporter	16	9	0.917	0.060	0.982	0.797	0.907	0.712	1.010	0.822	0.998	0.986
sync_2503	RND family efflux transporter MFP subunit	8	12	0.904	0.218	0.759	0.038	1.047	0.436	1.001	0.989	0.817	0.011
sync_2505	protein phosphatase 2C	90	13	0.859	0.021	0.894	0.066	1.034	0.735	1.021	0.713	1.001	0.989
sync_2508	bacterioferritin comigratory protein	9	7	1.285	0.153	0.964	0.891	0.878	0.857	0.928	0.355	0.845	0.809
sync_2509	transcriptional activator, putative, Baf family protein		1			1.284		1.056				1.022	
sync_2510	phosphoadenosine phosphosulfate reductase	8	1	1.124	0.872	0.833		0.832		1.088	0.620	1.003	
sync_2511	NADH dehydrogenase, FAD-containing subunit	5	1	0.950	0.615	0.836		0.782		0.968	0.812	0.906	
sync_2512	GTP-binding protein HflX-like protein	2	1	1.149	0.667	0.883	0.822	1.098	0.519	1.186	0.179	0.955	0.725
sync_2515	K+ transporter, Trk family protein	3	1	0.886	0.307	0.808	0.286	0.901	0.551	1.097	0.372	0.925	0.581
sync_2520	hypothetical protein sync_2520	1	3	1.954		0.947	0.826	0.871	0.699	0.446		0.903	0.605
sync_2523	peptidase, S1C (protease Do) family protein	7	5	1.121	0.167	0.830	0.150	1.096	0.453	1.118	0.240	1.066	0.520
sync_2524	hypothetical protein sync_2524		1			1.354		1.112				1.069	
sync_2525	hypothetical protein sync_2525	3	6	1.027	0.822	1.257	0.314	0.979	0.816	0.983	0.826	1.034	0.721
sync_2530	exodeoxyribonuclease VII, large subunit	2		0.864						0.999			
sync_2540	inositol monophosphate family protein		2			1.144		0.733				0.645	
sync_2541	RND family outer membrane efflux protein	12	24	0.965	0.559	1.130	0.099	0.932	0.375	1.089	0.367	0.987	0.791
sync_2542	Fe-S oxidoreductase		1			1.299	0.233	0.894	0.493			0.957	0.736
sync_2543	undecaprenyl pyrophosphate phosphatase		1			0.306		2.375				1.660	

sync_2545	photosystem II complex extrinsic protein precursor U	15	29	1.077	0.408	0.727	0.097	1.056	0.561	0.953	0.576	0.974	0.639
sync_2546	L-aspartate oxidase	2		0.946	0.785					0.975	0.838		
sync_2547	VKORC1/thioredoxin domain-containing protein	4	6	0.946	0.674	0.783	0.243	1.031	0.953	1.033	0.798	0.861	0.406
sync_2551	radical SAM domain/B12 binding domain-containing protein	5	11	1.039	0.505	1.339	0.148	1.190	0.083	0.948	0.396	1.168	0.071
sync_2553	hypothetical protein sync_2553	1		0.994						1.350			
sync_2556	6-pyruvoyl-tetrahydropterin synthase-like protein	5	1	1.097	0.946	1.220		0.962		1.230	0.370	1.090	
sync_2557	shikimate kinase	2	3	1.030	0.756	1.139	0.454	0.843	0.372	0.952	0.610	0.936	0.836
sync_2560	glutathione S-transferase zeta class	7	10	0.989	0.853	1.039	0.683	0.806	0.058	1.013	0.830	0.827	0.077
sync_2562	ribosome-binding factor A	4		1.042	0.803					0.877	0.864		
sync_2563	beta-N-acetylglucosaminidase	7		1.108	0.271					0.953	0.843		
sync_2564	TPR repeat-containing glycosyl transferase	9	8	1.043	0.471	0.993	0.933	0.915	0.328	1.000	0.997	0.960	0.469
sync_2565	uroporphyrinogen-III synthase	5	4	0.947	0.575	0.852	0.526	0.928	0.831	1.030	0.753	0.856	0.606
sync_2567	oligoketide cyclase/lipid transport protein	5	6	1.372	0.813	1.183	0.177	0.962	0.678	1.332	0.386	1.016	0.879
sync_2568	zeta-carotene desaturase	8	3	0.945	0.498	1.558	0.207	0.949	0.589	0.976	0.673	1.001	0.993
sync_2569	iron-sulfur cluster assembly accessory protein	4		1.138	0.453					0.982	0.896		
sync_2570	hypothetical protein sync_2570	8	13	1.049	0.574	1.020	0.831	0.750	0.486	1.063	0.486	0.835	0.447
sync_2571	hypothetical protein sync_2571	1		0.791	0.373					1.263	0.257		
sync_2573	hypothetical protein sync_2573	4	5	0.980	0.789	0.982	0.919	1.101	0.620	0.986	0.858	0.913	0.625
sync_2575	hypothetical protein sync_2575	4	2	0.992	0.930	1.290	0.373	1.255	0.293	0.884	0.270	0.928	0.704
sync_2577	cysteine synthase A	6	2	1.131	0.092	0.813		1.086		1.021	0.784	1.330	
sync_2579	porin	59	10	0.828	0.294	0.983	0.909	1.028	0.774	1.008	0.943	0.954	0.718
sync_2581	porin	94	6	0.923	0.471	0.783	0.064	1.107	0.436	1.034	0.707	0.919	0.627
sync_2586	photosystem II D2 protein (photosystem q(a) protein)	10	1	1.112	0.499	1.267	0.338	0.970	0.837	0.981	0.868	0.896	0.563
sync_2587	hypothetical protein sync_2587	6	8	0.832	0.154	0.927	0.621	0.996	0.989	1.021	0.838	1.039	0.827

sync_2591	DNA-binding response regulator RpaA	12	7	1.045	0.740	1.011	0.939	1.109	0.449	1.301	0.396	1.235	0.063
sync_2593	thymidylate kinase	3	1	1.106	0.577	0.647		0.997		0.940	0.567	1.068	
sync_2594	copper-translocating P-type ATPase	8	6	1.026	0.807	1.096	0.465	0.923	0.542	1.090	0.269	0.932	0.516
sync_2595	photosystem I assembly protein Ycf3	3	1	1.005	0.952	1.037	0.905	0.984	0.977	1.003	0.970	0.689	0.055
sync_2597	DNA-binding response regulator	22	21	0.963	0.601	0.929	0.523	1.156	0.426	0.957	0.435	1.045	0.619
sync_2598	putative glycerol-3-phosphate acyltransferase PlsX	1	3	0.837	0.343	1.021	0.927	0.958	0.742	1.123	0.782	1.103	0.505
sync_2599	3-oxoacyl-(acyl carrier protein) synthase III	4	3	0.970	0.700	1.001	0.996	1.036	0.836	0.942	0.486	1.052	0.704
sync_2600	malonyl CoA-acyl carrier protein transacylase	10	9	1.102	0.574	1.060	0.719	0.788	0.215	1.011	0.906	1.055	0.848
sync_2601	1-acyl-sn-glycerol-3-phosphate acyltransferase		2			0.842	0.362	1.054	0.699			0.914	0.532
sync_2603	glycoprotease family protein		2			0.658	0.593	1.279	0.498			1.216	0.457
sync_2606	putative RNA-binding protein	10	9	0.952	0.527	1.040	0.789	0.925	0.487	1.021	0.790	0.972	0.723
sync_2608	phytoene desaturase	7	4	0.999	0.992	1.017	0.915	0.939	0.604	0.968	0.595	0.985	0.912
sync_2609	hypothetical protein sync_2609	2	4	0.949	0.803	1.202	0.315	0.840	0.651	1.075	0.701	0.912	0.597
sync_2610	hypothetical protein sync_2610		1			0.595		0.878				0.609	
sync_2611	transcriptional regulator, LysR family protein	3		1.081						0.951			
sync_2613	NAD(P)H-quinone oxidoreductase subunit F	4	2	1.015	0.880	1.357	0.300	0.888	0.293	1.042	0.707	1.168	0.230
sync_2615	hypothetical protein sync_2615	3	3	1.084	0.459	0.833	0.469	0.893	0.558	0.932	0.496	0.875	0.267
sync_2617	nucleotidyl transferase family protein	18	13	1.016	0.828	1.068	0.451	1.087	0.344	1.016	0.767	1.077	0.250
sync_2618	methylenetetrahydrofolate reductase family protein	8	5	0.960	0.710	1.059	0.671	0.956	0.731	0.834	0.085	0.869	0.430
sync_2619	transcriptional regulator, LuxR family protein	2		1.018	0.972					1.225	0.519		

sync_2621	inorganic polyphosphate/ATP-NAD kinase	3	1	1.037	0.909	0.964		1.519		1.113	0.514	1.046	
sync_2623	NADH dehydrogenase subunit J	2	3	1.235		0.883		1.004		1.077		1.024	
sync_2624	NADH dehydrogenase subunit I	9	5	1.045	0.525	0.916	0.735	1.074	0.483	1.050	0.399	0.821	0.214
sync_2625	NADH dehydrogenase subunit H		2			1.290	0.430	1.065	0.803			0.916	0.763
sync_2626	methylcitrate synthase	4		1.105	0.821					0.839	0.506		
sync_2628	hypothetical protein sync_2628	6		0.993	0.958					1.011	0.891		
sync_2633	tryptophan synthase subunit beta	8	5	1.103	0.293	0.996	0.979	1.077	0.338	0.951	0.439	0.900	0.404
sync_2636	adenylylsulfate kinase	7	5	0.973	0.831	1.215	0.252	1.082	0.486	0.986	0.925	1.013	0.922
sync_2638	phosphoribosylaminoimidazole carboxylase, catalytic subunit	2		0.850						0.977			
sync_2639	N-acetylglucosamine-6-phosphate deacetylase	3		1.123						1.048			
sync_2640	Mg-protoporphyrin IX methyl transferase	3	1	1.143	0.589	0.872	0.235	1.160	0.208	0.999	0.992	0.907	0.354
sync_2642	DNA-binding response regulator	15	25	1.011	0.941	1.164	0.347	0.961	0.770	1.004	0.962	1.004	0.966
sync_2643	hypothetical protein sync_2643	5	4	1.026	0.714	0.990	0.912	1.030	0.754	1.047	0.516	0.933	0.635
sync_2644	NifS-like aminotransferase class-V	2	2	0.875	0.254	0.878		1.266		1.018	0.936	1.031	
sync_2645	hypothetical protein sync_2645	4	8	0.854	0.358	0.853	0.695	0.937	0.865	1.048	0.719	0.781	0.453
sync_2647	S-adenosyl-methyltransferase MraW	1		0.896						1.108			
sync_2648	NAD(P)H-quinone oxidoreductase subunit H	7	16	0.962	0.581	0.960	0.734	0.965	0.702	1.073	0.379	0.986	0.799
sync_2657	glutathione synthetase	7	5	1.110	0.189	0.914	0.336	0.910	0.451	1.090	0.406	1.011	0.933
sync_2658	glutaredoxin 3	4	3	0.959	0.701	0.774	0.468	0.917	0.609	0.813	0.070	0.865	0.606
sync_2659	peptide chain release factor 2	10	7	1.018	0.774	0.945	0.352	0.990	0.868	0.897	0.056	1.009	0.874
sync_2662	diacylglycerol kinase	1		1.220						0.730			

sync_2663	para-aminobenzoate synthase component II		4	2	1.130	0.512	1.464		0.603		1.014	0.916	1.148	
sync_2664	hydrolase, metallo-beta-lactamase family protein		23	15	1.134	0.105	0.926	0.348	0.819	0.100	0.941	0.381	1.031	0.679
sync_2666	histidinol-phosphate aminotransferase		6	2	1.010	0.872	2.178		1.116		0.955	0.534	0.667	
sync_2667	arginyl-tRNA synthetase		15	14	0.982	0.782	1.049	0.471	1.102	0.104	1.000	1.000	1.049	0.292
sync_2669	Iron-containing alcohol dehydrogenase	ISL22	2	1	0.963	0.755	1.115		0.988		1.080	0.448	0.941	
sync_2670	antibiotic biosynthesis monooxygenase	ISL22	3	3	0.972	0.809	0.847	0.395	1.075	0.467	1.038	0.833	0.997	0.984
sync_2671	sensory box/GGDEF family protein	ISL22	9	12	0.975	0.793	0.961	0.787	0.967	0.568	1.053	0.770	1.151	0.048
sync_2672	hypothetical protein sync_2672	ISL22	1	4	1.010	0.917	0.814		0.829		0.915	0.393	0.965	
sync_2674	hypothetical protein sync_2674	ISL22		1			0.958	0.750	0.993	0.975			1.119	0.469
sync_2676	hypothetical protein sync_2676	ISL22	4		1.247	0.910					1.249	0.549		
sync_2677	hypothetical protein sync_2677	ISL22	2	1	1.040	0.861	0.947		0.796		0.958	0.591	1.165	
sync_2678	carboxyvinyl-carboxyphosphonate phosphorylmutase	ISL22	6		1.079	0.257					0.929	0.350		
sync_2679	enantiomer-selective amidase	ISL22	6	3	0.898	0.311	1.078	0.594	1.098	0.524	1.082	0.319	0.911	0.831
sync_2681	vanadium-dependent bromoperoxidase 2	ISL22	23	63	2.771	0.000	8.294	0.000	6.787	0.000	1.117	0.477	1.141	0.015
sync_2685	mechanosensitive ion channel family protein	ISL22	11	14	0.932	0.350	1.014	0.925	0.949	0.487	0.961	0.584	1.044	0.697
sync_2686	hypothetical protein sync_2686	ISL22	12	4	1.061	0.652	1.009	0.950	1.017	0.837	1.181	0.049	0.946	0.511
sync_2692	nicotinate-nucleotide pyrophosphorylase	ISL22	2	1	1.097	0.543	0.786		1.007		1.115	0.598	1.683	
sync_2696	hypothetical protein sync_2696	ISL22	2	2	1.050		1.689		0.661		0.847		0.912	
sync_2699	tRNA modification GTPase TrmE		4		1.176	0.246					1.123	0.634		
sync_2702	RelA/SpoT family protein		1		1.029	0.825					1.019	0.880		

sync_2703	ABC transporter ATP-binding protein	1	1	0.999		0.992		0.542		0.810		0.927	
sync_2705	cellulase	2		2.689						2.075			
sync_2708	universal stress family protein	1	3	1.199		0.894	0.805	0.911	0.528	1.441		0.825	0.306
sync_2709	phosphoglycerate kinase	30	44	0.981	0.675	0.910	0.452	0.962	0.525	0.966	0.452	0.952	0.394
sync_2713	hypothetical protein sync_2713	5	4	0.985	0.876	1.020	0.920	0.916	0.562	1.121	0.317	0.978	0.868
sync_2714	undecaprenyldiphospho- muramoylpentapeptide beta-N- acetylglucosaminyltransferase		3			1.394	0.339	1.147	0.398			0.974	0.832
sync_2718	hypothetical protein sync_2718	1	2	1.084	0.565	1.012	0.950	0.774	0.235	0.998	0.987	0.930	0.831
sync_2720	hypothetical protein sync_2720	1		0.990						1.049			
sync_2721	dihydroorotate dehydrogenase 2	2	2	1.055		0.914	0.541	0.786	0.734	1.051		0.940	0.656
sync_2724	50S ribosomal protein L7/L12	25	29	0.931	0.242	1.100	0.591	0.966	0.531	1.010	0.858	0.952	0.427
sync_2725	50S ribosomal protein L10	11	14	1.020	0.709	1.193	0.110	1.088	0.403	0.997	0.959	0.879	0.292
sync_2726	50S ribosomal protein L1	17	14	1.048	0.941	1.129	0.091	1.035	0.691	1.066	0.662	0.919	0.190
sync_2727	50S ribosomal protein L11	7	11	0.997	0.969	1.060	0.606	1.143	0.118	1.007	0.922	1.012	0.863
sync_2728	transcription antitermination protein NusG	14	9	1.082	0.427	1.077	0.322	1.130	0.233	1.134	0.168	1.083	0.457
sync_2729	preprotein translocase subunit SecE	3		0.929	0.899					0.851	0.587		
sync_2730	ATPases with chaperone activity, ATP-binding subunit	12	21	1.026	0.590	1.102	0.318	0.921	0.425	0.944	0.240	0.935	0.195
sync_2732	phosphopyruvate hydratase	18	33	1.054	0.610	1.020	0.853	1.036	0.761	0.998	0.976	1.068	0.250
sync_2733	hypothetical protein sync_2733	5	5	0.985	0.888	0.930	0.331	0.884	0.406	1.079	0.319	1.000	1.000
sync_2734	hypothetical protein sync_2734	2		0.905						0.916			
sync_2735	hypothetical protein sync_2735		3			0.785	0.251	0.914	0.760			1.020	0.876
sync_2736	bifunctional ornithine acetyltransferase/N- acetylglutamate synthase protein	3	4	0.927	0.527	1.089	0.549	1.113	0.474	0.923	0.368	1.076	0.596
sync_2738	hypothetical protein sync_2738	4	4	1.165	0.559	0.745	0.068	1.227	0.178	0.830	0.712	0.978	0.812

sync_2739	aspartyl/glutamyl-tRNA amidotransferase subunit B			16	13	0.986	0.698	0.948	0.677	1.227	0.193	1.018	0.628	1.040	0.766
sync_2740	glycine oxidase ThiO			6		1.063	0.788					1.151	0.257		
sync_2741	nucleoside diphosphate kinase			7	7	0.971	0.701	0.944	0.455	1.127	0.279	1.044	0.582	1.011	0.909
sync_2742	arginine decarboxylase			13	7	1.009	0.850	1.033	0.853	1.113	0.332	0.921	0.109	0.845	0.184
sync_2748	hypothetical protein sync_2748	ISL23		7	10	0.895	0.467	1.147		0.964		1.109	0.548	0.974	
sync_2765	transcriptional regulator, Crp/Fnr family protein	ISL23		8	6	1.144	0.625	1.025	0.731	1.016	0.907	1.124	0.213	1.165	0.105
sync_2766	RND multidrug efflux transporter	ISL23	YES	16	10	0.942	0.123	0.892	0.199	1.043	0.559	0.934	0.081	0.921	0.173
sync_2767	RND family efflux transporter MFP subunit	ISL23	YES	3	3	1.059	0.667	1.234	0.573	0.993	0.982	1.002	0.990	1.149	0.231
sync_2768	alanyl-tRNA synthetase			13	5	1.039	0.572	1.060	0.385	0.895	0.127	0.982	0.708	0.943	0.580
sync_2770	helicase, Snf2 family protein			6	3	1.042	0.614	0.926	0.592	0.986	0.930	1.019	0.777	0.844	0.339
sync_2771	hypothetical protein sync_2771				1			1.305	0.227	0.840	0.385			0.867	0.468
sync_2772	hypothetical protein sync_2772				1			0.835		0.912				0.939	
sync_2776	TRAP-T family tripartite transporter, substrate binding protein			1	1	0.705		0.835		1.076		1.032		0.978	
sync_2779	flavoprotein			17	17	1.020	0.705	0.882	0.167	0.903	0.037	1.006	0.892	1.030	0.503
sync_2780	flavodoxin:flavin reductase-like domain-containing protein			15	14	1.006	0.990	1.111	0.208	0.985	0.850	1.054	0.627	1.114	0.530
sync_2781	rubredoxin			15	11	1.100	0.427	0.825	0.158	0.960	0.813	0.977	0.848	1.091	0.664
sync_2783	reductase			4	4	1.019	0.898	1.320	0.152	0.884	0.279	1.147	0.633	0.920	0.670
sync_2784	hypothetical protein sync_2784			1		1.097						1.111			
sync_2788	glycine dehydrogenase			12	4	0.980	0.749	0.775	0.044	1.090	0.728	0.975	0.685	1.040	0.825
sync_2789	glycine cleavage system protein H			16	8	1.104	0.282	0.876	0.495	1.198	0.234	0.960	0.577	1.034	0.860
sync_2790	aluminium resistance protein			5	2	0.967	0.608	1.932		0.556		0.913	0.236	1.294	
sync_2794	50S ribosomal protein L9			7	13	1.172	0.461	1.122	0.214	1.251	0.121	1.084	0.652	1.052	0.530
sync_2795	replicative DNA helicase			7	2	1.086	0.210	0.994	0.945	1.029	0.767	0.946	0.379	0.931	0.657

sync_2796	tRNA uridine 5-carboxymethylaminomethyl modification enzyme GidA		2		0.916	0.564				0.969	0.827			
sync_2803	hypothetical protein sync_2803		4	2	1.049	0.732	1.024	0.858	0.879	0.478	0.953	0.615	1.146	0.505
sync_2805	hypothetical protein sync_2805		7	5	0.956	0.486	1.209	0.262	0.863	0.083	1.034	0.594	0.998	0.977
sync_2806	NAD-dependent DNA ligase LigA		2	1	1.018	0.843	0.916		0.973		1.051	0.605	0.902	
sync_2811	hypothetical protein sync_2811			6			0.988	0.934	0.872	0.247			0.864	0.328
sync_2817	hypothetical protein sync_2817		4	5	0.998	0.977	1.139	0.518	0.939	0.811	1.092	0.504	0.811	0.280
sync_2819	ABC-type phosphate/phosphonate transport system, periplasmic component, putative		5	5	0.992	0.933	0.880	0.304	0.812	0.133	0.997	0.969	0.841	0.179
sync_2820	GGDEF/EAL domain-containing protein	YES	3		0.988	0.902					1.011	0.912		
sync_2824	transporter, small conductance mechanosensitive ion channel (MscS) family protein		7	2	0.985	0.991	1.334		1.122		1.042	0.658	0.873	
sync_2825	valyl-tRNA synthetase		16	9	1.051	0.347	0.966	0.789	1.170	0.072	0.925	0.174	0.992	0.960
sync_2829	hypothetical protein sync_2829			5			1.303	0.785	0.763	0.282			0.568	0.403
sync_2846	nucleoside triphosphate pyrophosphohydrolase		1	1	0.988	0.916	1.082	0.783	0.886	0.437	0.993	0.940	0.819	0.294
sync_2851	agmatinase		1		1.295						1.288			
sync_2853	glycine cleavage system aminomethyltransferase T		7	7	1.049	0.360	0.908	0.434	1.046	0.639	1.017	0.744	1.032	0.677
sync_2854	aspartyl-tRNA synthetase		21	13	1.060	0.700	1.117	0.556	1.057	0.710	0.983	0.739	1.086	0.687
sync_2856	DNA protection protein		4	7	1.035	0.740	1.081	0.459	1.052	0.782	1.010	0.919	1.028	0.738
sync_2857	short-chain dehydrogenase/reductase family protein			2			1.395		1.006				0.994	
sync_2858	CTP synthetase		10	7	1.014	0.785	1.151	0.213	1.016	0.860	0.949	0.312	1.056	0.369
sync_2860	hypothetical protein sync_2860		5	1	1.014	0.870	0.810		1.394		0.969	0.786	1.308	

sync_2861	ABC transporter, multi drug efflux family protein	6	4	0.970	0.771	0.968	0.941	0.897	0.321	0.996	0.945	0.956	0.692
sync_2862	transporter component	5	6	0.922	0.513	1.263	0.402	0.975	0.917	0.920	0.628	0.994	0.961
sync_2863	ecotin precursor	7	8	1.029	0.708	1.102	0.520	1.080	0.604	1.045	0.573	1.023	0.907
sync_2864	exsB protein	4	4	1.040	0.770	1.014	0.910	0.886	0.436	0.943	0.675	1.225	0.300
sync_2865	p-aminobenzoate synthetase	1		0.983						1.003			
sync_2866	aminotransferases class-IV	1		0.810						0.920			
sync_2868	ABC transporter, ATP-binding protein	5	7	1.101	0.494	0.855	0.308	0.862	0.520	0.902	0.392	0.953	0.785
sync_2869	ABC transporter ATP-binding protein		3			0.863	0.513	1.135	0.257			1.080	0.603
sync_2872	urea ABC transporter, periplasmic urea-binding protein	97	10 2	0.987	0.775	0.753	0.018	0.926	0.160	1.077	0.181	0.898	0.018
sync_2874	urease accessory protein UreF	3		0.928	0.480					0.933	0.613		
sync_2875	urease accessory protein UreE		1			1.004		1.171				1.118	
sync_2876	urease accessory protein UreD	1		1.100						0.688			
sync_2877	urease subunit gamma	2	3	1.049		0.853	0.233	1.492	0.276	0.883		1.187	0.565
sync_2878	urease subunit beta	8	8	1.004		0.684	0.427	1.053	0.724	1.007		0.990	0.943
sync_2879	urease subunit alpha	15	10	1.173	0.133	0.849	0.113	0.949	0.581	1.019	0.832	0.992	0.921
sync_2882	hypothetical protein sync_2882	1		1.113						1.067			
sync_2887	nitrate permease NapA	4	3	0.924	0.429	1.331	0.073	0.982	0.891	1.052	0.593	0.809	0.130
sync_2888	nitrate reductase	1		1.349						0.914			
sync_2889	nitrate reductase associated protein	2	1	1.177	0.966	0.712		0.728		1.485	0.632	0.278	
sync_2890	hypothetical protein sync_2890		1			1.658		0.835				0.914	
sync_2891	molybdenum cofactor biosynthesis protein C	4		0.945	0.491					0.982	0.817		
sync_2892	molybdopterin biosynthesis protein MoeA	5	5	1.144	0.878	1.018	0.793	0.977	0.746	1.125	0.669	1.265	0.094
sync_2894	molybdopterin biosynthesis	1		1.207						0.828			

sync_2895	molybdenum cofactor biosynthesis protein B1	2	1	0.932		0.954		0.863		0.728		1.064		
sync_2896	uroporphyrin-III C-methyltransferase	7	3	1.102	0.562	0.506	0.539	0.925	0.967	0.815	0.303	1.485	0.182	
sync_2897	hypothetical protein sync_2897		2			1.025		0.777				0.917		
sync_2898	ferredoxin-nitrite reductase	33	34	1.190	0.002	1.223	0.039	1.227	0.011	1.054	0.384	0.961	0.417	
sync_2899	formate and nitrite transporters	4	2	1.023	0.828	0.930		0.870		0.904	0.382	1.173		
sync_2900	homeobox domain	2	1	1.441	0.197	0.956		0.822		0.893	0.458	0.982		
sync_2901	cyanate hydratase	6	5	0.970	0.745	0.988	0.978	1.179	0.359	0.981	0.845	1.138	0.512	
sync_2904	hypothetical protein sync_2904	8	3	1.124	0.153	0.834		1.090		1.027	0.705	1.027		
sync_2906	polyphosphate kinase	6	6	0.843	0.097	0.852	0.746	1.137	0.613	0.918	0.317	0.840	0.645	
sync_2909	phospho-2-dehydro-3-deoxyheptonate aldolase	9	8	0.983	0.793	0.909	0.458	0.942	0.703	1.014	0.831	1.054	0.712	
sync_2910	bifunctional aconitate hydratase 2/2-methylisocitrate dehydratase	14	11	1.078	0.226	1.289	0.003	1.292	0.004	0.990	0.819	1.131	0.186	
sync_2916	O-antigen polymerase family protein		1			1.244		1.374				1.145		
sync_2917	formyltetrahydrofolate deformylase	4	3	1.018	0.823	0.914	0.496	0.940	0.665	0.990	0.911	1.093	0.398	
sync_2918	putative lipoprotein	11	14	0.979	0.730	0.757	0.069	0.974	0.760	0.958	0.495	0.943	0.358	
sync_2920	phosphate ABC transporter, phosphate-binding protein	63	91	0.920	0.112	0.800	0.096	0.992	0.944	0.984	0.802	0.848	0.051	
sync_2923	molecular chaperone DnaK	56	61	1.046	0.294	1.083	0.327	1.018	0.735	1.023	0.506	1.073	0.247	
sync_2924	shikimate 5-dehydrogenase	3	1	1.252		0.668		0.805		1.187		1.379		
sync_2925	hypothetical protein sync_2925	2		0.820	0.448					0.899	0.476			
sync_2926	30S ribosomal protein S6	11	11	1.007	0.940	1.021	0.856	1.152	0.187	0.975	0.705	1.015	0.866	
sync_2928	argininosuccinate synthase	17	9	1.012	0.822	0.842	0.053	1.102	0.116	1.004	0.939	0.951	0.309	
sync_2930	hypothetical protein sync_2930	6	5	1.038	0.756	1.631	0.310	0.974	0.876	1.643	0.072	1.115	0.492	
sync_2932	hypothetical protein sync_2932	YES	7	8	0.917	0.529	0.955	0.635	0.977	0.922	1.114	0.182	1.246	0.441
sync_2935	phosphoribosylglycinamide formyltransferase 2	11	5	0.948	0.571	0.936	0.533	1.007	0.954	0.992	0.917	1.044	0.711	

sync_2938	esterase/lipase/thioesterase family protein	8	6	0.945	0.481	0.942	0.448	1.029	0.863	1.022	0.691	0.883	0.544
sync_2939	excinuclease ABC subunit A	10	17	0.970	0.552	1.328	0.000	0.973	0.559	1.260	0.017	0.877	0.032
sync_2940	DNA repair protein RecN	1	2	1.089		1.048		1.110		1.123		0.814	
sync_2942	hypothetical protein sync_2942	3	13	0.900	0.248	1.318	0.107	1.158	0.375	0.999	0.993	1.155	0.106
sync_2943	threonine synthase	5	5	1.100	0.365	1.101		0.724		1.028	0.779	0.984	
	Kanr_amino_acids	6	1	0.929	0.682	0.555		1.203		0.955	0.563	0.995	